TWO-DIMENSIONAL MOBILE-BED DAM-BREAK MODEL

by

GAVEN TANG
B.Sc., University of Alberta, 2010

A THESIS SUBMITTED IN PARTIAL FULFILLMENT OF
THE REQUIREMENTS FOR THE DEGREE OF

MASTER OF APPLIED SCIENCE
in
THE FACULTY OF GRADUATE STUDIES
(Civil Engineering)

THE UNIVERSITY OF BRITISH COLUMBIA
(Vancouver)

October 2012

ABSTRACT

Sudden and catastrophic dam-breaks typically induce high bed shear stresses downstream as the flood-wave propagates over the alluvial channel and flood plain. In fact, the non-dimensionalized shear stresses are often high enough that they are comparable to those typically seen in the transport of sand. Despite the existence of these shear stresses, industry typically ignores sediment transport altogether and assumes a fixed-bed when modelling dam-breaks. This thesis will examine the validity of the fixed-bed assumption and create a depth-averaged 2D mobile-bed dam-break model. This model will then be tested by simulating the Malpasset (France) dam-break of 1959, and a sensitivity analysis will then be performed on the parameters of grain roughness, vegetation roughness, friction angle, grain size, and depth to bedrock to examine differences in inundation and flood-wave propagation.

TABLE OF CONTENTS

LIST OF TABLES

LIST OF FIGURES

LIST OF EQUATIONS

LIST OF SYMBOLS AND ABBREVIATIONS

1D	=	one-dimensional
2D	=	two-dimensional
3D	=	three-dimensional
ASCE	=	American Society of Civil Engineers
BRGM	=	Bureau de Recherches Géologiques et Minières
DHL	=	Delft Hydraulics Laboratory
EDF	=	Electricité de France
EWRI	=	Environmental and Water Resources Institute
HWM	=	High-water mark
IAHR	=	International Association for Hydro-Environment Engineering & Research
IGN	=	Institut Géographique National
KE	=	k-epsilon turbulence model
LFM	=	Laboratory of Fluid Mechanics
NSERC	=	Natural Sciences and Engineering Research Council of Canada
USACE	=	U.S. Army Corps of Engineers
D^*	=	particle parameter
D_{50}	=	mean grain diameter
D_s	=	mean grain diameter
K_s	=	Nikuradse roughness height
R_{ep}	=	particle Reynolds number
d_{50}	=	mean grain diameter
d_b	=	thickness of alluvium layer to bedrock
n	=	Manning's roughness coefficient
n_g	=	grain component of Manning's roughness coefficient
n_v	=	vegetation component of Manning's roughness coefficient
q^*	=	non-dimensional transport rate
u^*	=	shear velocity
u_b	=	mean transport velocity of particles moving as bedload
τ^*	=	non-dimensional bed shear stress

τ_b	=	bed shear stress
τ_c^*	=	non-dimensional critical shear stress
τ_g^*	=	grain component of total non-dimensional bed shear stress
τ_v^*	=	vegetation component of total non-dimensional bed shear stress
g	=	acceleration of gravity
s	=	specific gravity
t	=	time
v	=	flow velocity
w	=	settling velocity
Θ	=	τ^*
Φ	=	q^*
Ψ	=	$1/\Theta$
ρ	=	density
ϕ'	=	friction angle

ACKNOWLEDGEMENTS

I give my gratitude to Dr. Faye Hicks and Dr. Nallamuthu Rajaratnam, my former professors in the field of Water Resources Engineering at the University of Alberta, for inspiring me to pursue further studies and a career in this field. This work would have not been possible without guidance and support from Dr. Robert Millar, my supervisor at the University of British Columbia. Dr. Millar also provided an opportunity for me to travel to Paris for the XVIIIth TELEMAC Users Club Conference. This memorable trip to Europe was the first of many to come.

I am also very grateful for the modelling assistance that Dr. Jose Vasquez and Mr. Faizal Yusuf provided in the early stages of my research. I must give special thanks to Dr. Stephen Kwan for giving so much of his personal time to troubleshoot my models and provide extensive technical guidance. In the later stages of research, Dr. Jean-Michel Hervouet and the online TELEMAC community provided much needed programming support.

I dedicate this work to my family and friends for always supporting me in my decisions, and for encouraging me to continuously better myself. I also need to give special recognition to my best friend, Mr. Lawrence Lau, for never declining my requests to proofread and edit my papers. Lastly, I would like to thank my officemates, Mr. Curtis VanWerkhoven and Mr. Yapo Alle-Ando, for the Risk games and lunches that we were able to share.

1 INTRODUCTION

1.1 CURRENT PRACTICE

Dam-break analysis is commonly performed to create inundation maps and to determine flood-wave propagation time to populated regions or locations of critical infrastructure in the event of dam failure. Typically, one-dimensional fixed-bed simulations are used in the modelling of dam-break floods.

From **Newlin (2007)** and the **USACE (1997)** dam-break analysis guideline, it is apparent that dam-break analyses performed by industry have not progressed in quite a few years. The four steps involved in performing the industry standard dam-break analysis are as follows **(USACE, 1997)**:

(1) Dam-Breach Analysis: The causes of dam failure and dam-breach characteristics are determined.
(2) Dam Failure Hydrograph: A failed dam outflow hydrograph is produced based on input parameters (i.e., precipitation hydrograph, hydraulic and hydrologic routing, dam characteristics, and downstream river morphology).
(3) Dam-Break Routing: A usually one-dimensional, full unsteady flow routing model is run.
(4) Inundation Mapping: Maps of predicted inundated land are produced to assist in the identification of hazard zones and creation of evacuation plans.

It is of note that the **USACE (1997)** guideline to performing a dam-break analysis neither references sediment transport nor changes in river morphology; hence, the analysis is performed with the assumption that the riverbed is fixed. A fixed-bed assumption for the analysis of sudden dam-break flows in an alluvial river may or may not be appropriate depending on application. However, it is well recognized in the fluvial geomorphology community that flows equal to or greater than bankfull flows are channel forming. Thus, if sudden dam-break flows are channel-forming flows, the stream morphology may evolve.

Research to examine the morphologic change in a river following a dam-break will require the assumption of a mobile riverbed. In making this assumption, it is extremely likely that steps (3)

and (4) of the above **USACE (1997)** guideline will be impacted. By incorporating mobile-bed conditions, the process of performing dam-break analyses will be advanced.

1.2 DAM-BREAK CASE STUDIES

In 1996, the Ha! Ha! Lake in Quebec experienced a breach whereby a small earthen dyke situated south of the main concrete dam was overtopped. This resulted in a new channel being incised, allowing water to bypass the dam. The lake's water level rapidly dropped by 9 m with an estimated peak outflow of 1010 m^3/s **(Capart et al., 2007)**.

The Ha! Ha! Lake outbreak flood likely led to large amounts of sediment being entrained from the lake and floodway and being deposited downstream. Such a large mobilization of bed sediment caused morphologic changes along the entire downstream reach of the Ha! Ha! River as evidenced in **Figure 1-1**. In the figure, (b) shows the before aerial photograph of the river, and (c) shows the after. By comparing (b) and (c) it can be interpreted that following the lake outbreak, the channel was widened along the entire length of the river and there was lateral migration of some meanders. Both of these feed into the notion that flows on the scale of those observed following a sudden dam-break, or in this case, dyke-breach, will cause morphologic change.

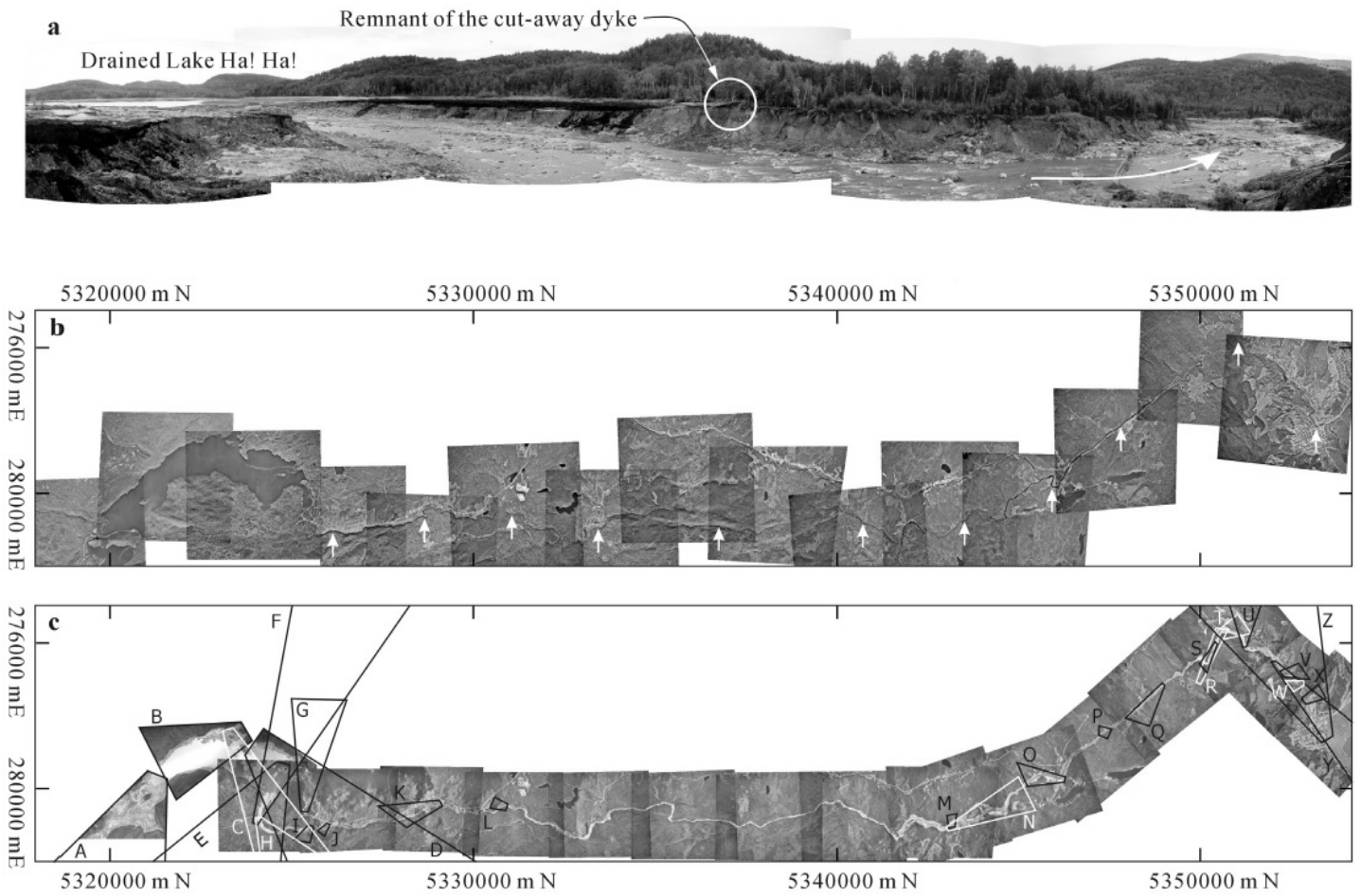

Figure 5 Photo mosaics of the dyke area and river course: (a) ground photos of the dyke area, with the drained lake to the left and a remnant of the earthen dyke circled in white (photos by G.R. Brooks) ; (b) and (c) air photos from 1994 and 1996, respectively before and after the flood, registered on the 1998 ortho-photo (*Source*: Photocartothèque Québécoise). White arrows on panel b mark the river course, and frames on panel c denote the projected outlines of helicopter photos A–Z.

Figure 1-1: Ha! Ha! Lake outbreak flood outcome photographs: (a) photo mosaic showing eroded river-bank; (b) and (c) aerial photographs of the river course before and after the flood, respectively. (Capart et al., 2007; © Taylor & Francis, 2007, by permission)

In 2008, a magnitude 8.0 earthquake shook Wenchuan, Sichuan Province, Southwest China, resulting in the formation of a barrier lake at Tangjiashan. Approximately a month after its formation, the lake breached and the water level in the lake fell $22\ m$ as it emptied. Peak discharge was determined to be about $6500\ m^3/s$ **(Liu et al., 2010)**.

Similar to the Ha! Ha! Lake outbreak, the Tangjiashan Barrier Lake breach also entrained and deposited large amounts of sediment. **Figure 1-2** shows a longitudinal profile of the original bed elevation and topography, before and after the dam-break. Comparing the original bed slope to the bed slope after the dam-breach, it can be seen that the slope angle has increased and up to $40\ m$ of sediment has been deposited on top of the original bed. It is also likely that the material deposited on top of the original riverbed has a different grain size distribution than that of the original bed. Both of these factors contribute to the development of a new morphology.

Figure 1-3 shows the cross-sections of the river channel with the original bed elevation and the bed elevation after the dam-breach. As a part of a changing morphology, the channel geometry has also changed.

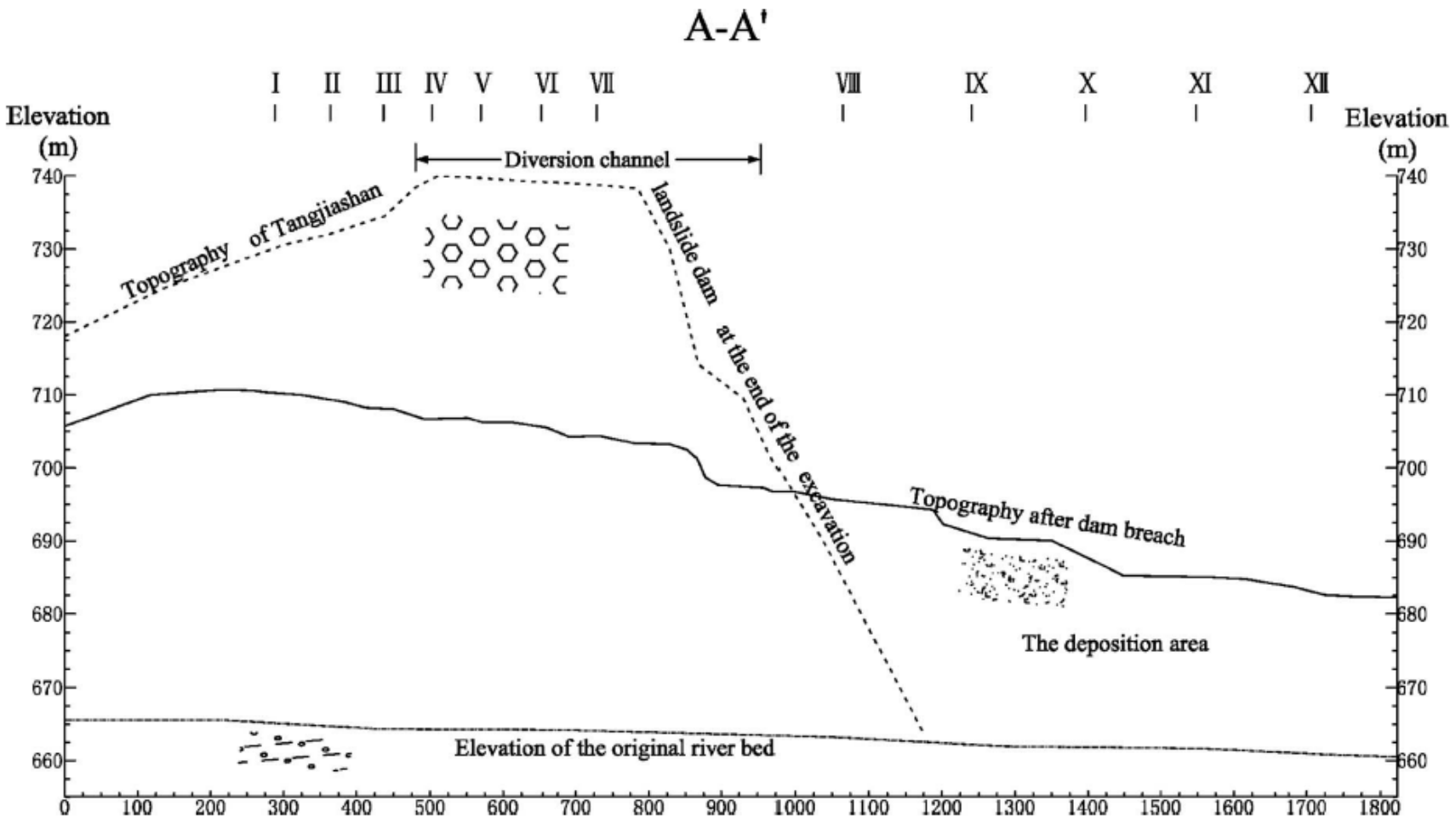

Fig. 13. Longitudinal cross section along the river channel showing the incision and deposition effects

Figure 1-2: Topography of the river channel before and after the Tangjiashan Barrier Lake dam-break (Liu et al., 2010; © ASCE, 2010, by permission)

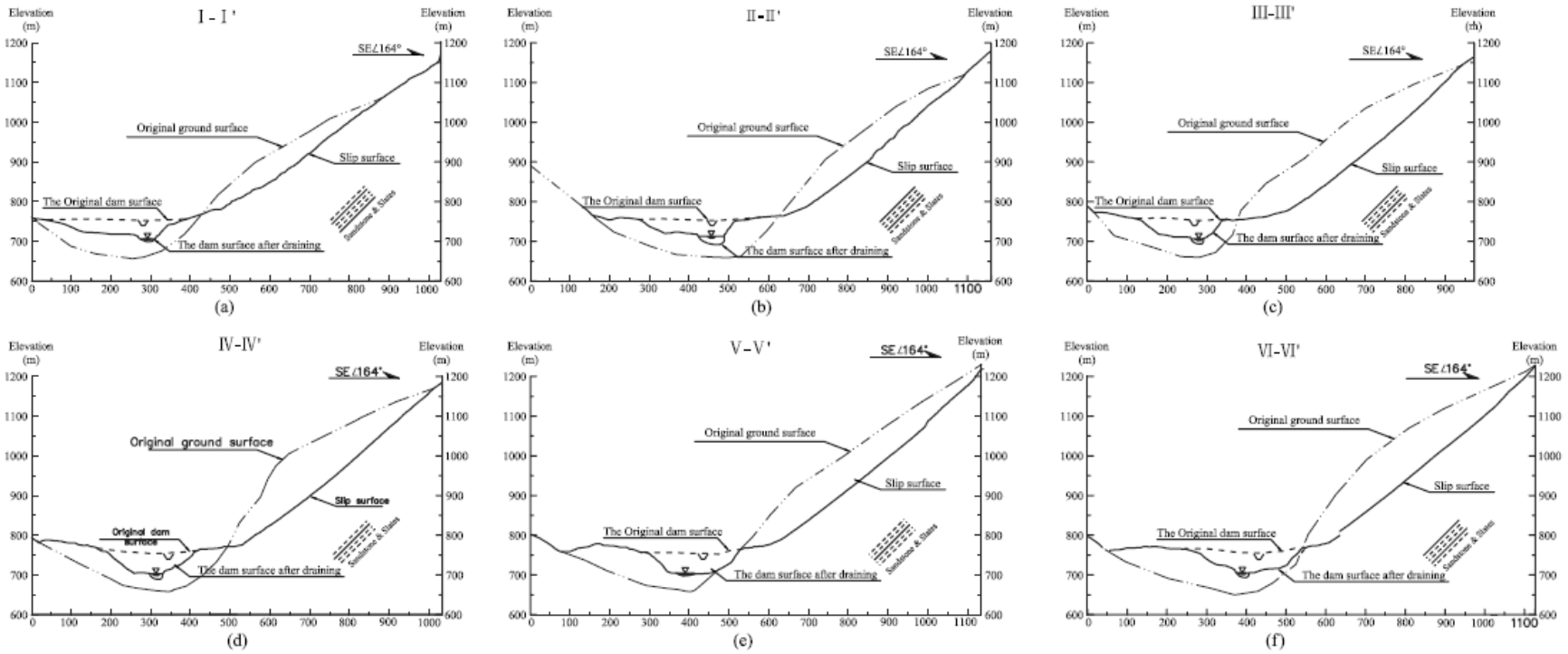
I - I '
II-II'
III-III'
IV-IV'
V-V'
VI-VI'
Elevation (m)
SE∠164°
Original ground surface
Slip surface
The Original dam surface
The dam surface after draining
Sandstone & Slates
Original dam surface
(a)
(b)
(c)
(d)
(e)
(f)

Figure 1-3a

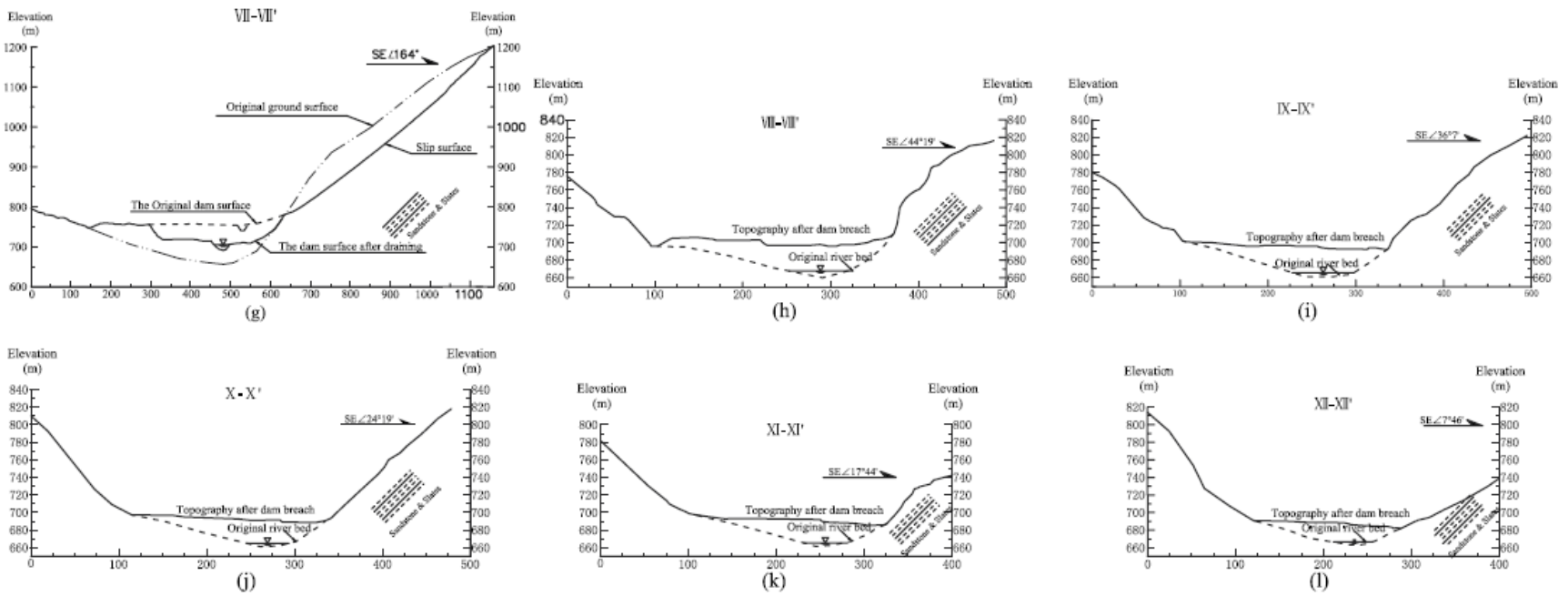

Fig. 14. Cross sections of the new river channel

Figure 1-3b

Figure 1-3: Before and after cross-sections of the river following the Tangjiashan Barrier Lake dam-break. (a) to (l) are cross-sections at various points along the river. (Liu et al., 2010; © ASCE, 2010, by permission)

The Ha! Ha! Lake and Tangjiashan Barrier Lake incidents both highlight the fact that dyke-breaches and dam-breaks are events with flows that can mobilize large amounts of sediment. Such large mobilizations of sediment are bound to have significant impacts on river morphology. Thus, it is more appropriate to assume mobile-bed conditions when attempting to model dam-break flows over alluvial rivers.

1.3 CURRENT METHODS OF MODELLING DAM-BREAK

The current state of practice, study of dam-break flows on alluvial rivers involves both numerical simulations and scaled physical models. Most scaled physical models are created to verify their numerical simulation counterparts **(Quanhong, 2009; Vasquez and Leal, 2006; Vasquez et al., 2007; Xia et al., 2010; Capart and Young, 1998)**. After a numerical model is verified, there can be confidence in the output yielded when applying the model to a case study.

Numerical simulation involves one-, two-, or three-dimensional models. Traditionally, 1D models have been widely used because they require the least computer resources. As the processing power of computers has grown over the years, 2D models have become more practical. Eventually, once computer processing power reaches the point where simulation time is reduced to an acceptable level, 3D models will become the standard. Having a mobile-bed over a fixed-bed also increases computational requirements; therefore, fixed-bed simulations are more prevalent for all three categories of numerical models **(Vasquez and Roncal, 2009; Cao et al., 2004; Ferrari et al., 2010; Hardy et al., 2005)**.

Scaled physical models of dam-break flows on alluvial rivers are typically used to develop and verify numerical models. Verification of a 1D model would entail the use of a simple rectangular or trapezoidal prismatic channel, such as that of **Soares Frazao et al. (2001)**, while verification of a 2D or 3D model would entail the use of more complex channel geometries and morphologies such as those of **Soares Frazao and Zech (2002)**, **Vasquez and Roncal (2009)**, and **Vasquez and Leal (2006)**. The bed of this type of set-up may or may not contain mobile sediment, depending on the type of numerical simulation being tested.

Because the focus of this research is on the morphologic impacts of dam-break flows over alluvial rivers, the different modeling methodologies will be examined within the context of mobile-bed.

1.4 STATEMENT OF PROBLEM

Dam-breaks can lead to a multitude of environmental and community impacts, including impacts on fish populations, river morphology, and human life. A topic of particular interest to stakeholders is the immediate impact of a dam-break on the morphology of a river, as this will allow the assessment of ecological recovery and resilience. Research into this area will allow the examination of sediment transport, with and without vegetation influences, and the prediction of possible changes in channel geometry. The scour, transport, and deposition that occur during dam-break may also affect travel time, duration, and inundation levels of the dam-break flood. The Malpasset dam in France, which failed catastrophically in 1959, will be used as a case study. A 2D mobile-bed model will be developed and used to examine the morphologic effect of having a dam-break flood propagate through the Reyran Valley downstream of the Malpasset Dam. Potential morphologic effects of dam-break floods will be studied through a sensitivity analysis that allows for the examination of differences in inundation and flood-wave characteristics for both the mobile-bed and fixed-bed simulations. This research is part of a larger NSERC-funded project that involves BC Hydro as an industry partner. It will assist BC Hydro, other utilities, and stakeholders in performing appropriate planning and design exercises where dam-breaks are a concern.

2 LITERATURE REVIEW

2.1 2D MOBILE-BED MODELS

To model a dam-break flood over a mobile-bed, a 1D model would not be sufficient as it is cross-sectionally averaged, and a 3D model would require extensive computing resources. A 2D depth-averaged model would be sufficient as it is capable of simulating changes in river depth and width, allowing subsequent examination of changes to morphology and channel geometry.

There have been relatively few attempts at modelling dam-break flows for mobile-bed rivers using 2D depth-averaged approaches in order to examine morphologic impacts on alluvial rivers. A search of the literature has yielded four studies: **Dewals et al., 2002; Vasquez and Leal, 2006; Quanhong, 2009;** and **Xia et al., 2010**. This work is discussed below.

2.1.1 WOLF 2D MODEL

The WOLF 2D model was developed by the University of Liege to solve 2D shallow-water equations on any evolutive grid, dealing with natural topography and mobile-beds. The sediment transport module in WOLF 2D assumes that only bedload transport occurs. This software suite was developed over a period of years to be an efficient analysis and optimization tool, and thus it features helpful graphical display techniques in powerful pre- and post-processing analyses **(Dewals et al., 2002)**.

To demonstrate the WOLF 2D model, **Dewals et al. (2002)** successfully applied it in the simulation of a hypothetical instantaneous and total failure of the large Eupen dam in Belgium. The focus of this study was to create functional risk maps, but the model was also able to monitor changes in bed topography due to erosion and deposition. This is particularly useful in monitoring how the morphology in an alluvial river changes over time after a sudden dam-break. While the accuracy of the model simulation of the Eupen dam is not stated by **Dewals et al. (2002)**, the tone suggests that the results had an acceptable level of accuracy.

During a simulation run, WOLF 2D is capable of displaying a 3D rendering of what is occurring at a specific location along the channel. This provides an additional perspective when trying to understand what is happening during the simulation. **Figure 2-1** is a sample of the 3D rendering

capabilities of WOLF 2D. While this example is presented in black and white, coloured renderings are also possible.

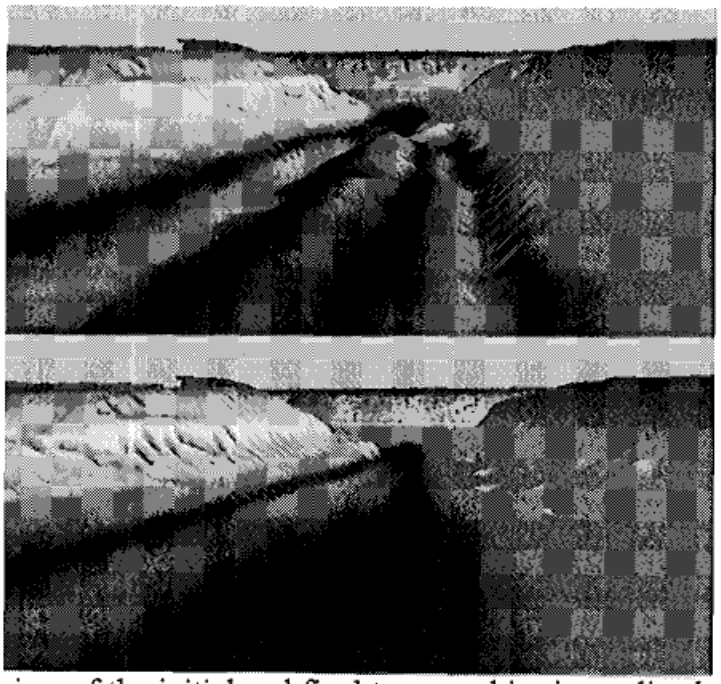

Figure 6 : 3D-view of the initial and final topographies immediately downstream the dam (not represented).

Figure 2-1: 3D-view in WOLF 2D (Dewals et al., 2002; Courtesy of WIT Press from: *Third International Conference Computer Simulation in Risk Analysis and Hazard Mitigation, Risk Analysis III, page 66*)

2.1.2 RIVER2D-MORPHOLOGY MODEL

River2D-Morphology (R2DM) is a 2D mobile-bed river morphology model developed as an extension of River2D (R2D), a fixed-bed hydrodynamic model **(Vasquez et al., 2007; Steffler and Blackburn, 2002)**. Similar to WOLF 2D, sediment transport in R2DM also accounts only for bedload transport.

Vasquez and Leal (2006) used R2DM to simulate a sudden release of water from a reservoir into an initially wetted channel with a 90° bend, and used experimental results to assess the model simulations. R2DM was capable of simulating the concavity of the bed and the formation of bars. It was also capable of predicting water levels with reasonable accuracy when compared

to experimental results. However, since the downstream water level had to be fixed, the accuracy of results deteriorated over time **(Vasquez and Leal, 2006)**.

It should be noted that **Vasquez and Leal**'s **(2006)** study involved an idealized rather than a real dam-break scenario. Water was only allowed to propagate along initially wetted channel cells and not on initially dry flood plain cells. Later testing by **Vasquez and Roncal (2009)** found that R2DM is not well suited to dam-break modelling in alluvial rivers due to the way that R2D handles wetting and drying of the bed. R2D always assumes that water moves over a pervious bed with a defined transmissivity, thus allowing some surface water to flow into an imaginary underlying aquifer when water depth decreases below a minimum low value. It was found that when the bed slope intersects the dam-break flood-wave, up to 100% of the incoming flood-wave could disappear into the aquifer. One possible solution to mitigate this was to reduce the groundwater transmissivity, but this caused numerical instabilities in River2D. As such, River2D-Morphology is not a candidate for use in researching morphologic change in alluvial rivers due to sudden dam-breaks.

2.1.3 QUANHONG'S MODEL

Quanhong (2009) developed a 2D morphodynamic model for a PhD thesis. However, this model has only been verified for straight channels without bends. In terms of dam-break simulations, it has only been tested on ideal dam-break and laboratory partial dam-break scenarios. This model is not suitable for simulating sudden dam-breaks since it is an uncoupled model with simplified governing equations. **Quanhong**'s **(2009)** approach appears to be similar to early renditions of River2D during its development.

2.1.4 XIA ET AL.'S MODEL

Xia et al. (2010) developed a 2D morphodynamic model that accounts for suspended-load and bedload sediment transport. It is noteworthy that this model couples the computation of flow motion and sediment transport.

To verify the model output, **Xia et al. (2010)** compared simulation data to existing numerical model outputs and experimental results. After the model was verified, it was used to simulate dam-break flows over a fixed-bed and then over a mobile-bed to examine the differences in

flood-wave speed and depth. Results indicated that dam-break flows behave substantially different over mobile-beds than over fixed-beds. **Xia et al.**'s **(2010)** findings justify the need to closely examine the differences between dam-break models with fixed-beds and mobile-beds.

2.1.5 CONCLUSIONS

The only models used to date to simulate real-case dam-breaks are WOLF2D, which was discussed above, and TELEMAC2D, which will be discussed in a later section. WOLF2D is the only model that has truly been verified to simulate mobile-bed dam-breaks. However, its development and popularity pales in comparison to the TELEMAC suite of models. It is therefore proposed that the TELEMAC models, TELEMAC2D and SISYPHE, be used for this research to simulate mobile-bed dam-breaks.

2.2 SEDIMENT TRANSPORT EQUATIONS

Dams are usually constructed on mountain streams, which are normally gravel-bed rivers. Since sediment starvation occurs downstream of dams, it is reasonable to assume that all rivers downstream of dams are gravel-bed.

In gravel-bed rivers, bedload transport typically occurs at or slightly above the threshold of motion of the gravel sediment **(Mays, 1999)**. As a consequence, most bedload transport equations for gravel-bed rivers are designed and verified at relatively low non-dimensional bed shear stresses (τ^*), and thus are unverified for cases of high τ^*. However, during dam-break analysis, τ^* will exceed the threshold of motion and, as a result, greatly exceed the intended and/or verified regions of validity for most bedload transport equations. It is, therefore, of interest to examine the degree to which the values of bed τ^* developed during dam-break flows deviate from verified τ^* regions. This examination will allow the selection of a suitable bedload transport relation to use during extreme flows.

For the determination of morphologic change downstream of a dam-break, it is of great interest to know what other regimes of sediment transport may occur or dominate. Consequently, suspension criteria will also be briefly examined.

2.2.1 DAM-BREAK SHEAR STRESS ESTIMATES

In order to determine the range of bed shear stresses (τ_b), PHOENICS, a 3D hydrodynamic model developed by CHAM, was employed to simulate a model previously created by **Vasquez and Roncal (2009)**.

It should be noted that this simulation only examines shear stresses that develop because of immobile boundary (bed) conditions; hence, the output shear stresses may not necessarily be representative of what would happen in an actual dam-break. For the purpose of quantifying the approximate degree of τ^* deviation, the condition of the mobile or immobile boundary is of no consequence.

It was found that under dam-break conditions, the maximum τ^* was on the order of 10, a value 100 times greater than the typical gravel transport condition. A preliminary observation from plotting the computed τ^* value on Parker's Shields Diagram **(Mays, 1999)** in **Figure 2-2** is that it plots much higher than the area specified for gravel-bed rivers. This indicates that under the dam-break scenario, flows are great enough to induce intense shear stresses. In addition, it can be deduced that the primary mode of sediment transport should be suspended-load transport since τ^* plots above the boundary where the ratio of shear velocity (u^*) to settling velocity (w) is 1.

Although the primary mode of sediment transport was determined to be suspension for the computed maximum value of τ^*, a review of bedload sediment transport equations is still warranted, as a wide range of τ^* was experienced by the river channel during the dam-break simulation.

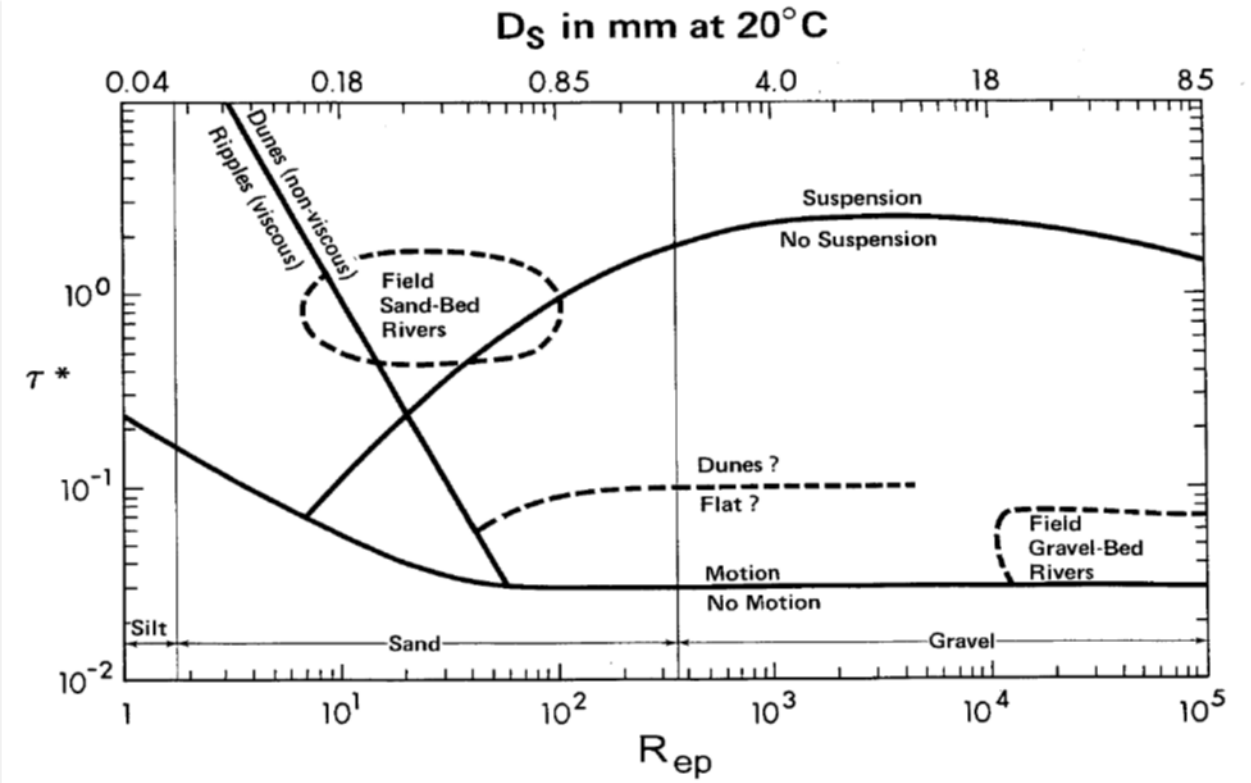

FIGURE 6.10 Shields regime diagram. (Source: Gary Parker)

Figure 2-2: Parker's Shields diagram (Mays, 1999; © The McGraw-Hill Companies, Inc., 1999, by permission)

2.2.2 REVIEW OF SELECT BEDLOAD TRANSPORT EQUATIONS

A number of bedload transport equations were examined and underlying assumptions in their development and verified ranges of τ^* compared. The purpose of comparing these bedload transport equations was to determine whether there exists a suitable q^* (non-dimensional transport rate) versus τ^* relationship that has been verified for values of τ^* up to 10.

2.2.2.1 ENGELUND AND FREDSOE EQUATION

Equation 2-1: Engelund and Fredsoe (1976) equation

$$q^* = 18.74(\tau^* - \tau_c^*)\left[\tau^{*\frac{1}{2}} - 0.7\tau_c^{*\frac{1}{2}}\right]$$

$$\tau_c^* = 0.05$$

This bedload transport equation was developed by first semi-empirically determining the motion of an immersed particle travelling as bedload. This allowed **Engelund and Fredsoe (1976)** to create a relationship between friction velocity (u^*) and mean transport velocity of particles moving as bedload (u_b), which then further allowed them to relate τ^* and q^*. The relationship developed assumed uniform grain size throughout the bed.

This formulation was verified for various u_b through laboratory experiments, where **Meland and Normann (1966)** used spherical glass beads moving over a bed of rhombohedrally packed spherical beads. Experiments were run where the beads travelling over the bed were larger, smaller, or the same size as the packed spherical beads.

The verified range of τ^* for **Engelund and Fredsoe**'s **(1976)** formulation is **0.04 to 0.3**, which covers the lower τ^* range of the gravel-bed river region in **Figure 2-2**.

2.2.2.2 MEYER-PETER AND MULLER EQUATION

Equation 2-2: Meyer-Peter and Muller (1948) equation

$$q^* = 8(\tau^* - \tau_c^*)^{\frac{3}{2}}$$

$$\tau_c^* = 0.047$$

The classic **Meyer-Peter and Muller (1948)** bedload transport equation was empirically developed through laboratory experiments in a rectangular flume. The experiments used a uniform grain size of $5.05\ mm$ and uniform flow conditions where friction slope equated to bed slope. Sediments of varying specific gravity were also used.

Figure 2-3 shows the experimental data that was collected by **Meyer-Peter and Muller (1948)** in creating their transport relation. It is noted that they were able to verify the relation for a τ^* range of **0.073 to 0.18**.

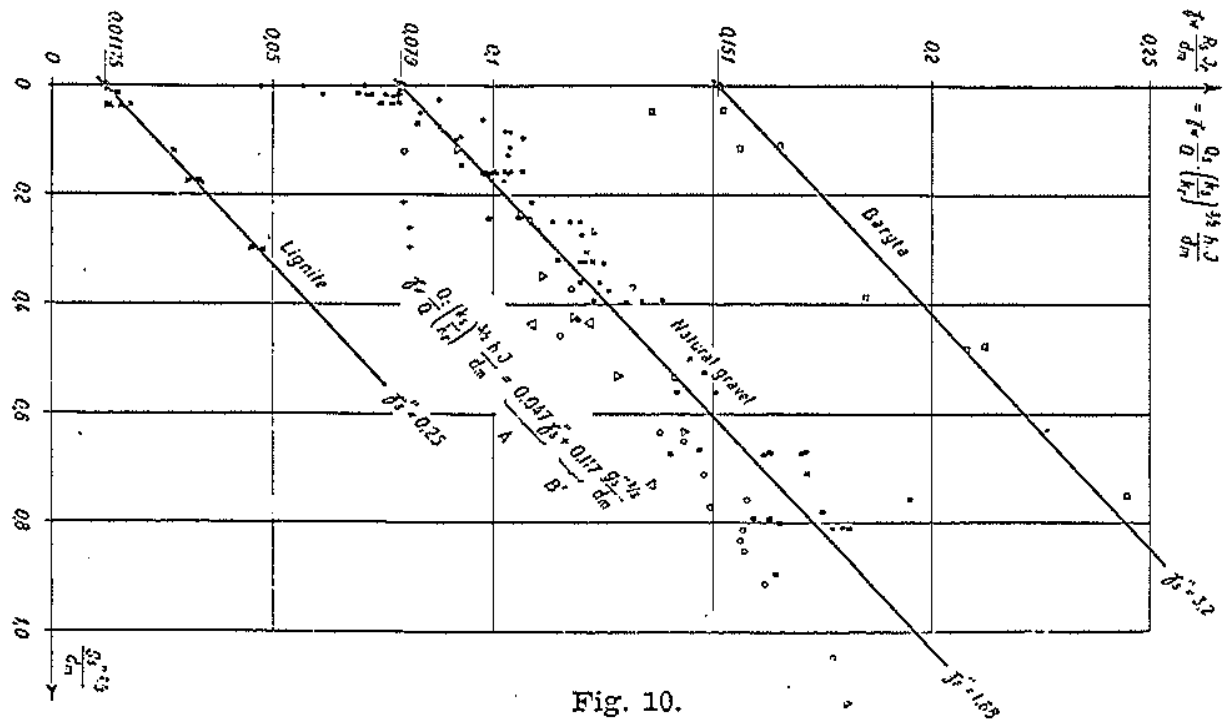

Figure 2-3: Data collected by Meyer-Peter and Muller (1948) (© IAHR, 1948, by permission)

2.2.2.3 WONG AND PARKER EQUATION

Equation 2-3: Modified Meyer-Peter and Muller equation (Wong and Parker, 2006)

$$q^* = 4.93(\tau^* - \tau_c^*)^{1.6}$$

$$\tau_c^* = 0.047$$

Wong and Parker (2006) re-examined **Meyer-Peter and Muller**'s **(1948)** derivation of their bedload transport equation and proposed that an unnecessary bed roughness correction was applied to cases of plane-bed morphodynamic equilibrium. They also highlighted that the characterization of flow resistance using Nikaradse roughness height (K_s) has been shown to be inappropriate in cases of mobile-bed rough conditions in rivers. Lastly, they proposed the incorporation of an improved correction of the boundary shear stress due to sidewall effects. Thus, **Wong and Parker (2006)** re-derived the **Meyer-Peter and Muller (1948)** formulation to create the Modified Meyer-Peter and Muller equation.

Figure 2-4 shows **Wong and Parker**'s **(2006)** fit of the same dataset from **Meyer-Peter and Muller (1948)**. It can be observed that τ^* is valid for the same range as the original **Meyer-Peter and Muller (1948)** method since no new data was used to verify this relationship.

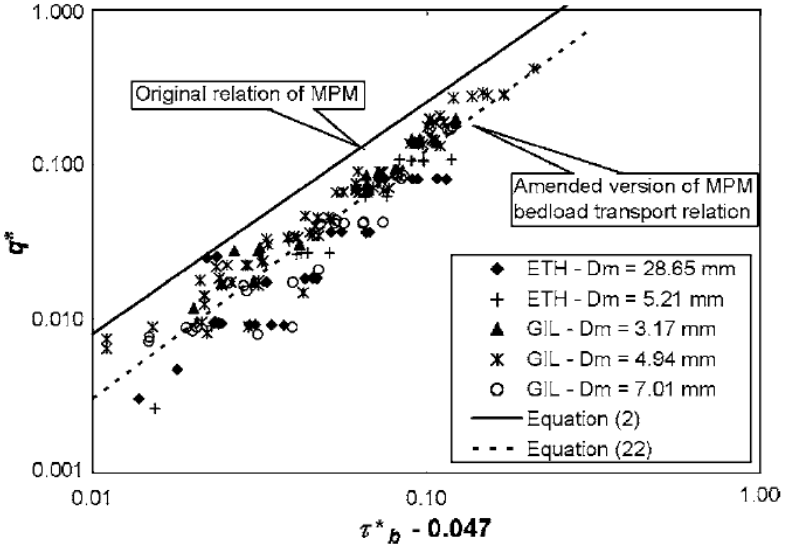

Fig. 8. Comparison of original empirical relation Eq. (2) proposed by MPM, and its amended version Eq. (22) recommended for case of lower-regime plane-bed normal flow equilibrium transport conditions

Figure 2-4: Modified Meyer-Peter Muller relation (Wong and Parker, 2006; © ASCE, 2006, by permission)

2.2.2.4 WILSON EQUATION

Equation 2-4: Wilson (1966) equation

$$q^* = 12(\tau^* - \tau_c^*)^{\frac{3}{2}}$$

$$\tau_c^* \, found \, from \, shields \, diagram$$

The **Wilson (1966)** bedload transport relation is an empirical relation that was fit to high rates of bedload transport. In particular, this relation is used extensively to estimate the transport of sand and industrial materials in pressurized flows **(EWRI, 2008)**. The range of τ^* used to fit this relation was **0.5 to 10 (Cheng, 2002)**.

2.2.2.5 CHENG EQUATION

Equation 2-5: Cheng (2002) equation

$$q^* = 13\tau^{*\frac{3}{2}} \exp\left(-\frac{0.05}{\tau^{*\frac{3}{2}}}\right)$$

Cheng (2002) created this bedload transport equation by fitting a continuous exponential function through data collected by **Meyer-Peter Muller (1948)**, **Gilbert (1914)**, and **Wilson (1966)**. The relation was fit to data over the range of τ^* from **0.03 to 10** (**Figure 2-5**).

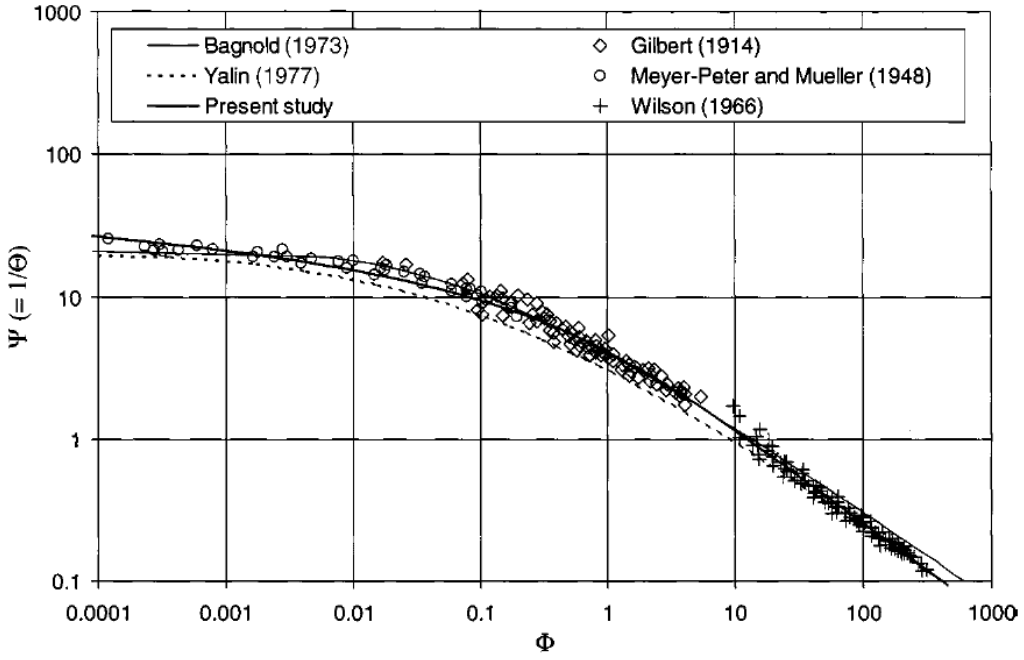

Fig. 4. Comparisons with formulas derived by Bagnold (1973) and Yalin (1977)

Figure 2-5: Cheng's (2002) bedload transport relation (© ASCE, 2002, by permission)

2.2.2.6 PARKER EQUATION

Equation 2-6: Parker (1979) equation

$$q^* = \frac{11.2(\tau^* - 0.03)^{4.5}}{\tau^{*3}}$$

According to **EWRI (2008)**, **Parker (1979)** developed this relation as a simplified fit to the **Einstein (1950)** method for the range of τ^* most likely to occur in gravel-bed rivers. This range of τ^* is the same as that in **Figure 2-2**.

The verified range of τ^* is thus **0.03 to 0.07**, which makes **Parker**'s **(1979)** relation reasonable to use for most gravel-bed rivers. Once again, however, this method only verifies a very minute portion of the dam-break range of τ^*.

2.2.3 SUSPENSION

The suspension boundary in **Figure 2-2** was proposed by **Bagnold (1966)**. He stated that a particle remains in suspension when turbulent eddies have vertical velocity components that exceed the particle fall velocity. After detailed studies were performed on turbulence, it was determined that the bed-shear velocity was on the same order as the maximum value of vertical turbulent velocity. Hence, **Bagnold**'s **(1966)** suspension criterion of $\frac{u^*}{w} = 1$ was formulated, where u^* is the bed-shear velocity, and w is the particle fall velocity.

Around the same time, **Engelund (1965)** developed a similar relation using a "rather crude" stability analysis **(van Rijn, 1984)**. This criterion was also based on a ratio between u^* and w: $\frac{u^*}{w} = 0.25$. Reducing the value from 1 to 0.25 indicates that **Engelund (1965)** thought that suspension occurred at much lower τ^* for a given sediment grain size.

Finally, based on experimental research performed at Delft Hydraulics Laboratory **(DHL, 1982)**, **van Rijn (1984)** developed a new set of suspension criteria that falls between the previous two criteria. He quantified the initiation of suspension as when the instantaneous upward turbulent motions of particles caused jump lengths of about 100 particle diameters. The developed suspension criteria were: $\frac{u^*}{w} = \frac{4}{D^*}$ for $1 < D^* \leq 10$, and $\frac{u^*}{w} = 0.4$ for $D^* > 10$, where $D^* = D_{50}\left[\frac{(s-1)g}{v^2}\right]^{\frac{1}{3}}$ is the dimensionless particle parameter.

Figure 2-6 presents a comparison between the three different suspension criteria, where the vertical axis is τ^*. The large variation between the suspension criteria is noteworthy because it indicates the need for more research into when the initiation of suspension actually occurs.

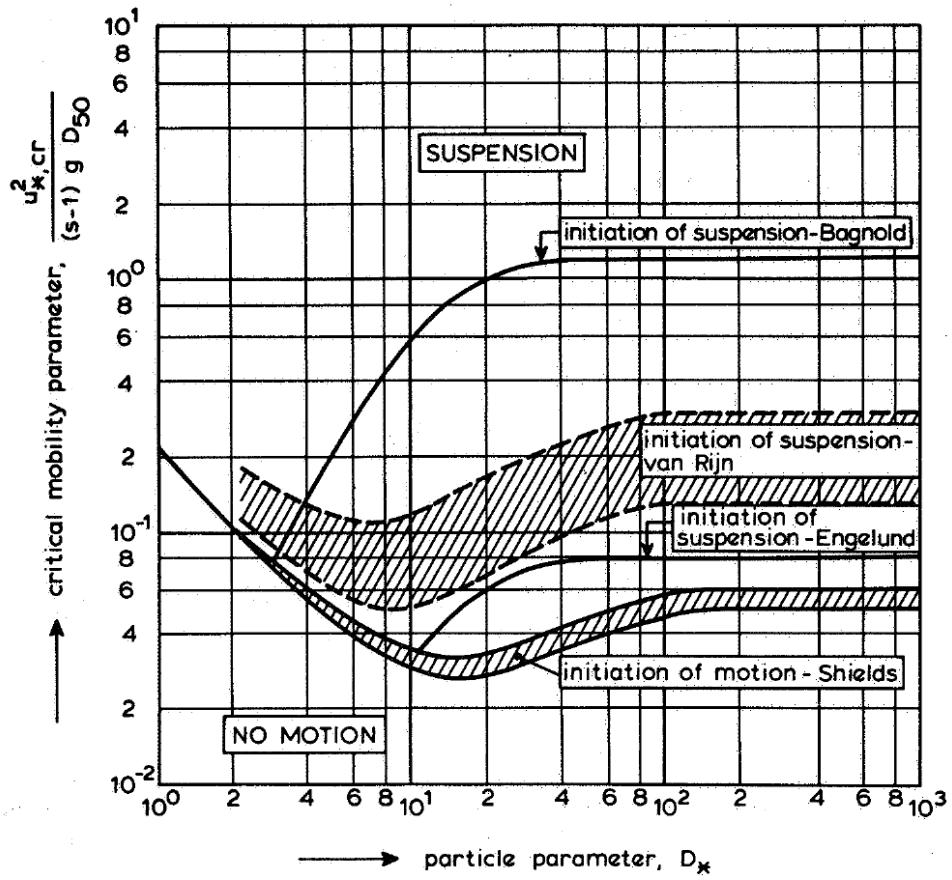

FIG. 1.—Initiation of Motion and Suspension

Figure 2-6: Criteria for the initiation of suspension (van Rijn, 1984; © ASCE, 1984, by permission)

2.2.4 DISCUSSION

From the review of select bedload transport equations in **Section 2.2.2**, a trend is observed in that q^* is proportional to $\tau^{*\frac{3}{2}}$. Consequently, for low values of τ^*, the bedload transport relation can be approximated by $q^* = B\tau^{*\frac{3}{2}}$, where B is a coefficient used by each of the methods to fit the transport relation to their dataset.

Figure 2-7 is a plot of the bedload transport relations reviewed in this paper for a wide range of τ^*. It is apparent that all of the relations plot similar in shape and form, but with a vertical shift along the q^* axis. This shift is caused by the fact that each relation was created based on fits of different datasets.

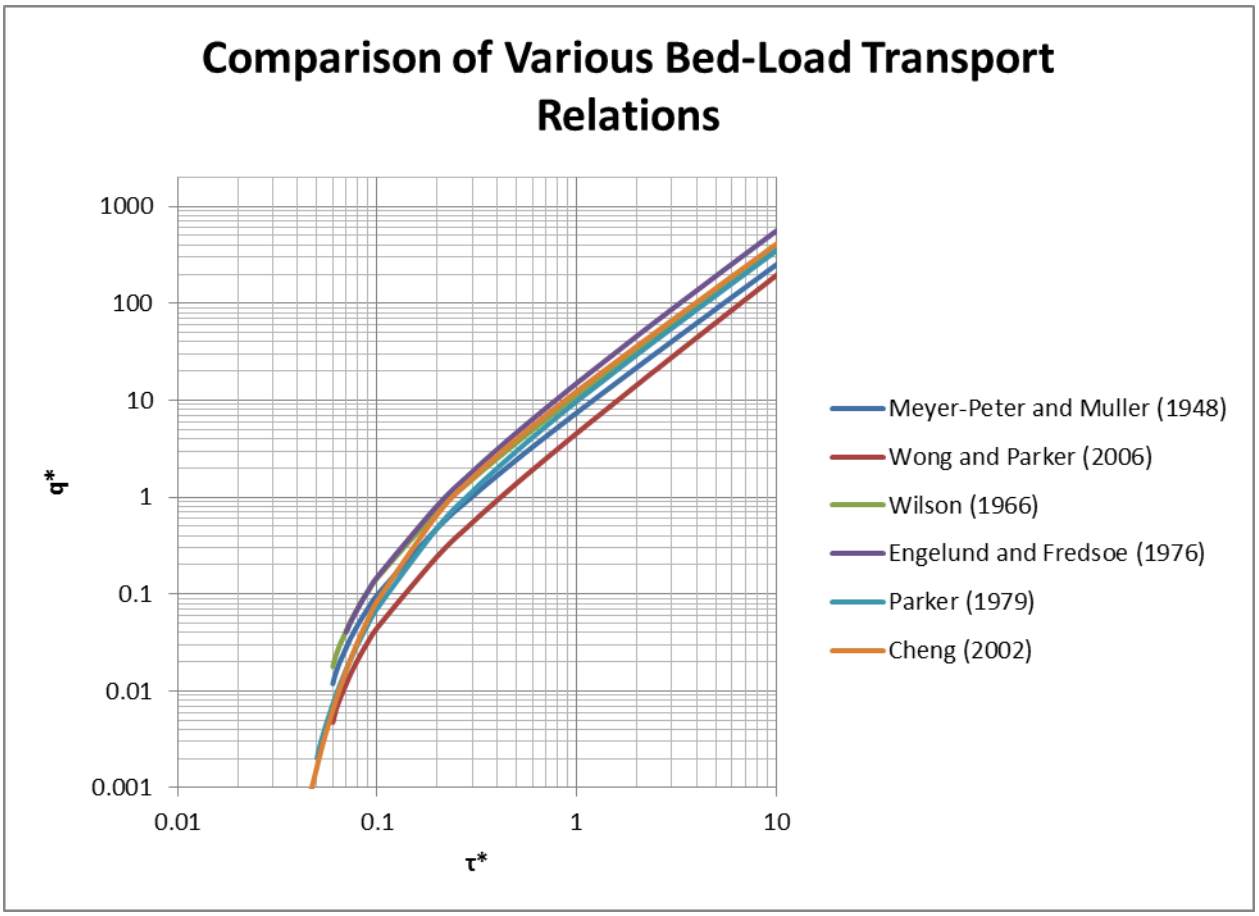

Figure 2-7: Comparison of various bedload transport relations for a wide range of τ^*

In the lower τ^* region of **Figure 2-7**, it is observed that q^* is very sensitive to the value of τ^*. Therefore, slight differences in the fitting of bedload transport relations to different datasets can lead to dramatically different computed values of q^*. This may explain the variation in q^*, since most of the relations were verified based on small τ^* values.

Table 2-1 shows the validated τ^* range of each reviewed bedload transport equation from **Figure 2-7**. **Figure 2-8** is similar to **Figure 2-7**, except that only the verified values of τ^* are plotted for each bedload transport relation. From the plot, it is observed that the relations developed by **Wilson (1966)** and **Cheng (2002)** have verified τ^* ranges that are suitable for the computed τ^* value due to dam-break flows (τ^* on the order of 10). However, it should be noted that the data used to verify these bedload transport relations were from sand-bed rivers rather than gravel-bed rivers. Hence, the validity of these equations in gravel-bed rivers remains

questionable, even though the predicted q^* in **Figure 2-7** falls between the relations of **Engelund and Fredsoe (1976)** and **Meyer-Peter and Muller (1948)**.

Table 2-1: Valid τ^* ranges of reviewed bedload transport equations

Sediment Transport Relation	Valid τ^* Range
Engelund and Fredsoe (1976)	0.04 to 0.3
Meyer-Peter and Muller (1948)	0.073 to 0.18
Wong and Parker (2006)	0.073 to 0.18
Wilson (1966)	0.5 to 10
Cheng (2002)	0.03 to 10
Parker (1979)	0.03 to 0.07

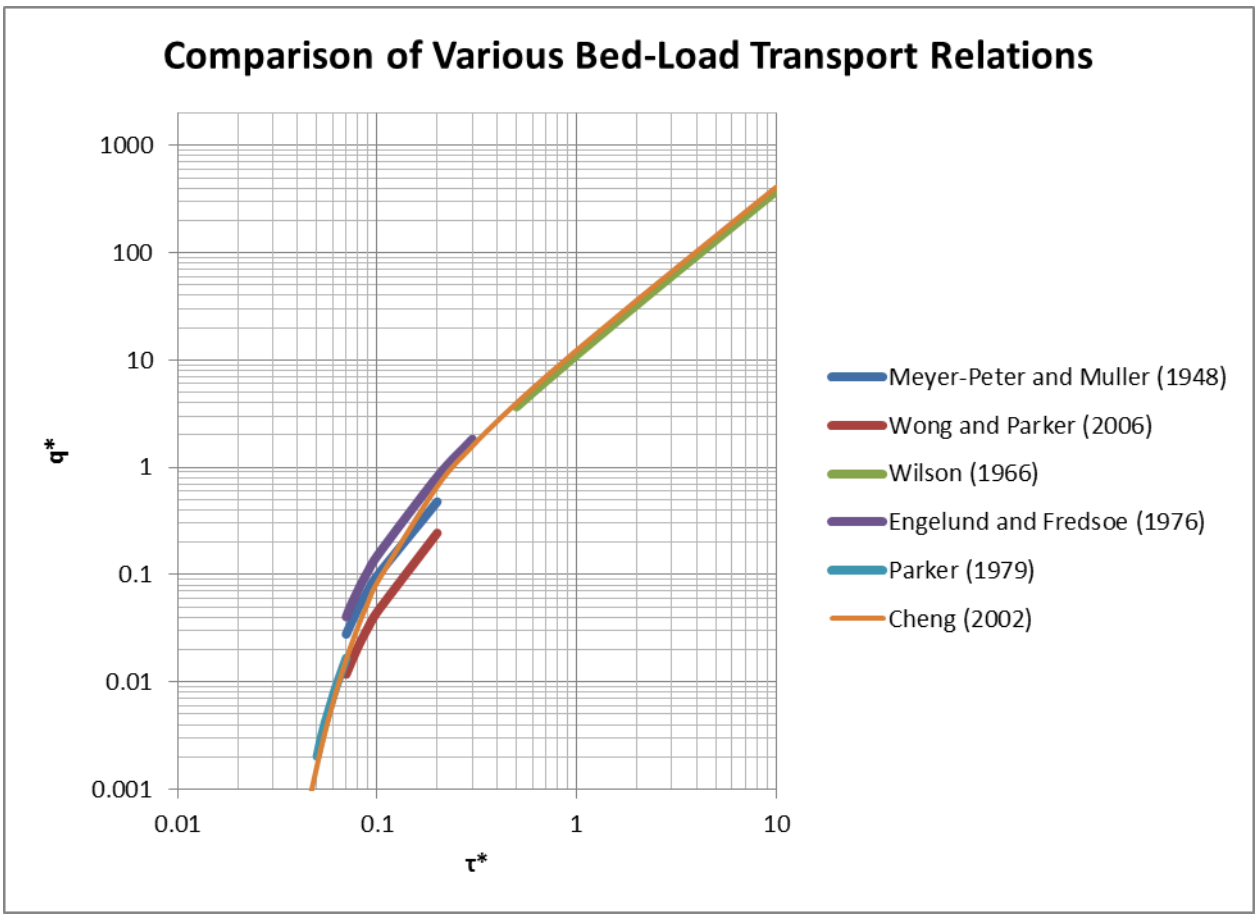

Figure 2-8: Comparison of various bedload transport relations for verified ranges of τ^*

Figure 2-6 shows a range of τ^* where initiation of suspension occurs. However, each of the three suspension criteria have a different definition of what suspension actually is. **Bagnold (1966)**

and **Engelund (1965)** defined suspension as where a particle would remain suspended in the flow due to vertical velocity components of turbulent eddies, while **van Rijn (1984)** defined suspension as when particles jump, or saltate, 100 particle diameters. As such, it is not entirely clear when sediment becomes entrained as suspended-load, and a better definition of the initiation of suspended-load transport is required before attempting to integrate it into a morphological model.

2.2.5 CONCLUSIONS

From the work of **van Rijn (1984)**, since maximum τ_b^* plots beyond all three suspension criteria (**Figure 2-6**) for the case of a catastrophic dam release, it can be concluded that sediments in that particular area of the simulated river will be transported in suspension. As such, none of the relations mentioned above for bedload transport and for grain flows apply. It is recommended that suspended-load transport relations be used in the case of extreme τ^*.

Since a spectrum of τ^* exists during a catastrophic dam release, the sediment transport regimes of bedload and suspended-load must both be considered together. For bedload transport, **Cheng**'s **(2002)** relation was verified for the largest range of τ^*, and hence, ideally, it should be used to estimate bedload transport for all τ^* values.

The problem with the use of **Cheng**'s **(2002)** relation is that, being an average of multiple bedload transport relations, it does not incorporate the feature of τ_c^*. Thus, it would not be possible to vary the critical shear stress at which sediment transport is initiated. It is therefore proposed that, for the mobile-bed dam-break model constructed for this research, a combination **Meyer-Peter and Muller (1948)** and **Wilson (1966)** equation **(Equation 2-7)** be created, whereby each equation would be used for its known range of validity with a logarithmic interpolation bridging the two. This is demonstrated in **Figure 2-9**.

Equation 2-7: Proposed combination sediment transport equation

$$q^* = \begin{cases} 8(\tau^* - \tau_c^*)^{\frac{3}{2}} & \tau^* \leq 0.18 \\ 8(0.18 - \tau_c^*)^{\frac{3}{2}} \left(\frac{\tau^*}{0.18}\right)^{\frac{\log\left(\frac{12(0.5-\tau_c^*)^{\frac{3}{2}}}{8(0.18-\tau_c^*)^{\frac{3}{2}}}\right)}{\log\left(\frac{0.5}{0.18}\right)}} & 0.18 < \tau^* < 0.5 \\ 12(\tau^* - \tau_c^*)^{\frac{3}{2}} & \tau^* \geq 0.5 \end{cases}$$

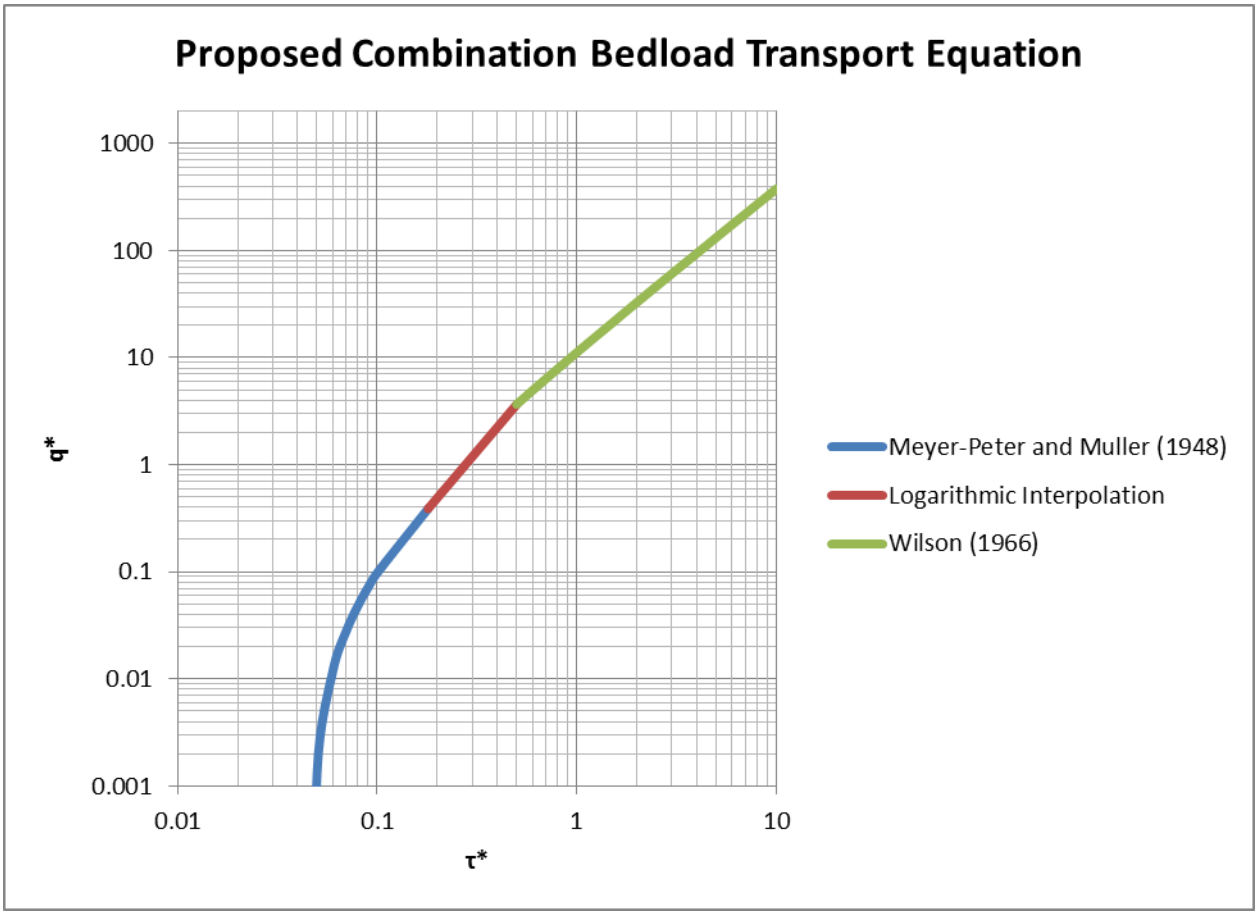

Figure 2-9: Proposed combination bedload transport equation

2.3 FLOOD PLAIN VEGETATION EFFECTS

Simulating a dam-break flood over a mobile-bed requires consideration of the effect of varying levels of vegetation on sediment transport rates. To account for this effect, **Li and Millar (2011)** introduced the concept of partitioning roughness into grain and vegetation components. This leads to a partitioning of ϕ' and τ^*, friction angle and bed shear stress respectively, whereby only the grain component (τ_g^*) of τ^* would contribute to the transport of sediment. This is based on the work of **Meyer-Peter and Muller (1948)** and **Einstein (1950)**, who partitioned shear stress into grain and form components.

The partitioning of τ^* yields two components: τ_g^* and τ_v^*. τ_v^* is the portion of shear stress acting on any vegetation present, while τ_g^* is the remainder of the shear stress acting upon the sediment responsible for inducing sediment transport. The presence of any appreciable amount of vegetation, hence τ_v^*, would lead to a reduced portion of τ_g^* available for sediment transport. This translates to a decrease in q^* as vegetation density increases.

Another effect of vegetation is that its roots can hold and stabilize the soil around it. For sediment with no vegetative root networks, the value of $\phi' = 40°$ (the angle of repose of gravel sediment). As vegetation density increases, so does the stability of the sediment, and hence ϕ' would also increase. To represent this in a model, τ_c^* can be increased through the relation $\tau_c^* = c\ tan\phi'$, where c is a constant that can be determined by setting τ_c^* to τ_c^* of the sediment transport equation being used, and $\phi' = 40°$ represents no vegetation being present.

The concept of partitioning τ^* and varying τ_c^* based on varied levels of vegetation is incorporated into the 2D mobile-bed dam-break model developed.

3 MODELLING METHODOLOGY

3.1 TELEMAC VERSION 6.1

After more than a decade of development, **Hervouet and Petitjean (1999)** used TELEMAC2D to model the Malpasset dam failure of 1959. What was unique about the Malpasset dam-break was the availability of parameters such as flood-wave travel time and high-water marks for validating physical and numerical models. The fixed-bed model that **Hervouet and Petitjean (1999)** created to simulate this dam-break yielded valid results. Yet they did not perform a mobile-bed dam-break analysis even though SISYPHE, a sediment transport module, could be coupled with TELEMAC2D to perform such an analysis. The research in this thesis takes the work of **Hervouet and Petitjean (1999)** one step further and incorporates sediment transport into their Malpasset dam-break model.

TELEMAC2D is a 2D hydrodynamic model that is part of the TELEMAC suite of models developed by Electricité de France (EDF). This suite also contains a 2D sediment transport module that can be coupled with TELEMAC2D. With this tool it would be simple to convert the Malpasset dam-break simulation from a fixed-bed model to a mobile-bed model. Another advantage of the TELEMAC suite of models is that the source code is available and can be modified.

The TELEMAC suite of models was initially built at Electricité de France (EDF) for dimensioning and impact studies. In 2010, TELEMAC became open source after 17 years of commercial distribution in order to improve access by consultants and researchers. The suite of models and a support forum can now be accessed at http://www.opentelemac.org.

The TELEMAC system contains a wide range of models to simulate free surface flows in a variety of conditions. These are listed below:

- TELEMAC2D: 2D hydrodynamics using Saint-Venant equations
- TELEMAC3D: 3D hydrodynamics using Navier-Stokes equations
- ARTEMIS: Hydrodynamics of waves in harbours
- TOMAWAC: Hydrodynamics of costal wave propagation
- SISYPHE: 2D sediment transport of bedload and suspended load

- SEDI-3D 3D sediment transport of suspended load
- ESTEL-2D: 2D groundwater flow
- ESTEL-3D: 3D groundwater flow

All of the models listed above can be run as coupled models. To simulate a dam-break flood over a mobile-bed, TELEMAC2D was coupled with SISYPHE to perform a morphodynamic simulation of a dam-break. TELEMAC2D and SISYPHE would interact at every timestep to update the bed elevation of the flood plain and channel for the next hydrodynamic computation.

The reason behind using these TELEMAC models is that **Hervouet and Petitjean (1999)** have applied TELEMAC2D, with fixed-bed assumptions, to simulate a real-case dam-break flood, the Malpasset dam failure of 1959. TELEMAC is versatile because it is open source and because all computations are coded as separate modules that can be easily modified. Overall, TELEMAC was chosen due to its versatility and because it has been verified as a means of simulating real-case dam-breaks.

3.1.1 TELEMAC2D

3.1.1.1 HYDRODYNAMICS

This is the 2D hydrodynamic model of the TELEMAC suite. This code solves the depth-averaged shallow water Saint-Venant equations that follow **(EDF, 2010)**:

Equation 3-1: Continuity

$$\frac{\partial h}{\partial t} + u \cdot \vec{\nabla}(h) + h\, div(\vec{u}) = S_h$$

Equation 3-2: Momentum along $\boldsymbol{x}$

$$\frac{\partial u}{\partial t} + \vec{u} \cdot \vec{\nabla}(u) = -g\frac{\partial Z}{\partial x} + S_x + \frac{1}{h} div(h\nu_t \vec{\nabla} u)$$

Equation 3-3: Momentum along $\boldsymbol{y}$

$$\frac{\partial v}{\partial t} + \vec{u} \cdot \vec{\nabla}(v) = -g\frac{\partial Z}{\partial y} + S_y + \frac{1}{h} div(h\nu_t \vec{\nabla} v)$$

Where:

- h = depth of water (m)
- u, v = velocity components (m/s)
- g = gravity acceleration (m/s^2)
- ν_t = momentum diffusion coefficient (m^2/s)
- Z = free surface elevation (m)
- t = time (s)
- x, y = horizontal space coordinates (m)
- S_h = source of sink of fluid (m/s)
- S_x, S_y = source or sink terms in dynamic equations (m/s^2)

Turbulent viscosity may be specified or determined by a model through the transport of turbulent quantities k (turbulent kinetic energy) and ε (turbulent dissipation). The equations are as follows:

Equation 3-4: Transport of $\boldsymbol{k}$ and $\boldsymbol{\varepsilon}$ (a)

$$\frac{\partial k}{\partial t} + \vec{u} \cdot \vec{\nabla}(k) = \frac{1}{h} div\left(h \frac{\nu_t}{\sigma_k} \vec{\nabla} k\right) + P - \varepsilon + P_{kv}$$

Equation 3-5: Transport of $\boldsymbol{k}$ and $\boldsymbol{\varepsilon}$ (b)

$$\frac{\partial \varepsilon}{\partial t} + \vec{u} \cdot \vec{\nabla}(\varepsilon) = \frac{1}{h} div\left(h \frac{\nu_t}{\sigma_\varepsilon} \vec{\nabla} \varepsilon\right) + \frac{\varepsilon}{k}(c_{1\varepsilon} P - c_{2\varepsilon} \varepsilon) + P_{\varepsilon v}$$

After completing a computation, TELEMAC2D is able to output h (water depth), u (velocity in the x-direction), and v (velocity in the y-direction) at each node. For a coupled model, this output is then fed into SISYPHE to calculate bed evolution.

3.1.1.2 COMPUTATIONAL OPTIONS IMPLEMENTED

A sample input file for TELEMAC2D is provided in **APPENDIX A**. Refer to **EDF**'s **(2010)** TELEMAC2D manual for a translation and description of the computational options implemented. **APPENDIX C** contains fortran-coded scripts that were modified or created for TELEMAC2D or SISYPHE to enable the simulation of mobile-bed dam-break modelling.

3.1.2 SISYPHE

3.1.2.1 MOBILIZATION OF THE BED

The volume of sediment transported is computed through the Exner equation:

Equation 3-6: Exner Equation

$$(1-n)\frac{\partial Z_f}{\partial t} + div\left(\overrightarrow{Q_b}\right) = 0$$

Where:

- Z_f = bed elevation (m)
- Q_b = bedload transport per unit width (m^2/s)
- n = porosity
- t = time (s)

3.1.2.2 SEDIMENT TRANSPORT EQUATION

Modifications to the sediment transport code were made to implement a combination **Meyer-Peter and Muller (1948)** and **Wilson (1966)** equation and to incorporate the effect of vegetation on the sediment transport rate.

As stated in previous sections, the **Meyer-Peter and Muller (1948)** and **Wilson (1966)** equations have different ranges of τ^* for which τ^* has been validated, $\tau^* = 0.073$ to 0.18 and $\tau^* = 0.5$ to 10 respectively. Thus, this dam-break model implements the **Meyer-Peter and Muller (1948)** equation for $\tau^* \leq 0.18$ and the **Wilson (1966)** equation for $\tau^* \geq 0.5$. For the τ^* range of 0.18 to 0.5, a logarithmic interpolation is used to bridge the two equations. Since the **Meyer-Peter and Muller (1948)** equation is used at the lower bounds of τ^*, it is assumed that $\tau_c^* = 0.047$. The following are the sediment transport equations implemented in the SISYPHE code:

Equation 3-7: Meyer-Peter and Muller (1948) equation

$$q^* = 8(\tau^* - \tau_c^*)^{\frac{3}{2}}$$

Equation 3-8: Logarithmic interpolation between Meyer-Peter and Muller (1948) and Wilson (1966)

$$q^* = 8(0.18 - \tau_c^*)^{\frac{3}{2}} \left(\frac{\tau^*}{0.18}\right)^{\frac{\log\left(\frac{12(0.5-\tau_c^*)^{\frac{3}{2}}}{8(0.18-\tau_c^*)^{\frac{3}{2}}}\right)}{\log\left(\frac{0.5}{0.18}\right)}}$$

Equation 3-9: Wilson (1966) equation

$$q^* = 12(\tau^* - \tau_c^*)^{\frac{3}{2}}$$

To account for the effect of vegetation on the sediment transport rate, τ^* is partitioned into τ_g^* and τ_v^* components, and τ_c^* is adjusted based on ϕ'. The shear stress partitioning is accomplished through **Li and Millar**'s **(2011)** shear stress partitioning equation:

Equation 3-10: Li and Millar's (2011) shear stress partitioning

$$\tau_g^* = \tau^* \frac{n_g}{\left(n_g^2 + n_v^2\right)^{\frac{1}{2}}}$$

Where:

- n_g = Manning's grain roughness
- n_v = Manning's vegetation roughness

Adjustments of τ_c^* are accomplished by assuming that $\tau_c^* = c\ tan\phi'$, where c is a constant, and that sediment with no vegetation influence has $\phi' = 40°$. Since $\tau_c^* = 0.047$ for conditions with no vegetation **(Meyer-Peter and Muller, 1948)**, then $c = 0.056$. τ^* can then be calculated for increasing ϕ', which corresponds to increasing levels of vegetation.

Adjustments to τ_c^* are limited to the top 1 m of the original bed elevation. The assumption was made that vegetation would only affect the top 1 m of sediment, and thus, when this top layer of sediment is eroded away, τ_c^* reverts to a value with no vegetation influence (0.047). Any sediment deposited on top of the original bed elevation is also assumed not to be influenced by vegetation and has a $\tau_c^* = 0.047$.

A similar scheme is used to adjust Manning's roughness. In regions where vegetation is present, $n = \left(n_v^2 + n_g^2\right)^{0.5}$ in only the top 1 m of sediment. After sediment is eroded past the top 1 m from the original bed elevation, or if sediment is deposited on top of the original bed elevation, $n = n_g$.

3.1.2.3 VERTICAL AND SPATIAL VARIATION OF SEDIMENT AND RIGID BOUNDARY

In SISYPHE, it is possible to vertically stratify and spatially vary sediment by specifying up to 10 different sediment layers at each node. Each of these layers can be assigned different d_{50}, n, ϕ', τ_c^*, and thickness. SISYPHE also has a subroutine to define bedrock elevation, or the rigid boundary; however, this may cause simulations to become unstable. As a remedy to these possible instabilities, it was found that defining one sediment layer with $\tau_c^* = \infty$ effectively makes it into a rigid boundary. The solution was implemented for all simulations run for this research.

3.1.2.4 COMPUTATIONAL OPTIONS IMPLEMENTED

A sample input file for TELEMAC2D is provided in **APPENDIX B**. Refer to **EDF**'s **(2010)** SISYPHE manual for a translation and description of the computational options implemented. **APPENDIX C** contains fortran-coded scripts that were modified or created for TELEMAC2D or SISYPHE to enable the simulation of mobile-bed dam-break modelling.

3.2 MODEL VALIDATION

To verify that TELEMAC2D outputs reasonable hydrodynamic results and that TELEMAC2D coupled with SISYPHE outputs reasonable morphodynamic results for the case of sudden dam-breaks, a series of models were created to simulate experiments run by **Soares-Frazao and Zech (2002)**, **Vasquez and Leal (2006)**, and **Vasquez (2005)**.

3.2.1 SOARES-FRAZAO AND ZECH (2002)

Soares-Frazao and Zech (2002) conducted a laboratory experiment to simulate how water would flow along a sharp 90° bend during a sudden dam-break style release from an upstream reservoir. This set-up consisted of a rectangular reservoir filled with water that was suddenly

released into a plastic channel containing a sharp 90° bend. **Figure 3-1** shows a schematic of the experimental set-up. Velocity of the fluid particles was measured using the Voronoi digital imaging technique, and water level measurements were taken at various times over the course of the experiment. This experimental data was used to validate a 2D hydrodynamic model that **Soares-Frazao and Zech (2002)** had created.

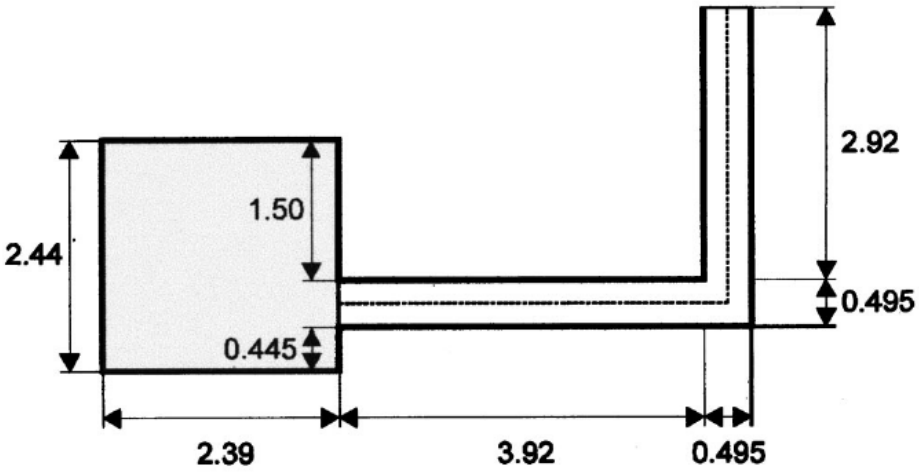

Fig. 3. Channel with 90° bend—Plane view (dimensions in m)

Figure 3-1: Soares-Frazao and Zech's (2002) experimental set-up (© ASCE, 2002, by permission)

To verify the TELEMAC2D's hydrodynamic outputs, a model with **Soares-Frazao and Zech**'s **(2002)** specifications was created. A graphical comparison of the simulated water level was made in **Figure 3-2** at $t = 3, 5, 7$ and 14 s between **Soares-Frazao and Zech**'s **(2002)** model and the TELEMAC2D model, which showed that both were in relatively good agreement.

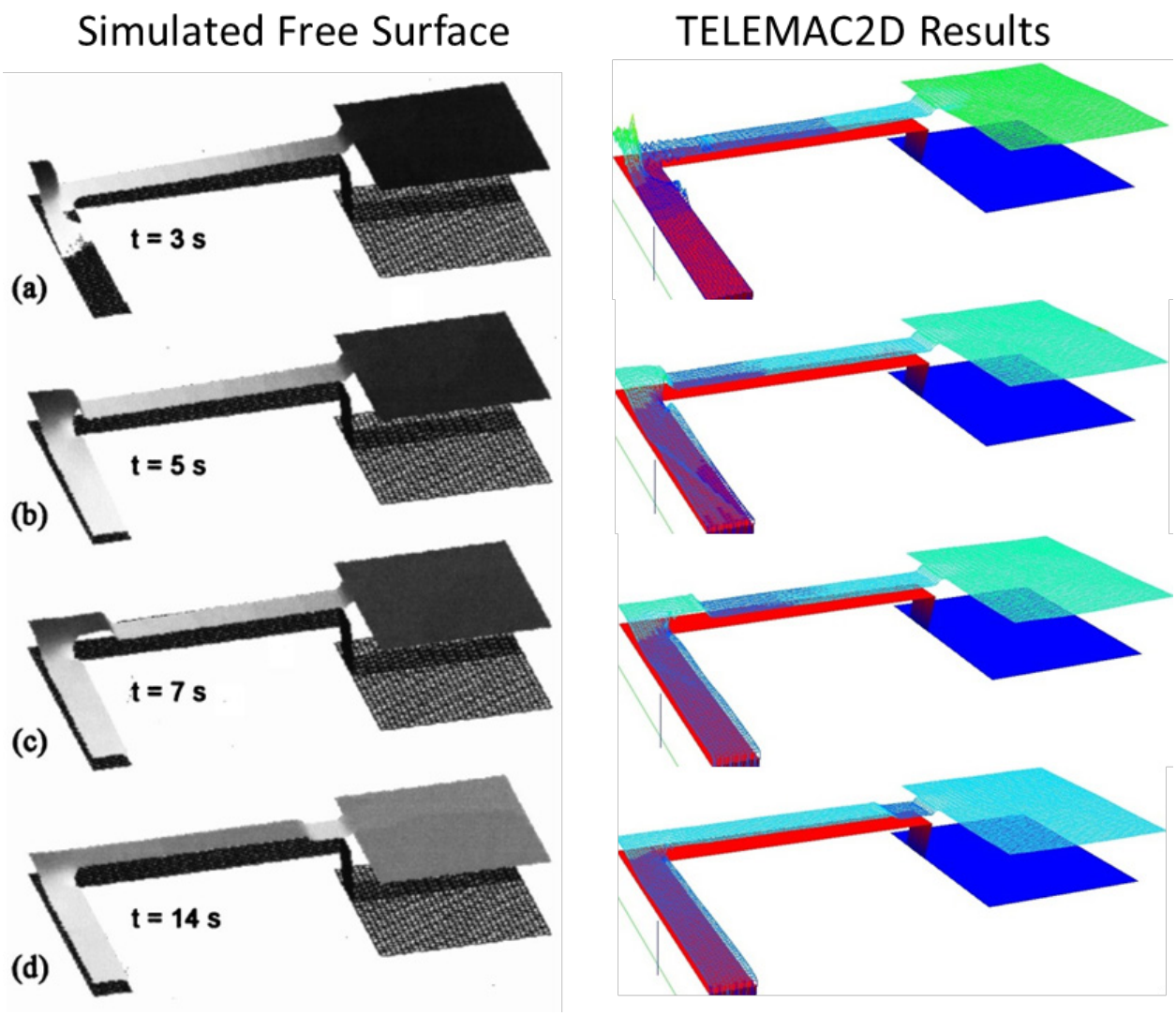

Figure 3-2: Graphical comparison of water levels between Soares-Frazao and Zech's (2002) model and TELEMAC2D output. The left part shows Soares-Frazao and Zech's (2002) simulated water levels, and the right part shows TELEMAC2D simulated water levels. (left part © ASCE, 2002, by permission)

A graphical comparison of the velocity field of the bend at $t = 7\ s$ was then made between the model output from the **Soares-Frazao and Zech (2002)** and the TELEMAC2D models as shown in **Figure 3-3**, and between the measured experimental results and TELEMAC2D model output as shown in **Figure 3-4**. It is apparent that both models are in reasonable agreement with the experimental results. Therefore, it is verified that TELEMAC2D outputs reasonable hydrodynamic results in this situation.

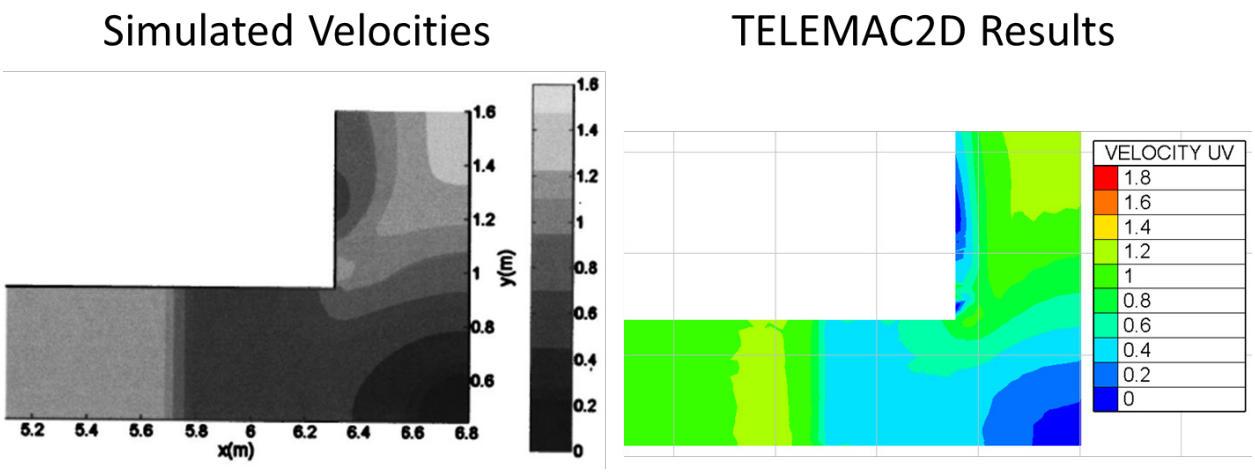

Figure 3-3: Graphical comparison of velocity field between Soares-Frazao and Zech's (2002) model and TELEMAC2D output (left part © ASCE, 2002, by permission)

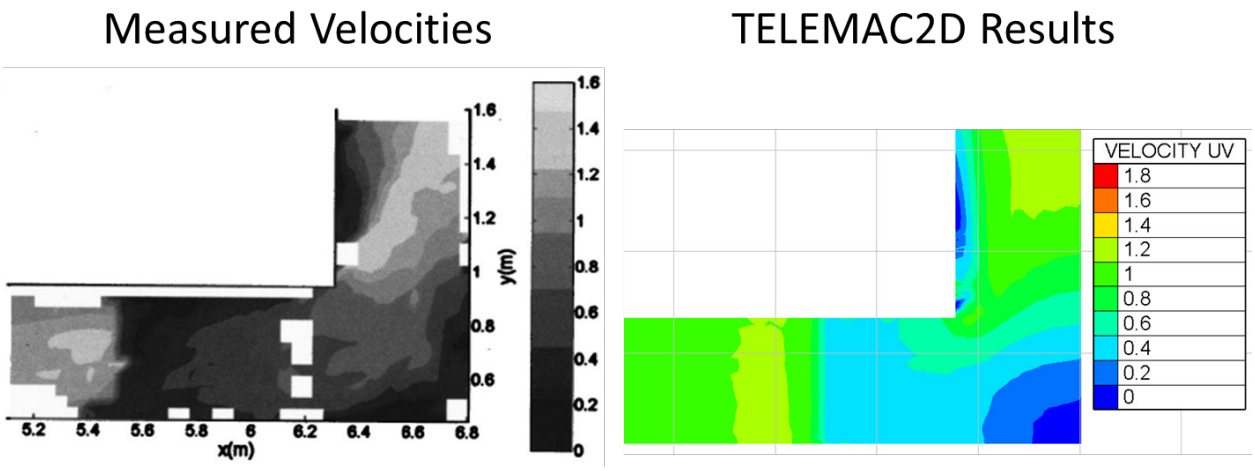

Figure 3-4: Graphical comparison of velocity field between Soares-Frazao and Zech's (2002) experimental results and TELEMAC2D output (left part © ASCE, 2002, by permission)

3.2.2 VASQUEZ AND LEAL (2006)

Leal et al. (2002) performed dam-break experiments in a rectangular flume that contained a stepped sediment-filled bed and a lift-gate in the middle. **Figure 3-5** shows the initial conditions of the experiment. **Vasquez and Leal (2006)** used the results from two sets of initial conditions, detailed in **Table 3-1**, to compare with the output of River2D.

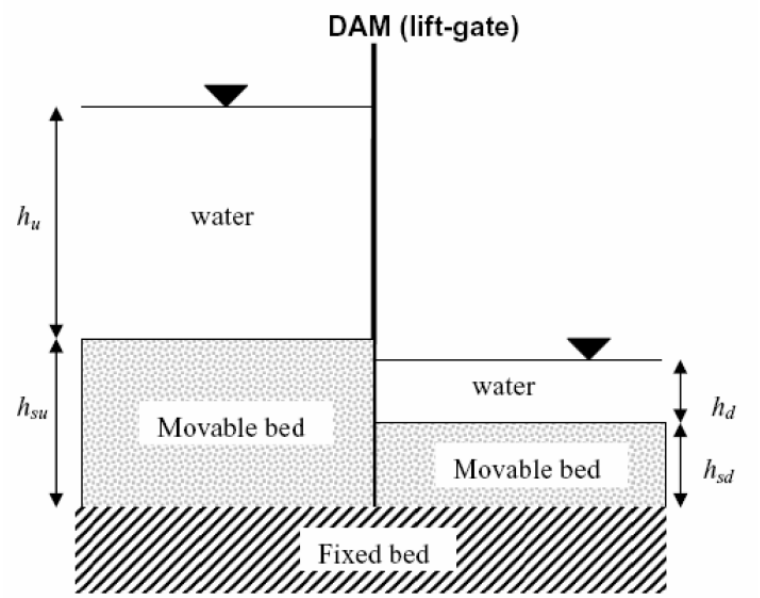

Figure 5. Initial conditions of Leal at al. (2002) experiments of dam-break over movable beds.

Figure 3-5: Initial conditions of Leal et al.'s (2002) experiments (Vasquez and Leal, 2006; © Jose Vasquez, 2006, by permission)

Table 3-1: Initial conditions of Leal et al.'s (2002) experiments

Test	$\boldsymbol{h_u}$ (m)	$\boldsymbol{h_d}$ (m)	$\boldsymbol{h_{su}}$ (m)	$\boldsymbol{h_{sd}}$ (m)
Ts.25	0.400	0.000	0.190	0.071
Ts.28	0.400	0.075	0.190	0.071

With the same initial conditions and model parameters as **Leal et al.**'s **(2002)** experimental set-up, the two tests were run in TELEMAC2D coupled with SISYPHE. Water surface elevations and bed elevations are compared at $t = 1$ and 4 s in **Figure 3-6** and **Figure 3-7**. The TELEMAC results appear to be in relatively good agreement with River2D and the experimental results. Thus, it is verified that a mobile-bed dam-break simulation in TELEMAC2D coupled with SISYPHE produces realistic and valid morphodynamic results.

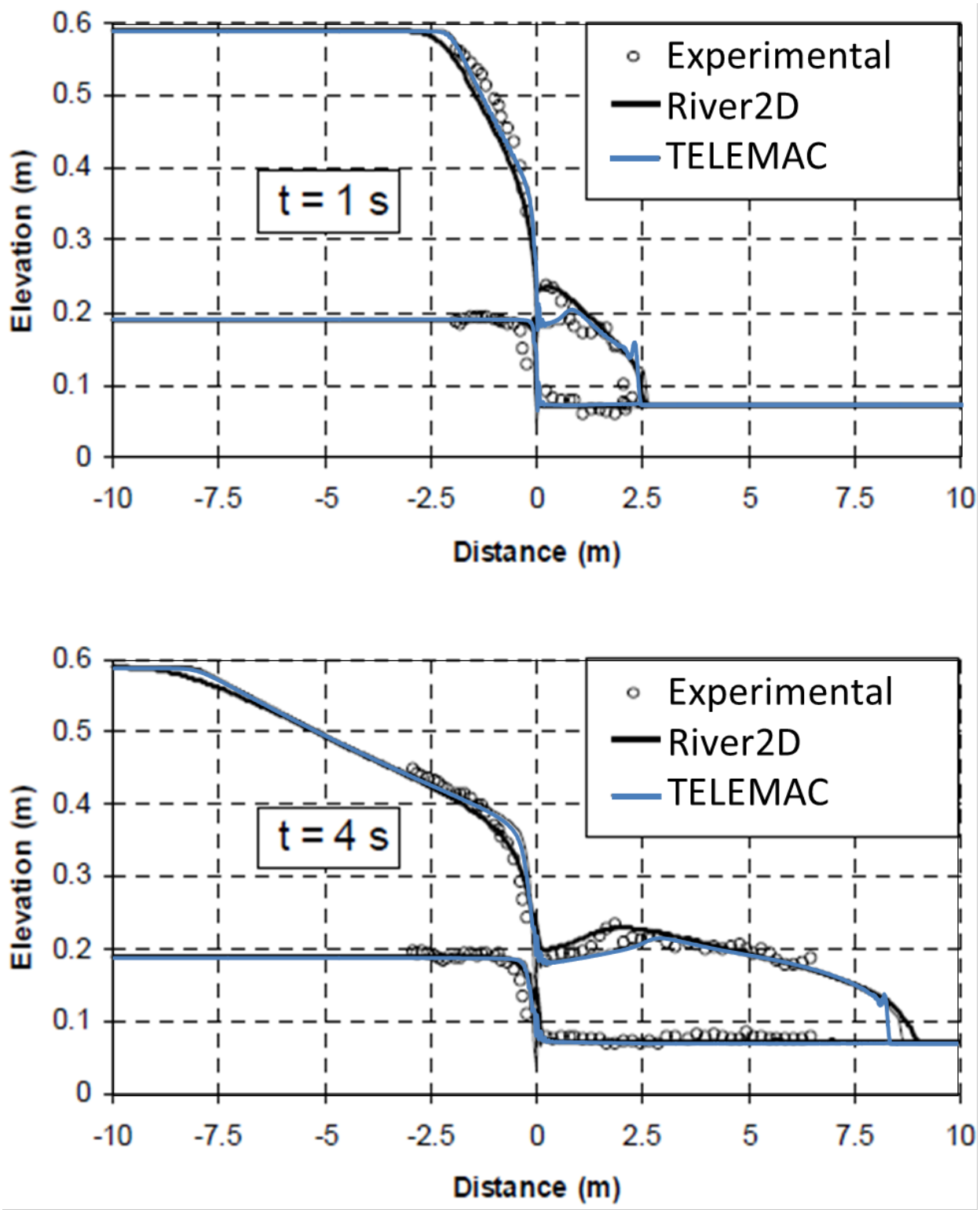

Figure 3-6: Experimental and simulated results for experiment Ts.25 (© Jose Vasquez, 2006, adapted by permission)

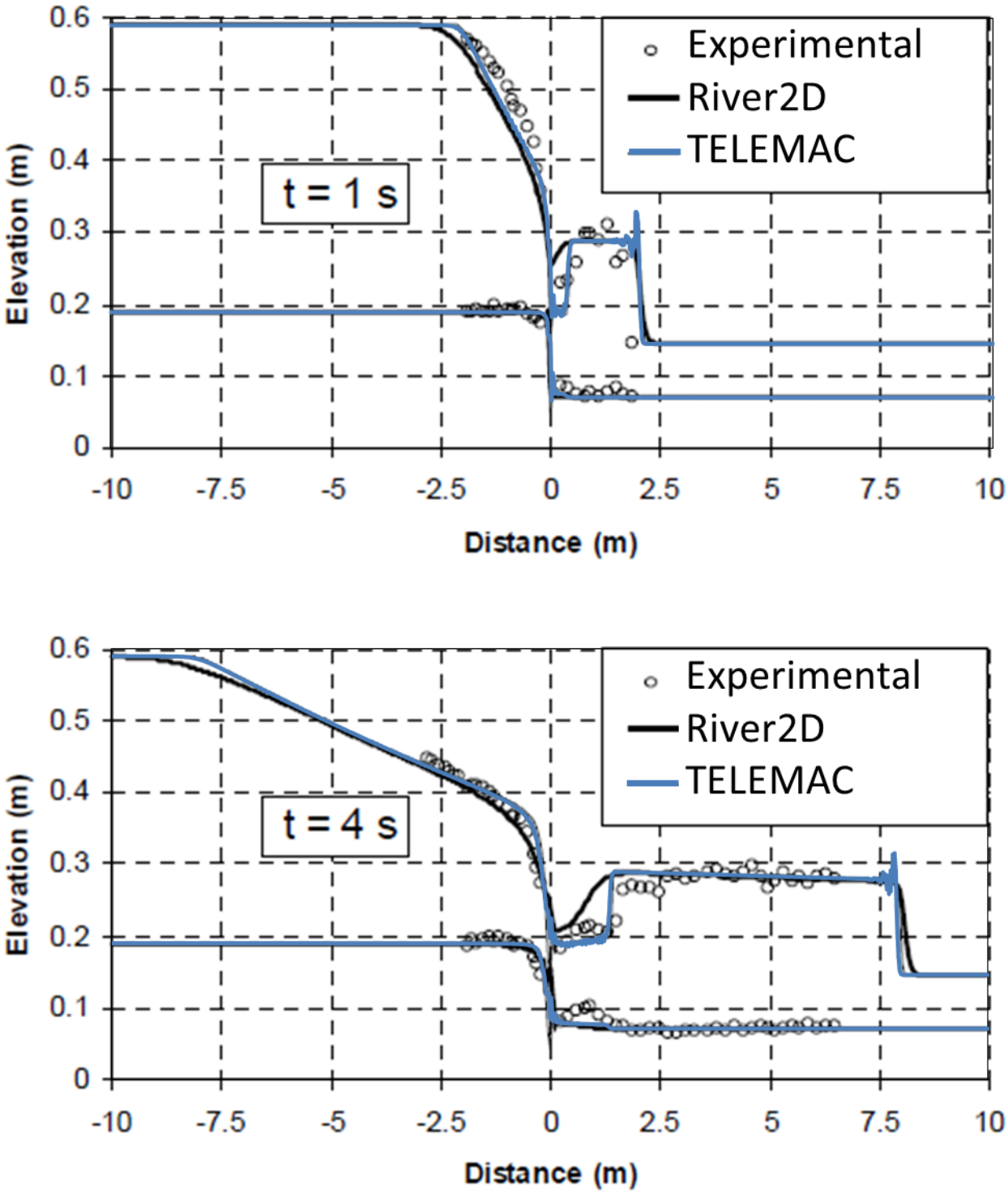

Figure 3-7: Experimental and simulated results for experiment Ts.28 (© Jose Vasquez, 2006, adapted by permission)

3.2.3 VASQUEZ (2005)

Accounting for secondary flows in morphodynamic simulations would yield significantly different bed topography where a channel meanders or bends. A subroutine exists in SISYPHE to account for such secondary flow effects. This subroutine was validated by simulating the Laboratory of Fluid Mechanics (LFM) experiment consisting of a long flume that has a 180° bend as shown in **Figure 3-8**.

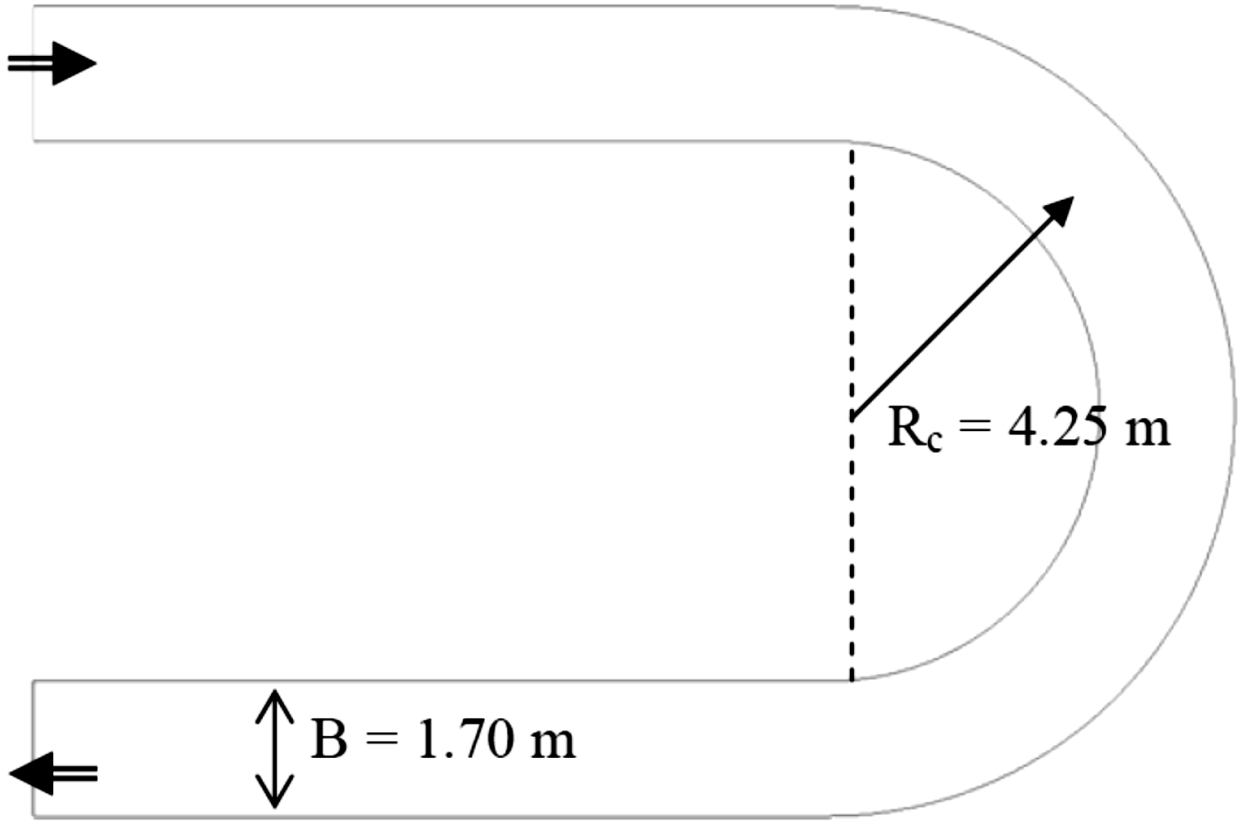

Figure 3-8: LFM secondary flow experiment (© Jose Vasquez, 2005, by permission)

A TELEMAC2D coupled with SISYPHE steady-state simulation was run to examine morphodynamics accounting for secondary flow effects. The parameters used in the numerical experiment were $Q = 170\ L/s$, $h = 20\ cm$, $S = 0.18\ \%$, $D_{50} = 0.78\ mm$, and $k = 0.083$. A comparison of modelled and experimental results, shown in **Figure 3-9**, suggests that the secondary flow correction built into SISYPHE does not fully capture the effect on morphology. However, it is not expected that morphodynamic evolution of the bed as a result of secondary

flow effects would dominate in the case of sudden dam-breaks. Therefore, the secondary flow correction in SISYPHE is considered adequate for the purposes of creating a 2D mobile-bed dam-break model.

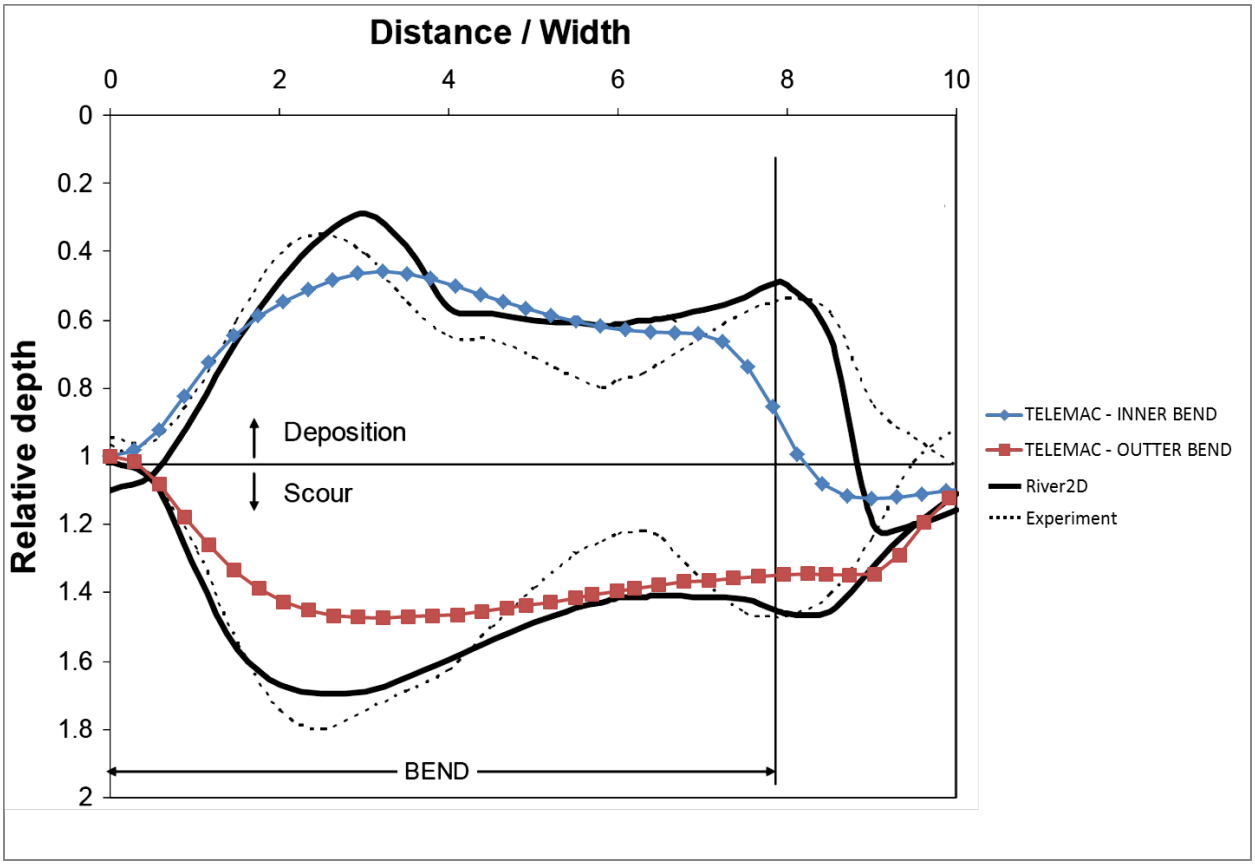

Figure 3-9: Comparison of model outputs and experimental results of secondary flow effects on LFM flume experiment for left and right banks (© Jose Vasquez, 2005, adapted by permission)

4 CASE STUDY: INPUT DATA AND MODELLING ASSUMPTIONS

4.1 STUDY SITE: MALPASSET DAM, FRANCE

4.1.1 BACKGROUND

The Malpasset dam failed explosively at 9:14 p.m. on December 2, 1959. This dam, built for irrigation and water storage, was located in a narrow gorge of the Reyran River approximately 12 km upstream of Frejus, France. It was a double-curvature arch dam with a maximum height of 66.5 m and a crest length of 223 m. The reservoir could store a maximum of 55 x 10^6 m^3 **(Hervouet, 2000; Hervouet and Petitjean, 1999)**.

In the days preceding November 30, 1959, the reservoir had been filling slowly, but, due to exceptionally heavy rains, the last 4 m were filled in three days. In response, the dam operators opened the bottom outlet gate at 6 p.m. on December 2 to prevent the dam from overtopping. Although this strategy was correct, the dam still failed following a violent trembling of the ground and a brief rumble. A massive flood-wave surged from the gorge and overran inhabited areas near Frejus. The Malpasset disaster caused 433 casualties **(Hervouet, 2000; Hervouet and Petitjean, 1999)**.

Engineering investigations after the accident showed that the reasons for the Malpasset dam failing were the pore pressure in the rock, the nature of the rock, and a geotechnical fault downstream of the dam. As the water level in the reservoir increased, the increased load caused the arch to separate from its foundation and rotate about its upper right end. Parts of the dam collapsed as this occurred **(Hervouet, 2000; Hervouet and Petitjean, 1999)**.

This disaster is an example of a catastrophic-type dam-break with a nearly instantaneous breach. As far as modelling considerations are concerned, this would be the worst-case scenario to model for dam-break analyses, yielding maximum high-water marks and maximum scouring of the channel bed and flood plain.

This disaster also supports the notion that it might be unreasonable to model dam-breaks with the fixed-bed assumption. The dam-break flood-wave eroded into the flood plain alluvium, and a wide, poorly defined channel developed, thus altering the morphology of the lower slopes and

bottom of the Reyran Valley. Post-dam-break investigators that visited the Reyran Valley witnessed undercut bridge abutments and pieces of the dam deposited far downstream, further exemplifying the morphologic changes that had occurred **(Hervouet, 2000; Hervouet and Petitjean, 1999)**.

Because the Malpasset dam-break was an example of a sudden and catastrophic dam-break, and because there was clear evidence that extreme sediment transport processes were involved, this presents a well-documented case study to test the use of a 2D mobile-bed dam-break model.

4.1.2 MALPASSET DAM-BREAK MODEL

To test the capabilities of the TELEMAC2D hydrodynamic model, **Hervouet and Petitjean (1999)** modelled the Malpasset dam-break with a fixed-bed simulation. It utilized the pre-event topography in generating the rather high-resolution bottom-elevation mesh, with mesh sizes ranging from $2\ m$ to $150\ m$, 53081 nodes, and 104000 elements (**Figure 4-1**). To simulate the sudden dam-break, the water level in the reservoir was initialized to an elevation yielding a $55\ m$ high wall of water at the location of the dam. This wall of water was instantaneously released into the valley when the simulation started. Calibration of the fixed-bed model indicated that setting a Manning's $n = 0.033$ across the entire domain would be appropriate to sufficiently match multiple recorded high-water marks and transit times between two transformers. This model is now available to the public at www.opentelemac.org in the TELEMAC validation cases package.

Using the **Hervouet and Petitjean (1999)** TELEMAC2D model as a base fixed-bed model, the SISYPHE module, subsequent subroutines and simulation options **(section 3.1)** were appended to create a new mobile-bed model of the Malpasset dam-break. It would have been ideal to be able to calibrate this new mobile-bed model of the Malpasset dam-break, but post-dam-break topographical data was not available as no post-dam-break survey had been performed. Thus, it was decided that a sensitivity analysis be run to examine differences in inundation and flood-wave characteristics (such as propagation time and maximum wave-heights).

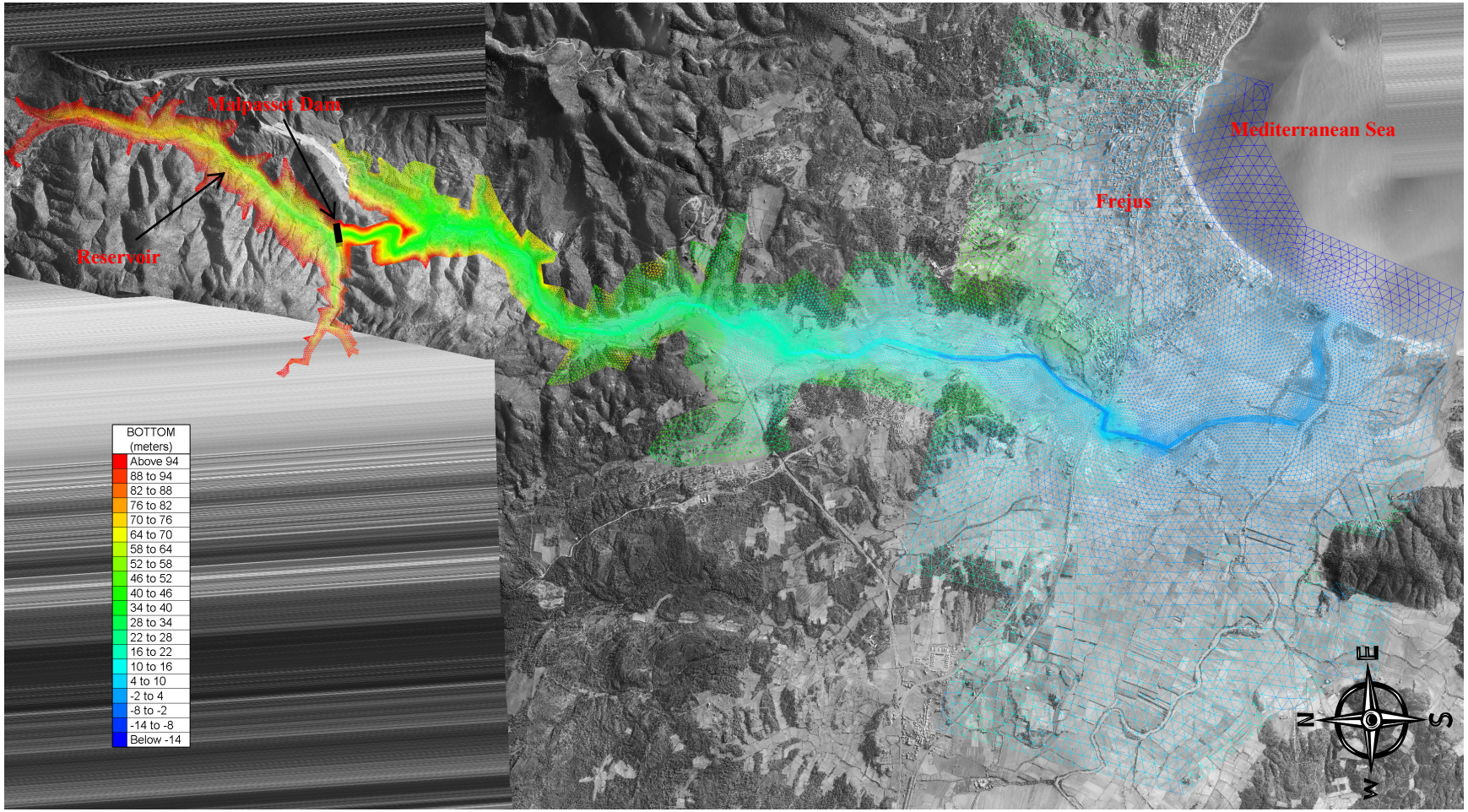

Figure 4-1: Malpasset dam-break model topography mesh (aerial photograph of Frejus [FR 177-150, #1 to #104] in 1959 © IGN, 2012, by permission)

4.2 SENSITIVITY ANALYSIS PARAMETERS

After an extensive literature search and consultations with both Institut Géographique National (IGN) and Bureau de Recherches Géologiques et Minières (BRGM), very little to no information about grain sizes and alluvium thicknesses (depth to bedrock) could be found. As a result, these parameters, coupled with the parameters of grain roughness, vegetation roughness, and friction angle, were varied in a sensitivity analysis to examine differences in inundation and flood-wave characteristics for both the mobile-bed and fixed-bed simulations.

4.2.1 MEAN GRAIN SIZE (d_{50})

Table 4-1 lists the mean grain sizes that were considered reasonable ranges for the Reyran River and its flood plain.

Table 4-1: Sensitivity parameter - mean grain sizes

Aggregate Class	d_{50} (mm)
Coarse Sand	1
Fine Gravel	5
Medium Gravel	10
Coarse Gravel	20
Very Coarse Gravel	40

4.2.2 DEPTH TO BEDROCK (d_b)

Table 4-2 lists the alluvium thicknesses (depths to bedrock) that were assumed throughout the whole domain for each sensitivity iteration.

Table 4-2: Sensitivity parameter - depth to bedrock

d_b (m)
0
2
5
10
15

4.2.3 GRAIN ROUGHNESS (n_g)

Table 4-3 lists the grain roughnesses in the form of Manning's n, which encompasses the fixed-bed calibrated roughness of $n_g = 0.033$. This will ensure that a somewhat realistic result is produced even with the influence of mobile-bed processes.

Table 4-3: Sensitivity parameter - grain roughness

n_g
0.025
0.030
0.035

4.2.4 VEGETATION ROUGHNESS (n_v) AND FRICTION ANGLE (ϕ')

Table 4-4 lists the vegetation roughness and friction angle combinations that range from no vegetation to heavy vegetation. This allows the examination of vegetation influences on sediment transport. Total roughness was computed using $n = \left(n_g^2 + n_v^2\right)^{0.5}$, which allows for the shear stress partitioning where $\tau^* = \tau_g^* + \tau_v^*$.

Table 4-4: Sensitivity parameter - vegetation density

Vegetation Density	n_v	ϕ'
None	0.000	40
Light	0.033	49
Medium	0.067	60
Heavy	0.090	70

4.2.4.1 DELINEATION OF VEGETATED AND URBANIZED ZONES

Vegetated zones were delineated from 1959 IGN aerial photographs of the Frejus area. A similar exercise was completed for urbanized areas. To avoid the complexity of determining calibrated roughnesses and friction angles for buildings and urban infrastructure, it was decided that urbanized areas would be treated as vegetated zones. To simplify this further, vegetated and urbanized zones would be assigned a uniform global n_v and ϕ' for each simulated sensitivity iteration. **Figure 4-2** shows the delineated vegetated and urbanized regions in red. As noted in

Section 3.1.2.2, the vegetation effects are limited to the top 1 m of sediment. After the top 1 m of sediment has been eroded away, the roughness and friction angle revert to the base values of n_g of the specific scenario and 40°, respectively.

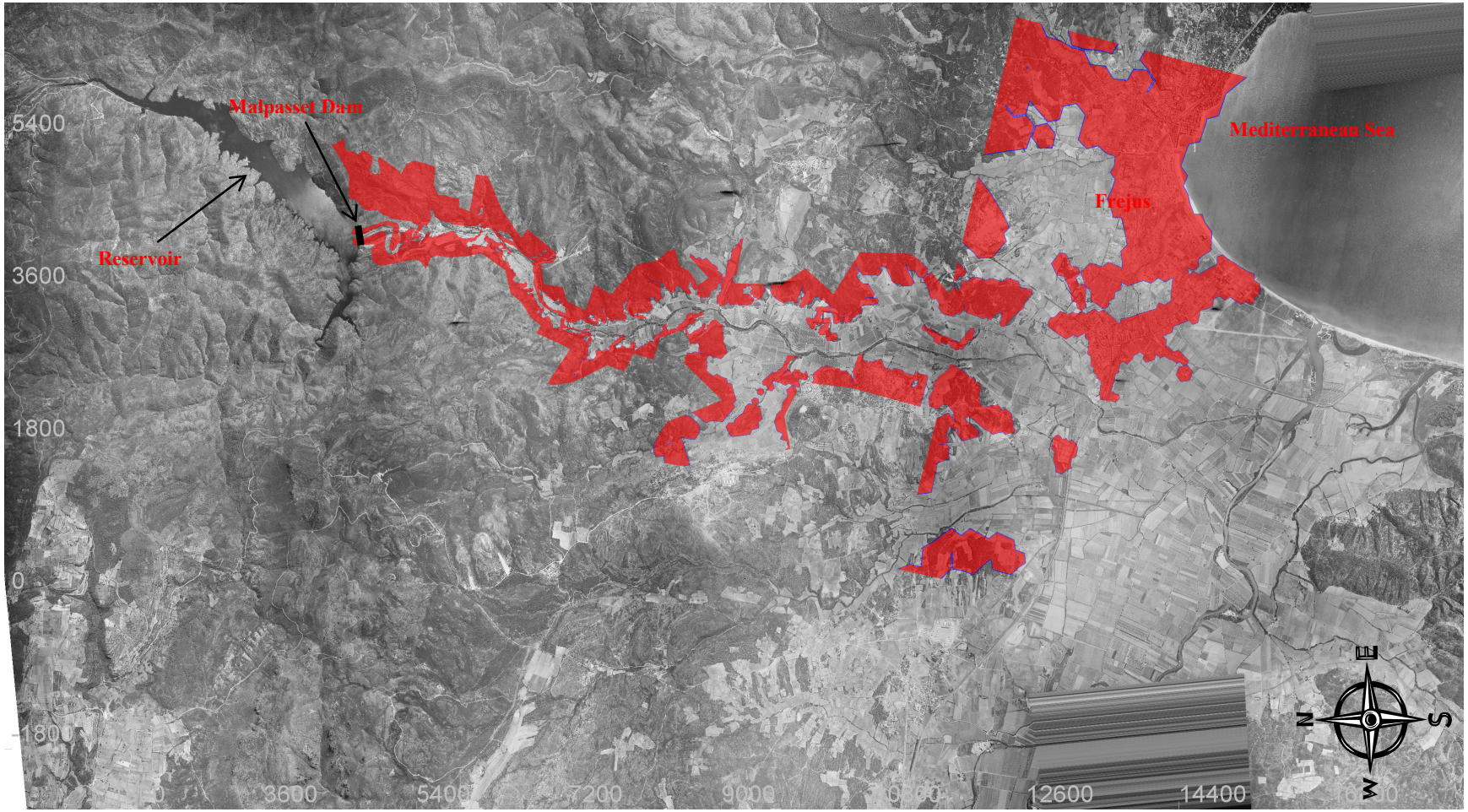

Figure 4-2: Vegetated and urbanized zones (aerial photograph of Frejus [3544-3644, #41 to #121] in 1955 © IGN, 2012, by permission)

5 RESULTS AND ANALYSIS

The flood plain inundation is examined using two approaches. The first is the high-water mark left by the propagation of the dam-break flood-wave towards the Mediterranean Sea; this is output by the transient simulations. The second is the extent of inundation during a mean annual flood event in the Reyran River, arbitrarily assumed to be $100\ m^3/s$ due to a lack of available hydrological data; this is output by the steady-state simulations. The steady-state simulations were run for a limited number of scenarios with varying degrees of vegetation as a proof-of-concept trial. The two methods combined paint a clear picture of how varying each of the sensitivity parameters would affect inundation.

The main method of examining flood-wave characteristics is by measuring the travel time for the flood-wave to reach the Mediterranean Sea and the distance the flood-wave has propagated at a certain time (30 minutes in this case). There is no need to examine maximum wave-height as this is accounted for by examining the HWMs left by the propagating dam-break flood-wave.

The change in morphology is quantified by comparing initial and final bed elevations at a sample of cross-sections and by looking at 2D plots of bed evolution for different simulations. This will help quantify morphological change due to the variation of sensitivity parameters. **Figure 5-1** shows the location of seven cross-sections where HWMs and final bed elevations will be compared. **Figure 5-2** shows the location of the 2D plots of bed evolution.

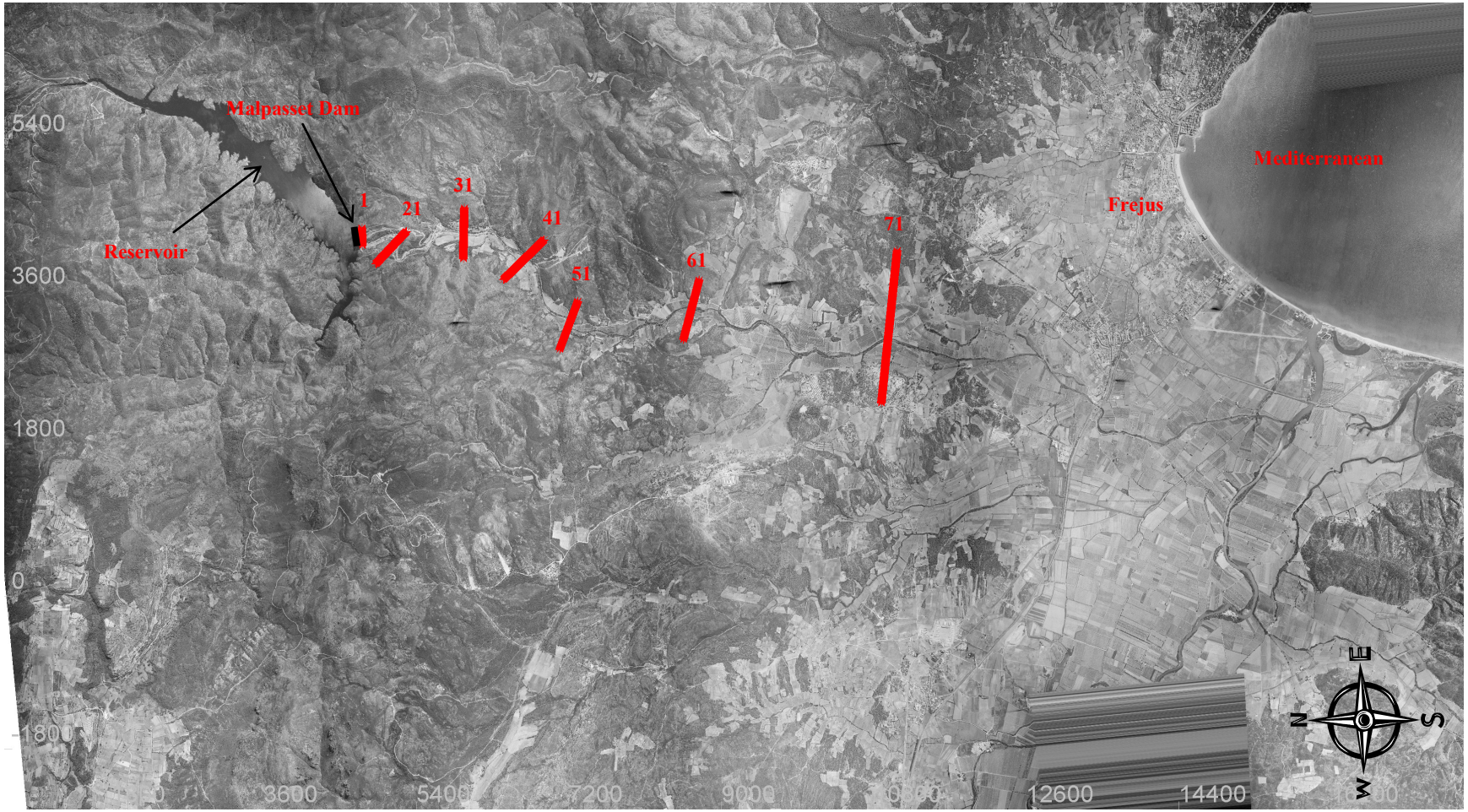

Figure 5-1: Cross-sections (aerial photograph of Frejus [3544-3644, #41 to #121] in 1955 © IGN, 2012, by permission)

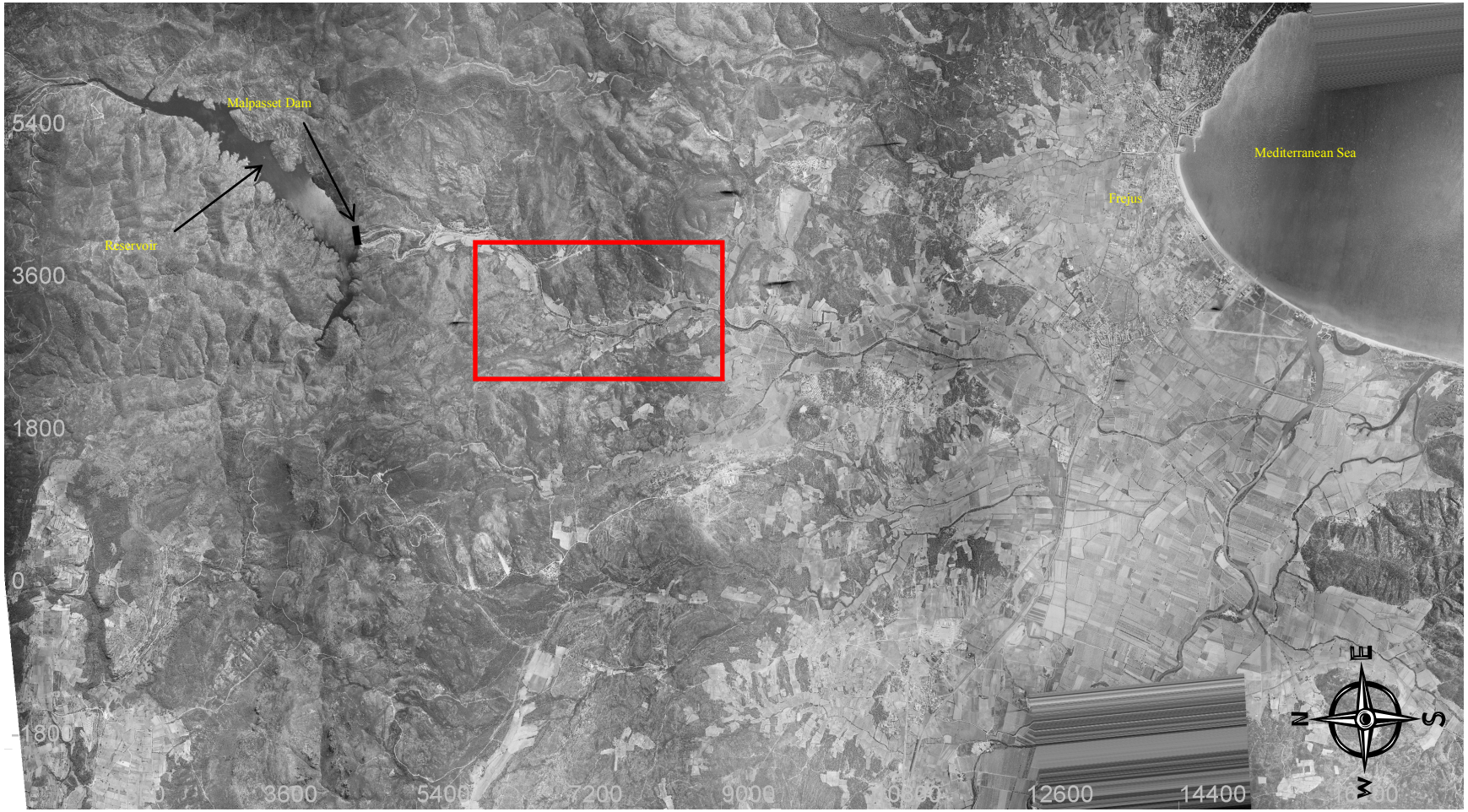

Figure 5-2: Location of 2D bed elevation plot of evolution (aerial photograph of Frejus [3544-3644, #41 to #121] in 1955 © IGN, 2012, by permission)

5.1 EFFECT OF VARYING GRAIN ROUGHNESS

The grain roughness (n_g) was varied with the values in **Table 4-3** for both mobile-bed and fixed-bed simulations. HWM and bed change were compared at the seven cross-sections **(Figure 5-1)** for both simulation types, and the 2D bed evolution at the location in **Figure 5-2** was examined for only the mobile-bed cases. Flood-wave propagation times were then compared for both the mobile-bed and fixed-bed simulations.

Only one set of results is presented for the comparison of cross-sections and 2D plots of bed evolution, but similar results are replicated when comparing scenarios with differing levels of vegetation and d_{50}. A full set of results is presented for flood-wave propagation time, as the number of plots is more manageable.

5.1.1 CROSS-SECTIONS OF HIGH-WATER MARKS AND BED CHANGE

The set of fixed-bed simulations used constant values of the following parameters: $n_v = 0.000$, and $t = 2\ hours$. To test the effect of grain roughness on high water levels, the value of n_g is varied among the three values of 0.025, 0.030, and 0.035. All of the cross-sections also display the original bed elevation (before dam-break) as a basis for comparison.

Results demonstrate that varying n_g does have a significant effect on the HWM for fixed-bed simulations. As n_g increases, the HWM **(Figure 5-3, Figure 5-5, Figure 5-7, Figure 5-9, Figure 5-11, Figure 5-13, Figure 5-15)** decreases in cross-sections 1 and 2 and in parts of 3, 4, 5, and 6, and increases in cross-section 7 and in parts of 3, 4, 5, and 6. The largest HWM difference was found to be a decrease of $5.4\ m$ when n_g increased from 0.025 to 0.035 in cross-section 2.

The set of mobile-bed simulations used constant values of the following parameters: $n_v = 0.000$, $\phi' = 40°$, $d_{50} = 1\ mm$, $d_b = 2\ m$, and $t = 2\ hours$. To test the effect of grain roughness on high water levels, the value of n_g is varied among the three values of 0.025, 0.030, and 0.035. All of the cross-sections also display the original bed elevation (before dam-break) as a basis for comparison.

Results demonstrate that varying n_g does have a significant effect on the HWM for mobile-bed simulations. As n_g increases, the HWM (**Figure 5-4, Figure 5-6, Figure 5-8, Figure 5-10, Figure 5-12, Figure 5-14, Figure 5-16**) decreases in cross-section 1 and in parts of 2, 3, 4, 5, and 6, and increases in cross-section 7 and in parts of 2, 3, 4, 5, and 6. The largest HWM difference was found to be a decrease of 5.5 m when n_g increased from 0.025 to 0.035 in cross-section 2. The effect of n_g on bed elevation is not discernible using this method of comparing cross-sections.

The maximum change in HWM and bed elevation when comparing fixed-bed and mobile-bed simulations with the same n_g was found to be 3.1 m and 78.9 m, respectively. Comparing the fixed-bed and mobile-bed HWM for each cross-section (**Figure 5-3 to Figure 5-16**) shows that the high water levels are relatively unaffected whether the dam-break is simulated with a fixed- or mobile-bed.

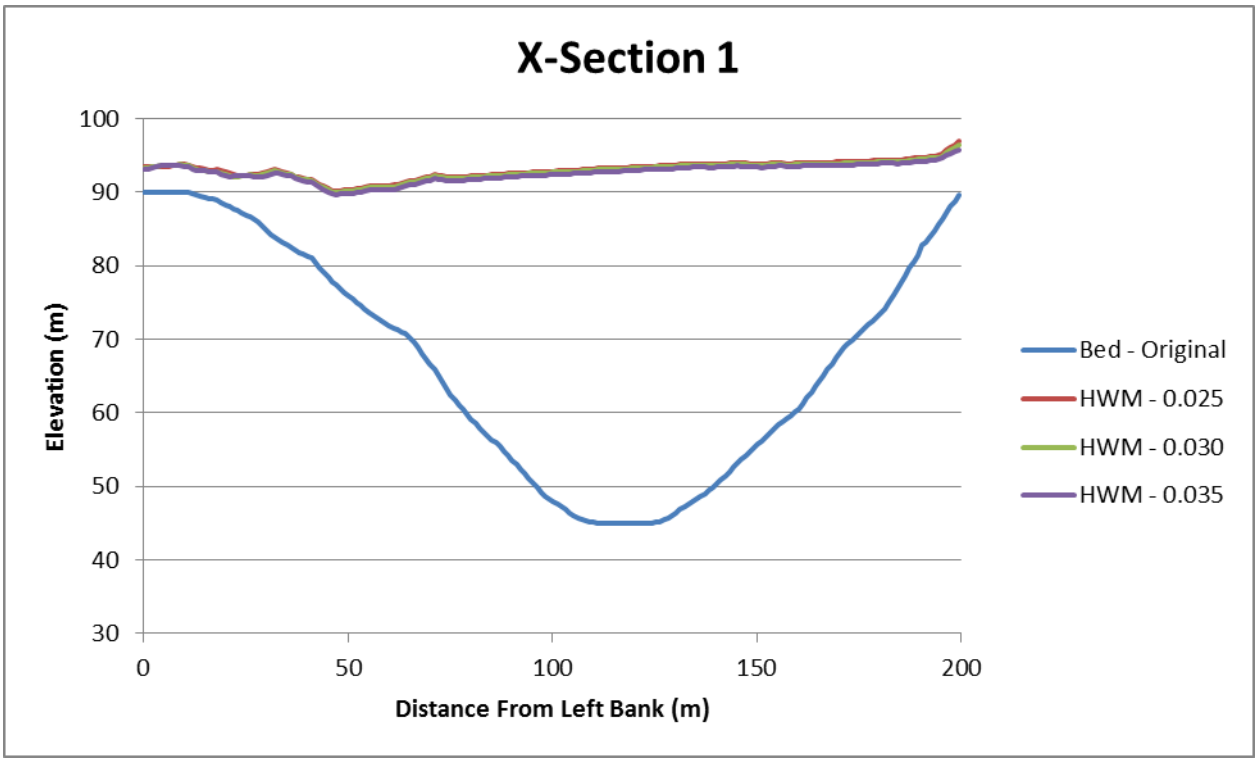

Figure 5-3: HWM at cross-section 1 varying n_g on a fixed-bed

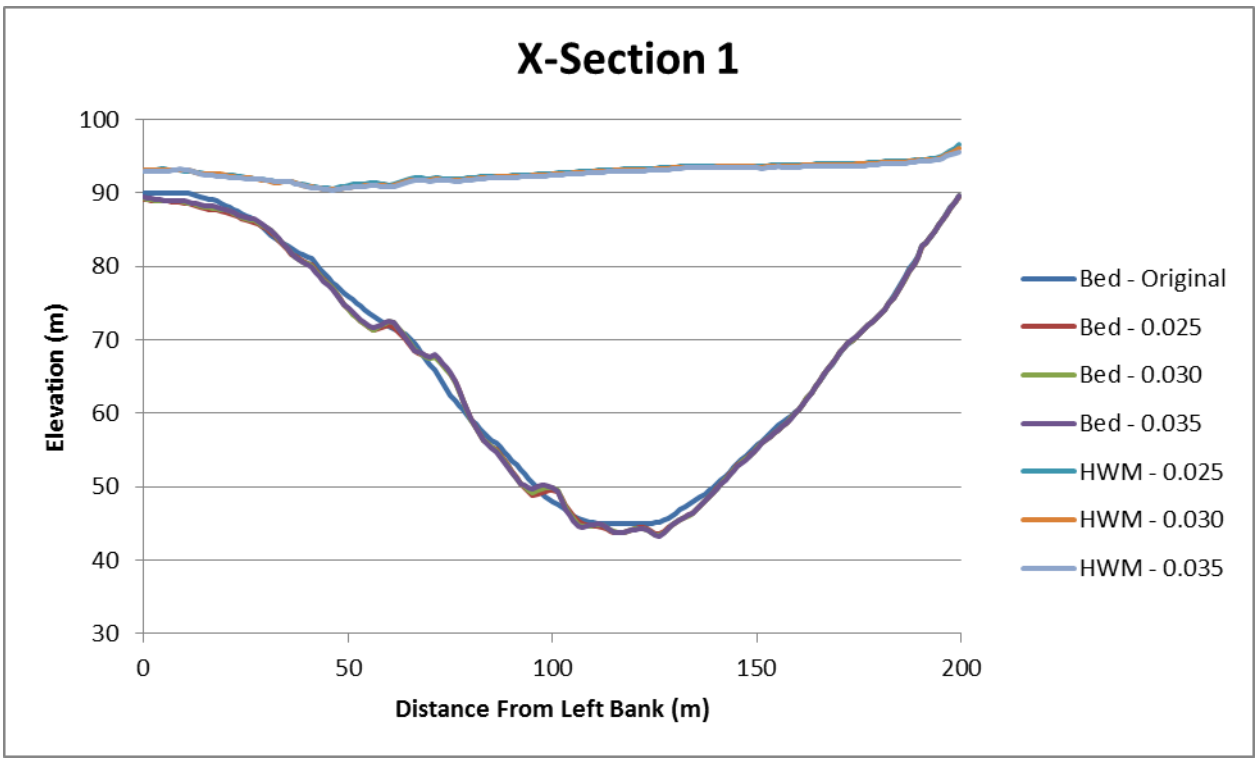

Figure 5-4: HWM and bed elevation at cross-section 1 varying n_g on a mobile-bed

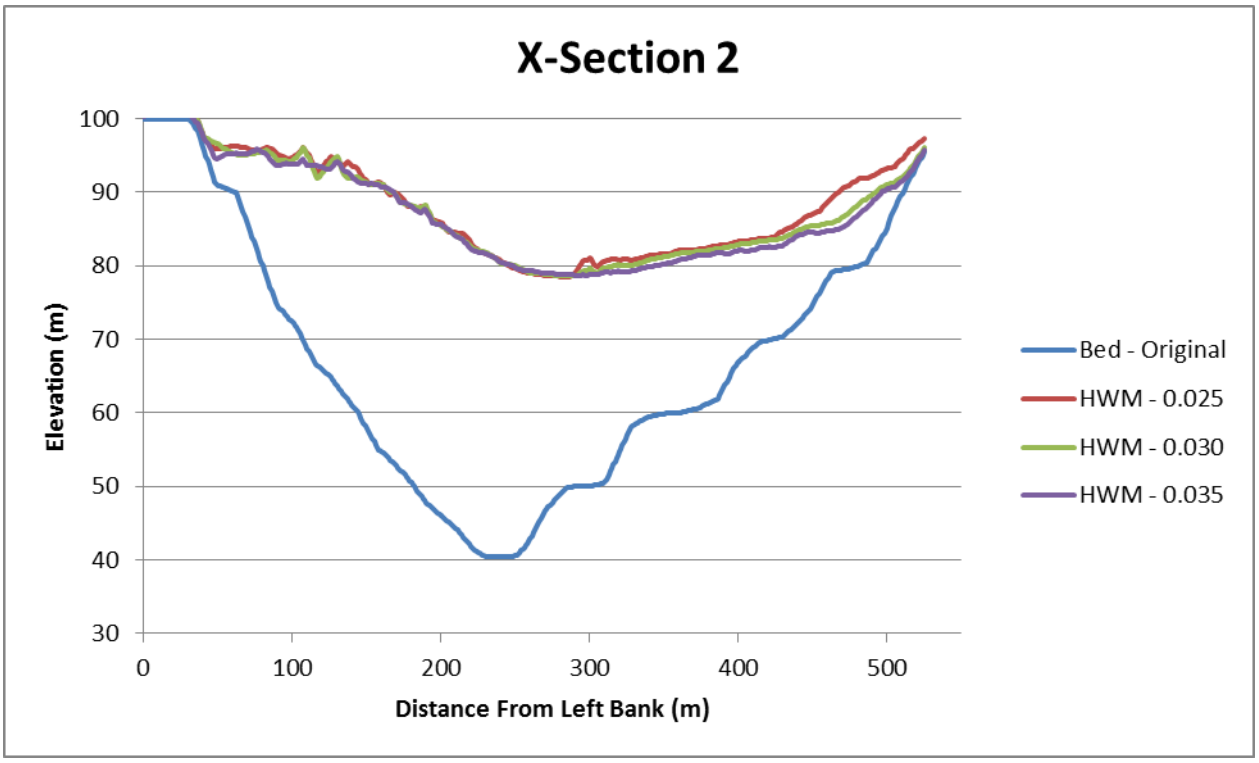

Figure 5-5: HWM at cross-section 2 varying n_g on a fixed-bed

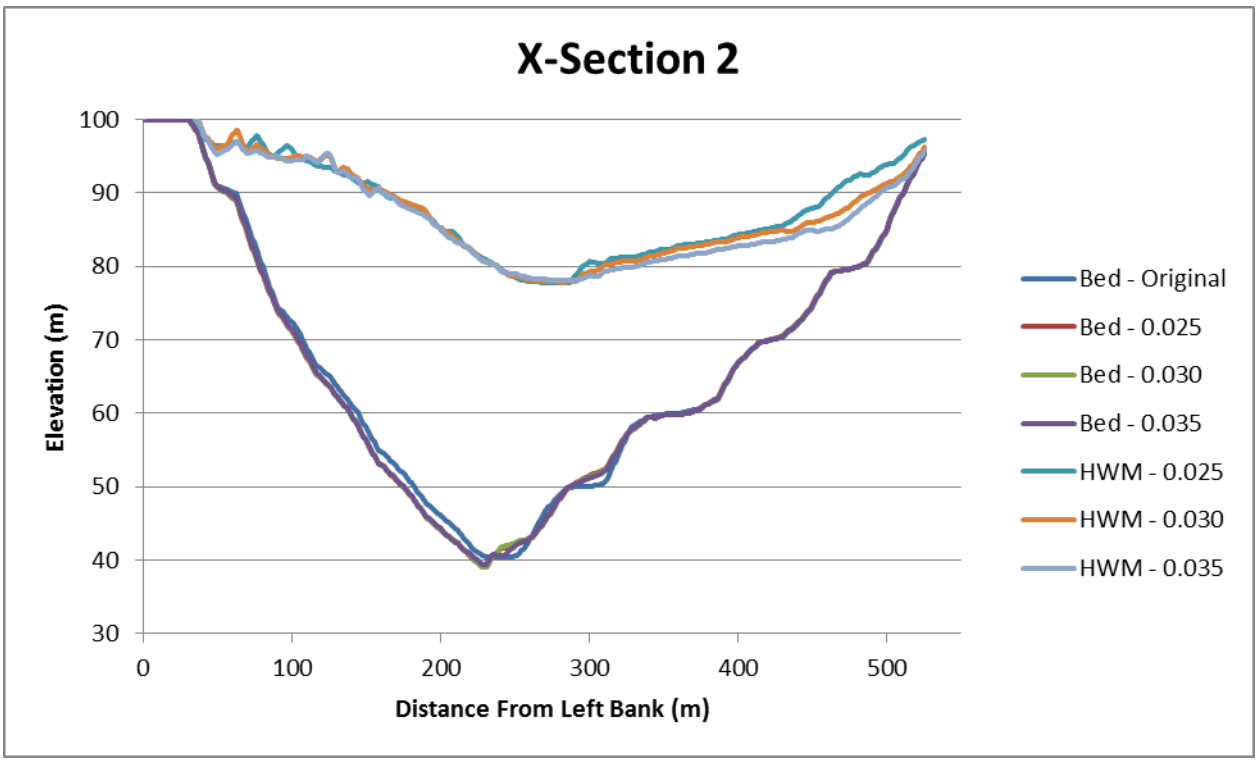

Figure 5-6: HWM and bed elevation at cross-section 2 varying n_g on a mobile-bed

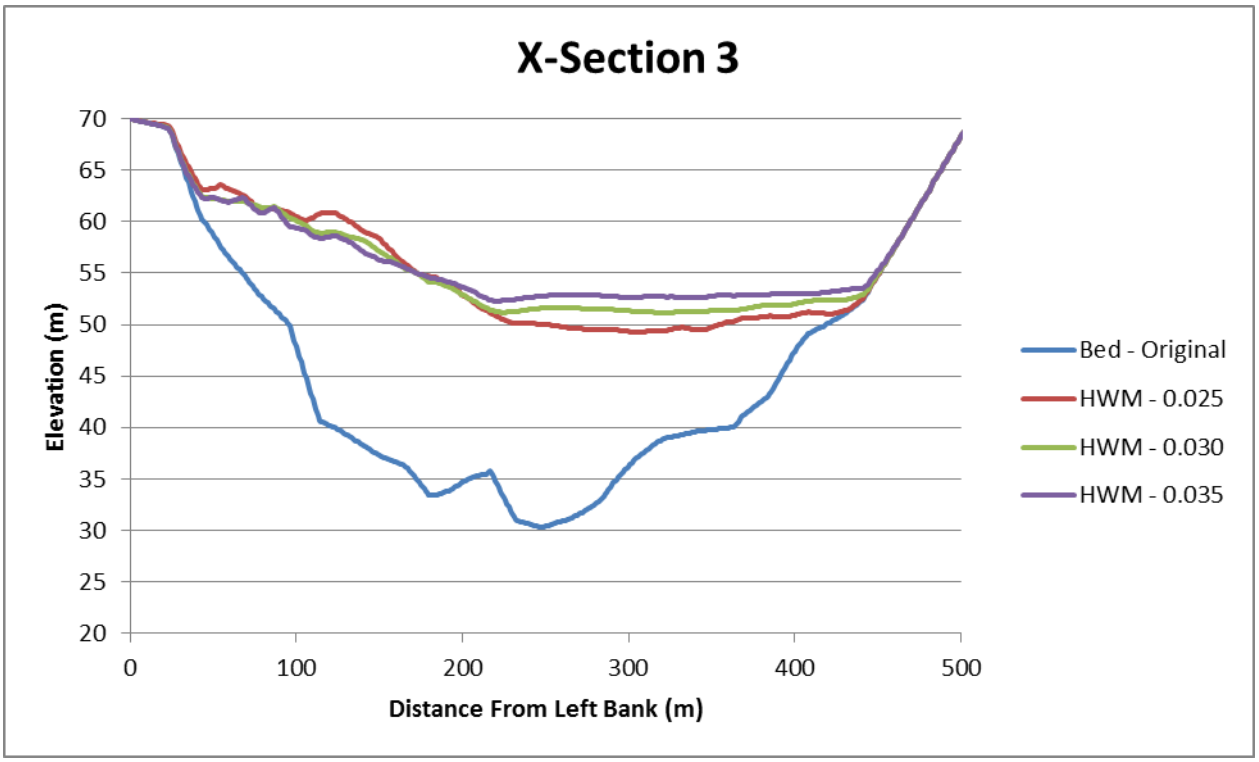

Figure 5-7: HWM at cross-section 3 varying n_g on a fixed-bed

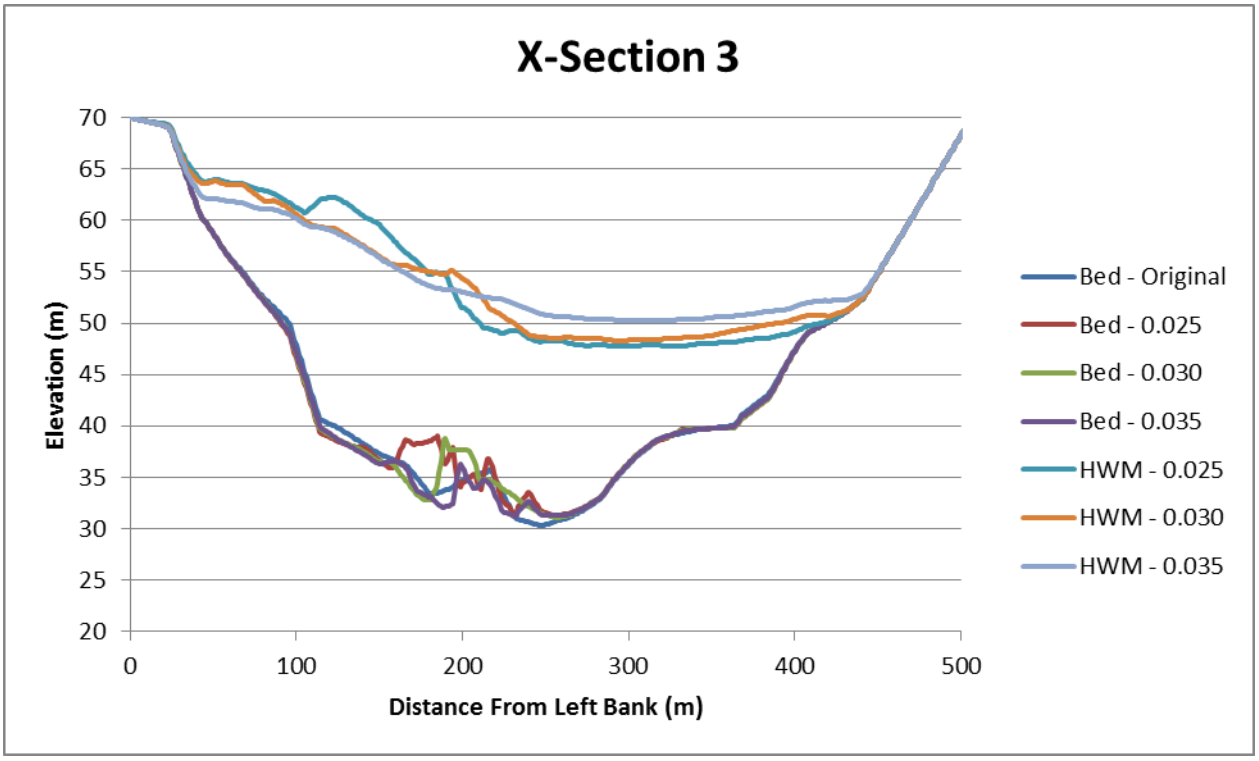

Figure 5-8: HWM and bed elevation at cross-section 3 varying n_g on a mobile-bed

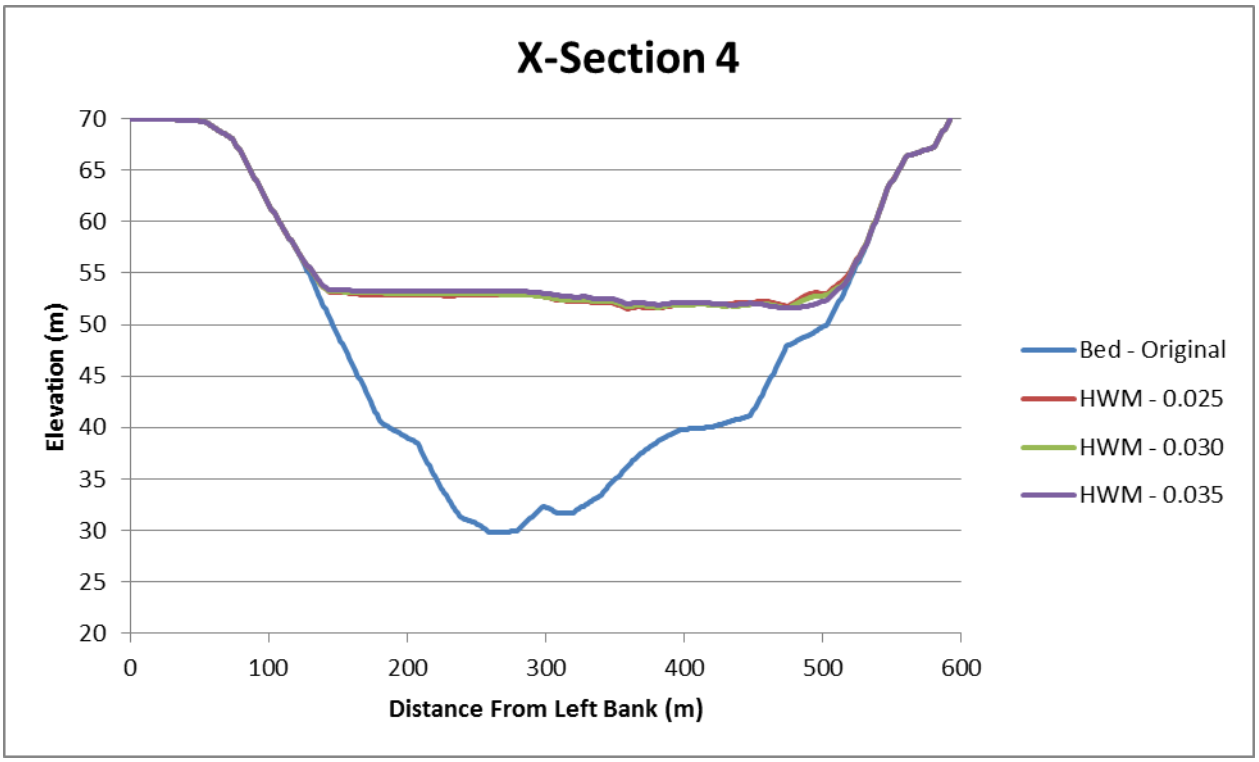

Figure 5-9: HWM at cross-section 4 varying n_g on a fixed-bed

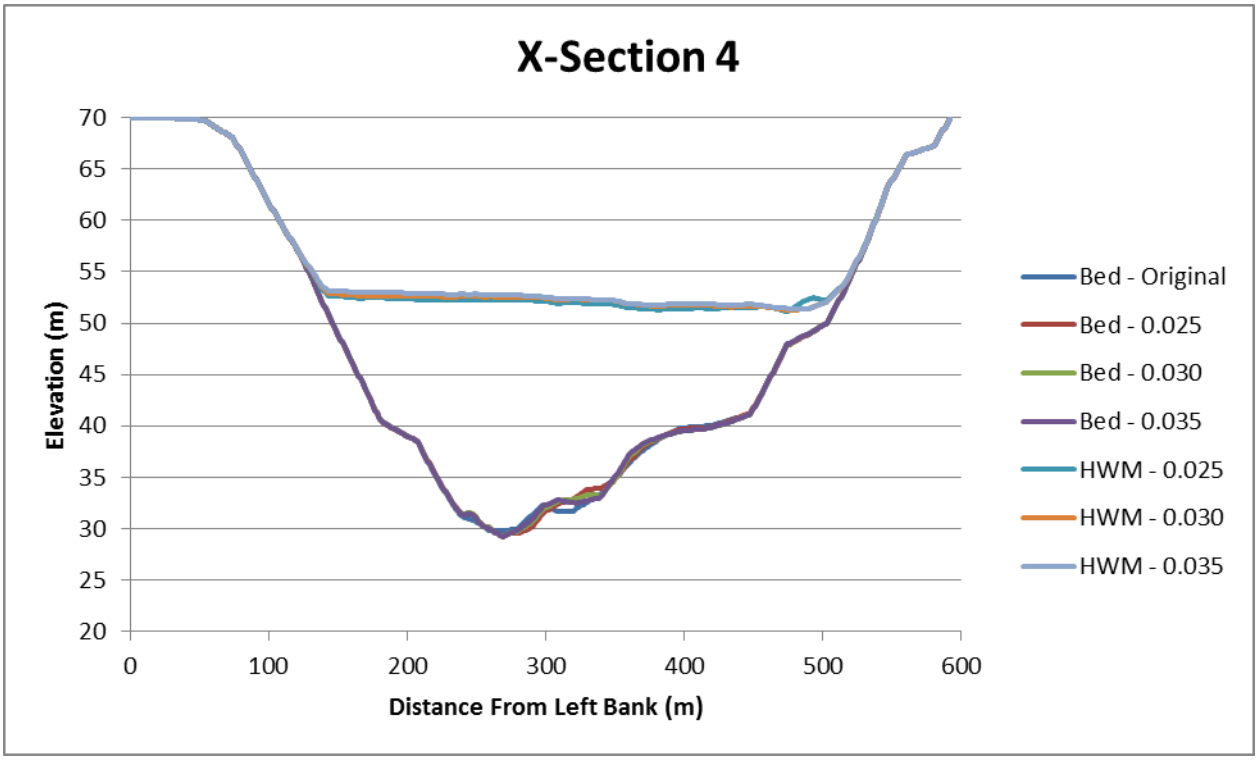

Figure 5-10: HWM and bed elevation at cross-section 4 varying n_g on a mobile-bed

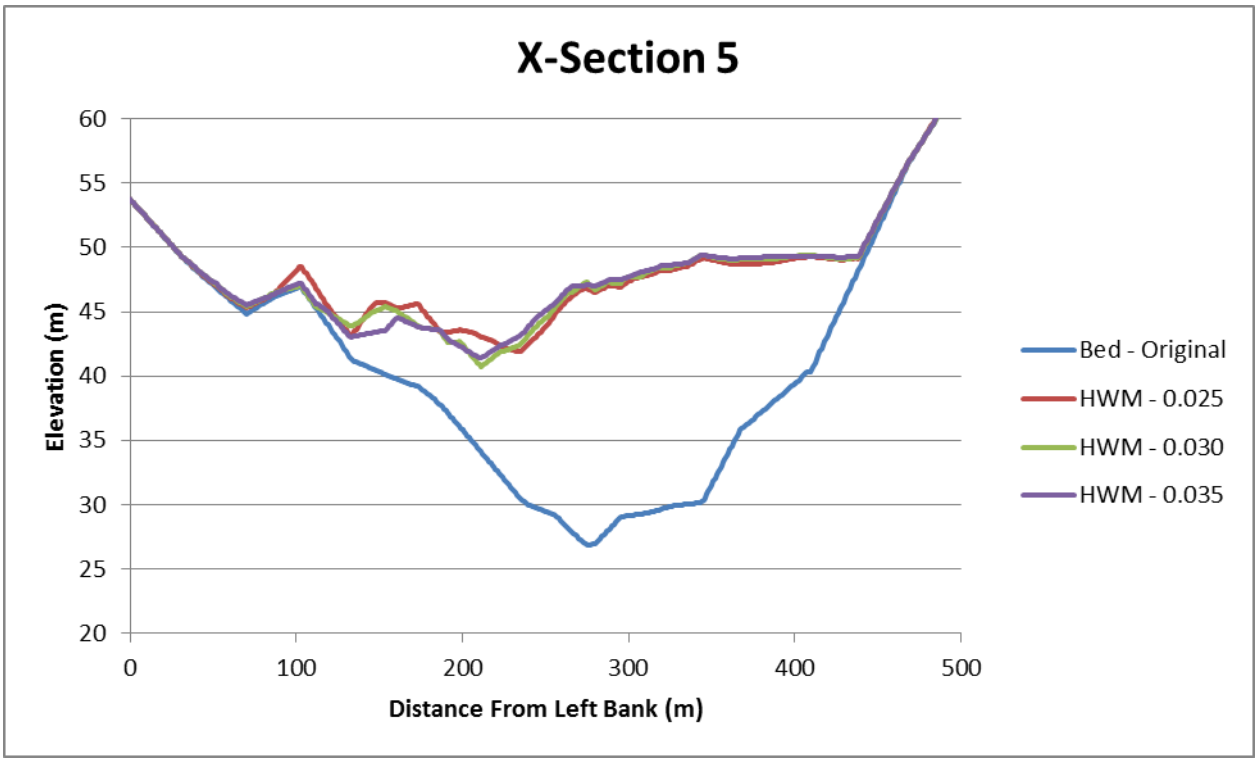

Figure 5-11: HWM at cross-section 5 varying n_g on a fixed-bed

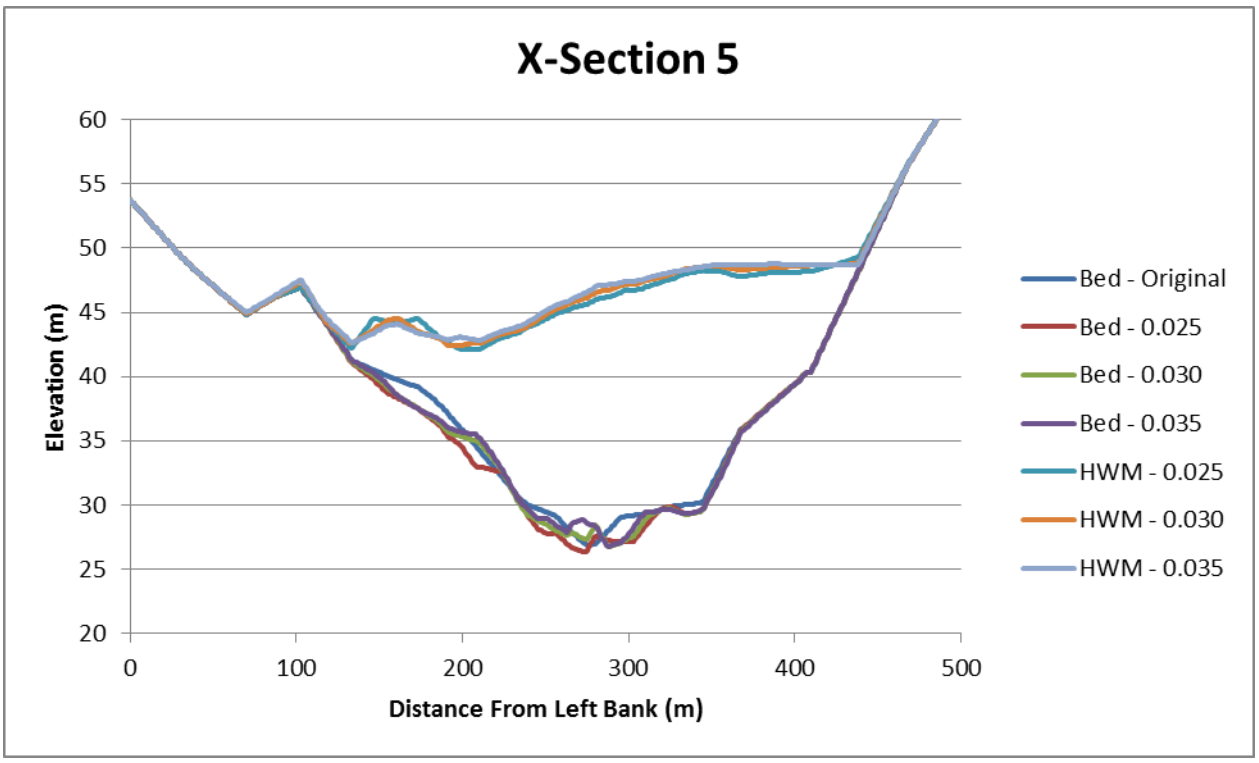

Figure 5-12: HWM and bed elevation at cross-section 5 varying n_g on a mobile-bed

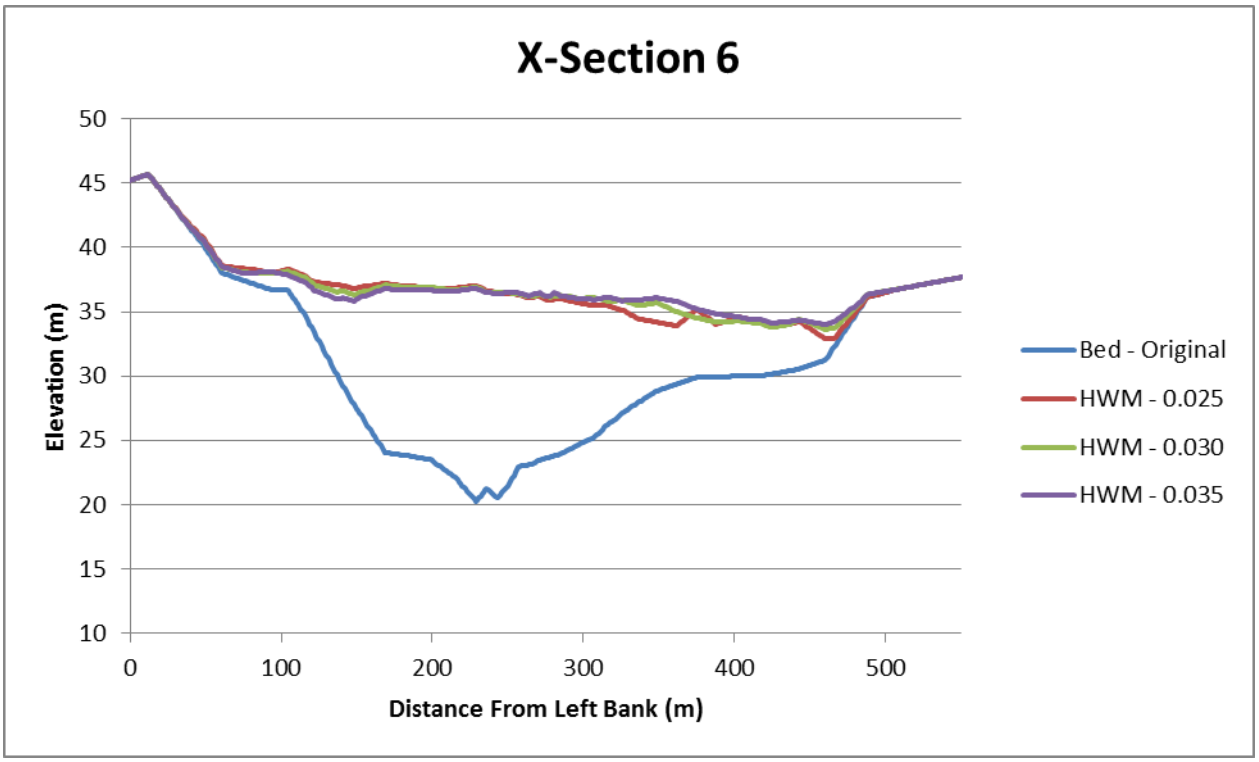

Figure 5-13: HWM at cross-section 6 varying n_g on a fixed-bed

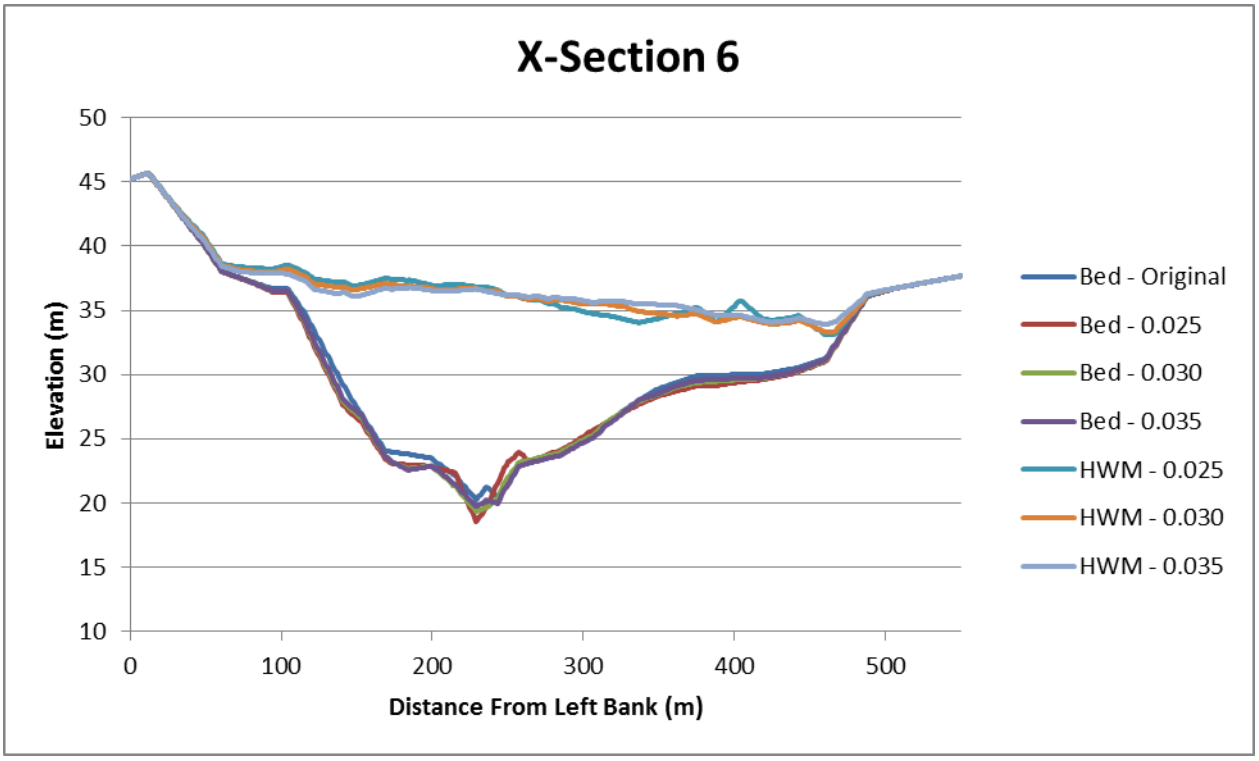

Figure 5-14: HWM and bed elevation at cross-section 6 varying n_g on a mobile-bed

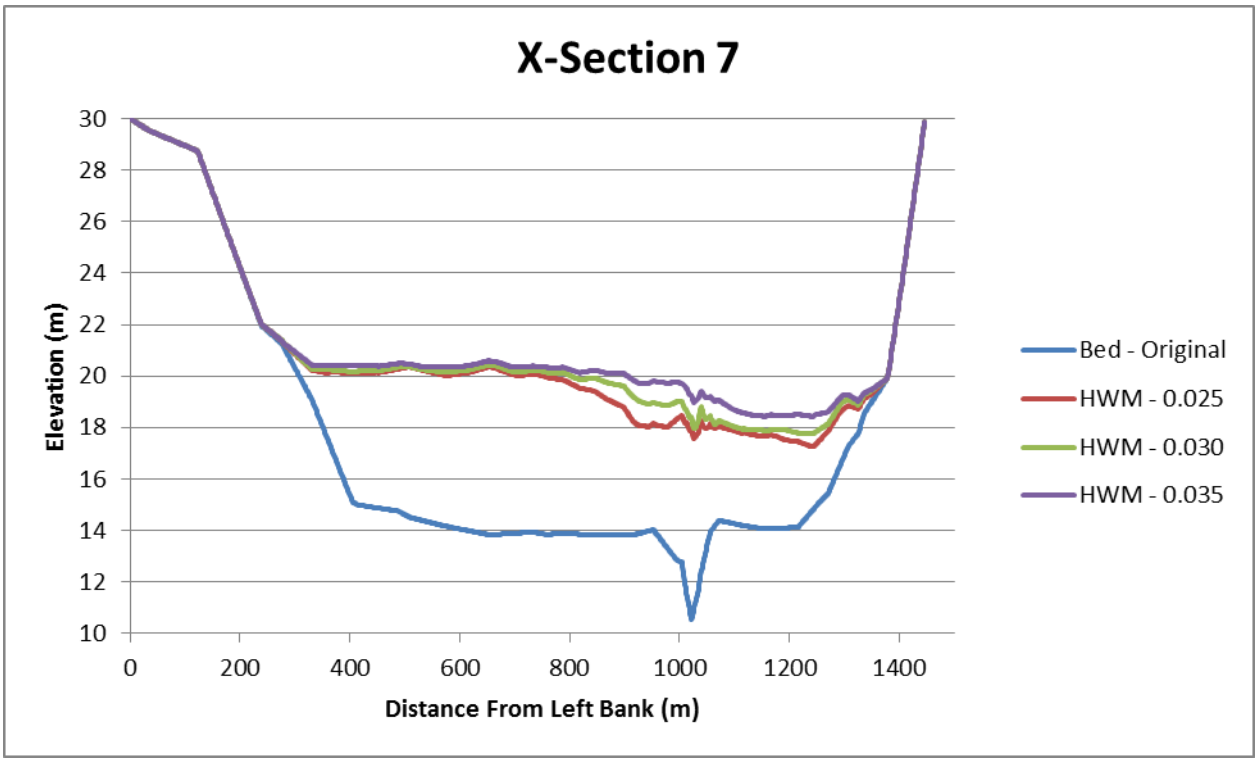

Figure 5-15: HWM at cross-section 7 varying n_g on a fixed-bed

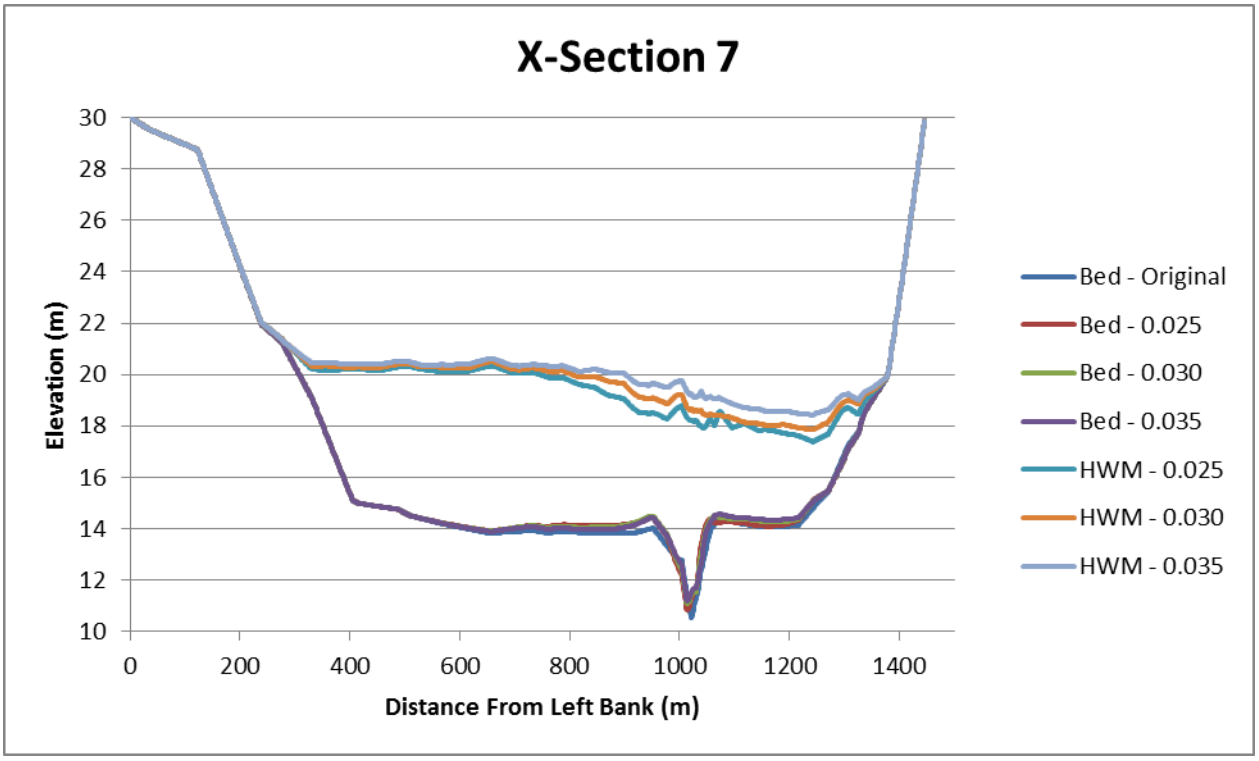

Figure 5-16: HWM and bed elevation at cross-section 7 varying n_g on a mobile-bed

5.1.2 2D BED EVOLUTION

Although the effect of varying n_g on bed elevation was indiscernible using the previous cross-sections, the effect of increasing n_g is clearly demonstrated in the 2D bed evolution plots **(Figure 5-17, Figure 5-18, and Figure 5-19**). As n_g is increased, the zones of significant erosion (blue) and deposition (red) shrink. This indicates that τ^* experienced by the bed decreases as n_g is increased.

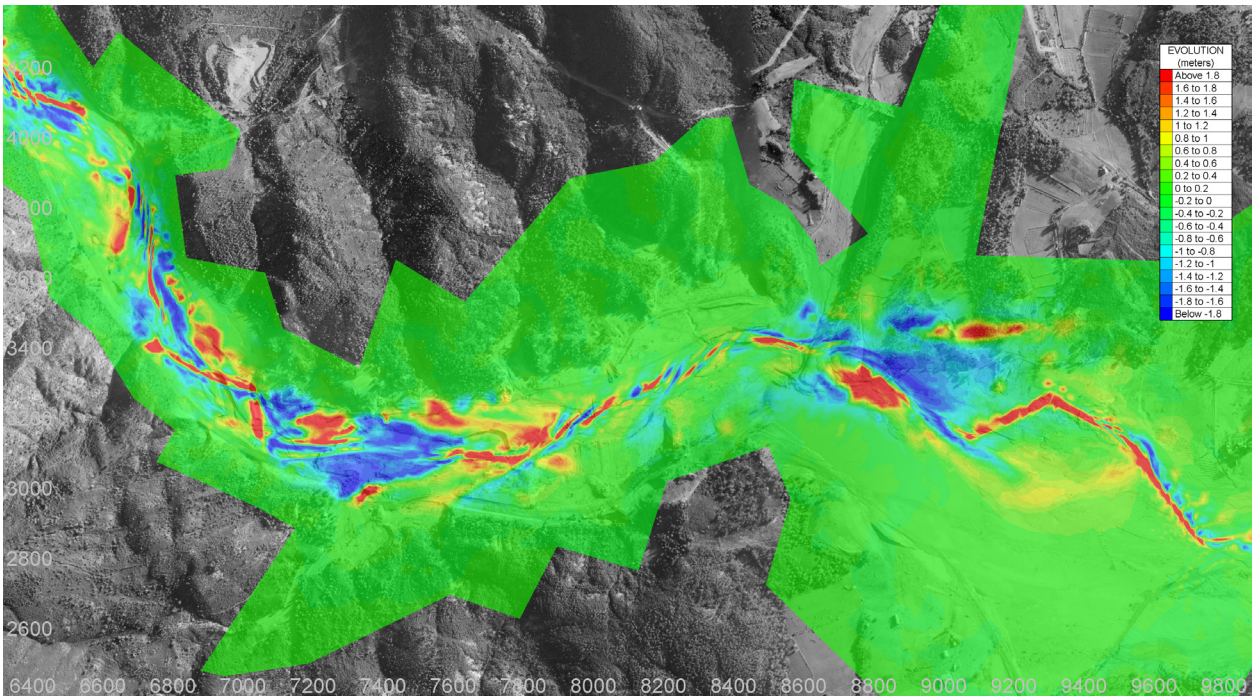

Figure 5-17

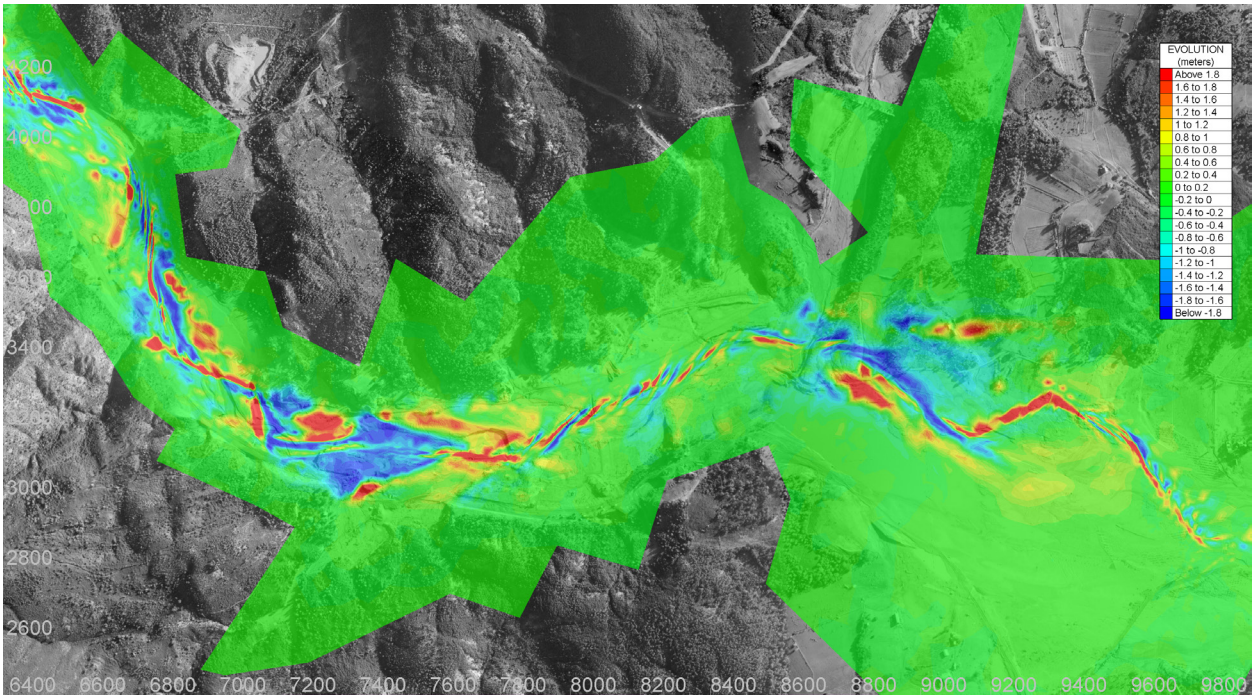

Figure 5-18

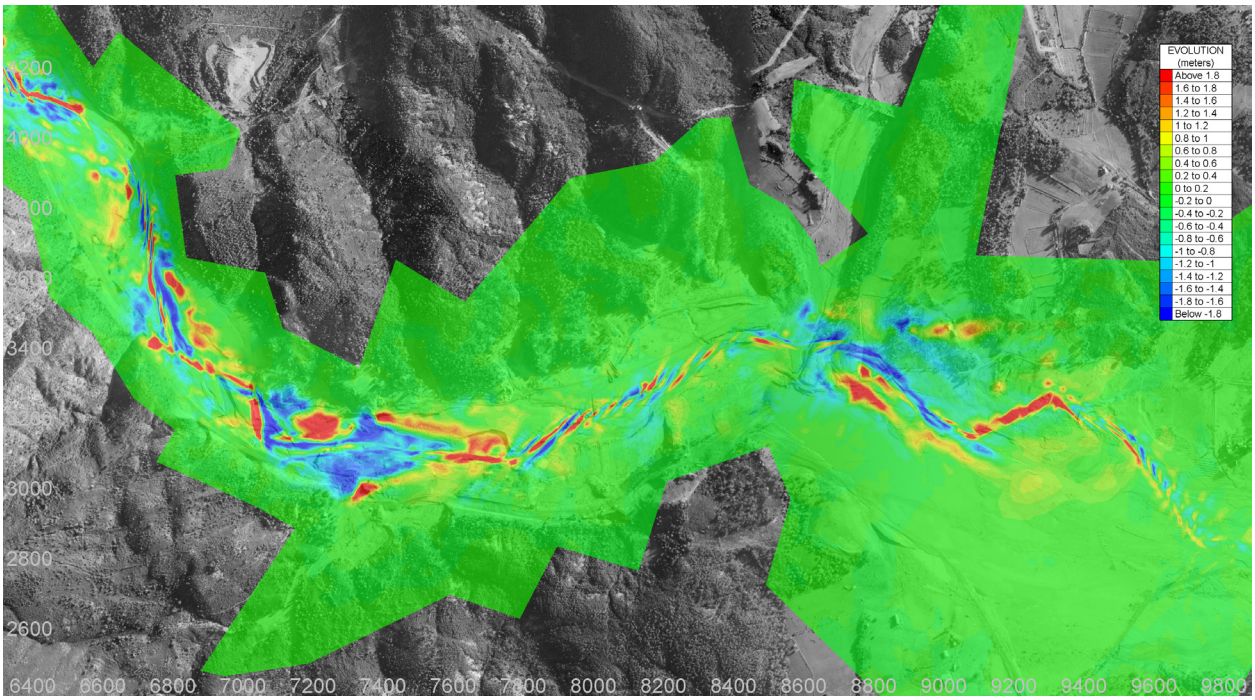

Figure 5-19

Figure 5-17: Bed evolution of case where: $n_g = 0.025$, $n_v = 0.000$, $\phi' = 40°$, and $d_{50} = 1\ mm$ (positive evolution = deposition, negative evolution = erosion) (aerial photograph of Frejus [FR 177-150, #1 to #104] in 1959 © IGN, 2012, by permission)

Figure 5-18: Bed evolution of case where: $n_g = 0.030$, $n_v = 0.000$, $\phi' = 40°$, and $d_{50} = 1\ mm$ (positive evolution = deposition, negative evolution = erosion) (aerial photograph of Frejus [FR 177-150, #1 to #104] in 1959 © IGN, 2012, by permission)

Figure 5-19: Bed evolution of case where: $n_g = 0.035$, $n_v = 0.000$, $\phi' = 40°$, and $d_{50} = 1\ mm$ (positive evolution = deposition, negative evolution = erosion) (aerial photograph of Frejus [FR 177-150, #1 to #104] in 1959 © IGN, 2012, by permission)

5.1.3 FLOOD-WAVE PROPAGATION TIME

5.1.3.1 MOBILE-BED SIMULATIONS

Figure 5-20 to **Figure 5-23** show the extent that the dam-break flood-wave has propagated after $t = 30\ min$ with assumptions of no vegetation to heavy vegetation for a mobile-bed. As the effect of vegetation increases, it can be observed that the distance travelled by the flood-wave after $t = 30\ min$ decreases; this is due to the increase in friction experienced by the flood-wave. Regardless of the effect of vegetation, it is observed that as n_g increases, the distance propagated by the flood-wave decreases. The figures below show this to be true for all levels of vegetation.

The reason for the presence of the streak patterns found in **Figure 5-20** and other figures alike, is that aerial photography was not readily available for the entire region. Aerial photograph coverage was found only for areas affected by the Malpasset dam-break. The streak patterns are a result of the photo software used to stitch together more than one hundred aerial photographs.

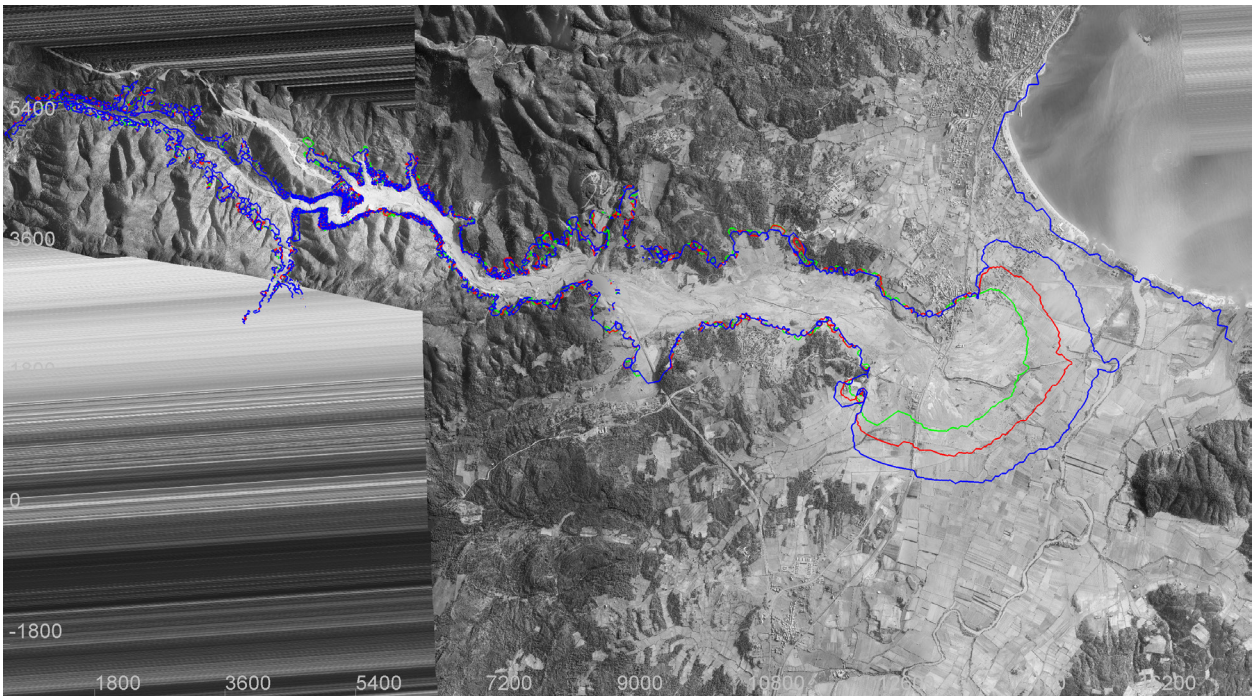

Figure 5-20

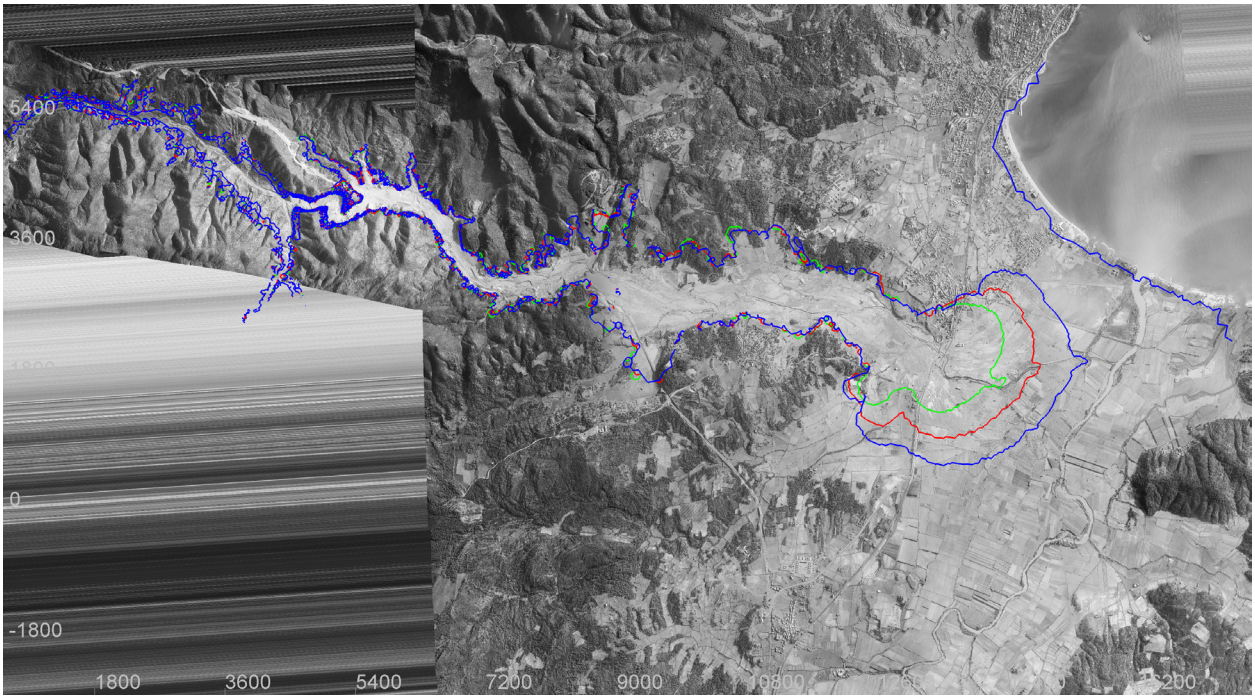

Figure 5-21

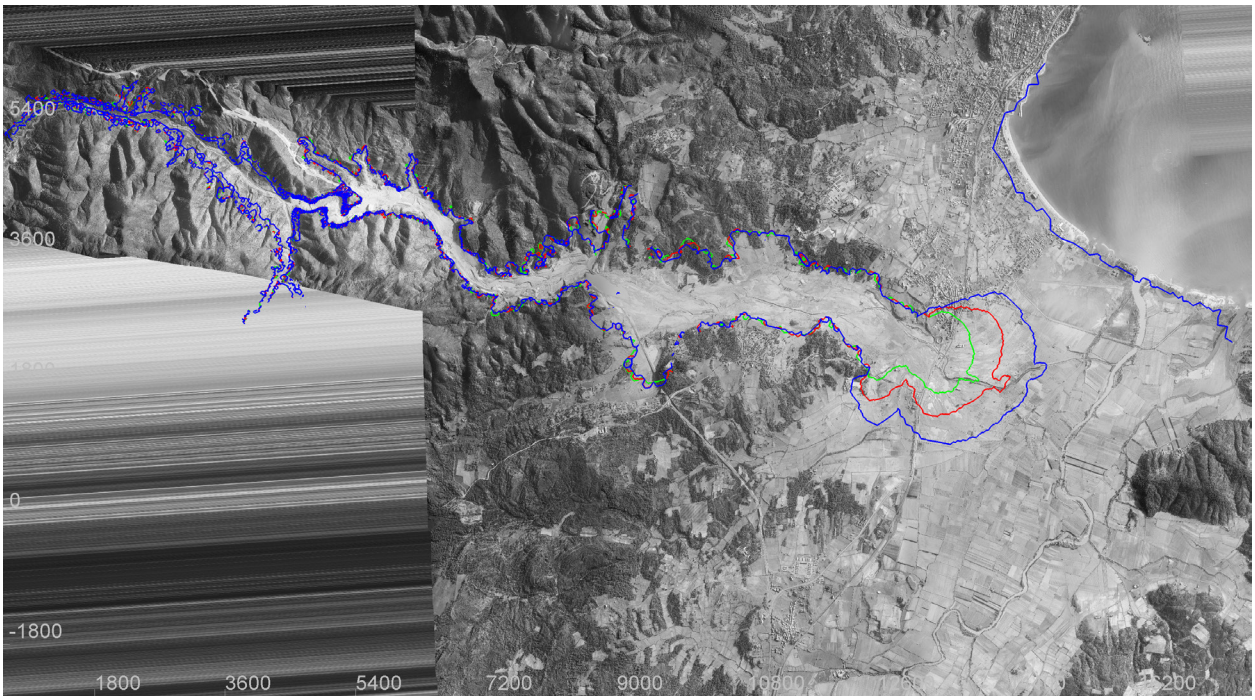

Figure 5-22

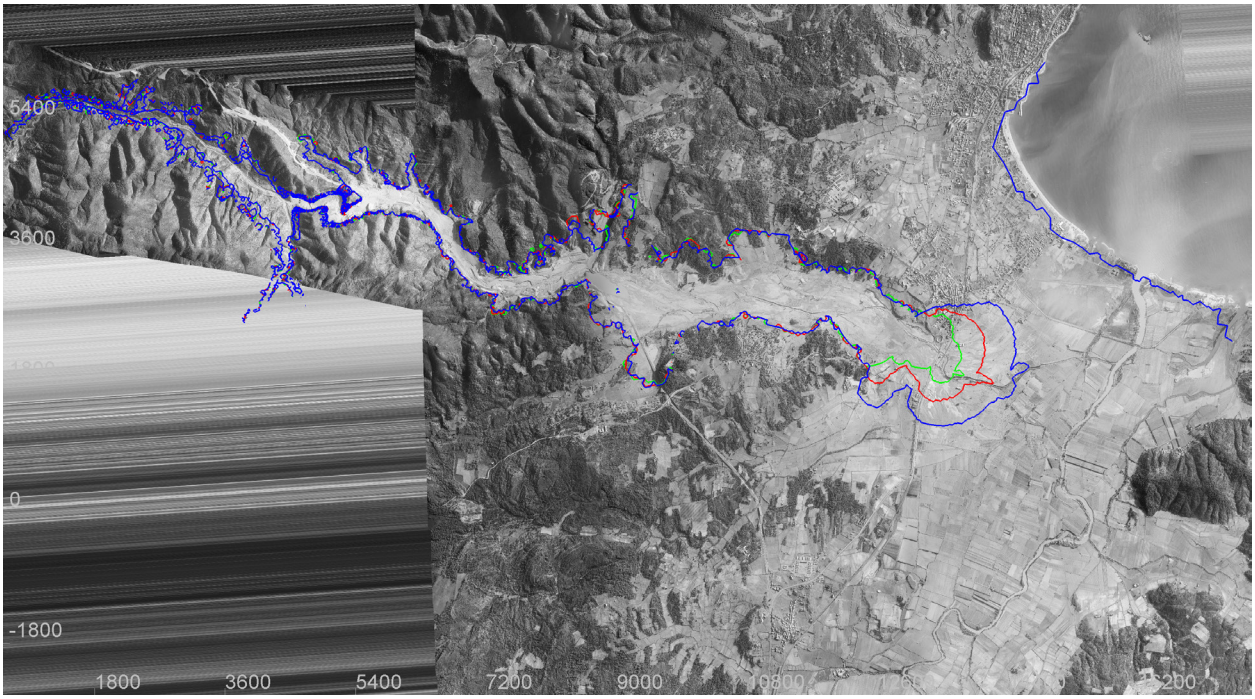

Figure 5-23

Figure 5-20: Extent of inundation 30 minutes after dam-break on a mobile-bed with $n_v = 0.000$, $\phi' = 40°$, and $d_{50} = 1\ mm$ (blue – $n_g = 0.025$, red – $n_g = 0.030$, green – $n_g = 0.035$) (aerial photograph of Frejus [FR 177-150, #1 to #104] in 1959 © IGN, 2012, by permission)

Figure 5-21: Extent of inundation 30 minutes after dam-break on a mobile-bed with $n_v = 0.033$, $\phi' = 49°$, and $d_{50} = 1\ mm$ (blue – $n_g = 0.025$, red – $n_g = 0.030$, green – $n_g = 0.035$) (aerial photograph of Frejus [FR 177-150, #1 to #104] in 1959 © IGN, 2012, by permission)

Figure 5-22: Extent of inundation 30 minutes after dam-break on a mobile-bed with $n_v = 0.067$, $\phi' = 60°$, and $d_{50} = 1\ mm$ (blue – $n_g = 0.025$, red – $n_g = 0.030$, green – $n_g = 0.035$) (aerial photograph of Frejus [FR 177-150, #1 to #104] in 1959 © IGN, 2012, by permission)

Figure 5-23: Extent of inundation 30 minutes after dam-break on a mobile-bed with $n_v = 0.090$, $\phi' = 70°$, and $d_{50} = 1\ mm$ (blue – $n_g = 0.025$, red – $n_g = 0.030$, green – $n_g = 0.035$) (aerial photograph of Frejus [FR 177-150, #1 to #104] in 1959 © IGN, 2012, by permission)

Table 5-1 tabulates the time it takes for the dam-break flood-wave to reach the Mediterranean Sea with varied sensitivity parameters. Selecting and holding constant values of n_v, ϕ', and d_{50}, then comparing different values of n_g consistently yields the conclusion that increasing n_g will lead to an increase in propagation time. Plotting t (propagation time) versus n (total roughness) for varying grain roughnesses **(Figure 5-24)** reveals that t is a function of n for each case of n_g, and that there is an approximate 3 $minute$ increase in t for every $n_g = 0.005$ increase.

Table 5-1: Flood-wave propagation time after dam-break to the Mediterranean Sea on mobile-bed

n_g	n_v	n	$\phi'(°)$	$d_{50}\ (m)$	$t\ (min)$
0.025	0.000	0.025	40	0.001	32
0.025	0.000	0.025	40	0.005	32
0.025	0.000	0.025	40	0.010	32
0.025	0.000	0.025	40	0.020	32
0.025	0.000	0.025	40	0.040	32
0.025	0.033	0.041	49	0.001	36
0.025	0.033	0.041	49	0.005	35
0.025	0.033	0.041	49	0.010	35
0.025	0.033	0.041	49	0.020	35
0.025	0.033	0.041	49	0.040	35
0.025	0.067	0.072	60	0.001	39
0.025	0.067	0.072	60	0.005	39
0.025	0.067	0.072	60	0.010	39
0.025	0.067	0.072	60	0.020	38
0.025	0.067	0.072	60	0.040	38
0.025	0.090	0.093	70	0.001	41
0.025	0.090	0.093	70	0.005	41
0.025	0.090	0.093	70	0.010	41
0.025	0.090	0.093	70	0.020	40
0.025	0.090	0.093	70	0.040	40
0.030	0.000	0.030	40	0.001	36
0.030	0.000	0.030	40	0.005	36
0.030	0.000	0.030	40	0.010	36
0.030	0.000	0.030	40	0.020	35
0.030	0.000	0.030	40	0.040	35
0.030	0.033	0.045	49	0.001	39
0.030	0.033	0.045	49	0.005	39
0.030	0.033	0.045	49	0.010	39
0.030	0.033	0.045	49	0.020	38
0.030	0.033	0.045	49	0.040	38

0.030	0.067	0.073	60	0.001	42
0.030	0.067	0.073	60	0.005	42
0.030	0.067	0.073	60	0.010	42
0.030	0.067	0.073	60	0.020	42
0.030	0.067	0.073	60	0.040	41
0.030	0.090	0.095	70	0.001	44
0.030	0.090	0.095	70	0.005	44
0.030	0.090	0.095	70	0.010	44
0.030	0.090	0.095	70	0.020	44
0.030	0.090	0.095	70	0.040	44
0.035	0.000	0.035	40	0.001	39
0.035	0.000	0.035	40	0.005	39
0.035	0.000	0.035	40	0.010	39
0.035	0.000	0.035	40	0.020	39
0.035	0.000	0.035	40	0.040	39
0.035	0.033	0.048	49	0.001	42
0.035	0.033	0.048	49	0.005	42
0.035	0.033	0.048	49	0.010	42
0.035	0.033	0.048	49	0.020	42
0.035	0.033	0.048	49	0.040	41
0.035	0.067	0.076	60	0.001	46
0.035	0.067	0.076	60	0.005	45
0.035	0.067	0.076	60	0.010	45
0.035	0.067	0.076	60	0.020	45
0.035	0.067	0.076	60	0.040	45
0.035	0.090	0.097	70	0.001	48
0.035	0.090	0.097	70	0.005	47
0.035	0.090	0.097	70	0.010	47
0.035	0.090	0.097	70	0.020	47
0.035	0.090	0.097	70	0.040	47

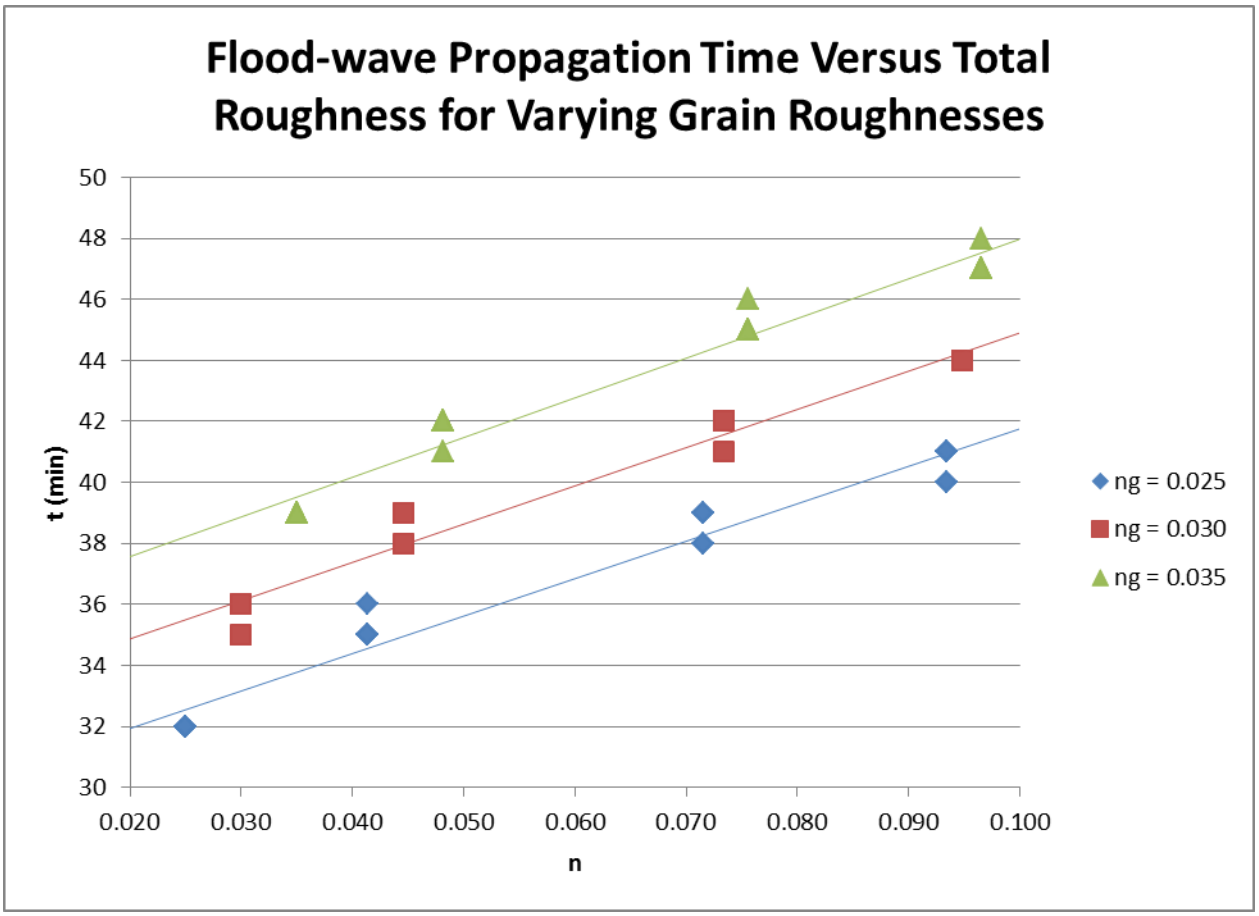

Figure 5-24: Flood-wave propagation time versus total roughness for varying grain roughnesses in mobile-bed model

5.1.3.2 FIXED-BED SIMULATIONS

Figure 5-25 to **Figure 5-28** show the extent that the dam-break flood-wave has propagated after $t = 30\ min$ with assumptions of no vegetation to heavy vegetation for a fixed-bed. As the effect of vegetation increases, it can be observed that the distance travelled by the flood-wave after $t = 30\ min$ decreases; this is due to the increase in friction experienced by the flood-wave. Regardless of the effect of vegetation, it is observed that as n_g increases, the distance propagated by the flood-wave decreases. The figures below show this to be true for all levels of vegetation.

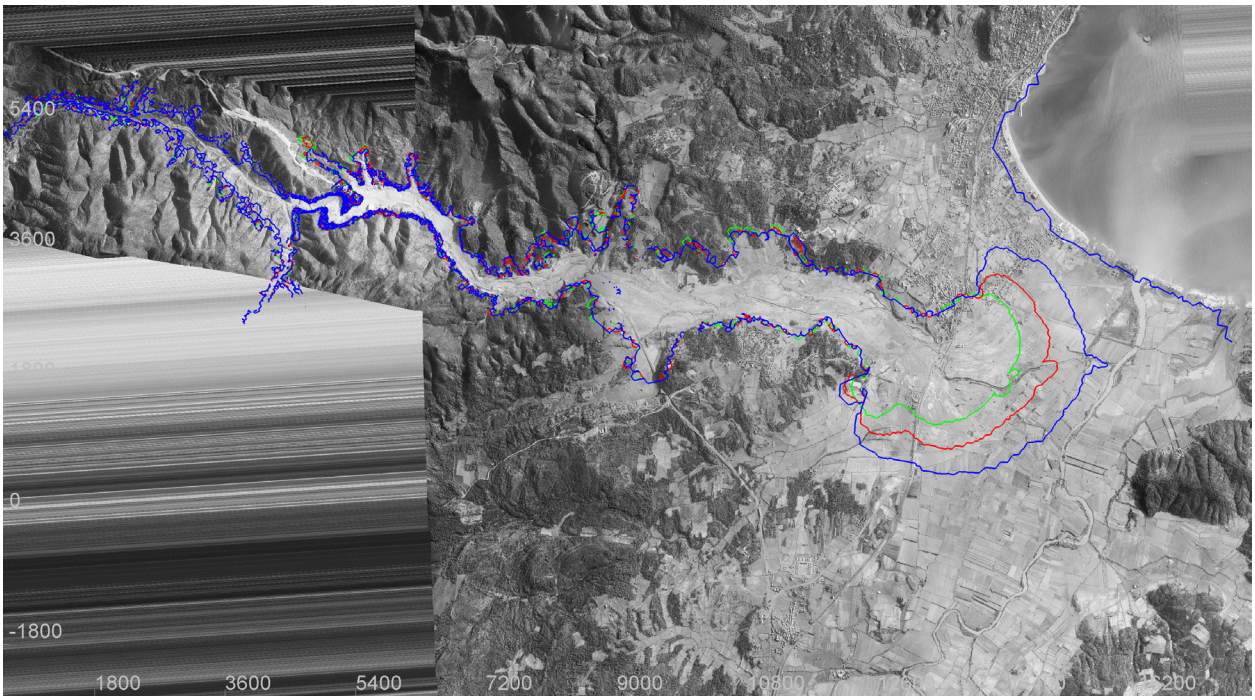

Figure 5-25

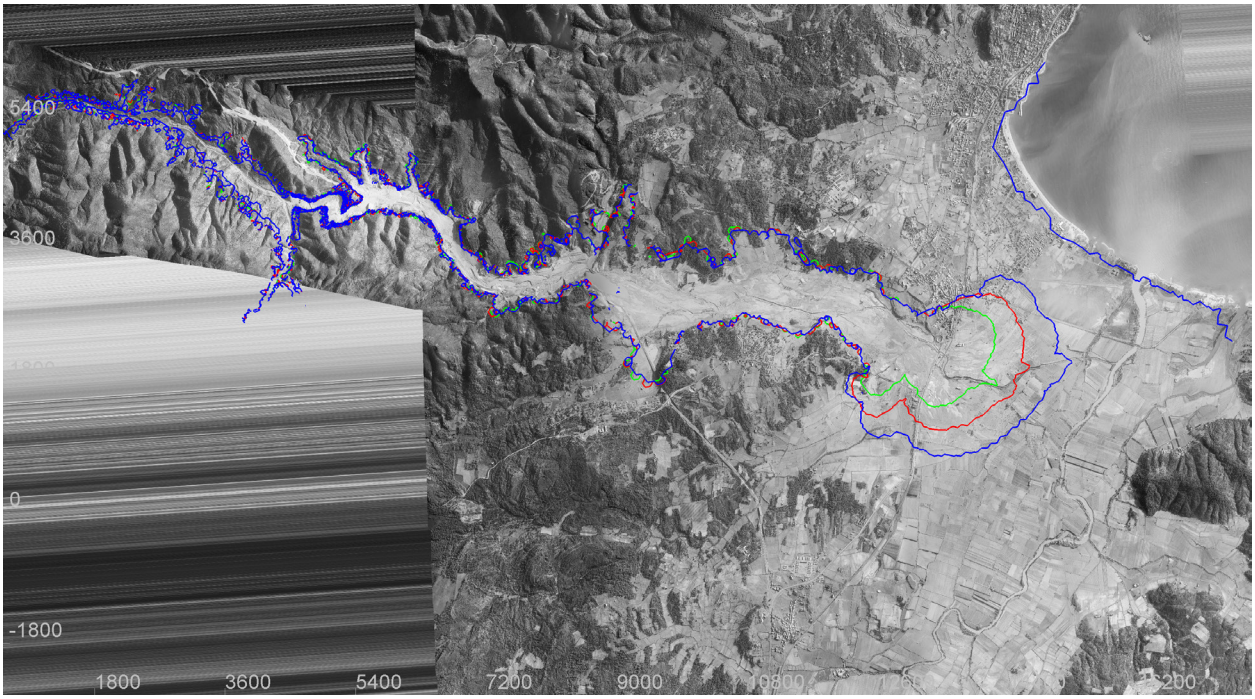

Figure 5-26

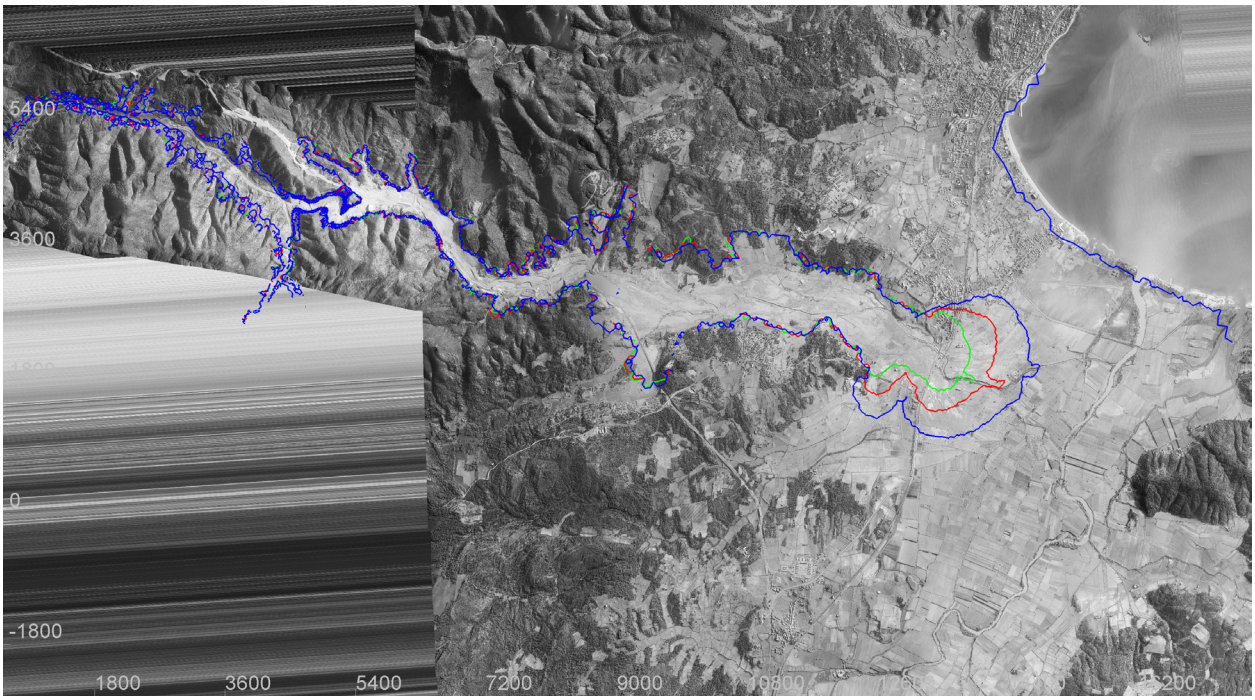

Figure 5-27

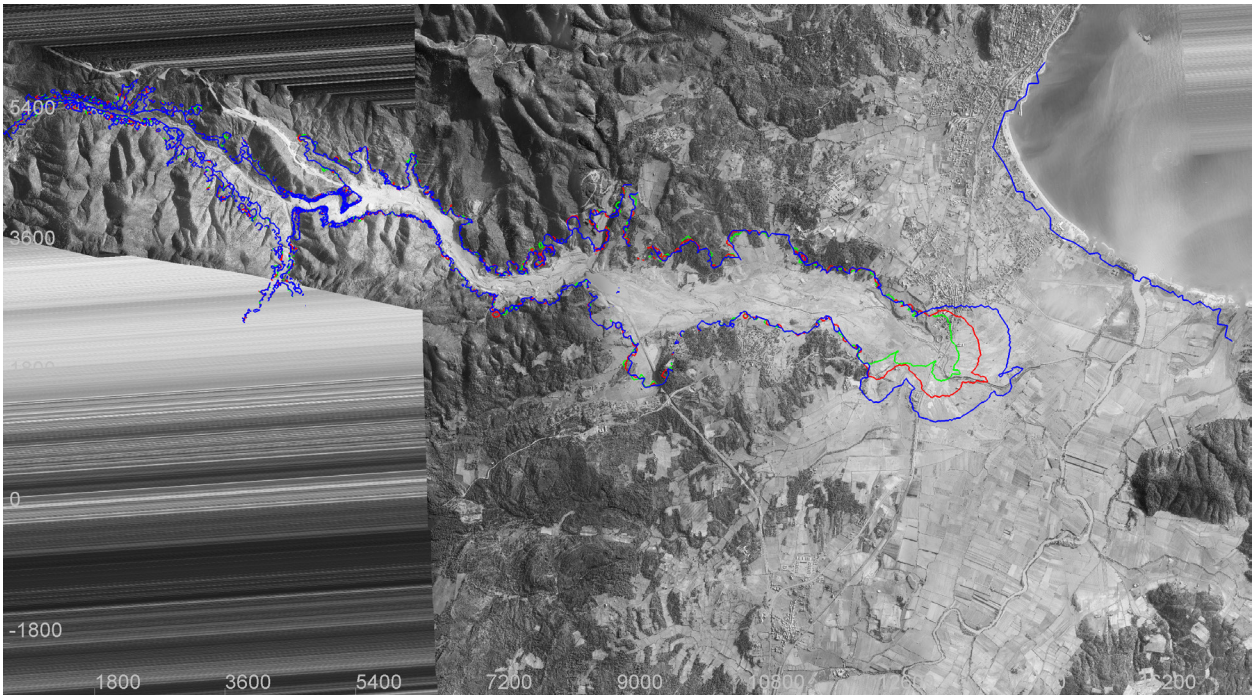

Figure 5-28

Figure 5-25: Extent of inundation 30 minutes after dam-break on a fixed-bed with $n_v = 0.000$ (blue – $n_g = 0.025$, red – $n_g = 0.030$, green – $n_g = 0.035$) (aerial photograph of Frejus [FR 177-150, #1 to #104] in 1959 © IGN, 2012, by permission)

Figure 5-26: Extent of inundation 30 minutes after dam-break on a fixed-bed with $n_v = 0.033$ (blue – $n_g = 0.025$, red – $n_g = 0.030$, green – $n_g = 0.035$) (aerial photograph of Frejus [FR 177-150, #1 to #104] in 1959 © IGN, 2012, by permission)

Figure 5-27: Extent of inundation 30 minutes after dam-break on a fixed-bed with $n_v = 0.067$ (blue – $n_g = 0.025$, red – $n_g = 0.030$, green – $n_g = 0.035$) (aerial photograph of Frejus [FR 177-150, #1 to #104] in 1959 © IGN, 2012, by permission)

Figure 5-28: Extent of inundation 30 minutes after dam-break on a fixed-bed with $n_v = 0.090$ (blue – $n_g = 0.025$, red – $n_g = 0.030$, green – $n_g = 0.035$) (aerial photograph of Frejus [FR 177-150, #1 to #104] in 1959 © IGN, 2012, by permission)

Table 5-2 tabulates the time it takes for the dam-break flood-wave to reach the Mediterranean Sea with varied sensitivity parameters. Selecting and holding constant values of n_v, then comparing different values n_g consistently yields the conclusion that increasing n_g will lead to an increase in propagation time. Plotting t (propagation time) versus n (total roughness) for varying grain roughnesses **(Figure 5-29)** reveals that t is a function of n for each case of n_g, and that there is an approximate 3 $minute$ increase in t for every $n_g = 0.005$ increase.

Table 5-2: Flood-wave propagation time after dam-break to the Mediterranean Sea on fixed-bed

n_g	n_v	n	$t\ (min)$
0.025	0.000	0.025	33
0.025	0.033	0.041	37
0.025	0.067	0.072	40
0.025	0.090	0.093	42
0.025	0.100	0.103	43
0.030	0.000	0.030	37
0.030	0.033	0.045	40
0.030	0.067	0.073	43
0.030	0.090	0.095	45
0.030	0.100	0.104	46
0.035	0.000	0.035	40
0.035	0.033	0.048	43
0.035	0.067	0.076	46
0.035	0.090	0.097	48
0.035	0.100	0.106	49

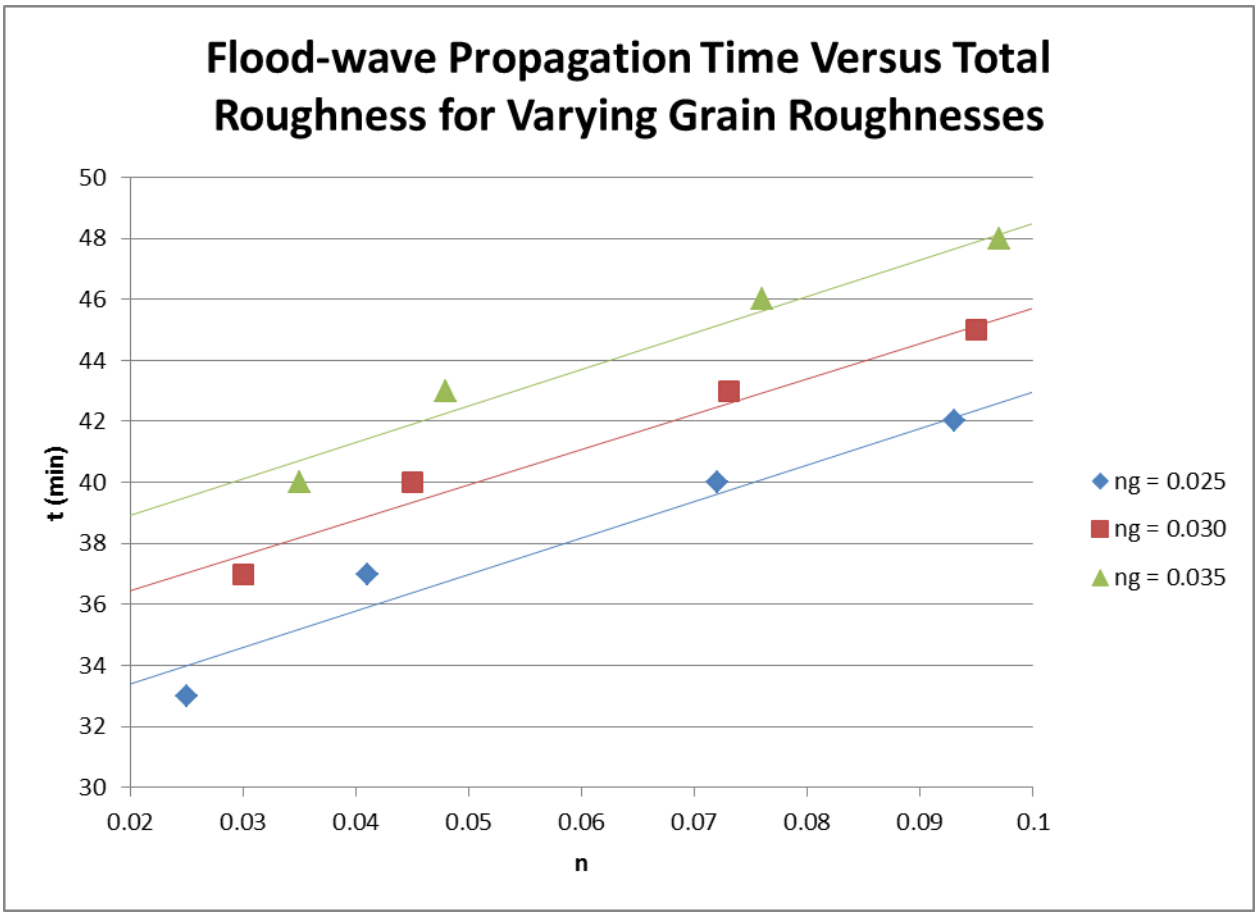

Figure 5-29: Flood-wave propagation time versus total roughness for varying grain roughnesses in fixed-bed model

5.2 EFFECT OF VARYING VEGETATION ROUGHNESS AND FRICTION ANGLE

The vegetation roughness (n_v) and friction angle (ϕ') were varied with the values in **Table 4-4** for both mobile-bed and fixed-bed simulations. HWM and bed change were compared at the seven cross-sections **(Figure 5-1)** for both simulation types, and the 2D bed evolution at the location in **Figure 5-2** was examined for only the mobile-bed cases. Flood-wave propagation times were then compared for both the mobile-bed and fixed-bed simulations. Lastly, pre- and post- dam-break steady state hydrodynamic simulations were performed to examine pre- and post-dam-break inundation.

5.2.1 CROSS-SECTIONS OF HIGH-WATER MARKS AND BED CHANGE

The set of fixed-bed simulations used constant values of the following parameters: $n_g = 0.025$ and $t = 2\ hours$. To test the effect of vegetation density on high water levels, the value of n_v is varied among the four values of 0.000, 0.033, 0.067, and 0.090. All of the cross-sections also display the original bed elevation (before dam-break) as a basis for comparison.

Results demonstrate that varying n_v does have an effect on the HWM for fixed-bed simulations. As vegetation density increases, the HWM **(Figure 5-30, Figure 5-32, Figure 5-34, Figure 5-36, Figure 5-38, Figure 5-40, Figure 5-42)** increases in cross-sections 1, 2, and 7, and has a mixed effect in cross-sections 3, 4, 5, and 6.

The set of mobile-bed simulations used constant values of the following parameters: $n_g = 0.025$, $d_{50} = 1\ mm$, $d_b = 2\ m$, and $t = 2\ hours$. To test the effect of vegetation density on high water levels, the values of n_v and ϕ' are varied among the four pairs of values in **Table 4-4** representing no vegetation to heavy vegetation. All of the cross-sections also display the original bed elevation (before dam-break) as a basis for comparison.

Results demonstrate that varying vegetation density does have an effect on the HWM for mobile-bed simulations. As vegetation density increases, the HWM **(Figure 5-31, Figure 5-33, Figure 5-35, Figure 5-37, Figure 5-39, Figure 5-41, Figure 5-43)** decreased in cross-sections 1, 2, and 7, increased in cross-sections 4 and 5, and had a mixed effect on cross-sections 3 and 6. It is not obvious what the effect of varying vegetation density is on bed elevations.

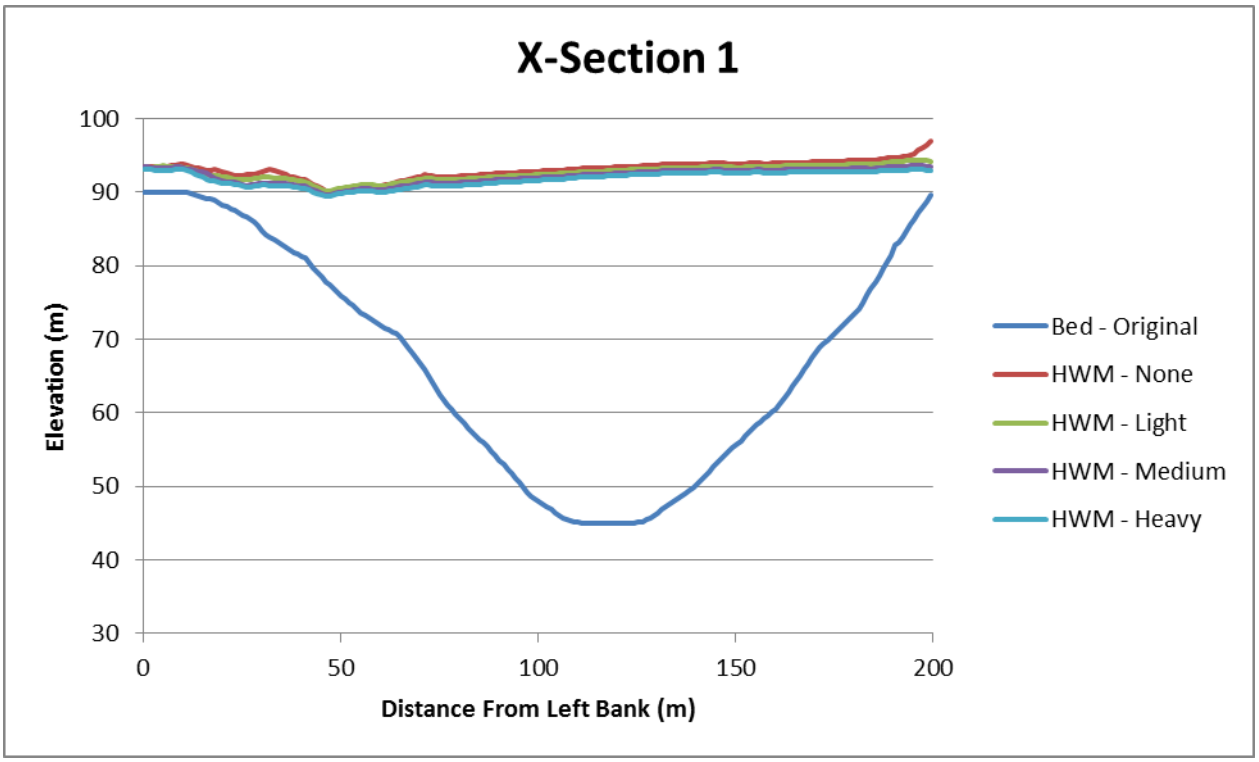

Figure 5-30: HWM at cross-section 1 varying n_v and ϕ' on a fixed-bed

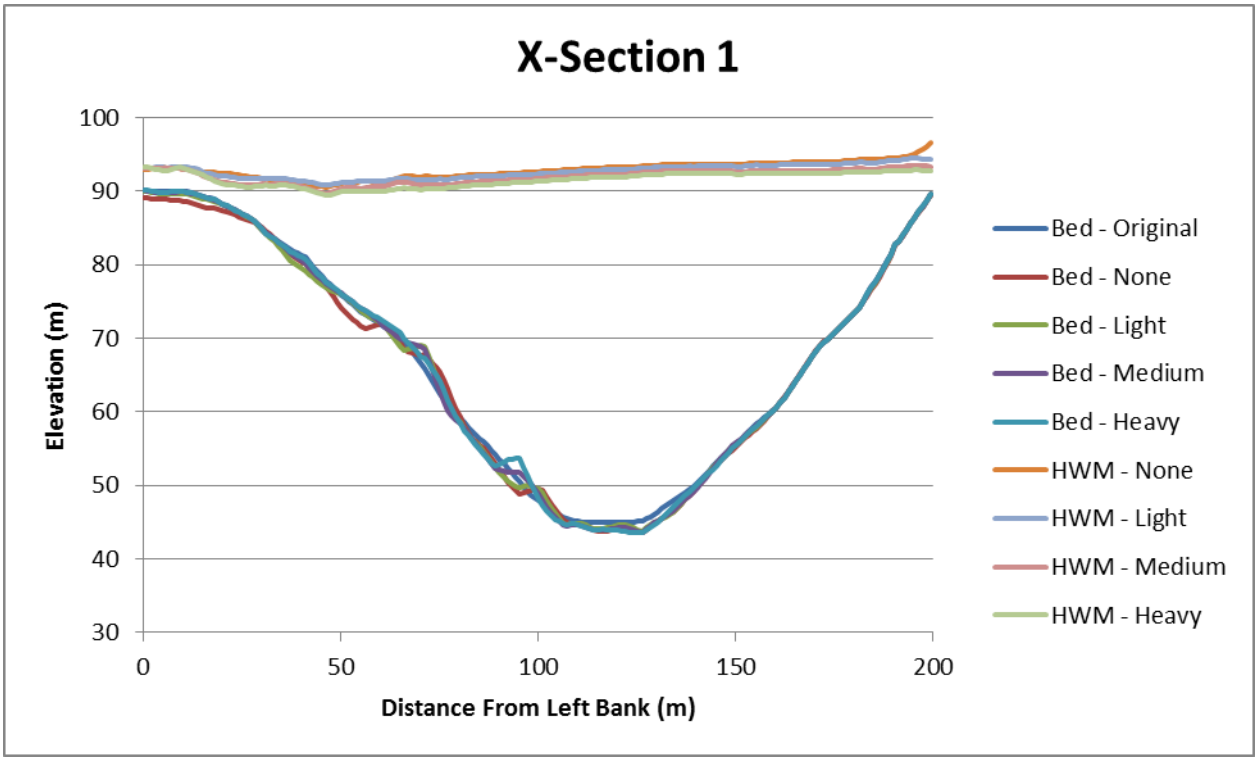

Figure 5-31: HWM and bed elevation at cross-section 1 varying n_v and ϕ' on a mobile-bed

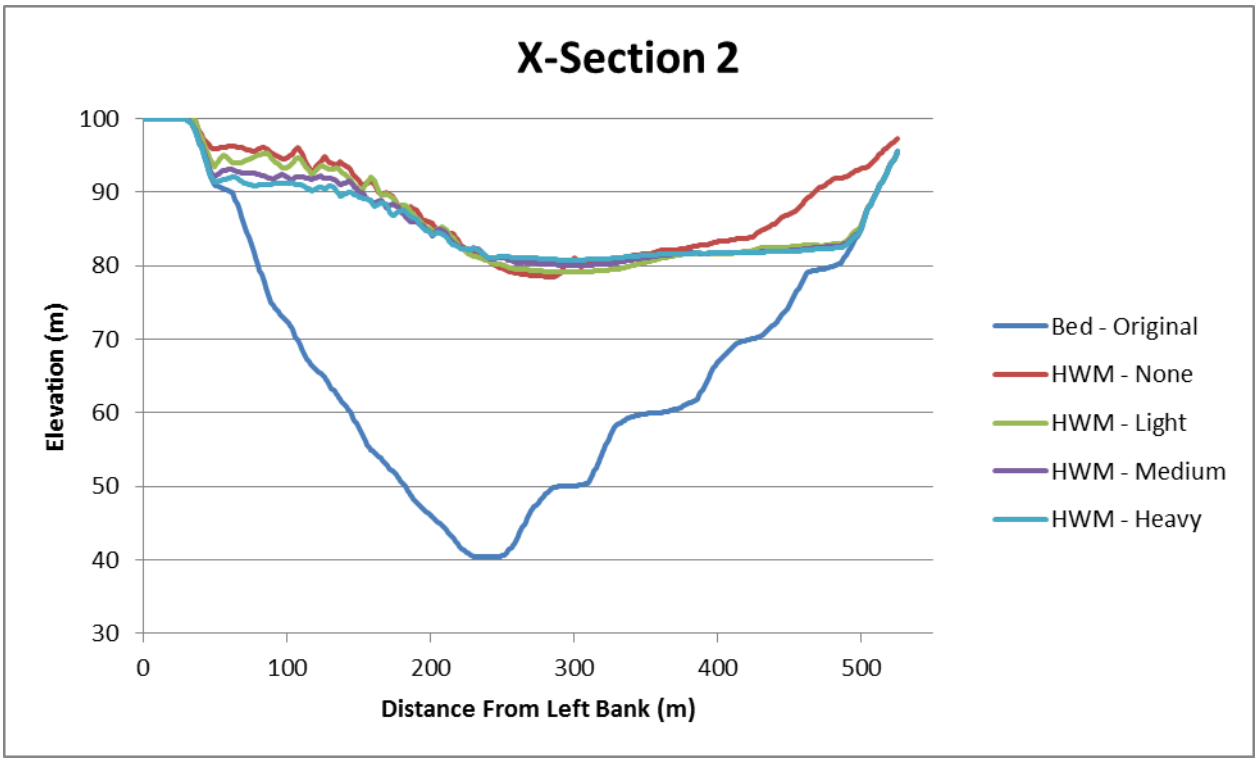

Figure 5-32: HWM at cross-section 2 varying n_v and ϕ' on a fixed-bed

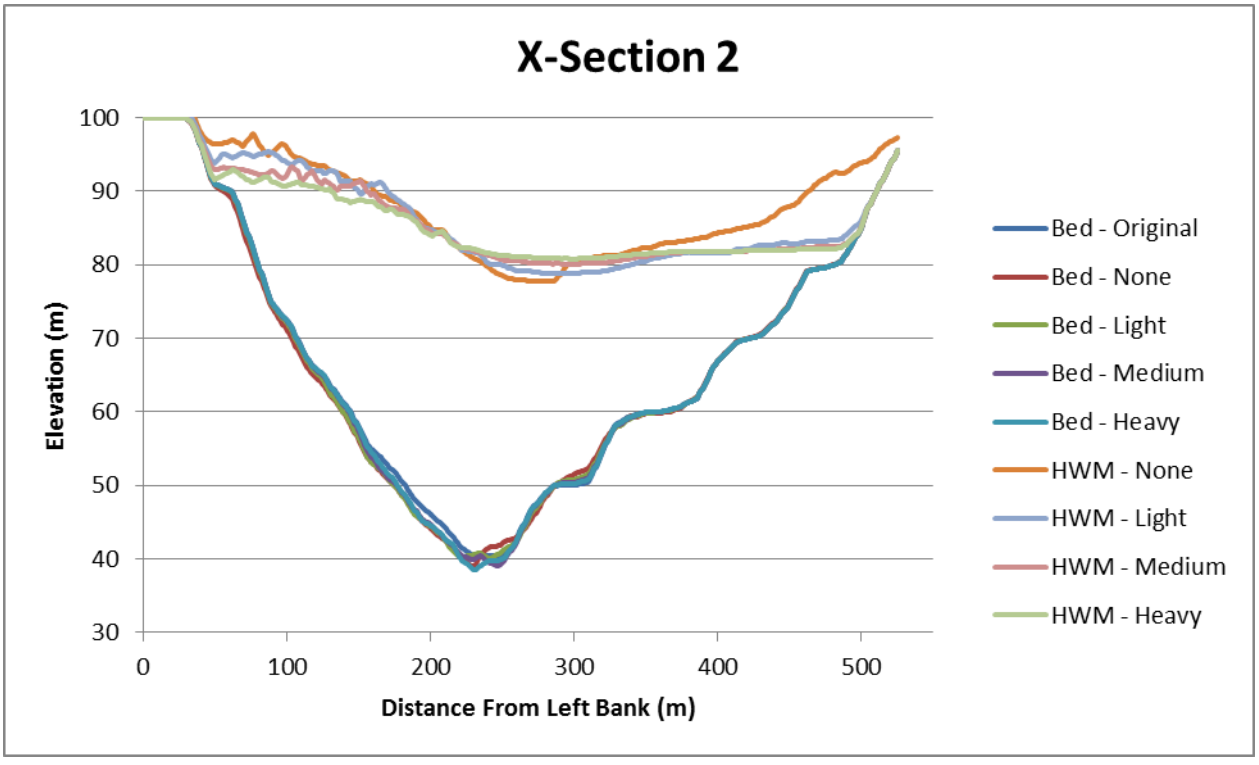

Figure 5-33: HWM and bed elevation at cross-section 2 varying n_v and ϕ' on a mobile-bed

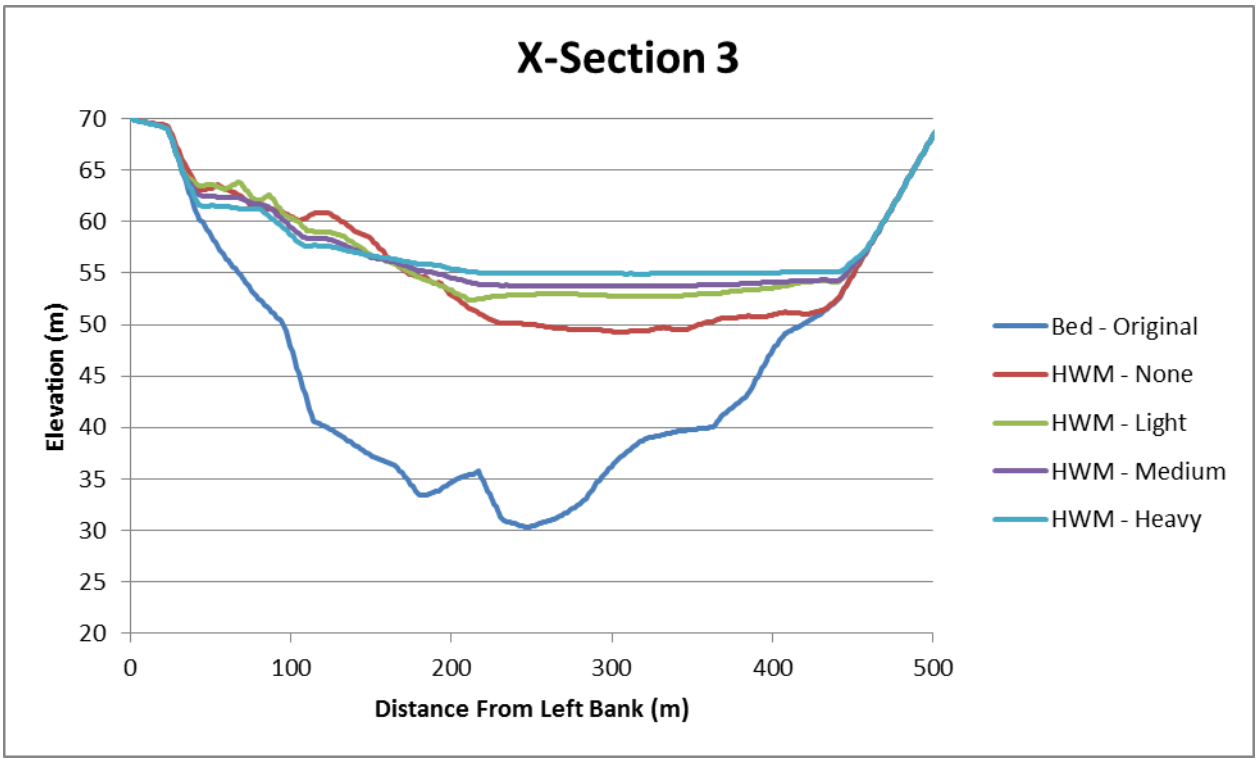

Figure 5-34: HWM at cross-section 3 varying n_v and ϕ' on a fixed-bed

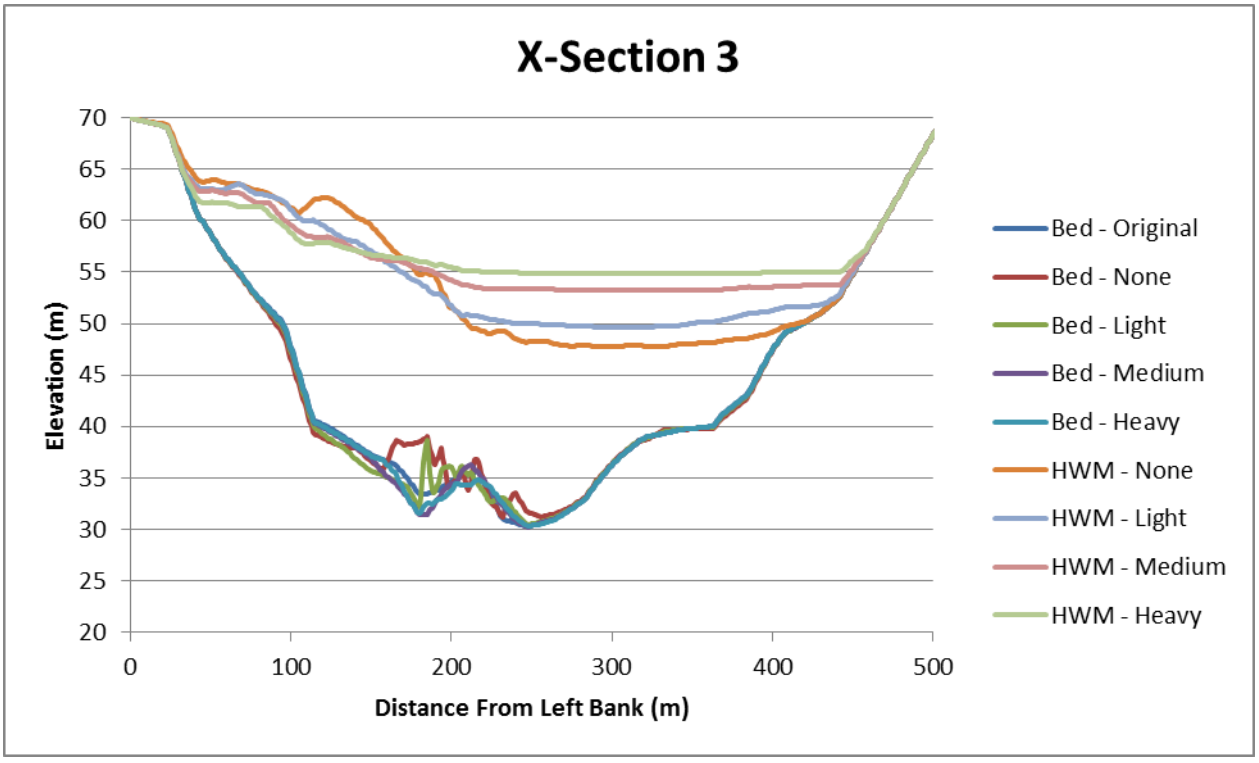

Figure 5-35: HWM and bed elevation at cross-section 3 varying n_v and ϕ' on a mobile-bed

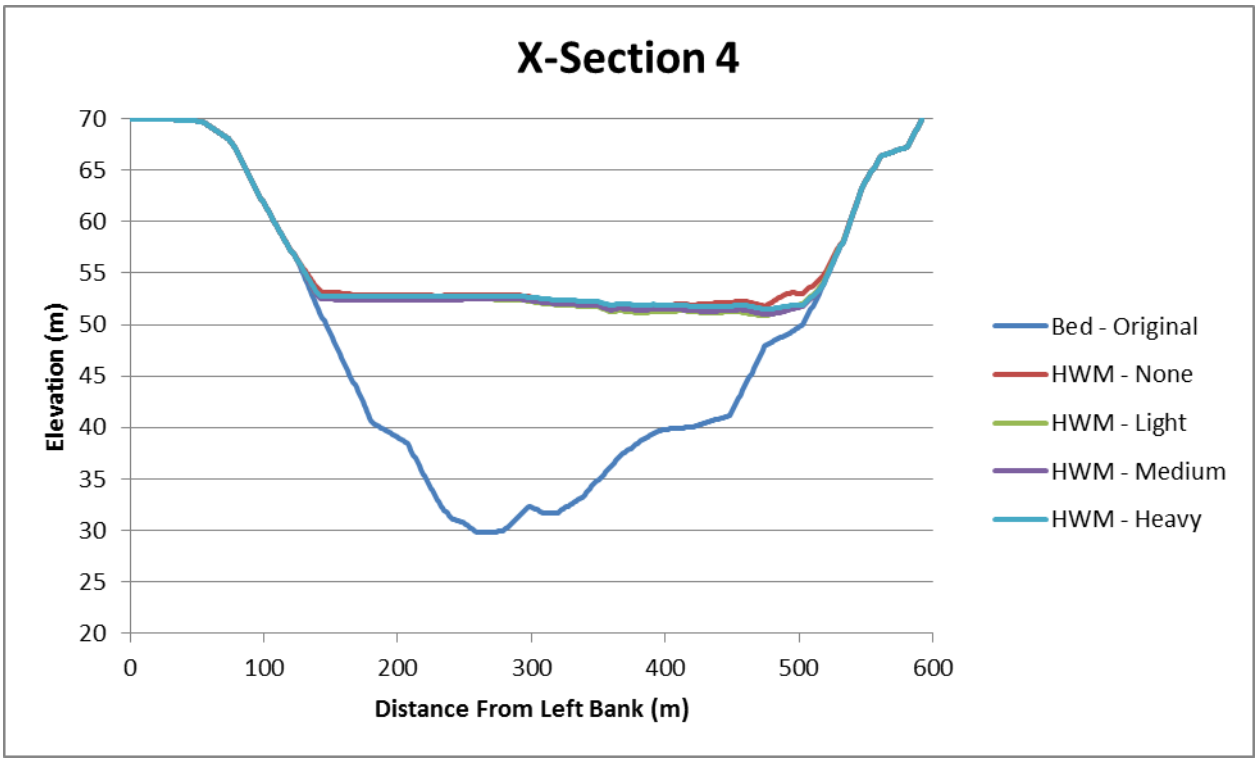

Figure 5-36: HWM at cross-section 4 varying n_v and ϕ' on a fixed-bed

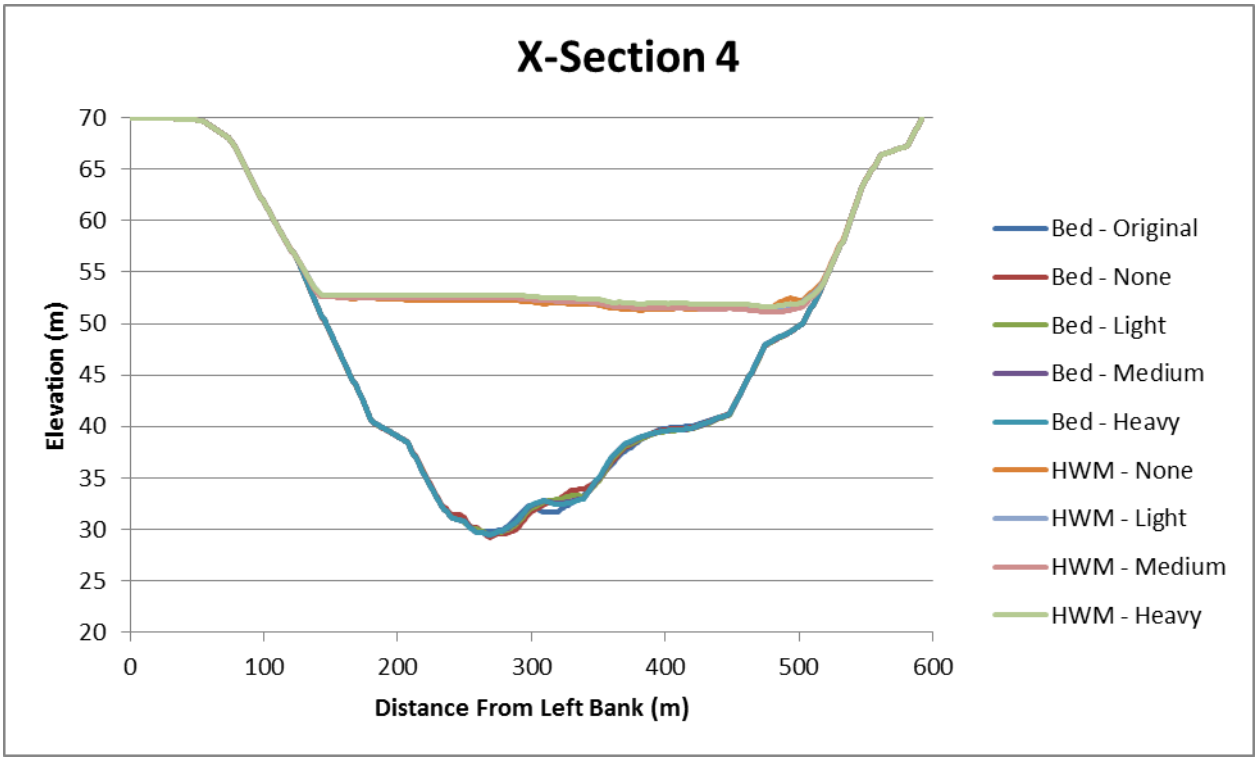

Figure 5-37: HWM and bed elevation at cross-section 4 varying n_v and ϕ' on a mobile-bed

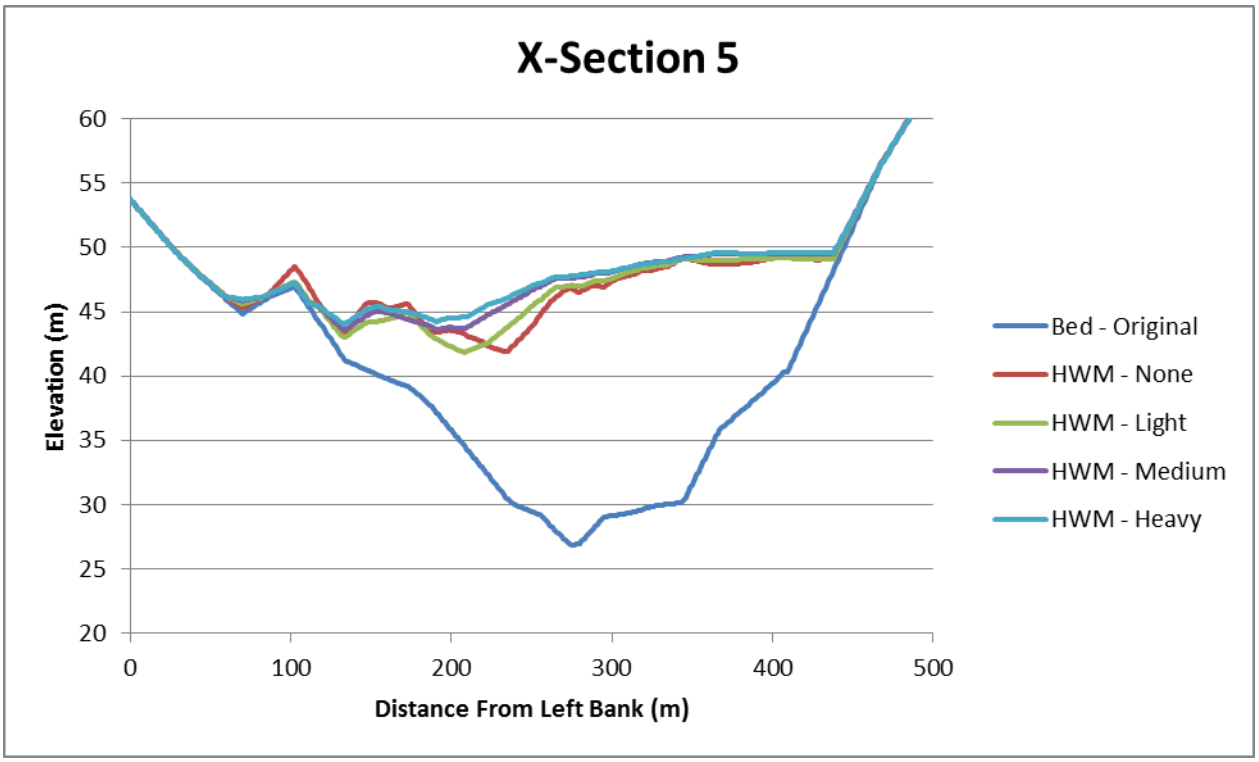

Figure 5-38: HWM at cross-section 5 varying n_v and ϕ' on a fixed-bed

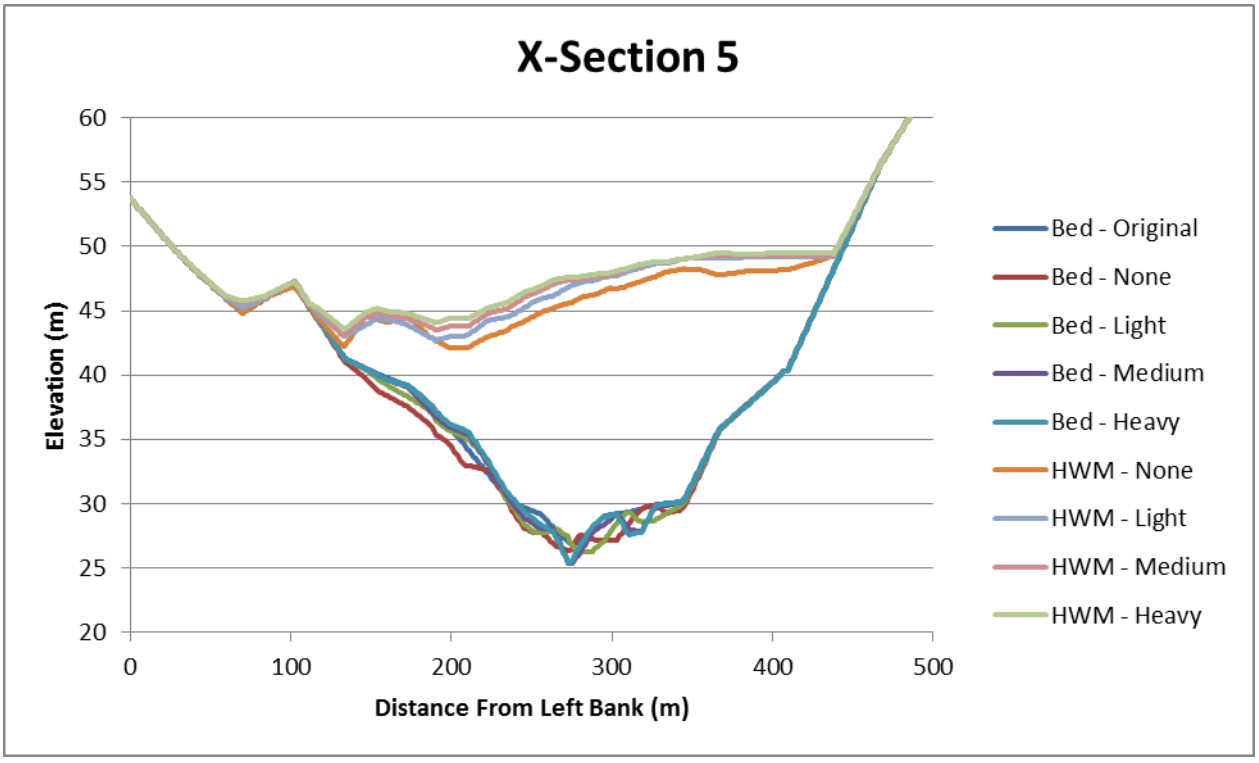

Figure 5-39: HWM and bed elevation at cross-section 5 varying n_v and ϕ' on a mobile-bed

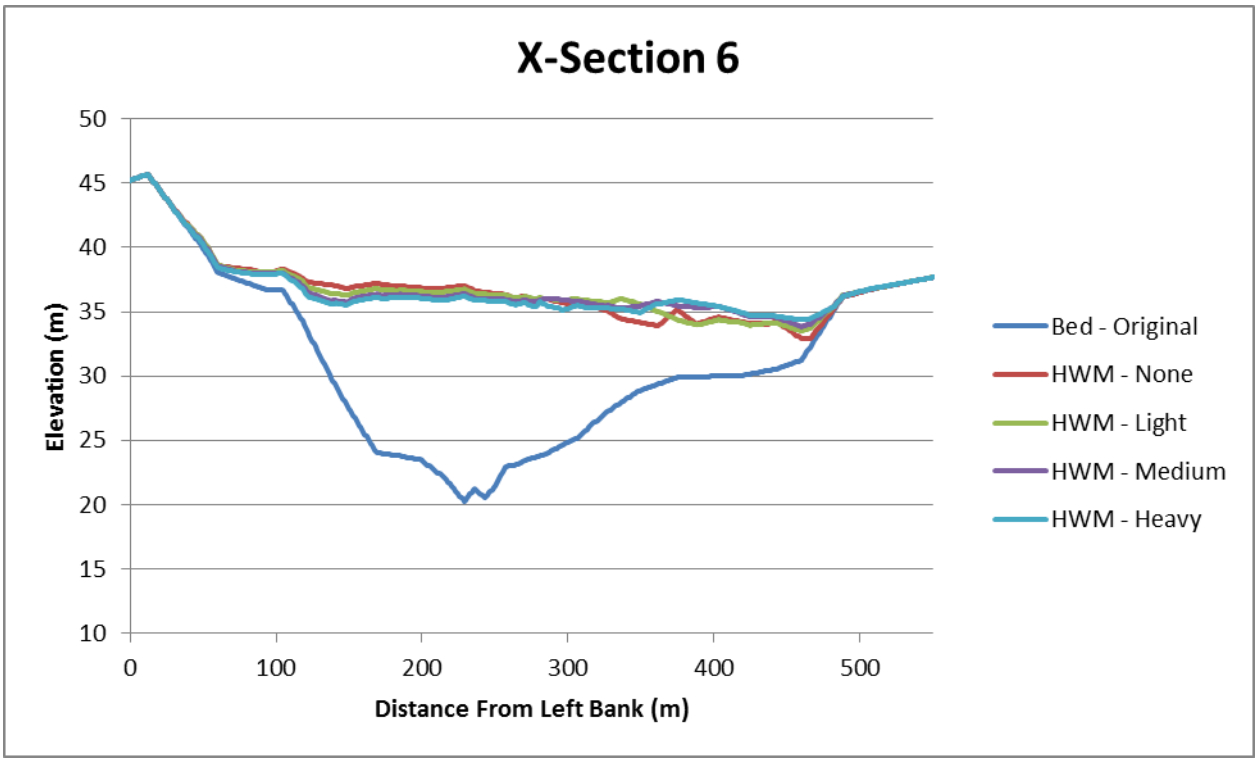

Figure 5-40: HWM at cross-section 6 varying n_v and ϕ' on a fixed-bed

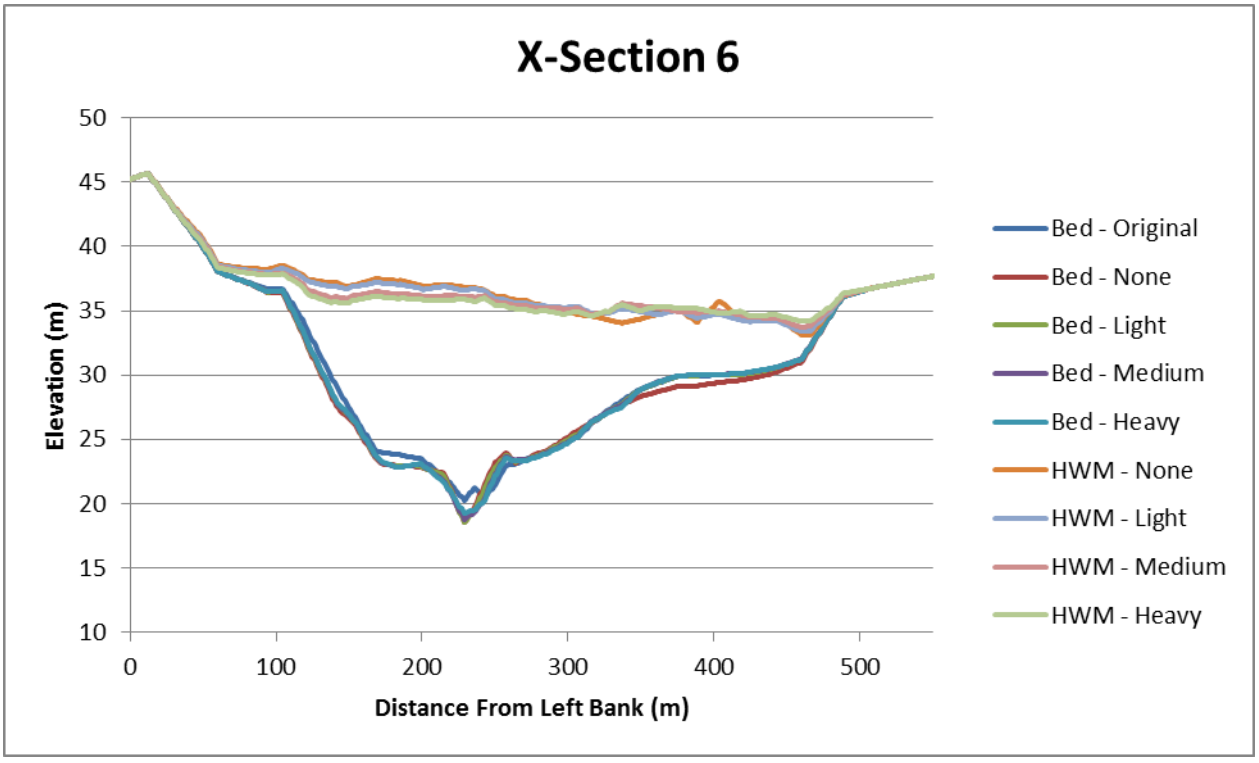

Figure 5-41: HWM and bed elevation at cross-section 6 varying n_v and ϕ' on a mobile-bed

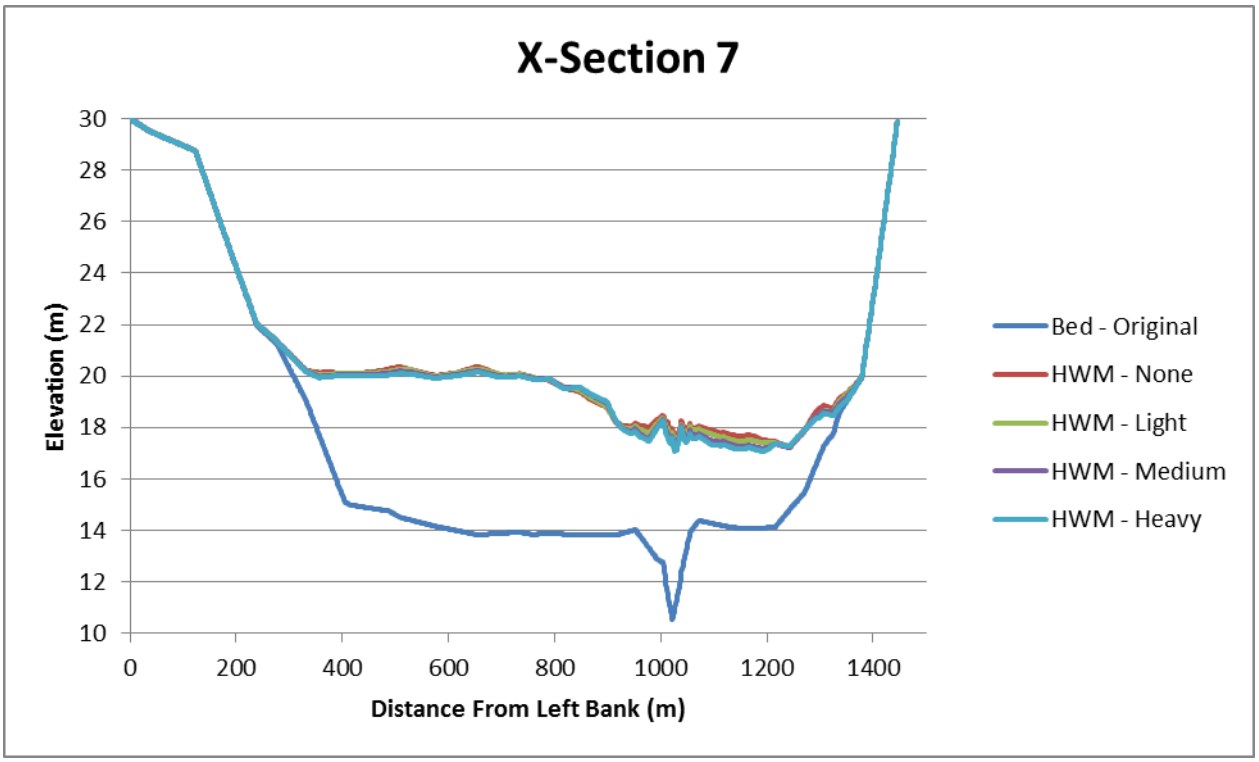

Figure 5-42: HWM at cross-section 7 varying n_v and ϕ' on a fixed-bed

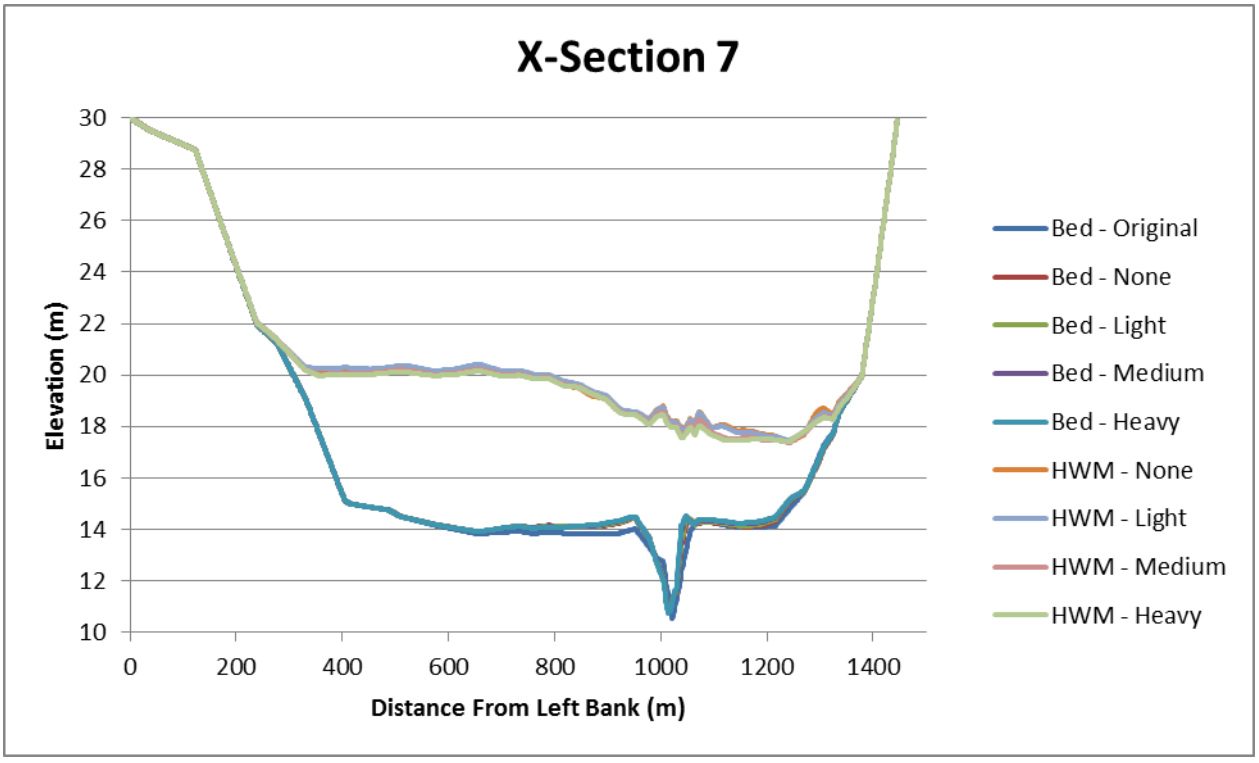

Figure 5-43: HWM and bed elevation at cross-section 7 varying n_v and ϕ' on a mobile-bed

5.2.2 2D BED EVOLUTION

Although the effect of varying vegetation density on bed elevation was indiscernible using the previous cross-sections, the effect of increasing vegetation density is clearly demonstrated in the 2D bed evolution plots **(Figure 5-44 to Figure 5-47)**. As vegetation density is increased, the zones of significant erosion (blue) and deposition (red) shrink, especially in regions on the flood plain. This indicates that τ_v^* increases, leading to a decrease in τ_g^* as vegetation density increases.

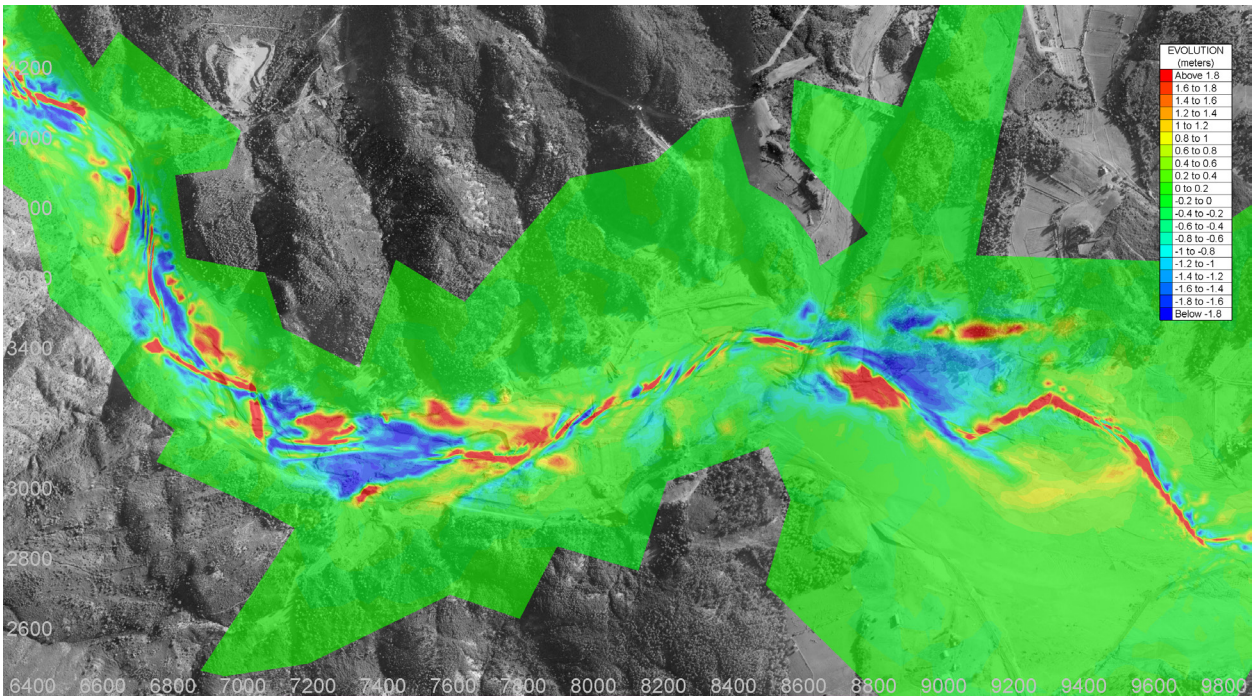

Figure 5-44

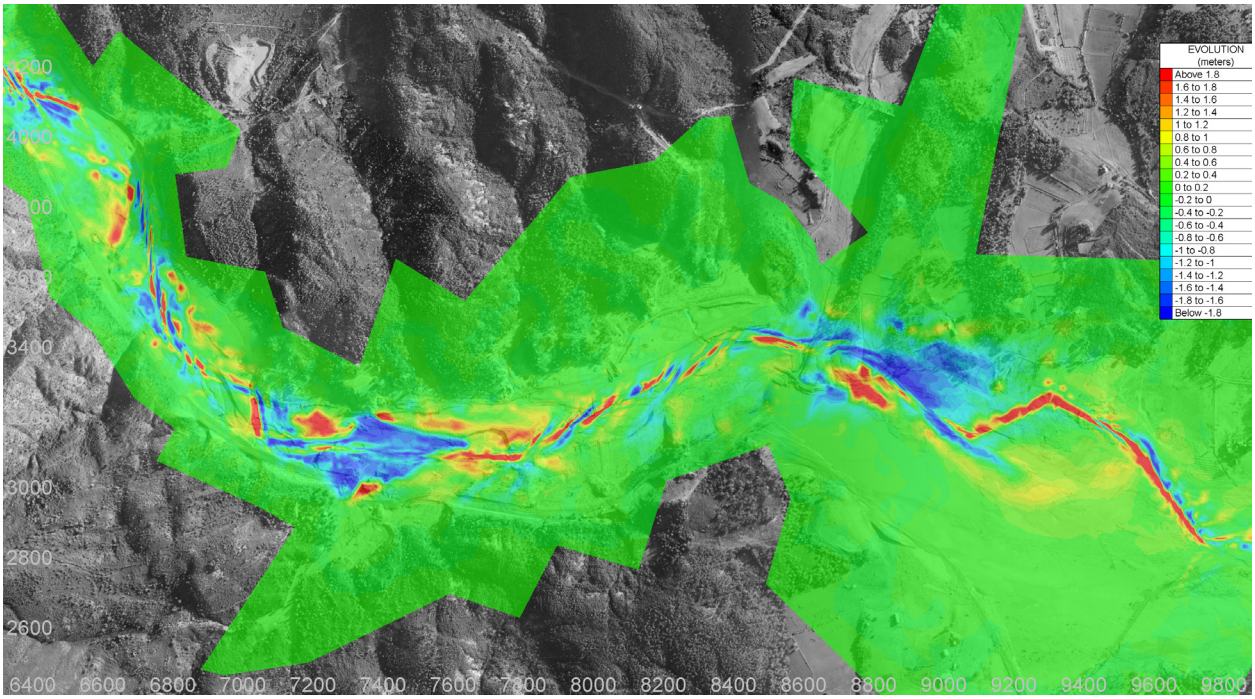

Figure 5-45

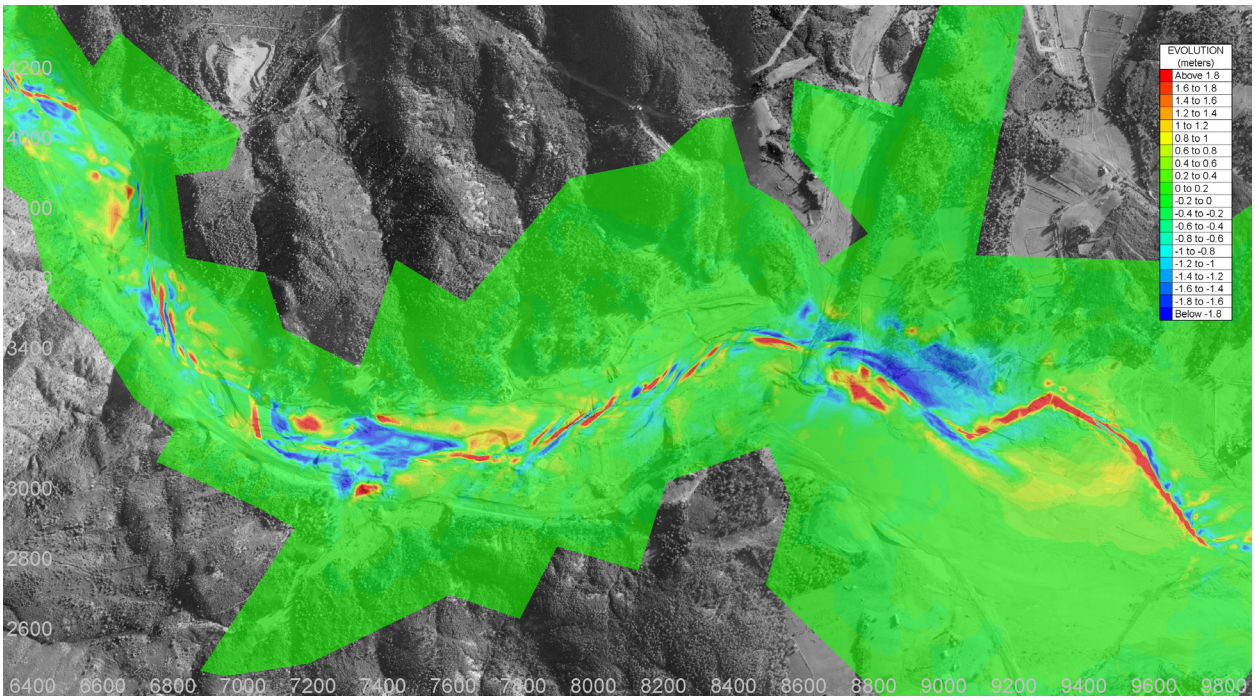

Figure 5-46

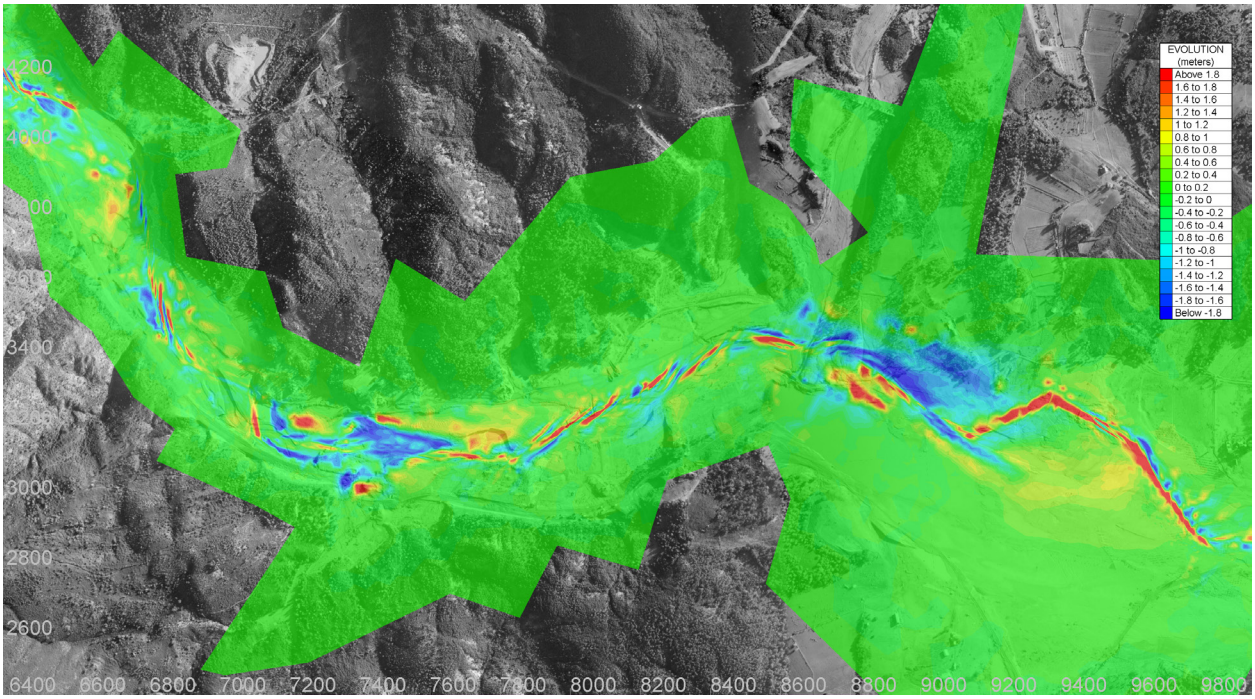

Figure 5-47

Figure 5-44: Bed evolution of case where: $n_g = 0.025$, $n_v = 0.000$, $\phi' = 40°$, and $d_{50} = 1\ mm$ (positive evolution = deposition, negative evolution = erosion) (aerial photograph of Frejus [FR 177-150, #1 to #104] in 1959 © IGN, 2012, by permission)

Figure 5-45: Bed evolution of case where: $n_g = 0.025$, $n_v = 0.033$, $\phi' = 49°$, and $d_{50} = 1\ mm$ (positive evolution = deposition, negative evolution = erosion) (aerial photograph of Frejus [FR 177-150, #1 to #104] in 1959 © IGN, 2012, by permission)

Figure 5-46: Bed evolution of case where: $n_g = 0.025$, $n_v = 0.067$, $\phi' = 60°$, and $d_{50} = 1\ mm$ (positive evolution = deposition, negative evolution = erosion) (aerial photograph of Frejus [FR 177-150, #1 to #104] in 1959 © IGN, 2012, by permission)

Figure 5-47: Bed evolution of case where: $n_g = 0.025$, $n_v = 0.090$, $\phi' = 70°$, and $d_{50} = 1\ mm$ (positive evolution = deposition, negative evolution = erosion) (aerial photograph of Frejus [FR 177-150, #1 to #104] in 1959 © IGN, 2012, by permission)

5.2.3 FLOOD-WAVE PROPAGATION TIME

5.2.3.1 MOBILE-BED SIMULATIONS

Figure 5-48 to **Figure 5-50** show the extent that the dam-break flood-wave has propagated after $t = 30\ min$ with $n_g = 0.025$, 0.030, and 0.035 respectively for a mobile-bed. As n_g increases, it can be observed that the distance travelled by the flood-wave after $t = 30\ min$ decreases; this is due to the increase in friction experienced by the flood-wave. Regardless of the effect of n_g, it is observed that as vegetation density increases, the distance propagated by the flood-wave decreases. The figures below show this to be true for all values of n_g.

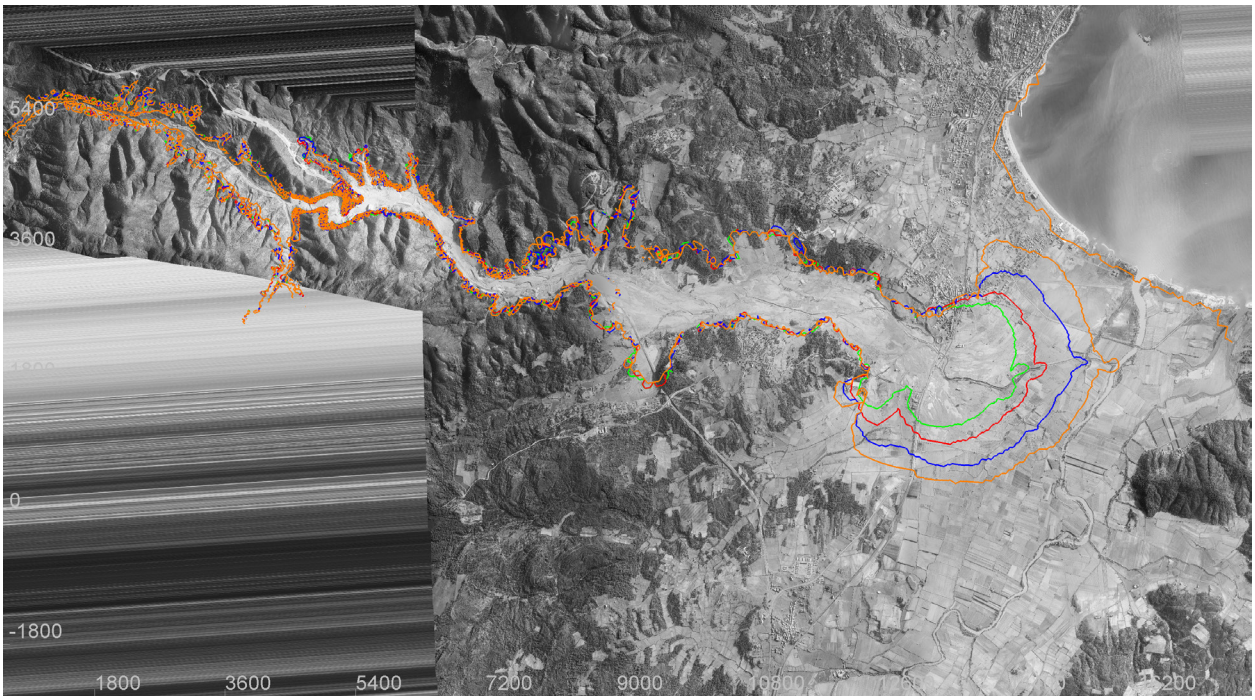

Figure 5-48

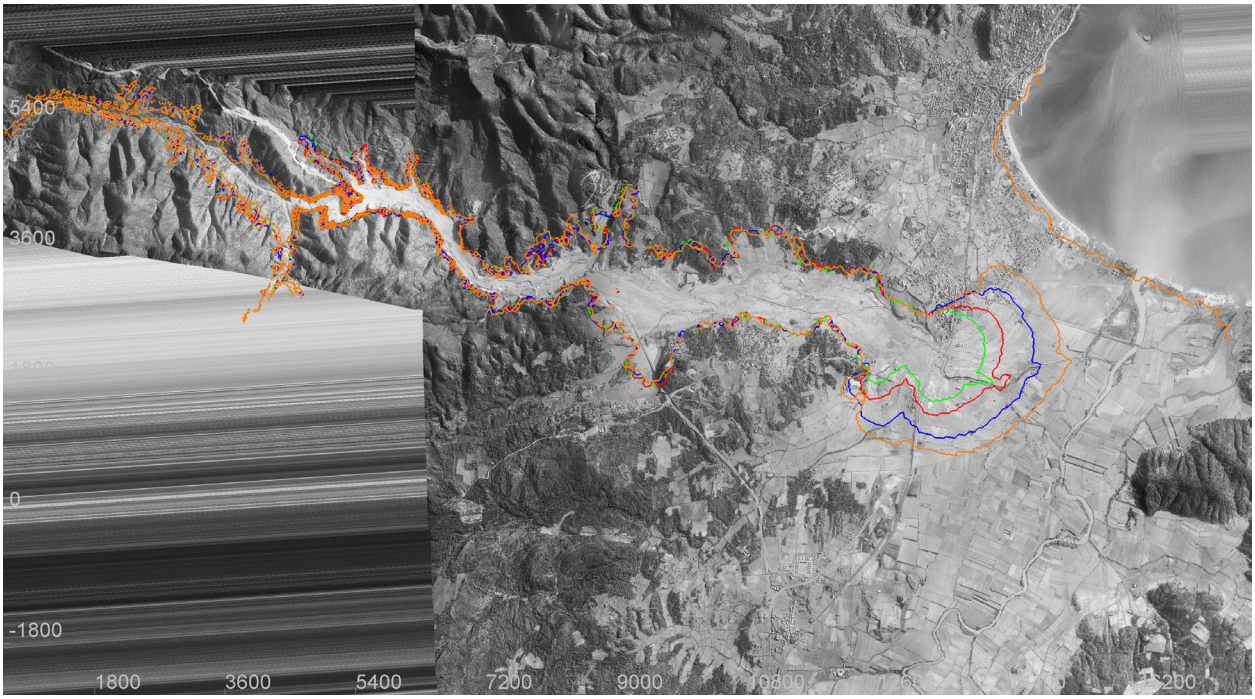

Figure 5-49

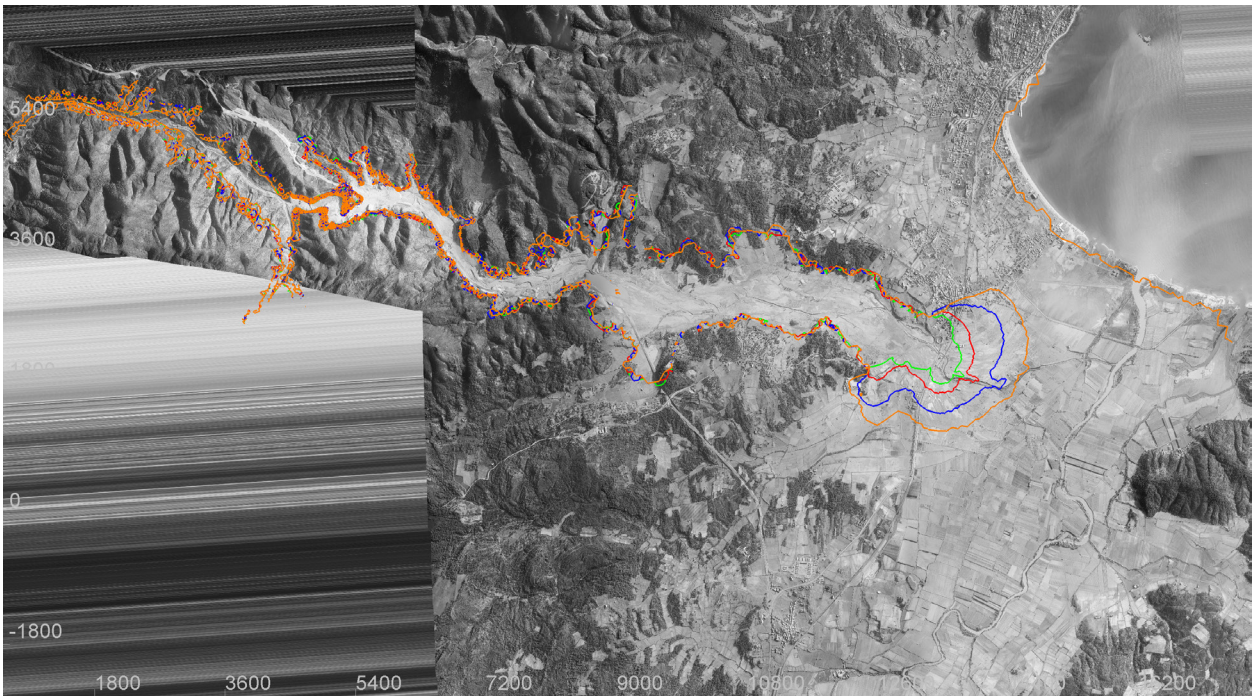

Figure 5-50

Figure 5-48: Extent of inundation 30 minutes after dam-break on a mobile-bed with $n_g = 0.025$, and $d_{50} = 1\ mm$ (orange – $n_v = 0.000$ and $\phi' = 40°$, blue – $n_v = 0.033$ and $\phi' = 49°$, red – $n_v = 0.067$ and $\phi' = 60°$, green – $n_v = 0.090$ and $\phi' = 70°$) (aerial photograph of Frejus [FR 177-150, #1 to #104] in 1959 © IGN, 2012, by permission)

Figure 5-49: Extent of inundation 30 minutes after dam-break on a mobile-bed with $n_g = 0.030$, and $d_{50} = 1\ mm$ (orange – $n_v = 0.000$ and $\phi' = 40°$, blue – $n_v = 0.033$ and $\phi' = 49°$, red – $n_v = 0.067$ and $\phi' = 60°$, green – $n_v = 0.090$ and $\phi' = 70°$) (aerial photograph of Frejus [FR 177-150, #1 to #104] in 1959 © IGN, 2012, by permission)

Figure 5-50: Extent of inundation 30 minutes after dam-break on a mobile-bed with $n_g = 0.035$, and $d_{50} = 1\ mm$ (orange – $n_v = 0.000$ and $\phi' = 40°$, blue – $n_v = 0.033$ and $\phi' = 49°$, red – $n_v = 0.067$ and $\phi' = 60°$, green – $n_v = 0.090$ and $\phi' = 70°$) (aerial photograph of Frejus [FR 177-150, #1 to #104] in 1959 © IGN, 2012, by permission)

Referring to **Table 5-1**, it can be seen that if n_g and d_{50} are held constant with only n_v and ϕ' varying, the conclusion that increasing vegetation density will increase flood-wave travel time to the Mediterranean Sea is consistently true.

5.2.3.2 FIXED-BED SIMULATIONS

Figure 5-51 to **Figure 5-53** show the extent that the dam-break flood-wave has propagated after $t = 30\ min$ with $n_g = 0.025$, 0.030, and 0.035 respectively for a fixed-bed. As n_g increases, it can be observed that the distance travelled by the flood-wave after $t = 30\ min$ decreases; this is due to the increase in friction experienced by the flood-wave. Regardless of the effect of n_g, it is observed that as vegetation density increases, the distance propagated by the flood-wave decreases. The figures below show this to be true for all values of n_g.

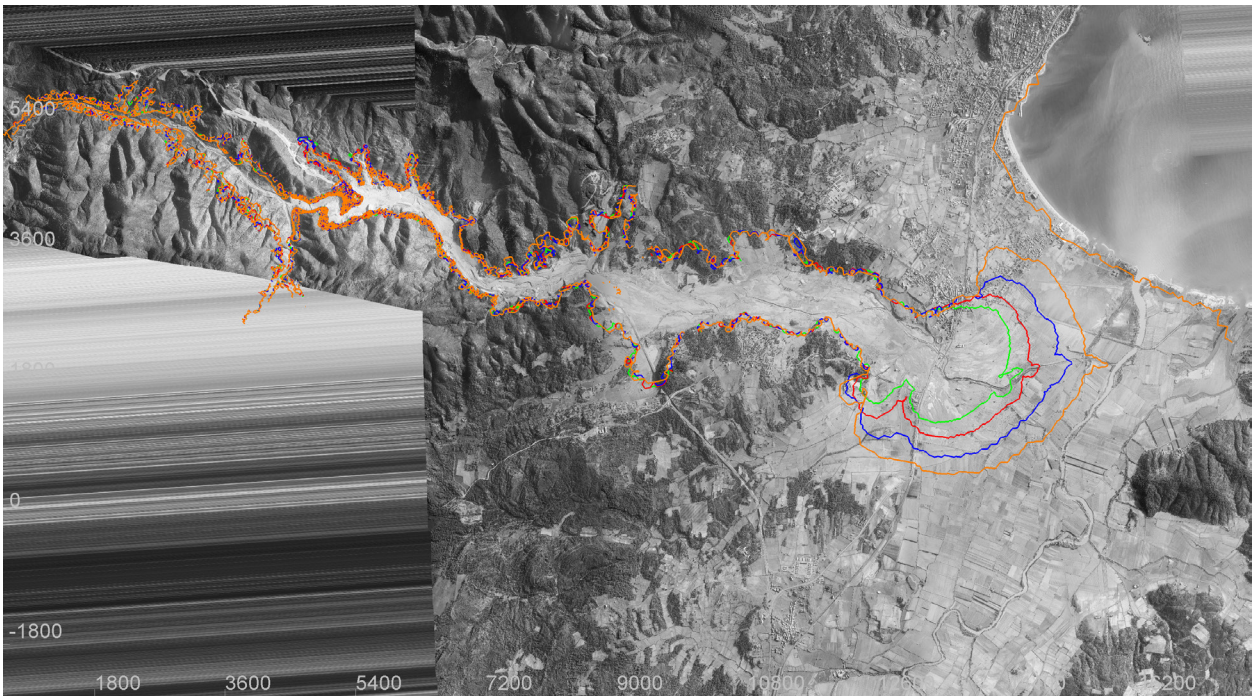

Figure 5-51

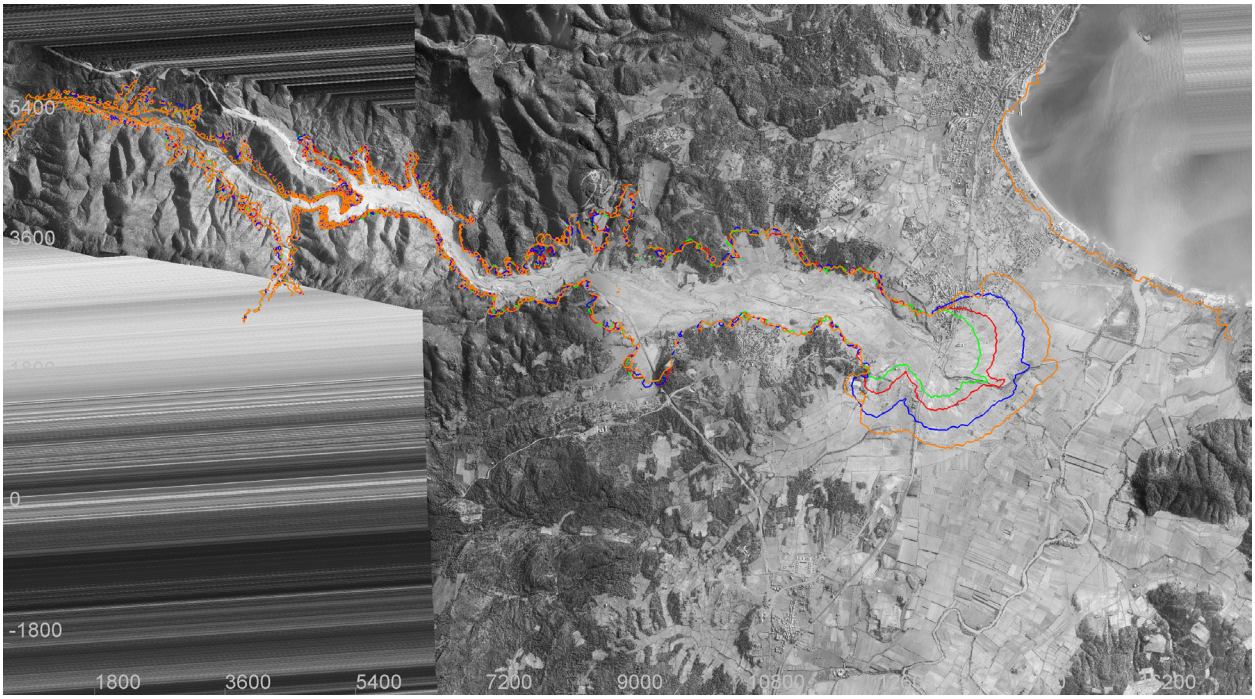

Figure 5-52

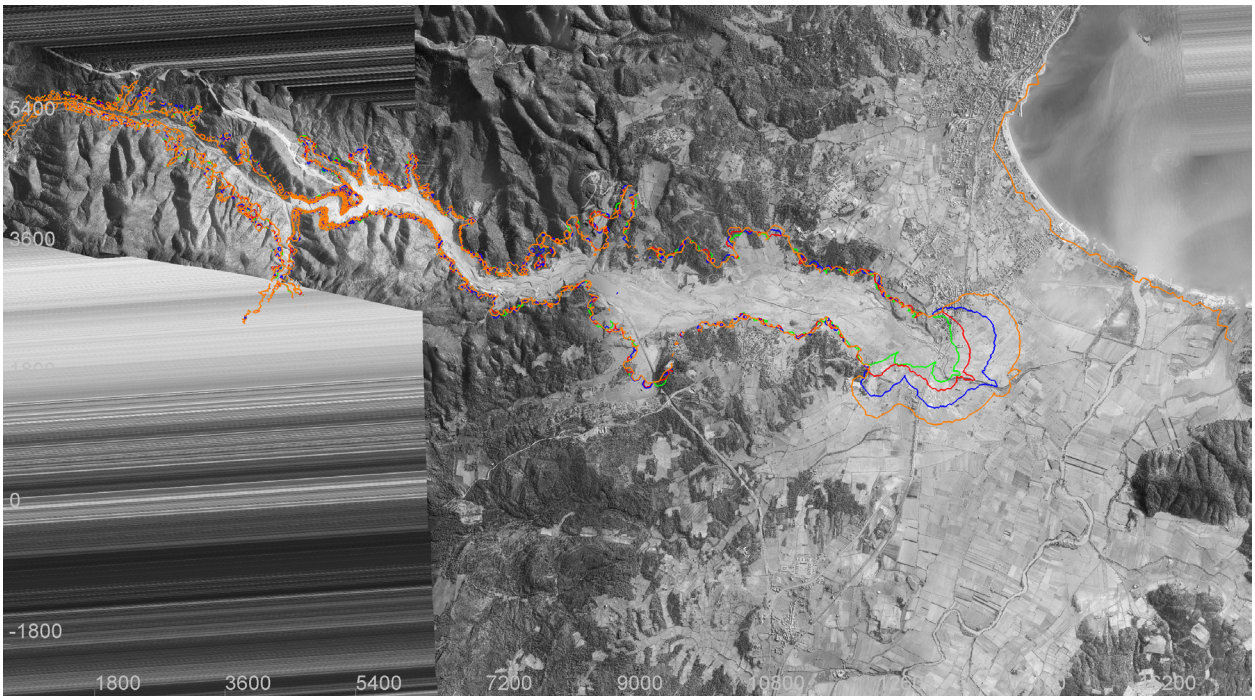

Figure 5-53

Figure 5-51: Extent of inundation 30 minutes after dam-break on a fixed-bed with $n_g = 0.025$ (orange – $n_v = 0.000$, blue – $n_v = 0.033$, red – $n_v = 0.067$, green – $n_v = 0.090$) (aerial photograph of Frejus [FR 177-150, #1 to #104] in 1959 © IGN, 2012, by permission)

Figure 5-52: Extent of inundation 30 minutes after dam-break on a fixed-bed with $n_g = 0.030$ (orange – $n_v = 0.000$, blue – $n_v = 0.033$, red – $n_v = 0.067$, green – $n_v = 0.090$) (aerial photograph of Frejus [FR 177-150, #1 to #104] in 1959 © IGN, 2012, by permission)

Figure 5-53: Extent of inundation 30 minutes after dam-break on a fixed-bed with $n_g = 0.035$ (orange – $n_v = 0.000$, blue – $n_v = 0.033$, red – $n_v = 0.067$, green – $n_v = 0.090$) (aerial photograph of Frejus [FR 177-150, #1 to #104] in 1959 © IGN, 2012, by permission)

Referring to **Table 5-2**, it can be seen that if n_g is held constant with only n_v varying, the conclusion that increasing vegetation density will increase flood-wave travel time to the Mediterranean Sea is consistently true.

5.2.4 PRE-/POST-DAM-BREAK STEADY-STATE HYDRODYNAMICS

To compare how the morphology of the Reyran River and its flood plain changed as a result of the propagation of a dam-break flood-wave, steady-state fixed-bed hydrodynamic simulations were run. From these simulations, it was possible to examine how zones of inundation were affected under the assumed mean annual flood of $Q = 100\ m^3/s$.

As a proof-of-concept trial, steady-state hydrodynamic simulations were run with parameters of $n_g = 0.035$, $d_{50} = 40\ mm$, and $Q = 100\ m^3/s$, and vegetation density varying from no vegetation ($n_v = 0.000$ and $\phi' = 40°$) to heavy vegetation ($n_v = 0.090$ and $\phi' = 70°$). **Figure 5-54**, **Figure 5-56**, **Figure 5-58**, and **Figure 5-60** show the pre-dam-break inundated zones, and **Figure 5-55**, **Figure 5-57**, **Figure 5-59**, and **Figure 5-61** show the post-dam-break inundated zones for the different vegetation density scenarios.

From the following figures, it is clear that zones of inundation are somewhat different. For example, in the pre-dam-break figures, the area directly west of Frejus and the river is inundated; this region is no longer inundated post-dam-break. The morphological changes caused by propagation of the dam-break flood-wave yield many alterations in zones of inundation.

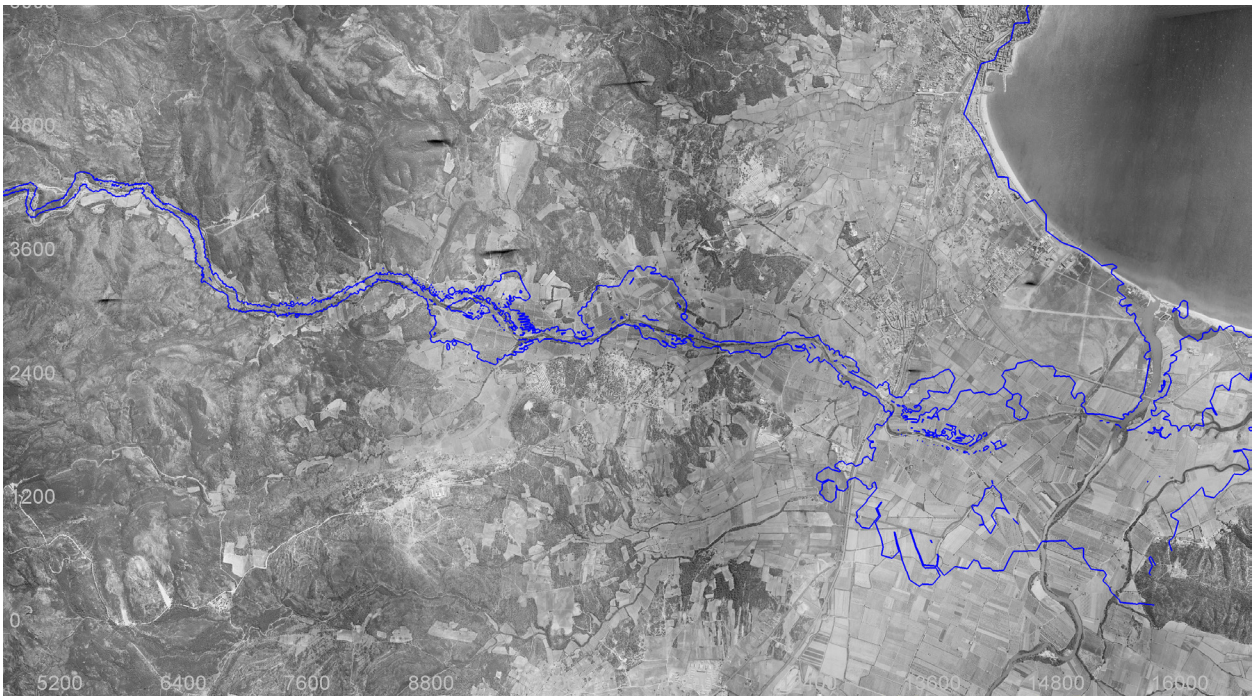

Figure 5-54

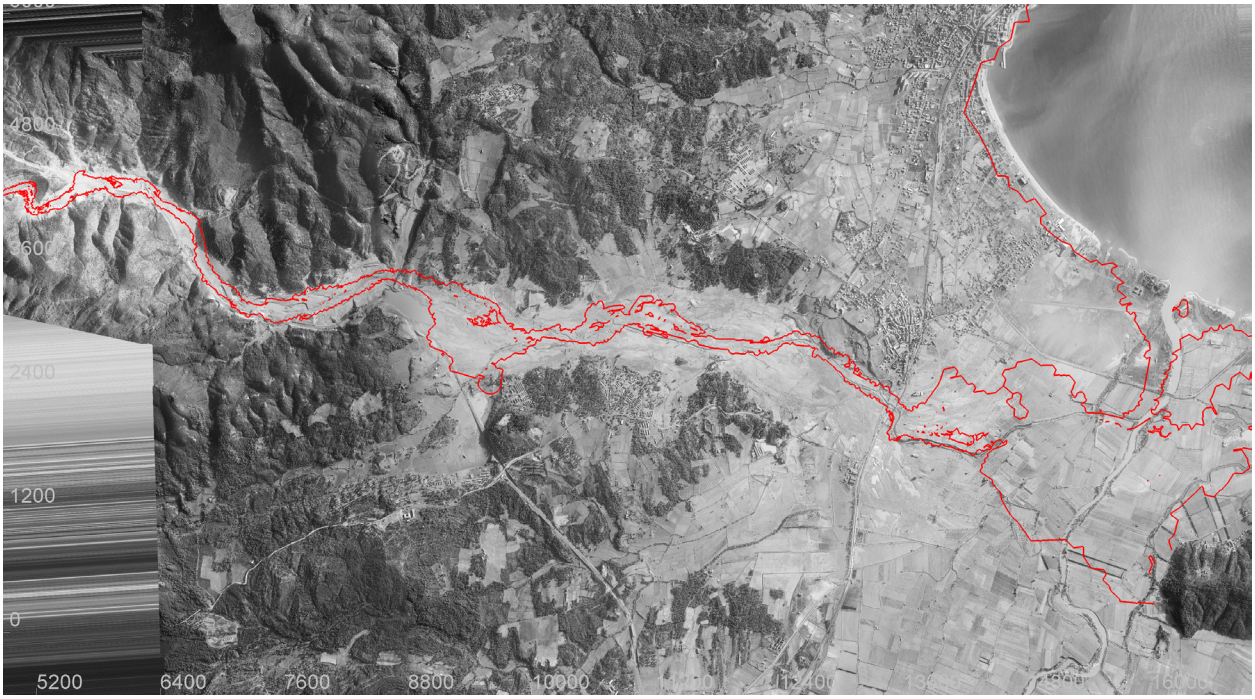

Figure 5-55

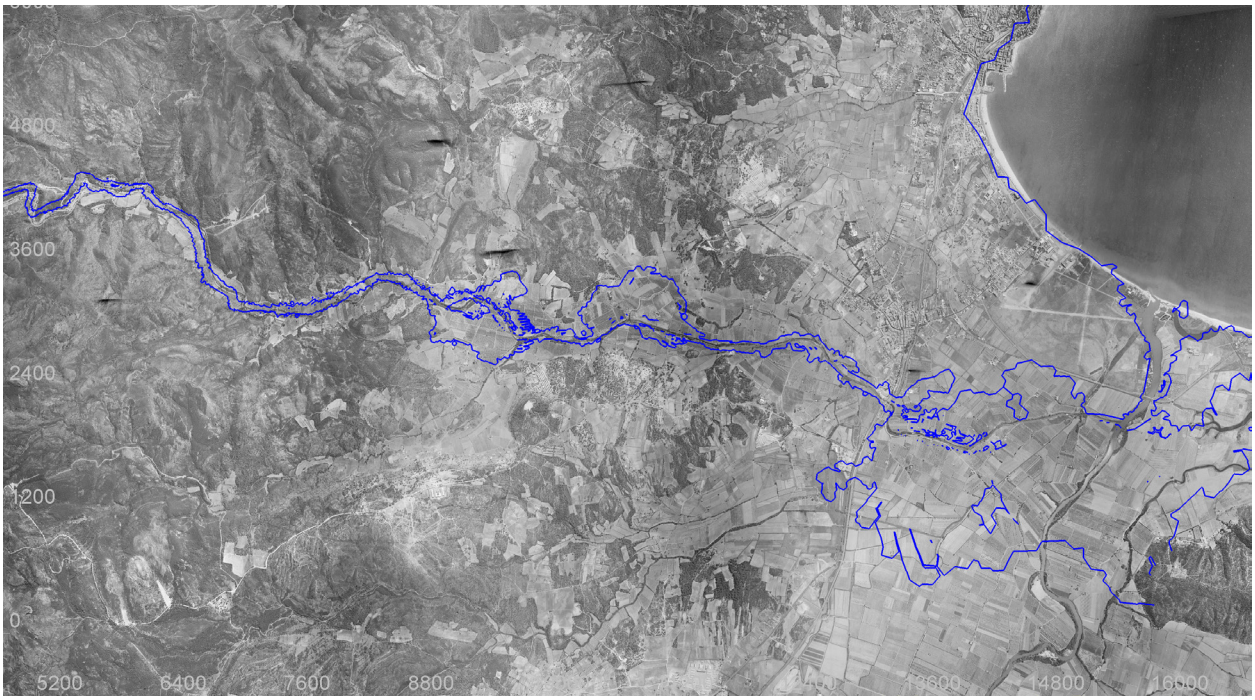

Figure 5-56

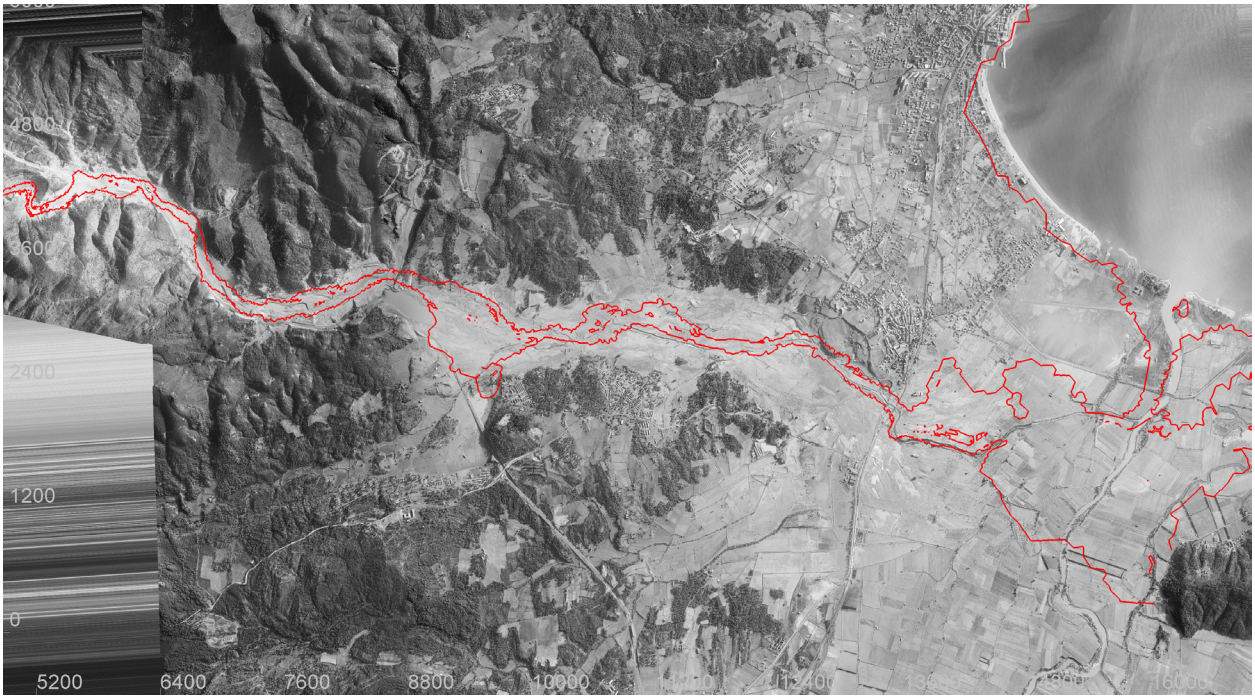

Figure 5-57

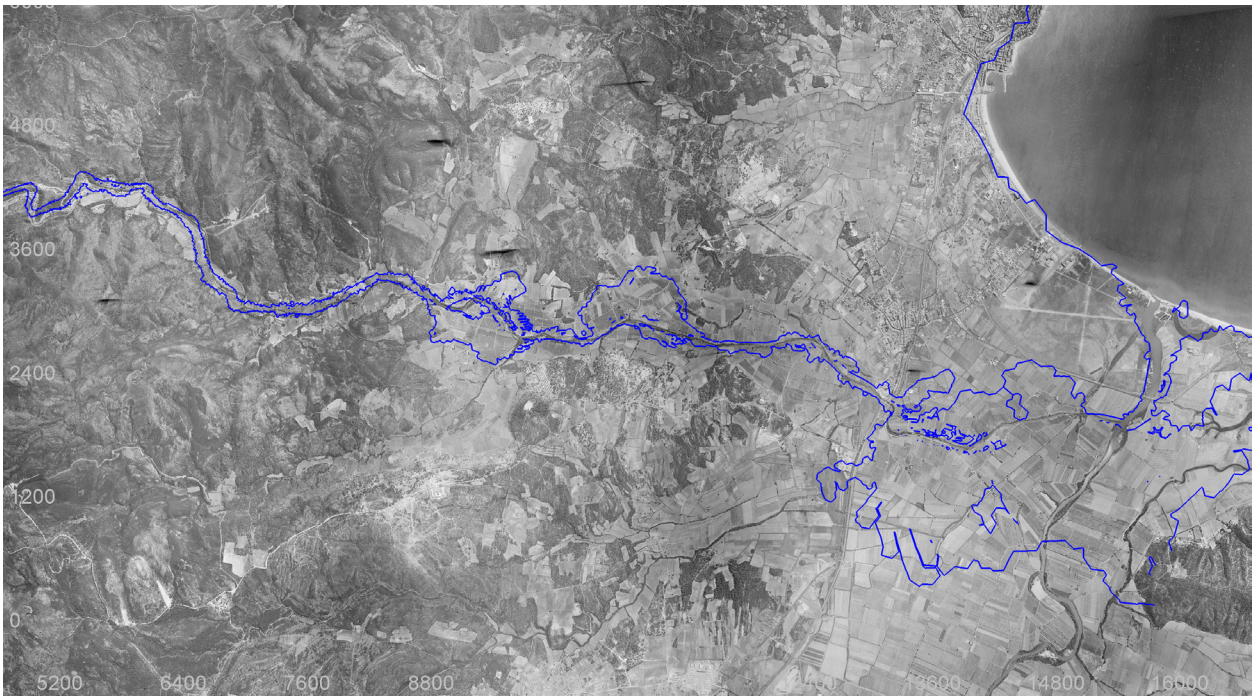

Figure 5-58

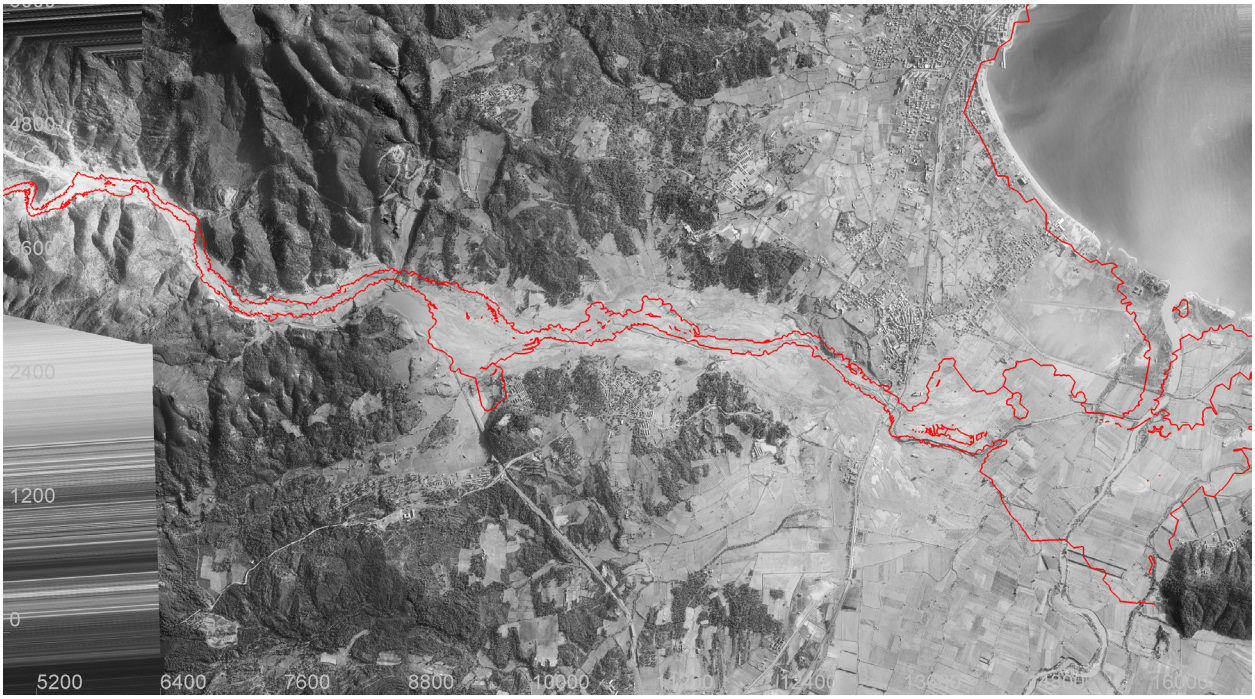

Figure 5-59

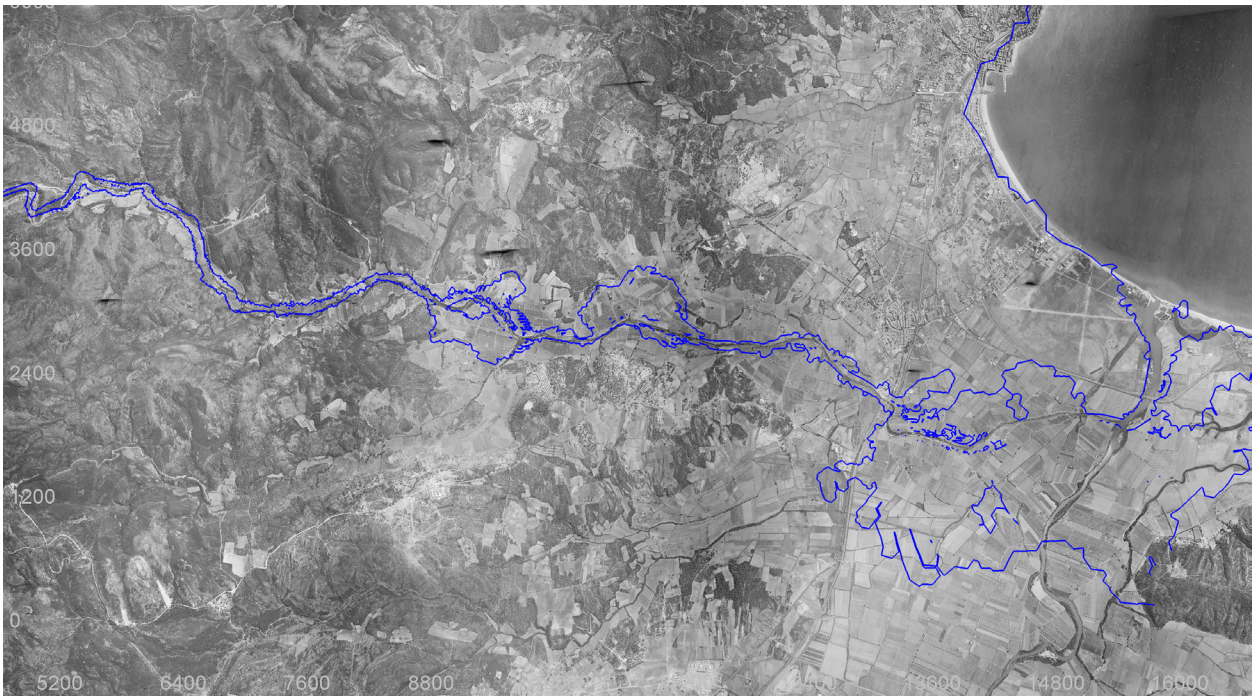

Figure 5-60

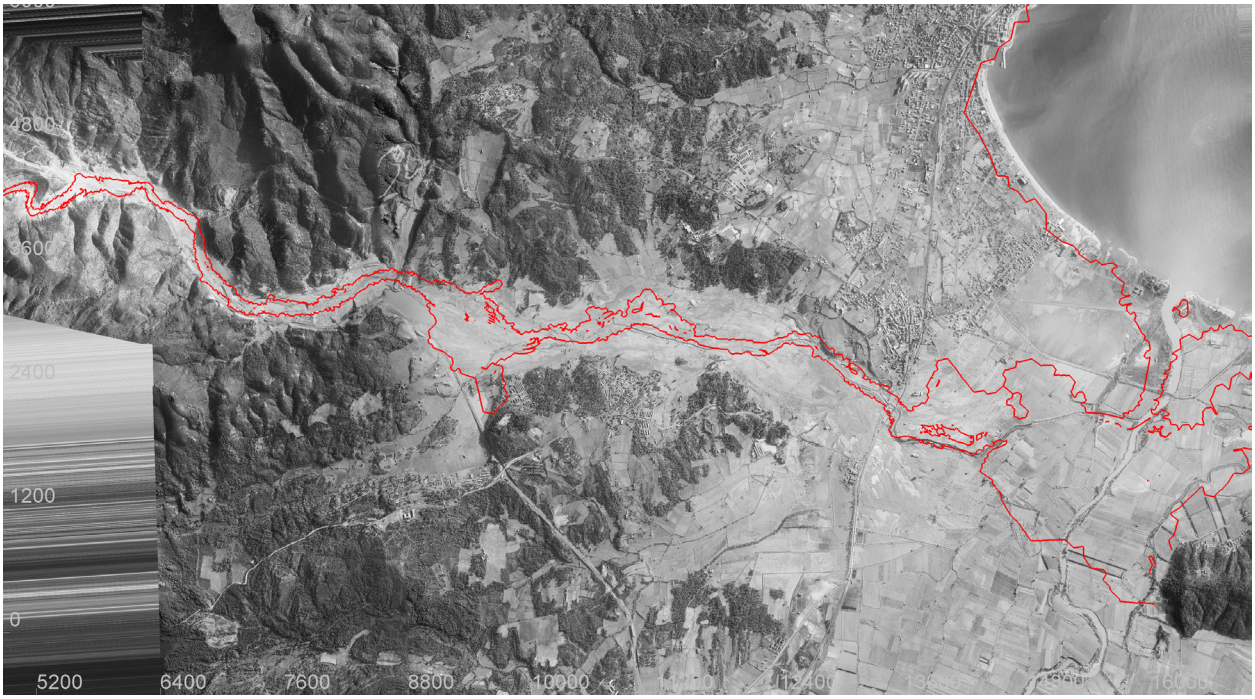

Figure 5-61

Figure 5-54: Pre-dam-break inundation under steady-state fixed-bed conditions with $n_g = 0.035$, $n_v = 0.000$, $\phi' = 40°$, $d_{50} = 40\ mm$, and $Q = 100\ m^3/s$ (aerial photograph of Frejus [3544-3644, #41 to #121] in 1955 © IGN, 2012, by permission)

Figure 5-55: Post-dam-break inundation under steady-state fixed-bed conditions with $n_g = 0.035$, $n_v = 0.000$, $\phi' = 40°$, $d_{50} = 40\ mm$, and $Q = 100\ m^3/s$ (aerial photograph of Frejus [FR 177-150, #1 to #104] in 1959 © IGN, 2012, by permission)

Figure 5-56: Pre-dam-break inundation under steady-state fixed-bed conditions with $n_g = 0.035$, $n_v = 0.033$, $\phi' = 49°$, $d_{50} = 40\ mm$, and $Q = 100\ m^3/s$ (aerial photograph of Frejus [3544-3644, #41 to #121] in 1955 © IGN, 2012, by permission)

Figure 5-57: Post-dam-break inundation under steady-state fixed-bed conditions with $n_g = 0.035$, $n_v = 0.033$, $\phi' = 49°$, $d_{50} = 40\ mm$, and $Q = 100\ m^3/s$ (aerial photograph of Frejus [FR 177-150, #1 to #104] in 1959 © IGN, 2012, by permission)

Figure 5-58: Pre-dam-break inundation under steady-state fixed-bed conditions with $n_g = 0.035$, $n_v = 0.067$, $\phi' = 60°$, $d_{50} = 40\ mm$, and $Q = 100\ m^3/s$ (aerial photograph of Frejus [3544-3644, #41 to #121] in 1955 © IGN, 2012, by permission)

Figure 5-59: Post-dam-break inundation under steady-state fixed-bed conditions with $n_g = 0.035$, $n_v = 0.067$, $\phi' = 60°$, $d_{50} = 40\ mm$, and $Q = 100\ m^3/s$ (aerial photograph of Frejus [FR 177-150, #1 to #104] in 1959 © IGN, 2012, by permission)

Figure 5-60: Pre-dam-break inundation under steady-state fixed-bed conditions with $n_g = 0.035$, $n_v = 0.090$, $\phi' = 70°$, $d_{50} = 40\ mm$, and $Q = 100\ m^3/s$ (aerial photograph of Frejus [3544-3644, #41 to #121] in 1955 © IGN, 2012, by permission)

Figure 5-61: Post-dam-break inundation under steady-state fixed-bed conditions with $n_g = 0.035$, $n_v = 0.090$, $\phi' = 70°$, $d_{50} = 40\ mm$, and $Q = 100\ m^3/s$ (aerial photograph of Frejus [FR 177-150, #1 to #104] in 1959 © IGN, 2012, by permission)

5.3 EFFECT OF VARYING MEAN GRAIN SIZE

5.3.1 CROSS-SECTIONS OF HIGH-WATER MARKS AND BED CHANGE

The set of simulations used to produce these cross-sections has the following parameters: $n_g = 0.025$, $n_v = 0.000$, $\phi' = 40°$, $d_b = 2\ m$, and $t = 2\ hours$. d_{50} is varied among the five values in **Table 4-1**. All of the cross-sections also display the original bed elevation (before dam-break) as a basis for comparison.

Figure 5-62 to **Figure 5-68** show cross-sections 1 to 7. From the figures, it is clear that varying d_{50} does have an effect on the HWM. As d_{50} increases, the HWM decreases in cross-sections 1, 4, and 6, increases in cross-sections 3 and 7, and has a mixed effect on cross-sections 2 and 5. It is also clear that varying d_{50} has an impact on final bed elevations. This is exemplified in **Figure 5-67** and **Figure 5-68**, where the increase in d_{50} yields increased deposition and increased erosion.

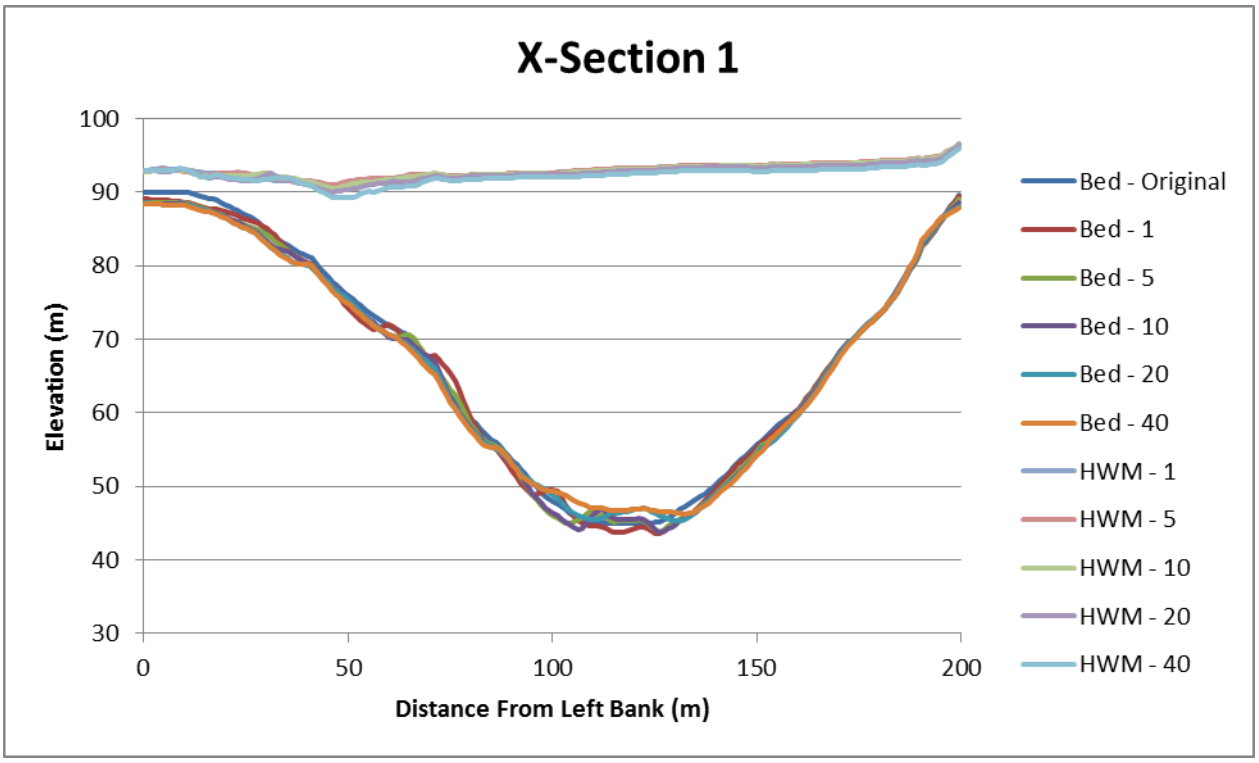

Figure 5-62: HWM and bed elevation at cross-section 1 varying d_{50} on a mobile-bed

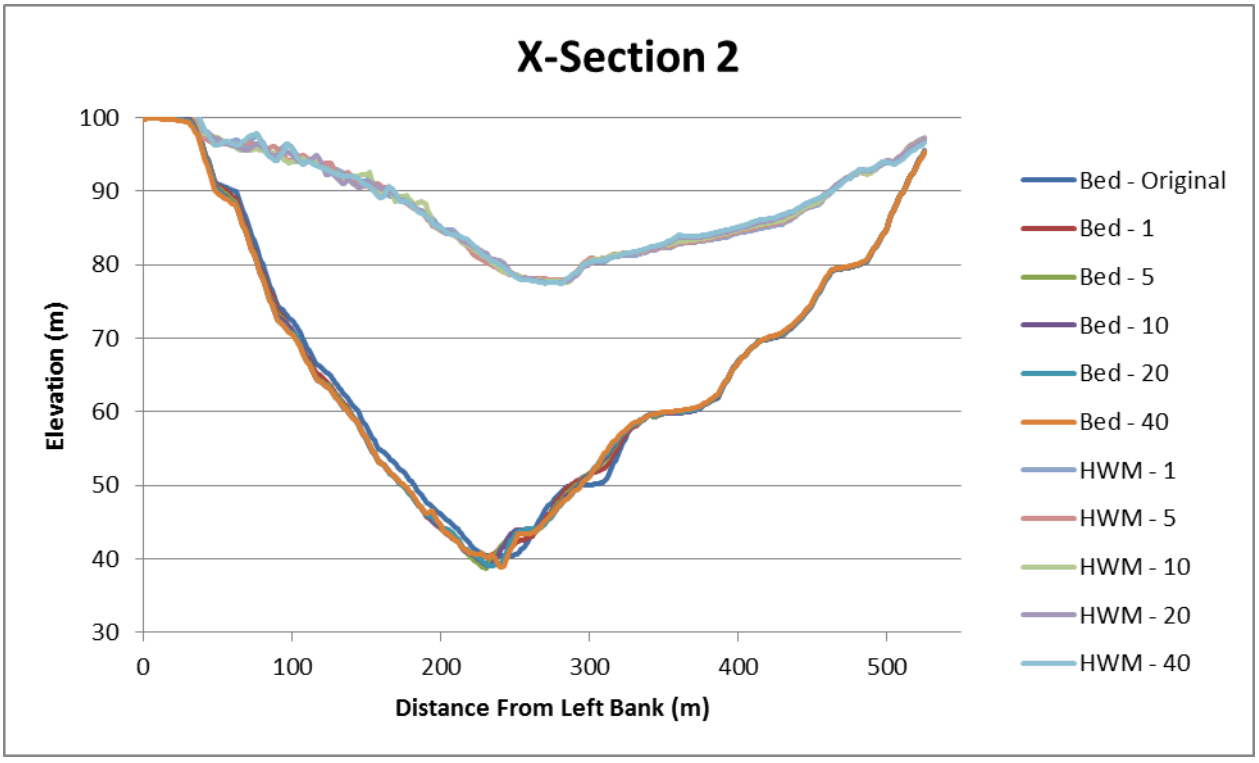

Figure 5-63: HWM and bed elevation at cross-section 2 varying d_{50} on a mobile-bed

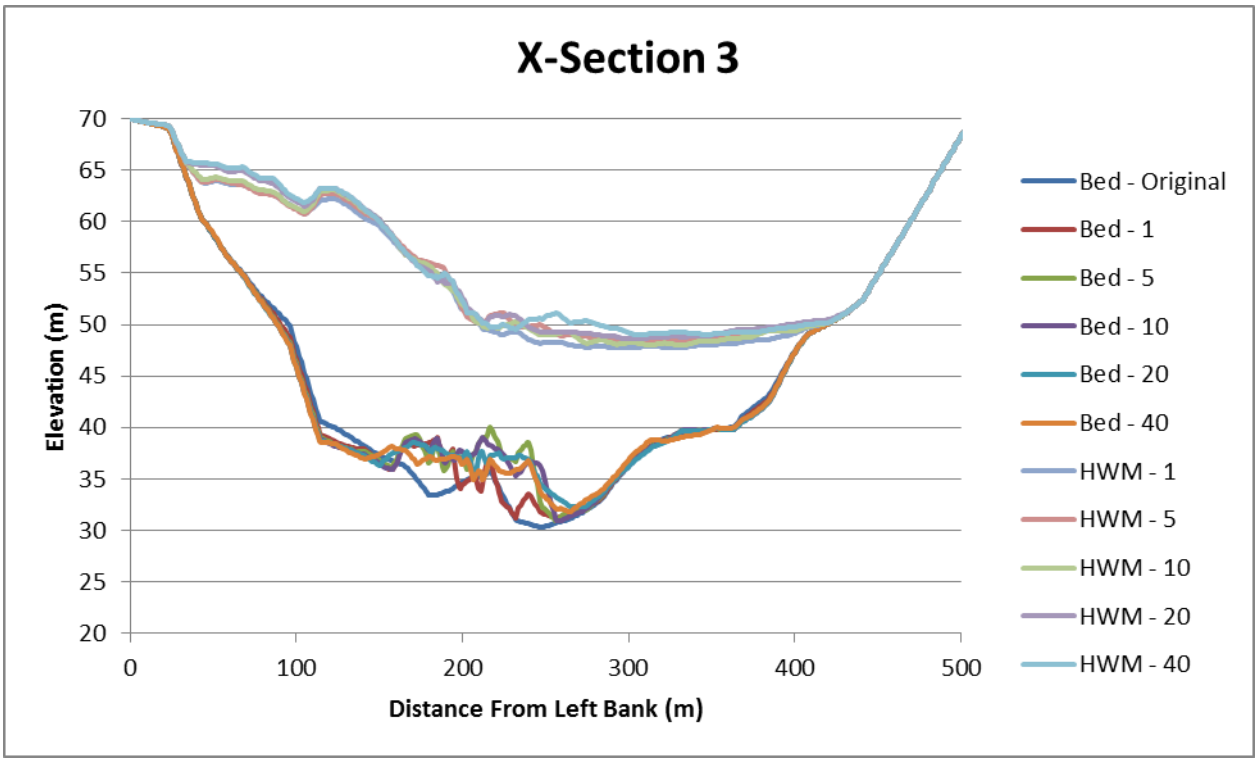

Figure 5-64: HWM and bed elevation at cross-section 3 varying d_{50} on a mobile-bed

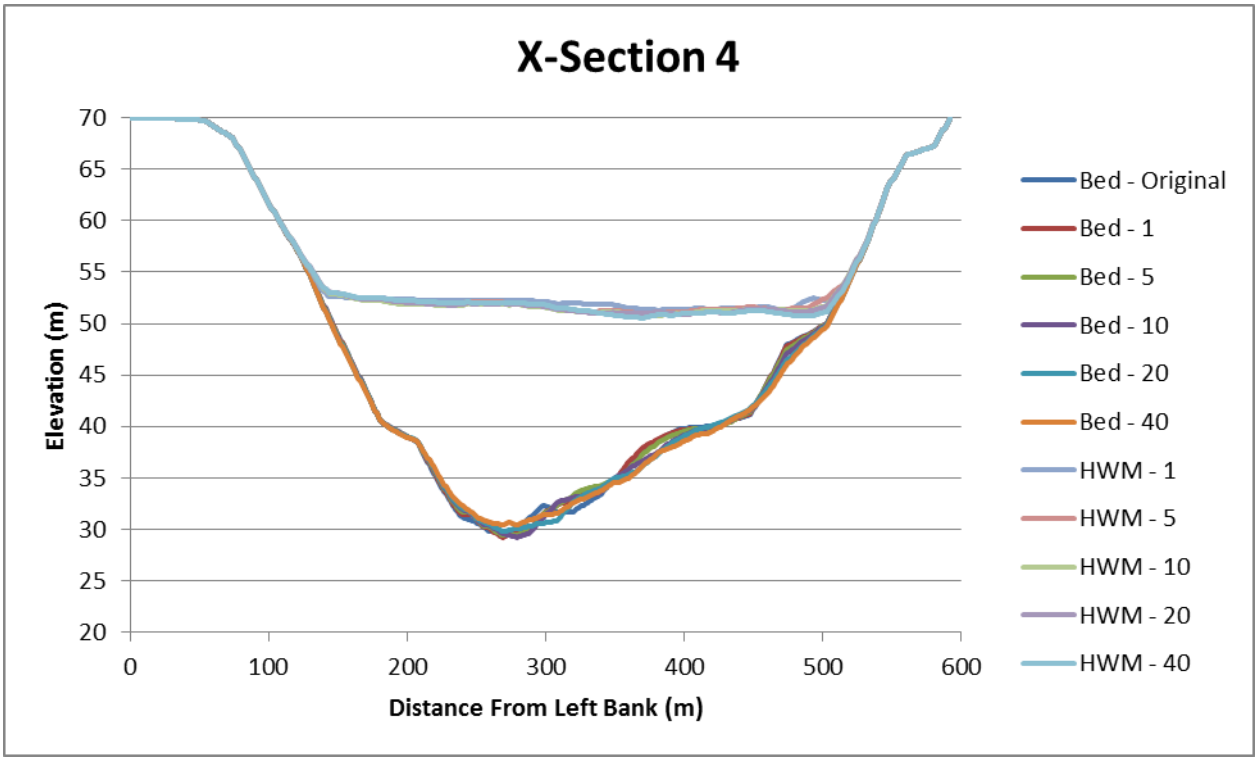

Figure 5-65: HWM and bed elevation at cross-section 4 varying d_{50} on a mobile-bed

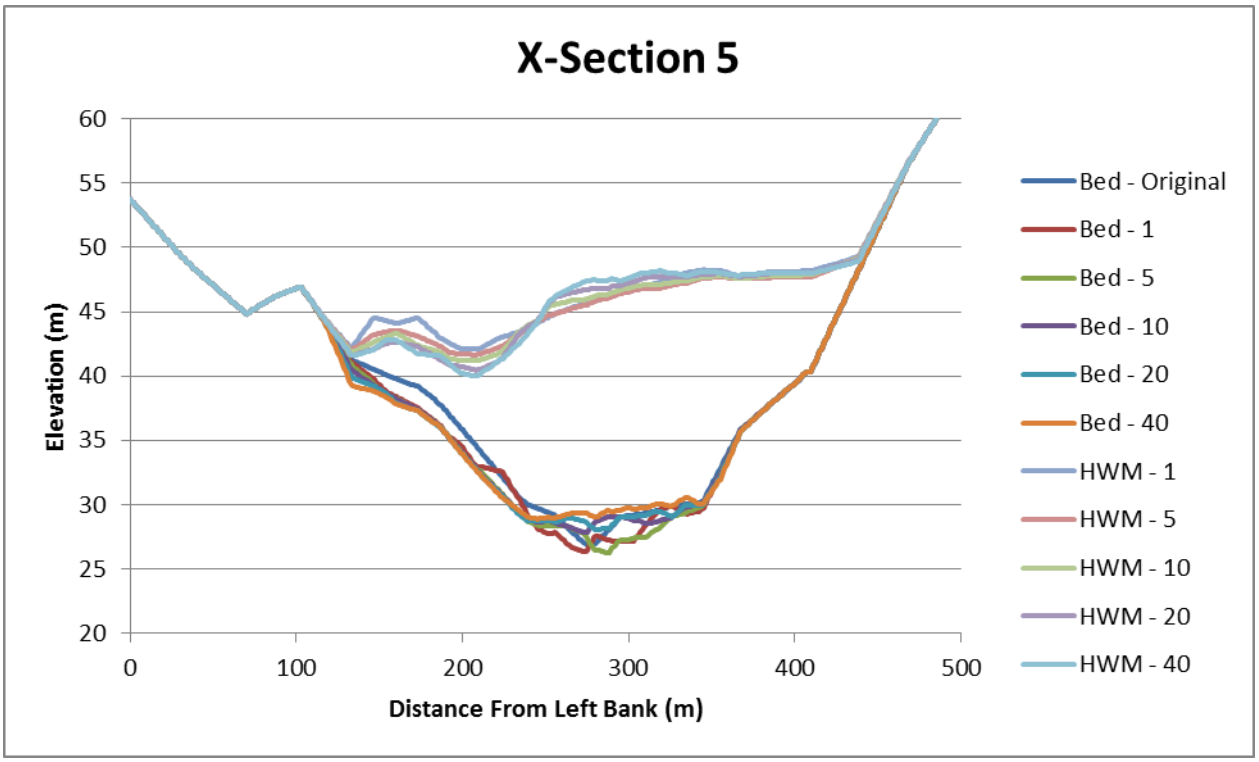

Figure 5-66: HWM and bed elevation at cross-section 5 varying d_{50} on a mobile-bed

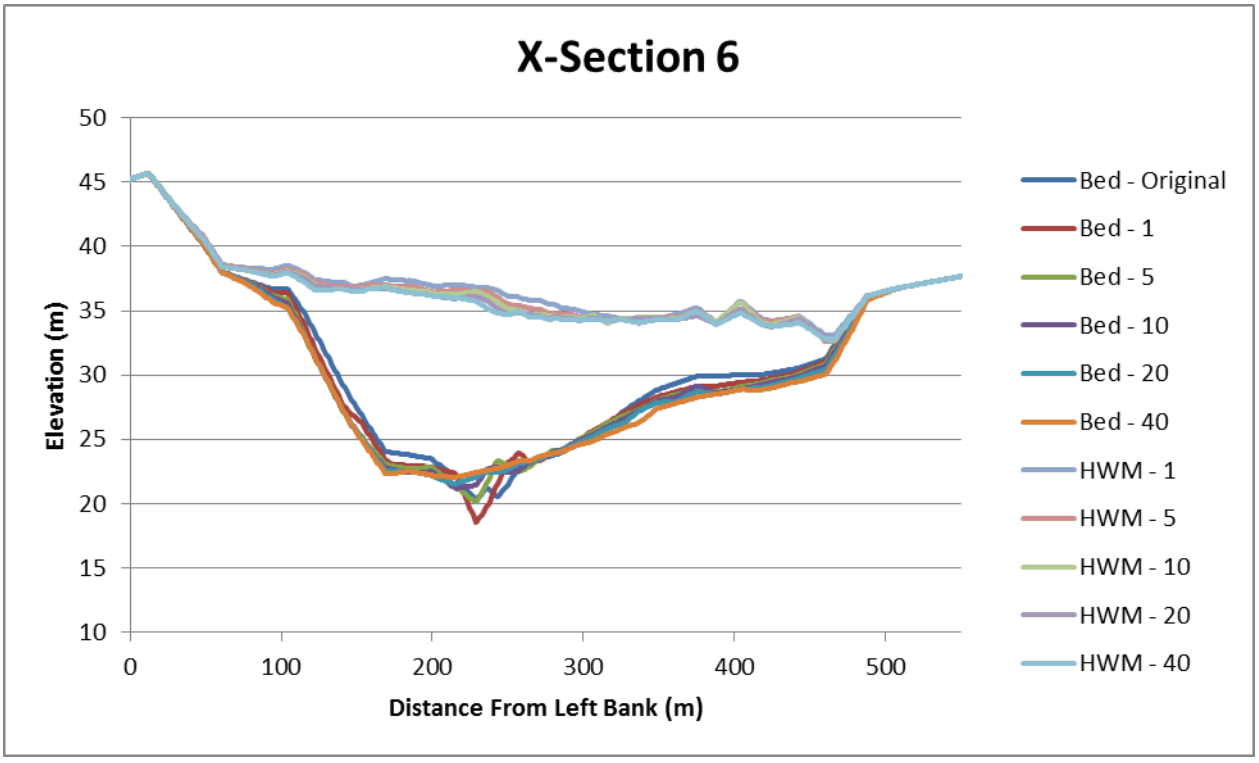

Figure 5-67: HWM and bed elevation at cross-section 6 varying d_{50} on a mobile-bed

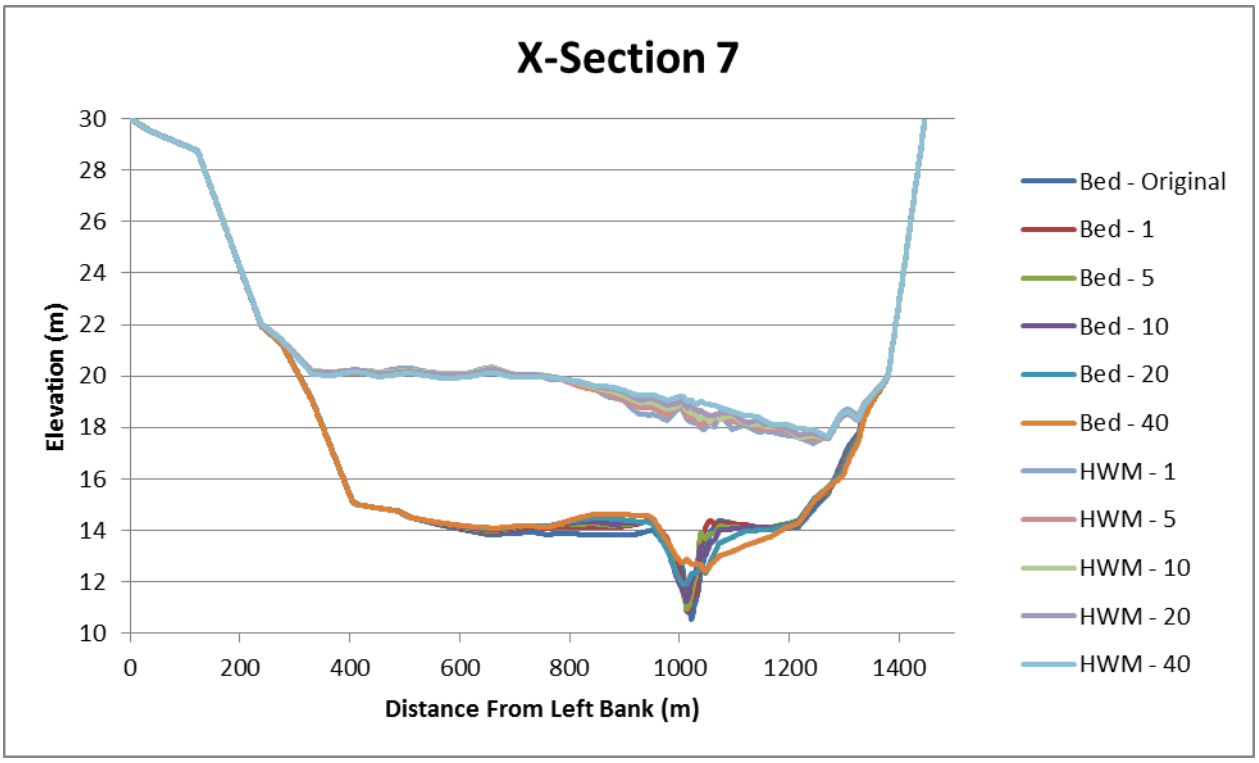

Figure 5-68: HWM and bed elevation at cross-section 7 varying d_{50} on a mobile-bed

5.3.2 2D BED EVOLUTION

The selection of d_{50} has a significant impact on the zones of erosion (blue) and deposition (red) shown in **Figure 5-69** to **Figure 5-73**. As d_{50} increases from 1 mm to 40 mm, the erosion and deposition zones grow. The simulations used to produce the figures are not influenced by vegetation. However, similar results are expected after the first metre of vegetation-influenced sediment is eroded away in those simulations. The reason that an increase in d_{50} leads to more erosion, and hence deposition, is not entirely clear. It is possibly caused by the way SISYPHE computes sediment transport using the active layer and active stratum concept (more information on this may be found in the SISYPHE manual at www.opentelemac.org).

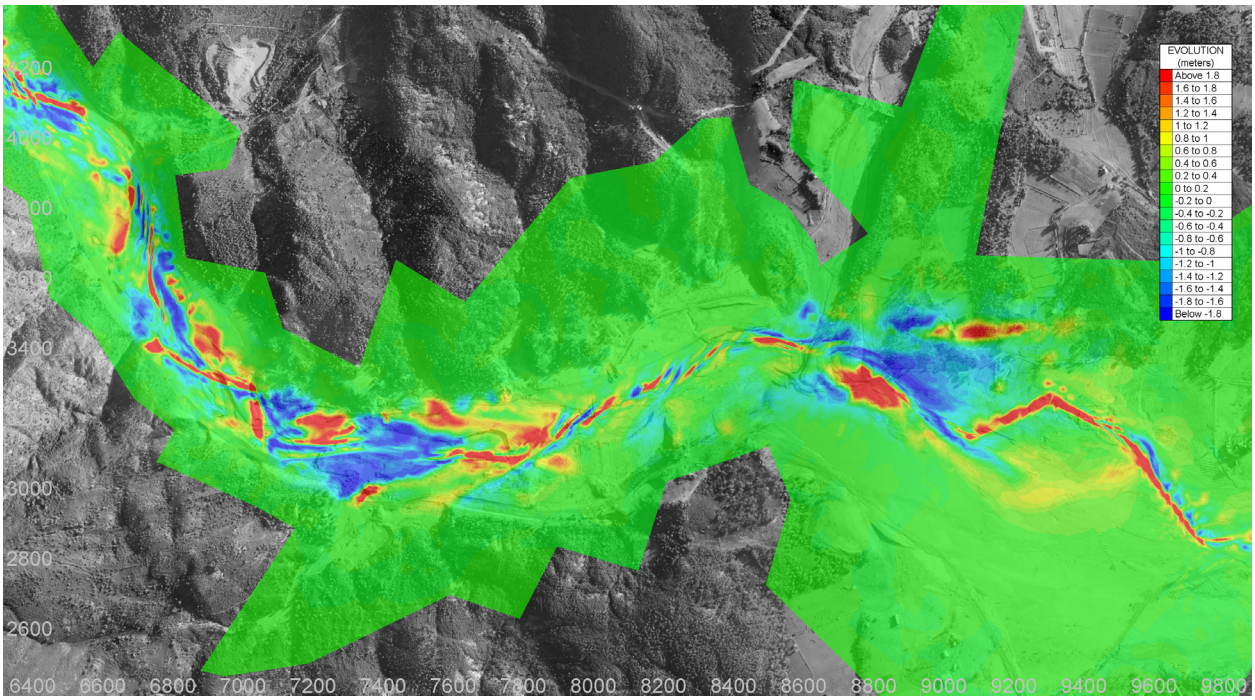

Figure 5-69

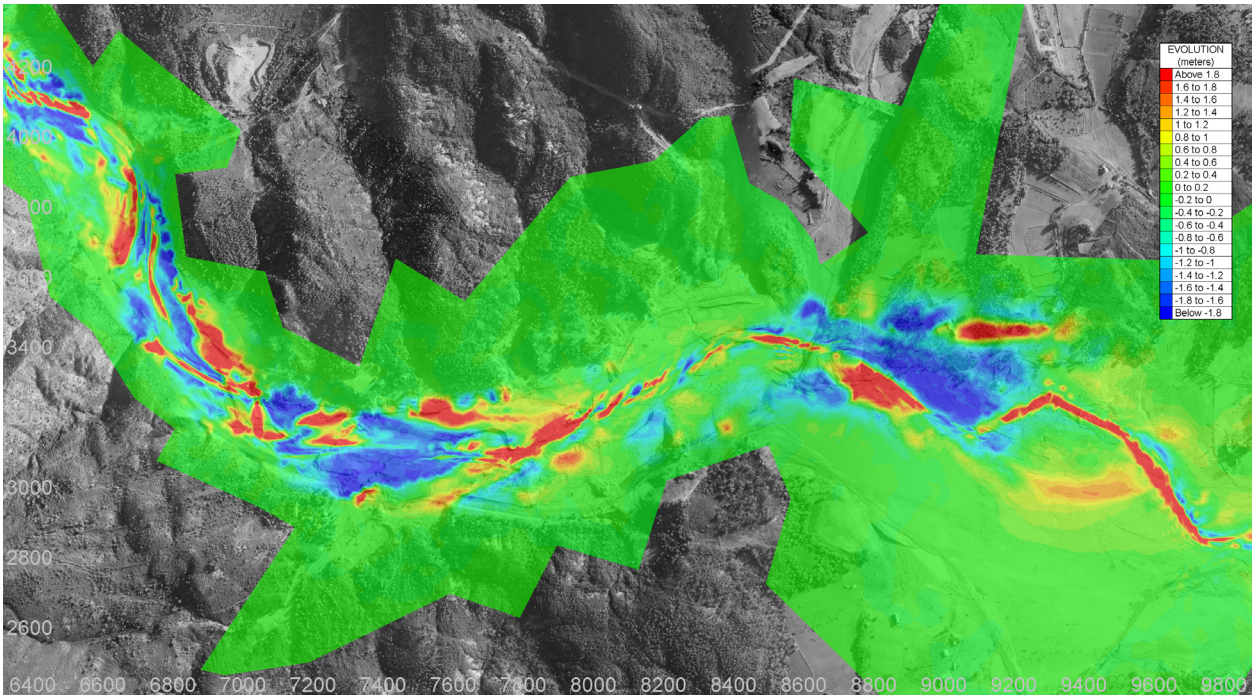

Figure 5-70

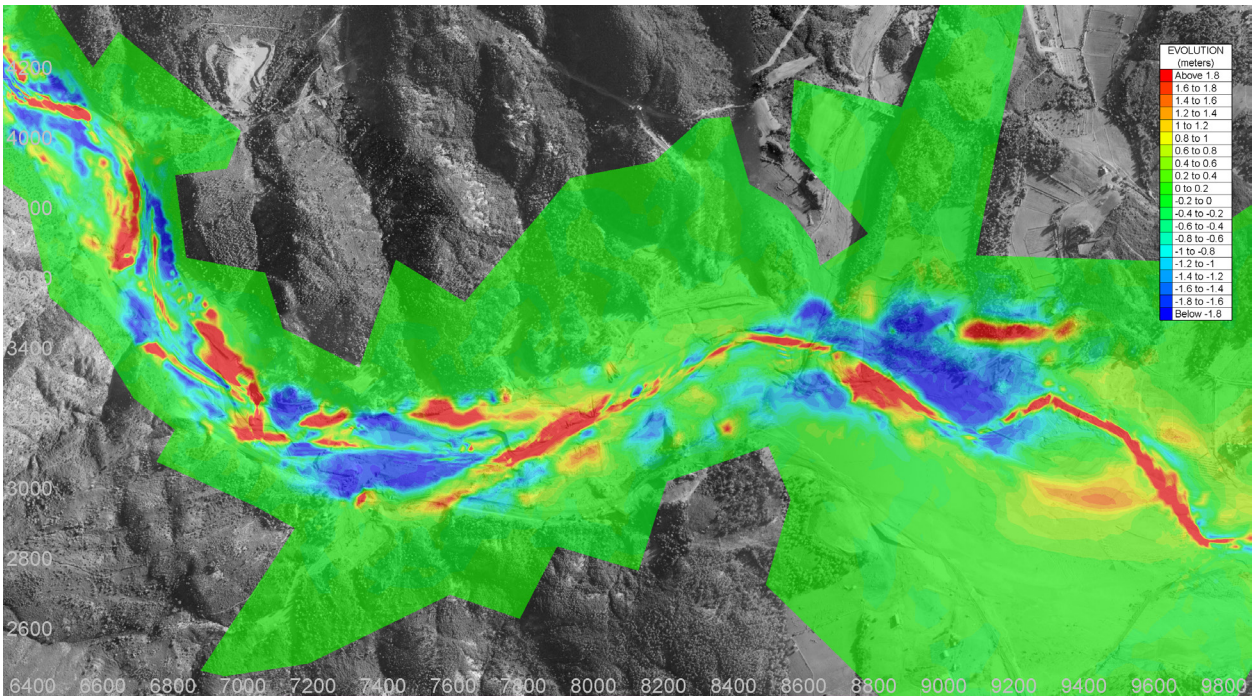

Figure 5-71

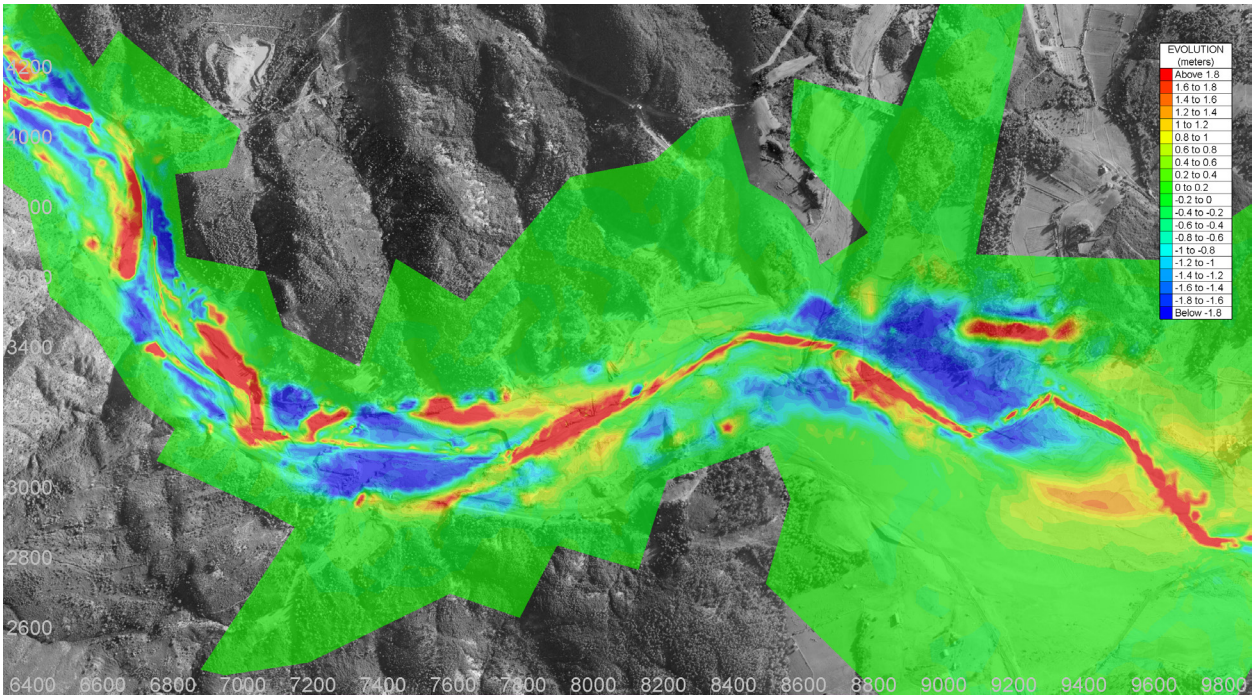

Figure 5-72

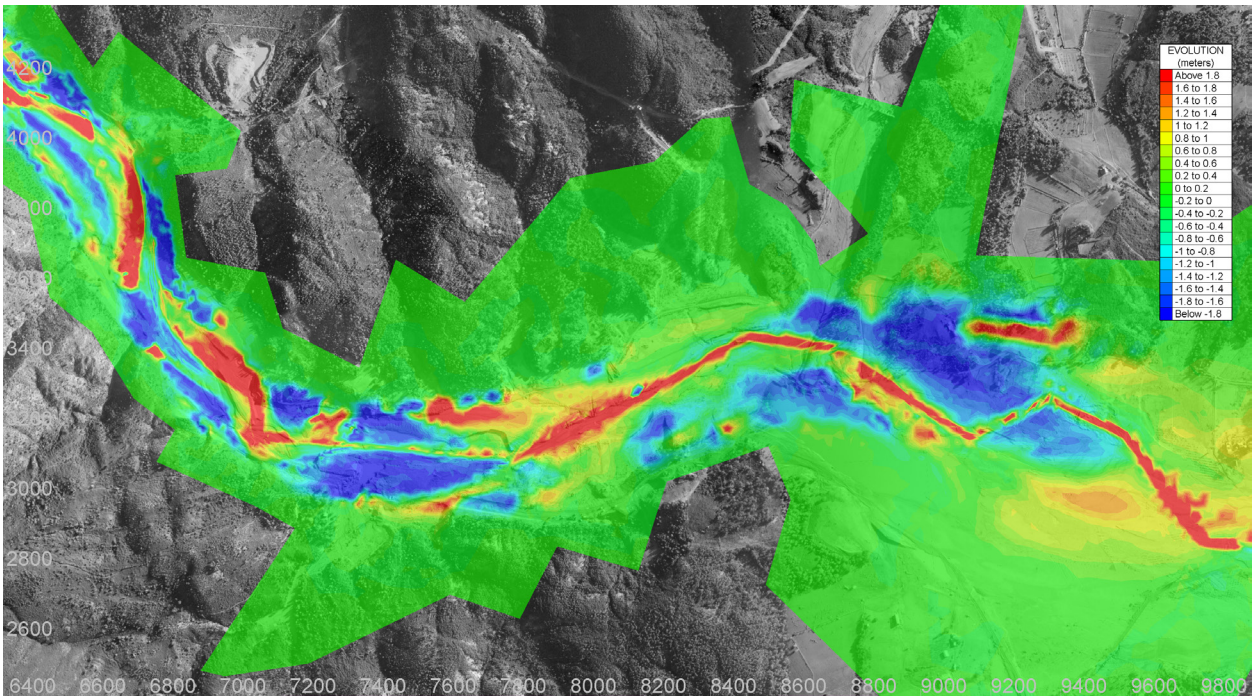
EVOLUTION
(meters)
Above 1.8
1.6 to 1.8
1.4 to 1.6
1.2 to 1.4
1 to 1.2
0.8 to 1
0.6 to 0.8
0.4 to 0.6
0.2 to 0.4
0 to 0.2
-0.2 to 0
-0.4 to -0.2
-0.6 to -0.4
-0.8 to -0.6
-1 to -0.8
-1.2 to -1
-1.4 to -1.2
-1.6 to -1.4
-1.8 to -1.6
Below -1.8
3400
3000
2800
2600
6400
6600
6800
7000
7200
7400
7600
8000
8200
8400
8600
8800
9000
9200
9400
9600
9800

Figure 5-73

Figure 5-69: Bed evolution of case where: $n_g = 0.025$, $n_v = 0.000$, $\phi' = 40°$, and $d_{50} = 1\ mm$ (positive evolution = deposition, negative evolution = erosion) (aerial photograph of Frejus [FR 177-150, #1 to #104] in 1959 © IGN, 2012, by permission)

Figure 5-70: Bed evolution of case where: $n_g = 0.025$, $n_v = 0.000$, $\phi' = 40°$, and $d_{50} = 5\ mm$ (positive evolution = deposition, negative evolution = erosion) (aerial photograph of Frejus [FR 177-150, #1 to #104] in 1959 © IGN, 2012, by permission)

Figure 5-71: Bed evolution of case where: $n_g = 0.025$, $n_v = 0.000$, $\phi' = 40°$, and $d_{50} = 10\ mm$ (positive evolution = deposition, negative evolution = erosion) (aerial photograph of Frejus [FR 177-150, #1 to #104] in 1959 © IGN, 2012, by permission)

Figure 5-72: Bed evolution of case where: $n_g = 0.025$, $n_v = 0.000$, $\phi' = 40°$, and $d_{50} = 20\ mm$ (positive evolution = deposition, negative evolution = erosion) (aerial photograph of Frejus [FR 177-150, #1 to #104] in 1959 © IGN, 2012, by permission)

Figure 5-73: Bed evolution of case where: $n_g = 0.025$, $n_v = 0.000$, $\phi' = 40°$, and $d_{50} = 40\ mm$ (positive evolution = deposition, negative evolution = erosion) (aerial photograph of Frejus [FR 177-150, #1 to #104] in 1959 © IGN, 2012, by permission)

5.3.3 FLOOD-WAVE PROPAGATION TIME

Figure 5-74 and **Figure 5-75** show the extent that the dam-break flood-wave has propagated after $t = 30\ min$ with two different scenarios of n_g, n_v, and ϕ', but with a varying spectrum of d_{50}. From both figures, it is clear that as d_{50} increases, the distance propagated by the flood-wave increases. Unlike the parameters of n_g and n_v, flood-wave propagation distance is not as sensitive to variations in d_{50}. Nonetheless, d_{50} does affect flood-wave propagation characteristics and is noteworthy when modelling dam-breaks with mobile-beds.

Table 5-1 shows that for scenarios where all parameters are constant except d_{50}, the flood-wave propagation time will vary at most by 1 or 2 minutes. This supports the conclusion that flood-wave propagation time is not very sensitive to the d_{50} parameter.

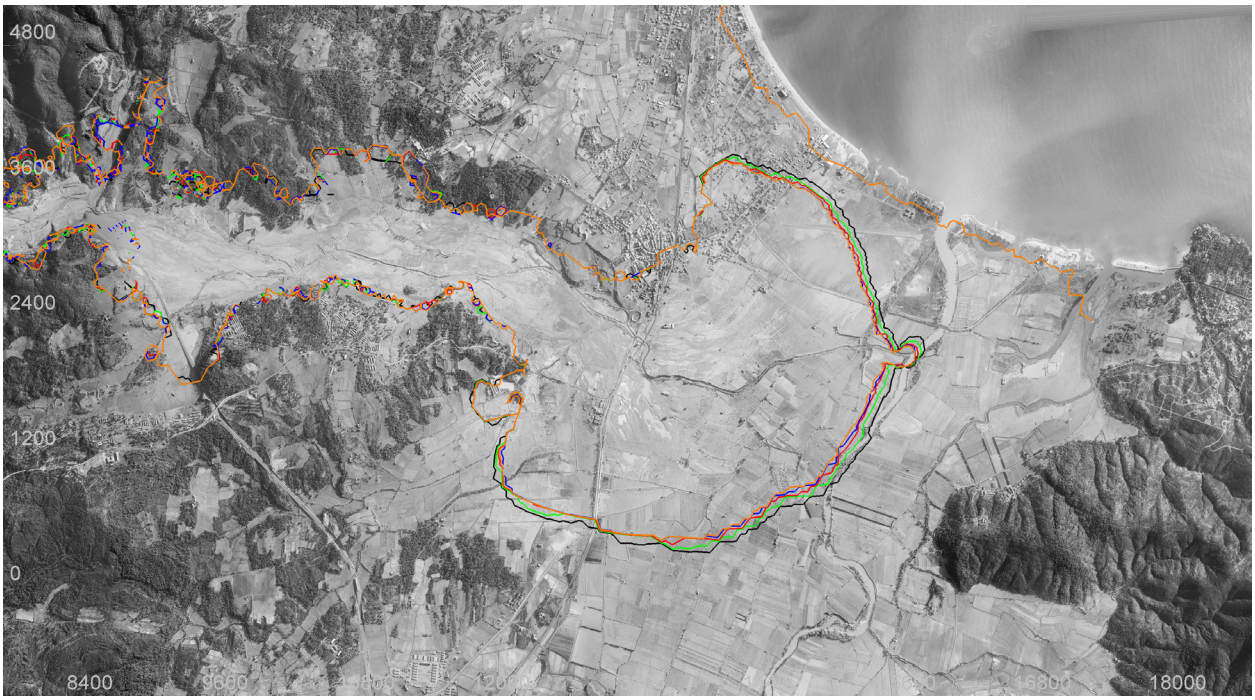

Figure 5-74

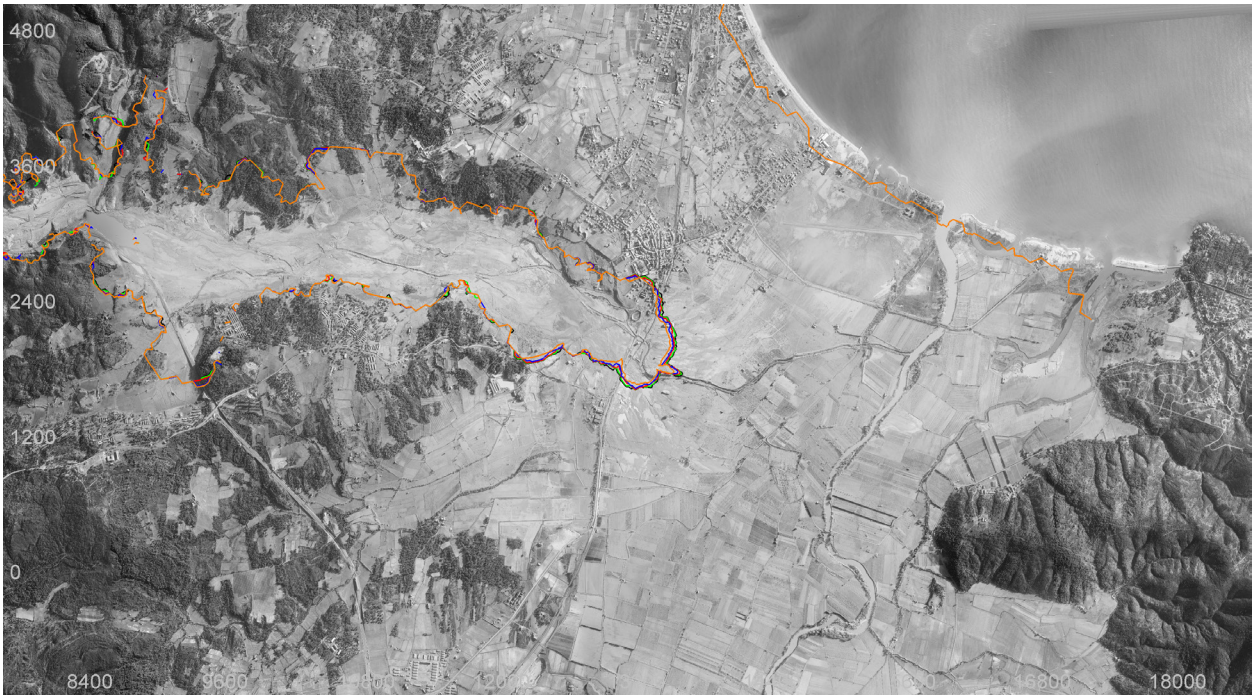

Figure 5-75

Figure 5-74: Extent of inundation 30 minutes after dam-break on a mobile-bed with $n_g = 0.025$, $n_v = 0.000$, and $\phi' = 40°$ (orange – $d_{50} = 1\ mm$, blue – $d_{50} = 5\ mm$, red – $n_v = d_{50} = 10\ mm$, green – $n_v = d_{50} = 20\ mm$, black – $d_{50} = 40\ mm$) (aerial photograph of Frejus [FR 177-150, #1 to #104] in 1959 © IGN, 2012, by permission)

Figure 5-75: Extent of inundation 30 minutes after dam-break on a mobile-bed with $n_g = 0.035$, $n_v = 0.090$, and $\phi' = 70°$ (orange – $d_{50} = 1\ mm$, blue – $d_{50} = 5\ mm$, red – $n_v = d_{50} = 10\ mm$, green – $n_v = d_{50} = 20\ mm$, black – $d_{50} = 40\ mm$) (aerial photograph of Frejus [FR 177-150, #1 to #104] in 1959 © IGN, 2012, by permission)

5.4 EFFECT OF VARYING DEPTH TO BEDROCK

5.4.1 CROSS-SECTIONS OF HIGH-WATER MARKS AND BED CHANGE

The set of simulations used to produce these cross-sections has the following parameters: $n_g = 0.030$, $n_v = 0.000$, $\phi' = 40°$, $d_{50} = 1\ mm$, and $t = 2\ hours$. d_b is varied among the five values in **Table 4-1**. All of the cross-sections also display the original bed elevation (before dam-break) as a basis for comparison.

Figure 5-76 to **Figure 5-82** show cross-sections 1 to 7. From the figures, it is clear that varying d_b has no impact on HWM, with the exception of cross-section 3, where the variation is likely a result of extreme bed elevation differences. Varying d_b should not have an impact on the development of erosion and deposition zones; it merely affects how deep the alluvial layer can erode. In regions of high velocities, hence high τ^*, erosion will occur until a depth is reached where $\tau^* < \tau_c^*$. This depth may or may not be greater than d_b. In the case of cross-section 3, it is clear that this depth exceeds $d_b = 2$, 5, 10, and 15 m. Thus, erosion is limited by d_b, resulting in varied HWMs.

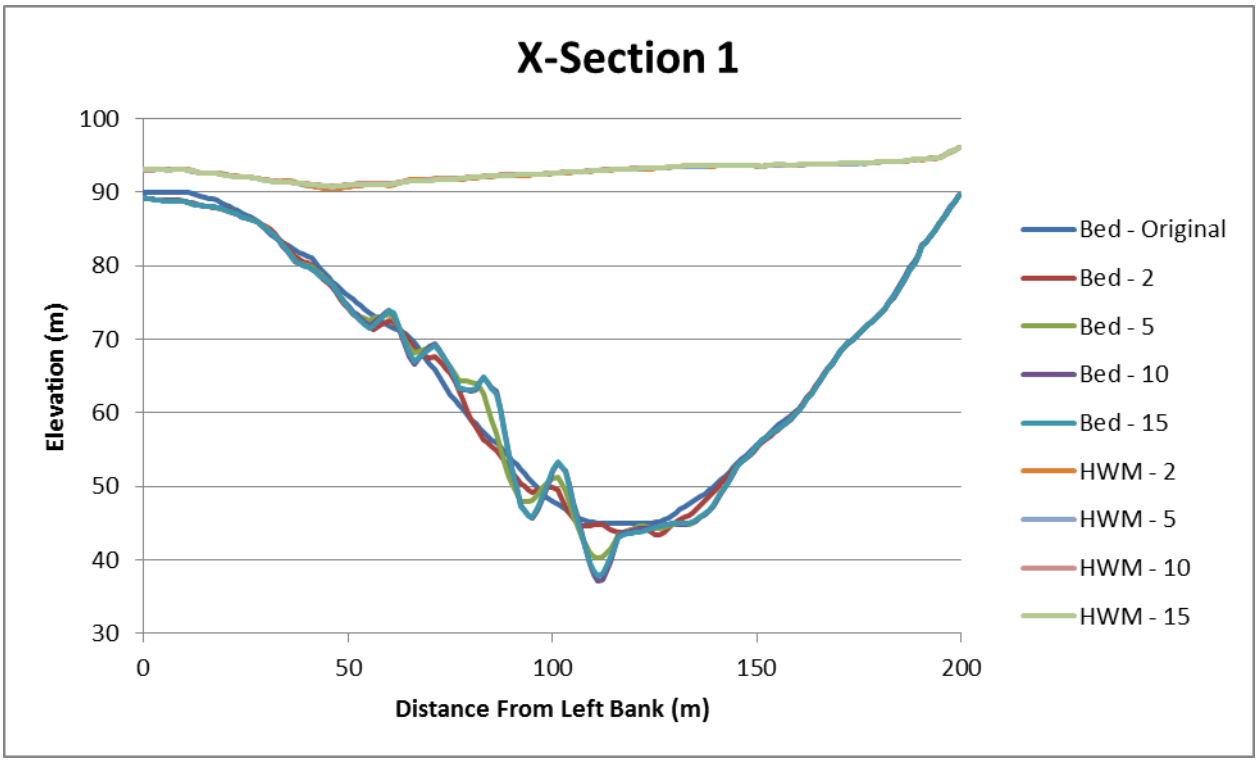

Figure 5-76: HWM and bed elevation at cross-section 1 varying d_b on a mobile-bed

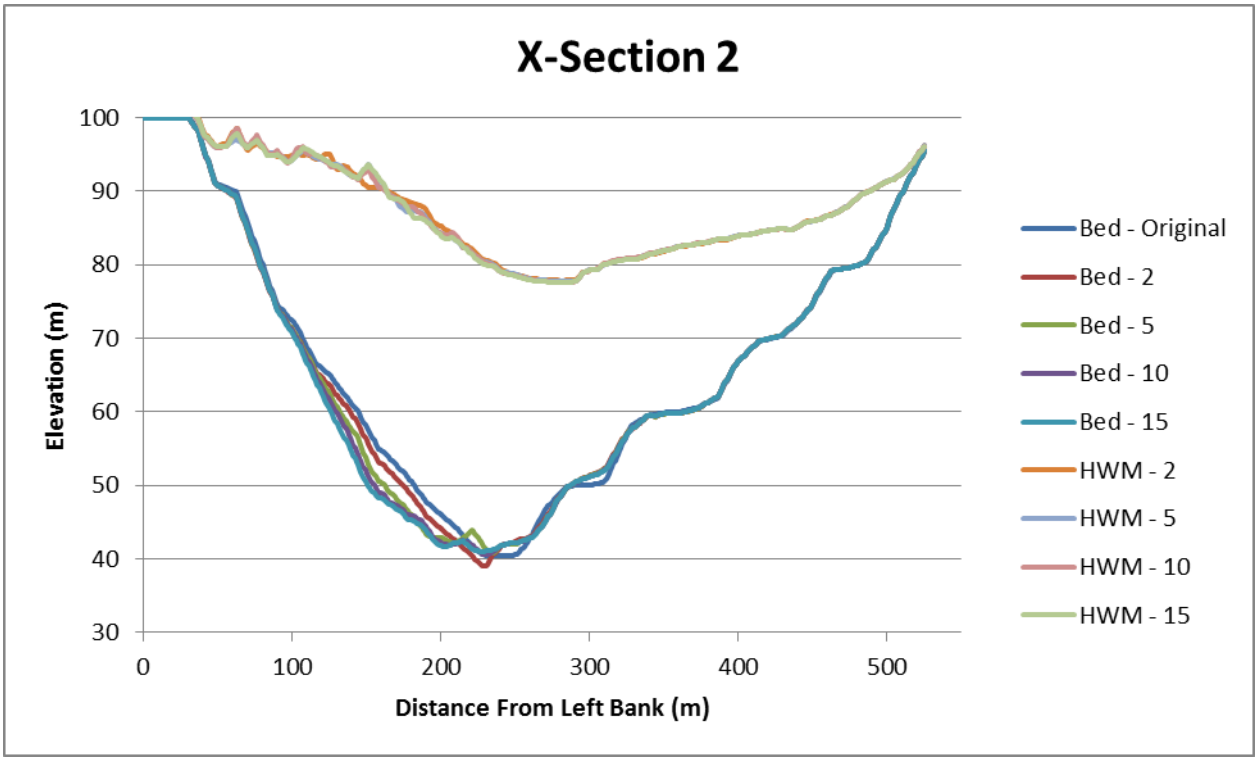

Figure 5-77: HWM and bed elevation at cross-section 2 varying d_b on a mobile-bed

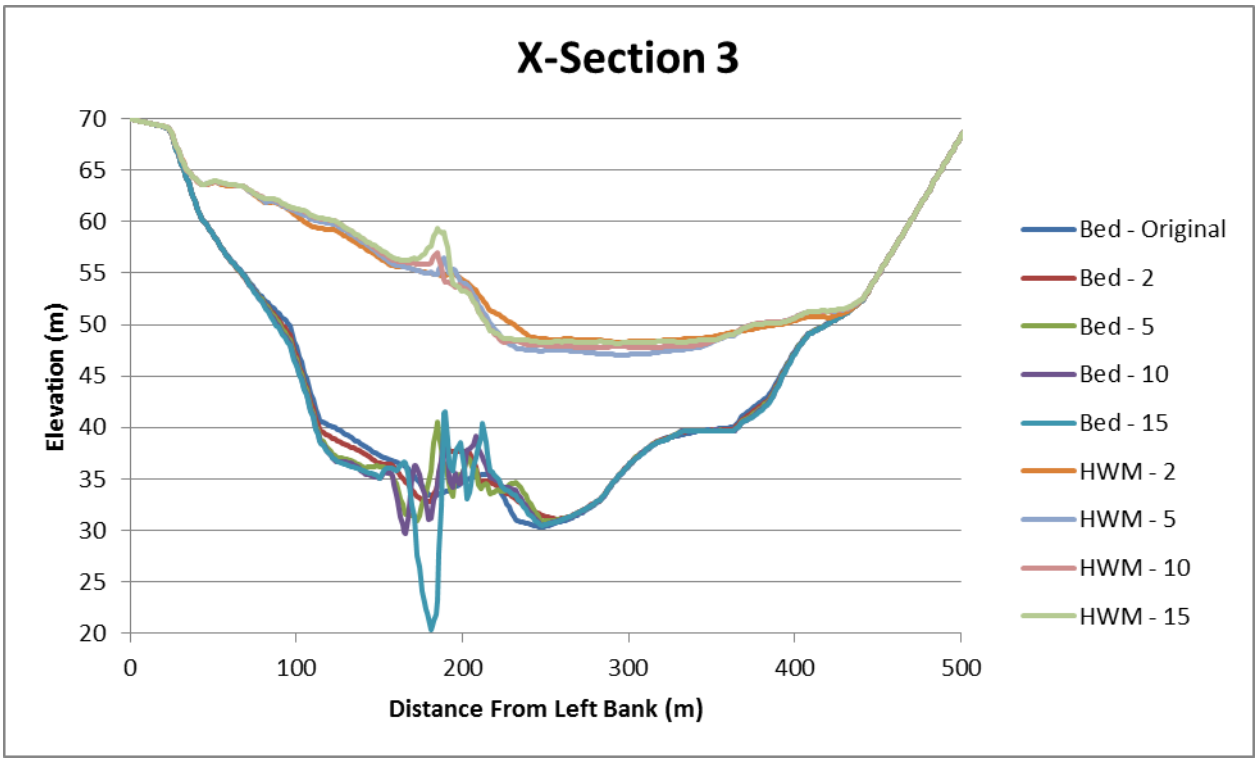

Figure 5-78: HWM and bed elevation at cross-section 3 varying d_b on a mobile-bed

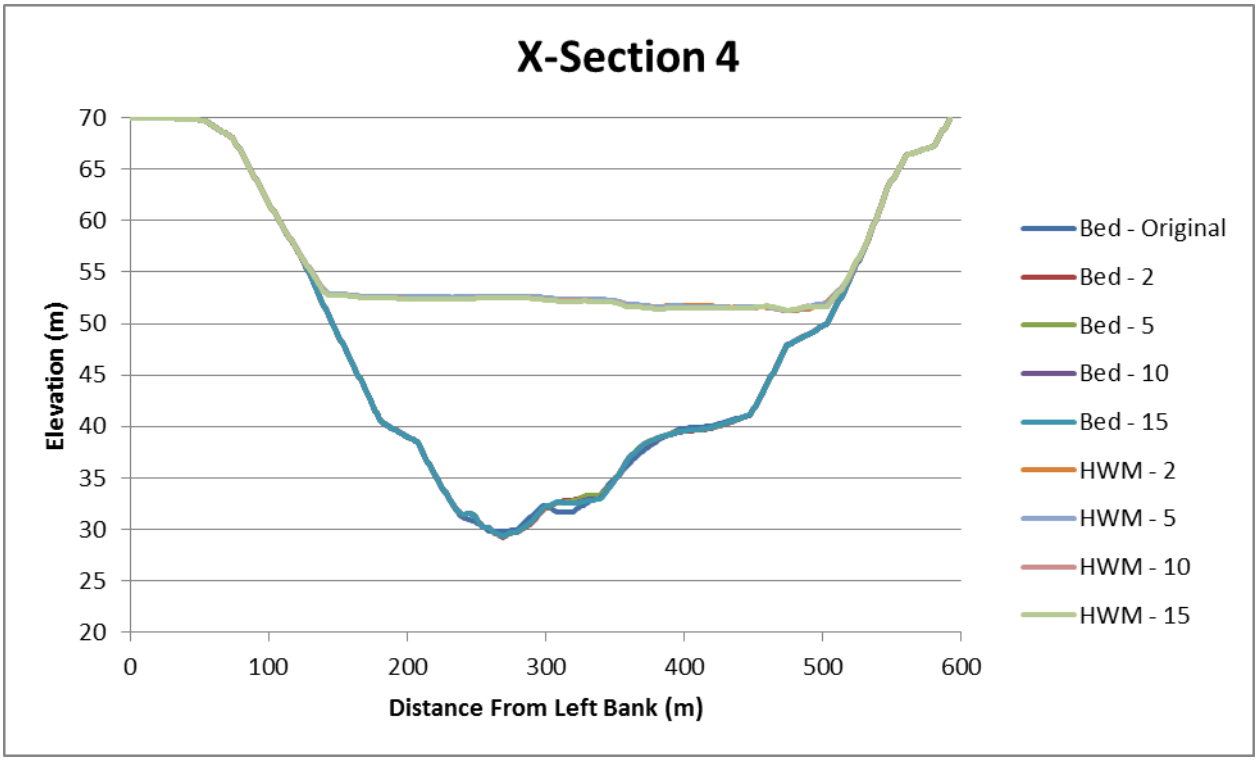

Figure 5-79: HWM and bed elevation at cross-section 4 varying d_b on a mobile-bed

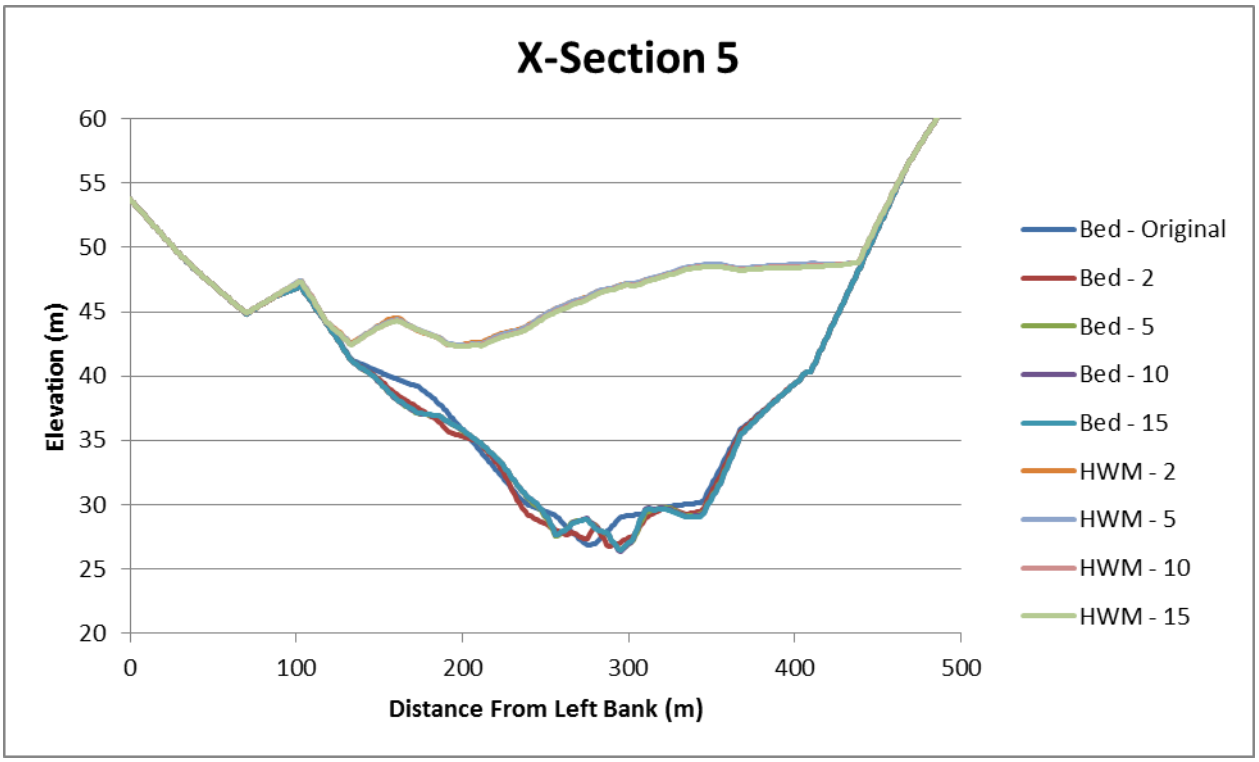

Figure 5-80: HWM and bed elevation at cross-section 5 varying d_b on a mobile-bed

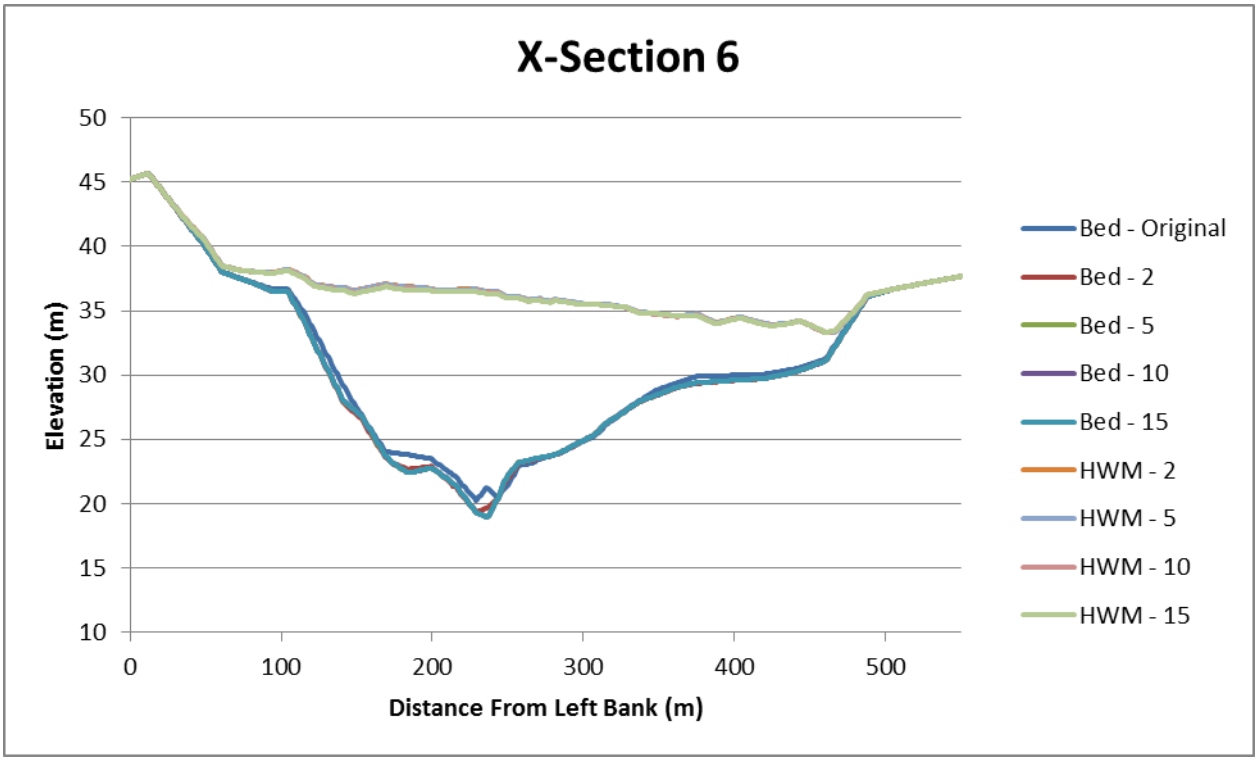

Figure 5-81: HWM and bed elevation at cross-section 6 varying d_b on a mobile-bed

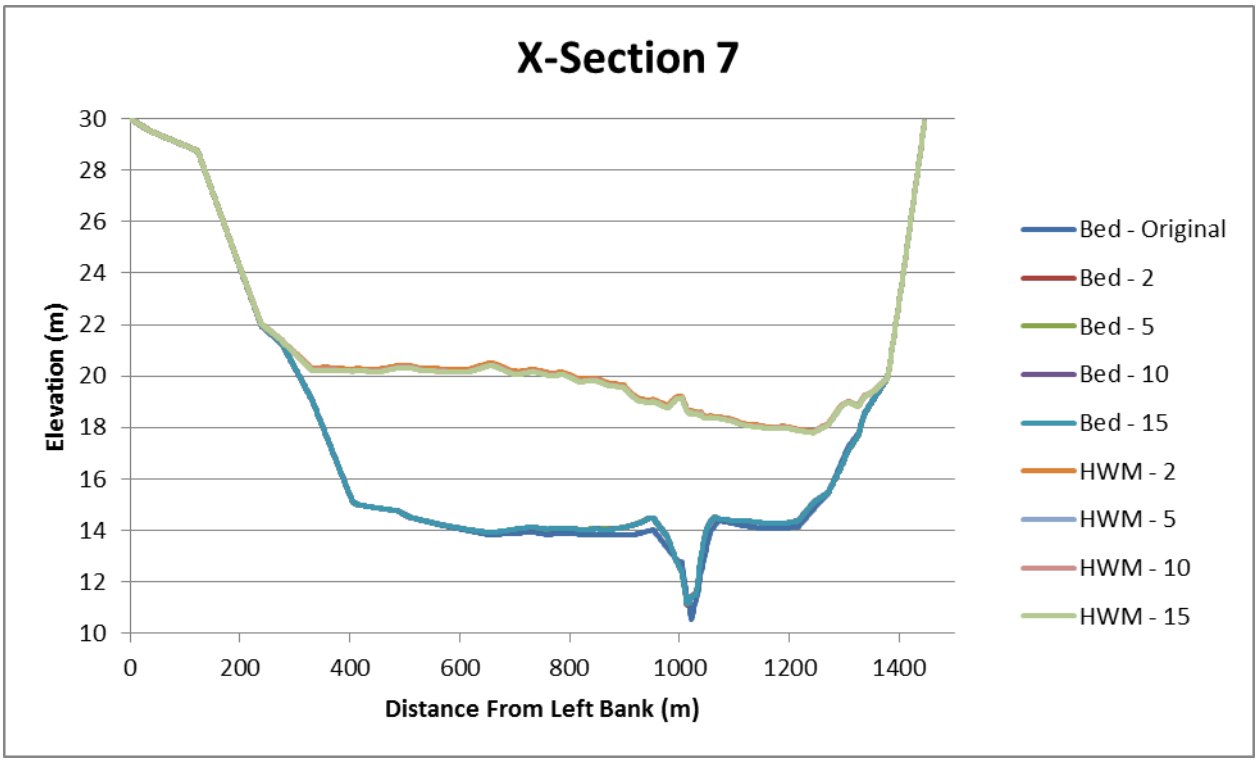

Figure 5-82: HWM and bed elevation at cross-section 7 varying d_b on a mobile-bed

5.4.2 2D BED EVOLUTION

Figure 5-83 to **Figure 5-89** show plots of 2D bed evolution, where n_g, n_v, ϕ', and d_{50} are fixed; only d_b is varied with values of 2, 5, 10, and 15 m. **Figure 5-84** to **Figure 5-89** are presented in pairs of differing scales so that the locations that have scoured down to bedrock can be detected.

Comparing **Figure 5-83**, **Figure 5-84**, **Figure 5-86**, and **Figure 5-88**, which have the same scale, it can be deduced that varying d_b has no impact on the location or the erosion (blue) and deposition (red) zones, nor does it have an impact on their size. Further examination of **Figure 5-85**, **Figure 5-87**, and **Figure 5-89** leads to the conclusion that d_b merely limits how deep the bed can be eroded. Although increased erosion means increased deposition, zones with increased deposition appear to be small and inconsequential.

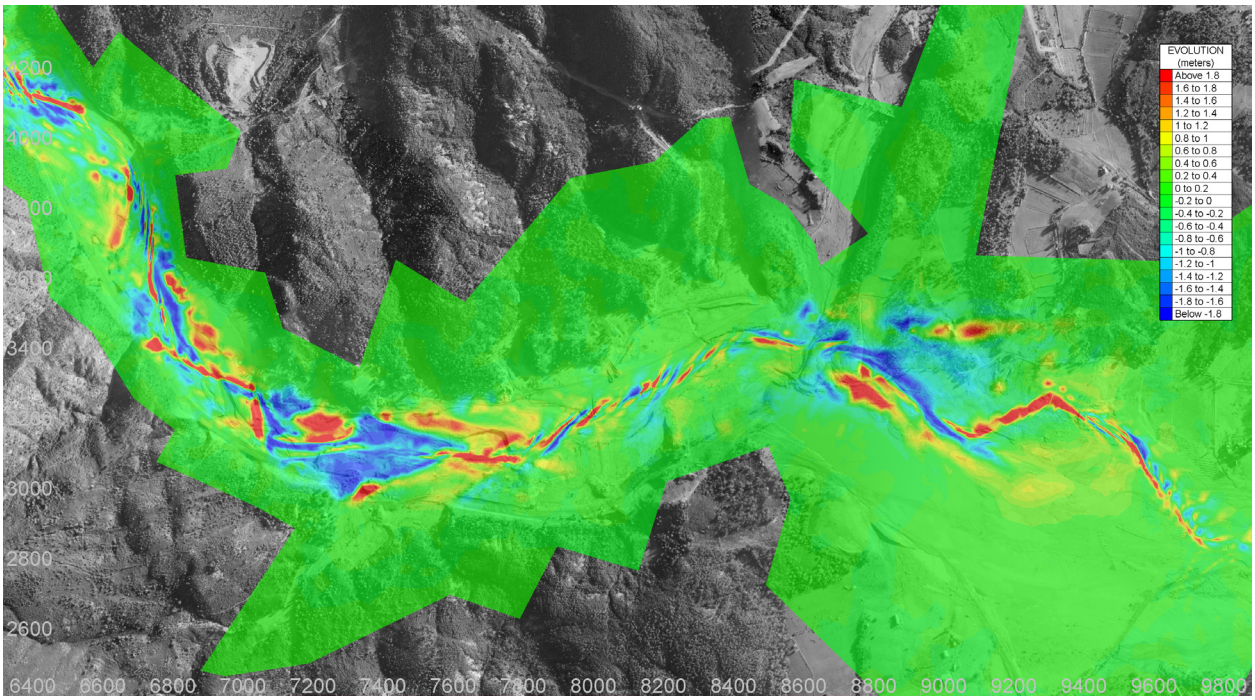

Figure 5-83

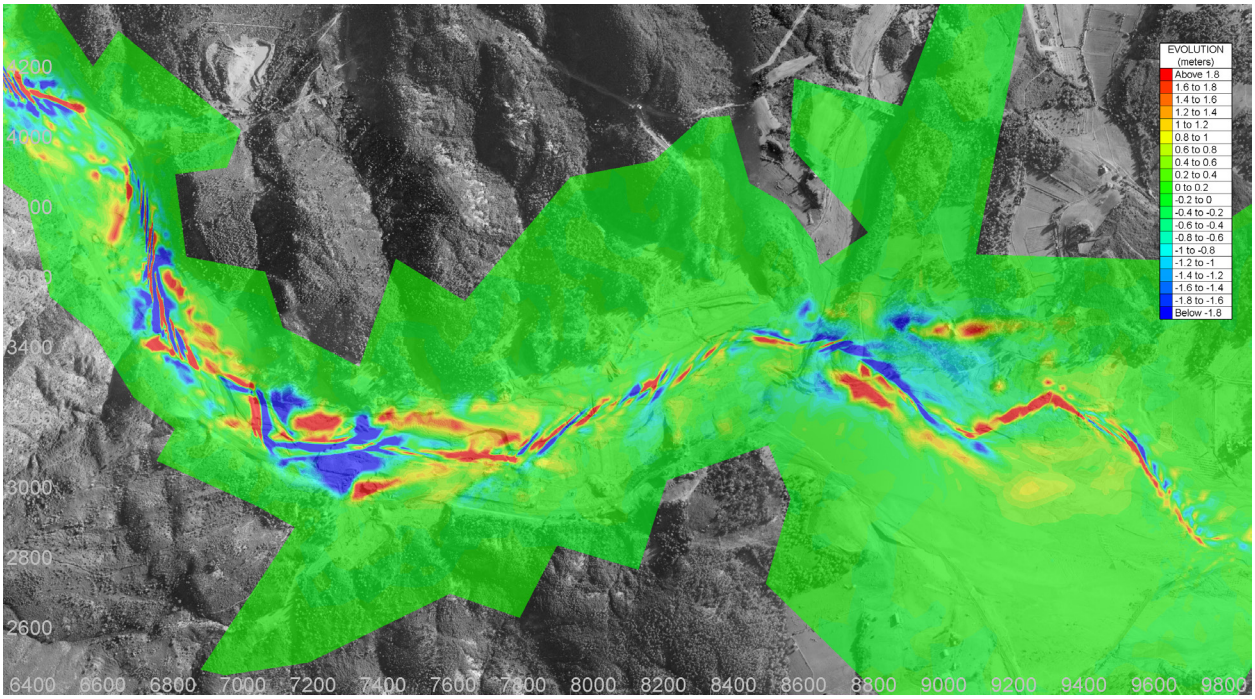

Figure 5-84

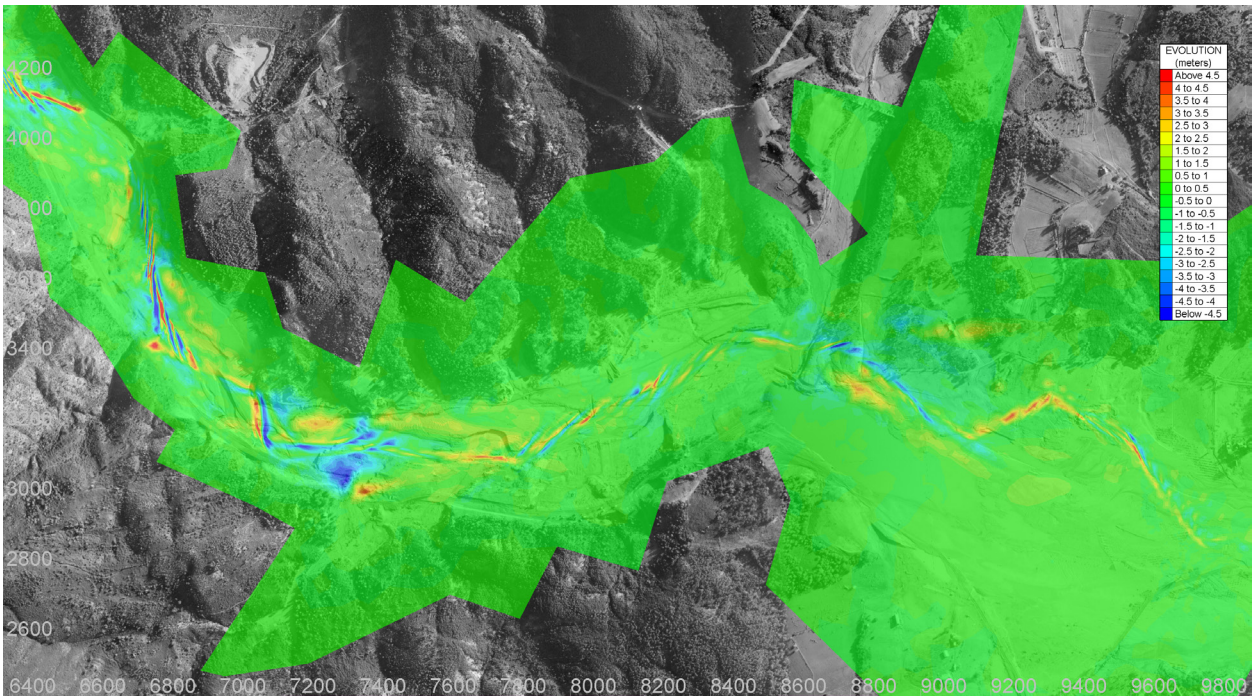

Figure 5-85

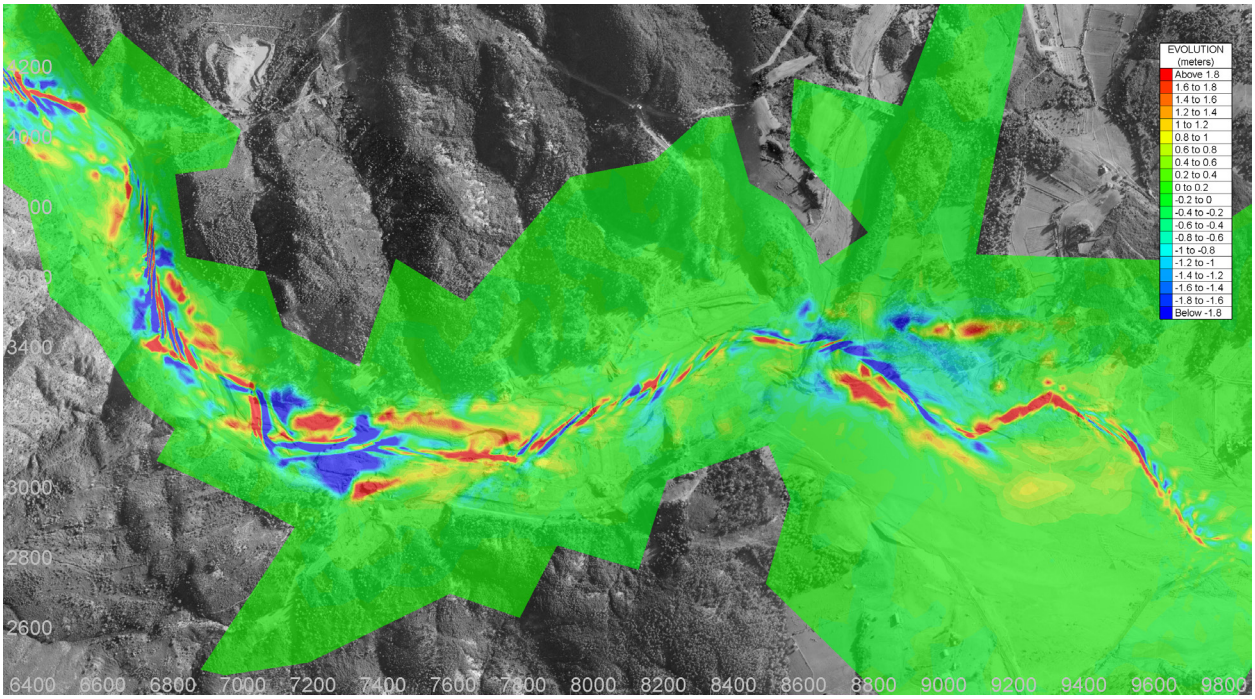

Figure 5-86

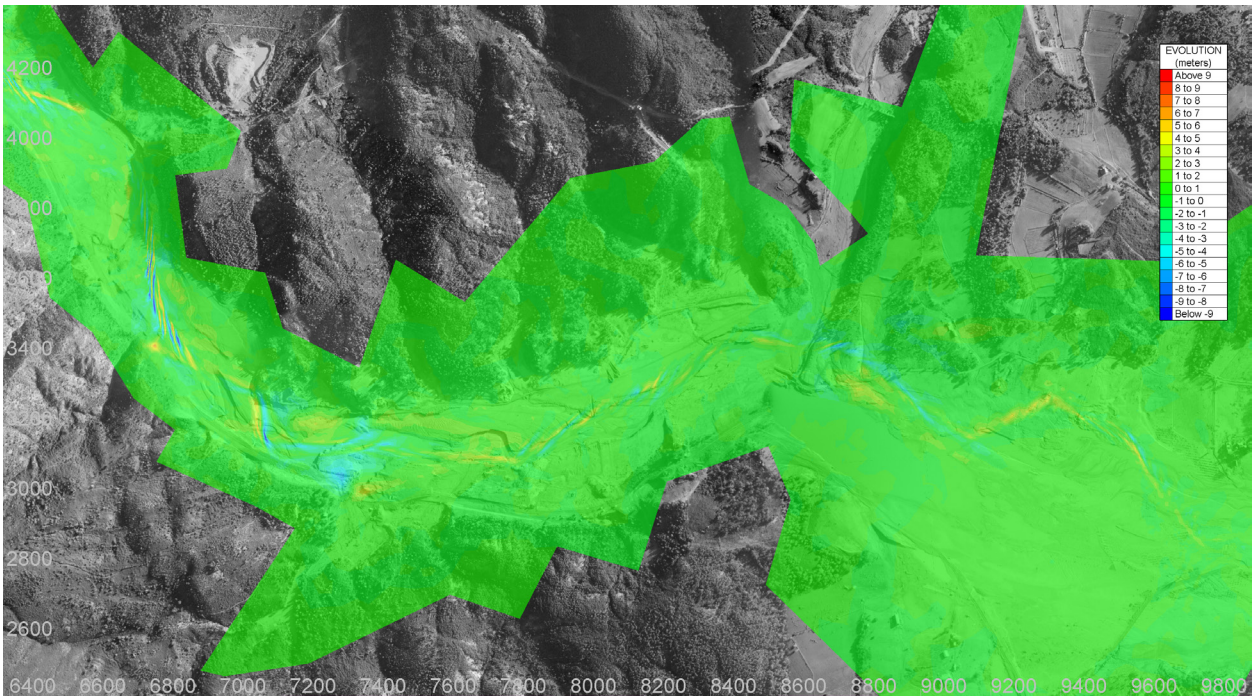

Figure 5-87

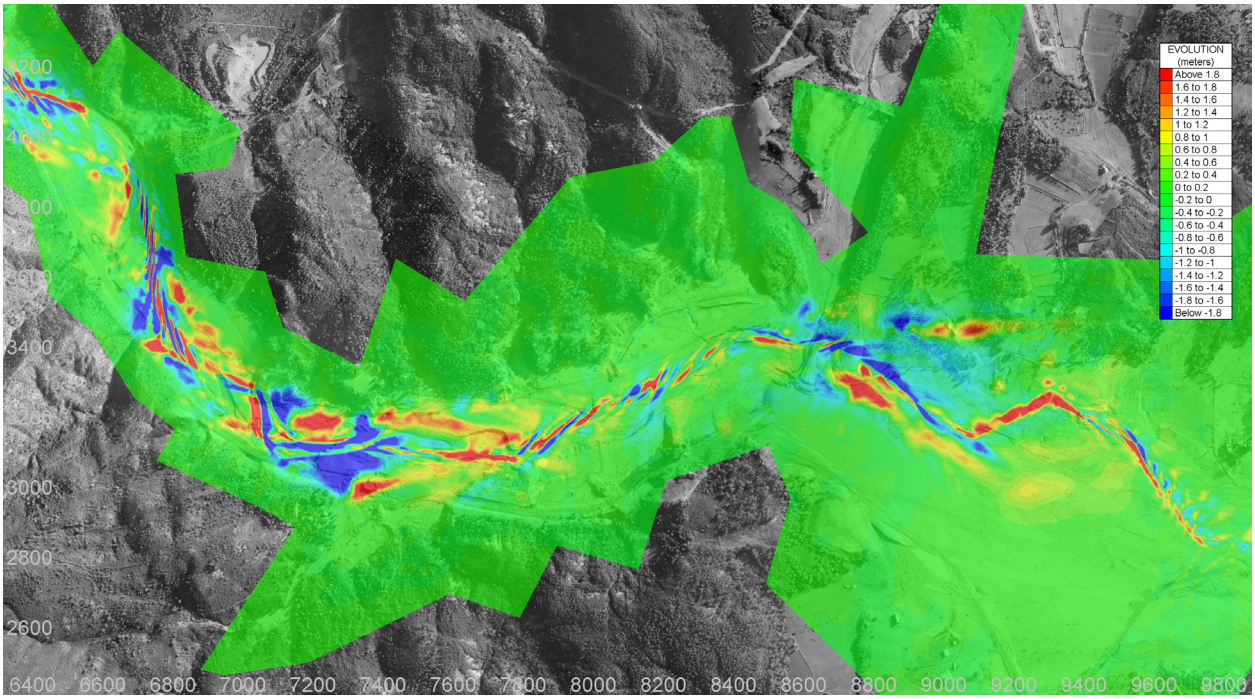

Figure 5-88

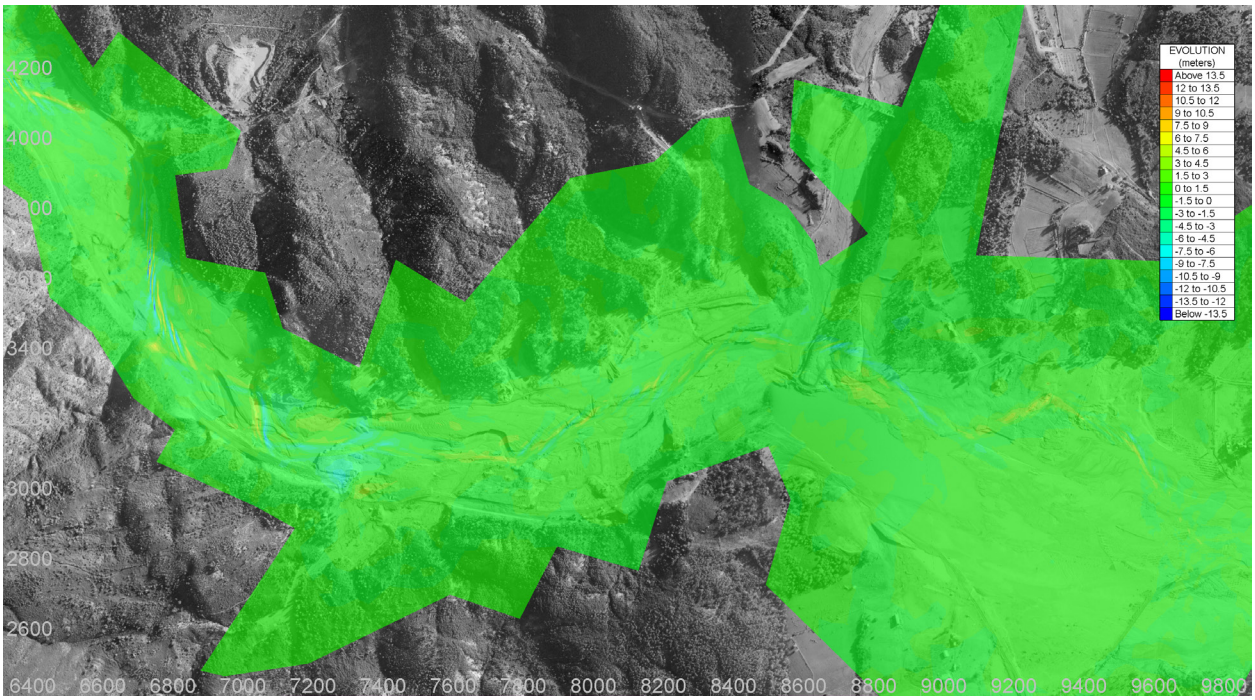
EVOLUTION
(meters)
Above 13.5
12 to 13.5
10.5 to 12
9 to 10.5
7.5 to 9
6 to 7.5
4.5 to 6
3 to 4.5
1.5 to 3
0 to 1.5
-1.5 to 0
-3 to -1.5
-4.5 to -3
-6 to -4.5
-7.5 to -6
-9 to -7.5
-10.5 to -9
-12 to -10.5
-13.5 to -12
Below -13.5
4200
4000
3400
3000
2800
2600
6400
6600
6800
7000
7200
7400
7600
8000
8200
8400
8600
8800
9000
9200
9400
9600
9800

Figure 5-89

Figure 5-83: Bed evolution of case where: $n_g = 0.030$, $n_v = 0.000$, $\phi' = 40°$, $d_{50} = 1\ mm$, and $d_b = 2\ m$ (positive evolution = deposition, negative evolution = erosion) (aerial photograph of Frejus [FR 177-150, #1 to #104] in 1959 © IGN, 2012, by permission)

Figure 5-84: Bed evolution of case where: $n_g = 0.030$, $n_v = 0.000$, $\phi' = 40°$, $d_{50} = 1\ mm$, and $d_b = 5\ m$ (positive evolution = deposition, negative evolution = erosion) (aerial photograph of Frejus [FR 177-150, #1 to #104] in 1959 © IGN, 2012, by permission)

Figure 5-85: Bed evolution of case where: $n_g = 0.030$, $n_v = 0.000$, $\phi' = 40°$, $d_{50} = 1\ mm$, and $d_b = 5\ m$ (positive evolution = deposition, negative evolution = erosion) (aerial photograph of Frejus [FR 177-150, #1 to #104] in 1959 © IGN, 2012, by permission)

Figure 5-86: Bed evolution of case where: $n_g = 0.030$, $n_v = 0.000$, $\phi' = 40°$, $d_{50} = 1\ mm$, and $d_b = 10\ m$ (positive evolution = deposition, negative evolution = erosion) (aerial photograph of Frejus [FR 177-150, #1 to #104] in 1959 © IGN, 2012, by permission)

Figure 5-87: Bed evolution of case where: $n_g = 0.030$, $n_v = 0.000$, $\phi' = 40°$, $d_{50} = 1\ mm$, and $d_b = 10\ m$ (positive evolution = deposition, negative evolution = erosion) (aerial photograph of Frejus [FR 177-150, #1 to #104] in 1959 © IGN, 2012, by permission)

Figure 5-88: Bed evolution of case where: $n_g = 0.030$, $n_v = 0.000$, $\phi' = 40°$, $d_{50} = 1\ mm$, and $d_b = 15\ m$ (positive evolution = deposition, negative evolution = erosion) (aerial photograph of Frejus [FR 177-150, #1 to #104] in 1959 © IGN, 2012, by permission)

Figure 5-89: Bed evolution of case where: $n_g = 0.030$, $n_v = 0.000$, $\phi' = 40°$, $d_{50} = 1\ mm$, and $d_b = 15\ m$ (positive evolution = deposition, negative evolution = erosion) (aerial photograph of Frejus [FR 177-150, #1 to #104] in 1959 © IGN, 2012, by permission)

5.4.3 FLOOD-WAVE PROPAGATION TIME

Figure 5-90 to **Figure 5-92** show the distance that the flood-wave has propagated after $t = 30\ min$, holding constant all parameters other than d_b. It is clear that d_b has a negligible effect on flood-wave propagation, since the distance travelled by the flood-wave in each case of d_b is exactly the same. The notion that d_b does not affect flood-wave propagation is further supported by **Table 5-3**, where flood-wave travel times to the Mediterranean Sea are equal for cases where all other parameters are held constant.

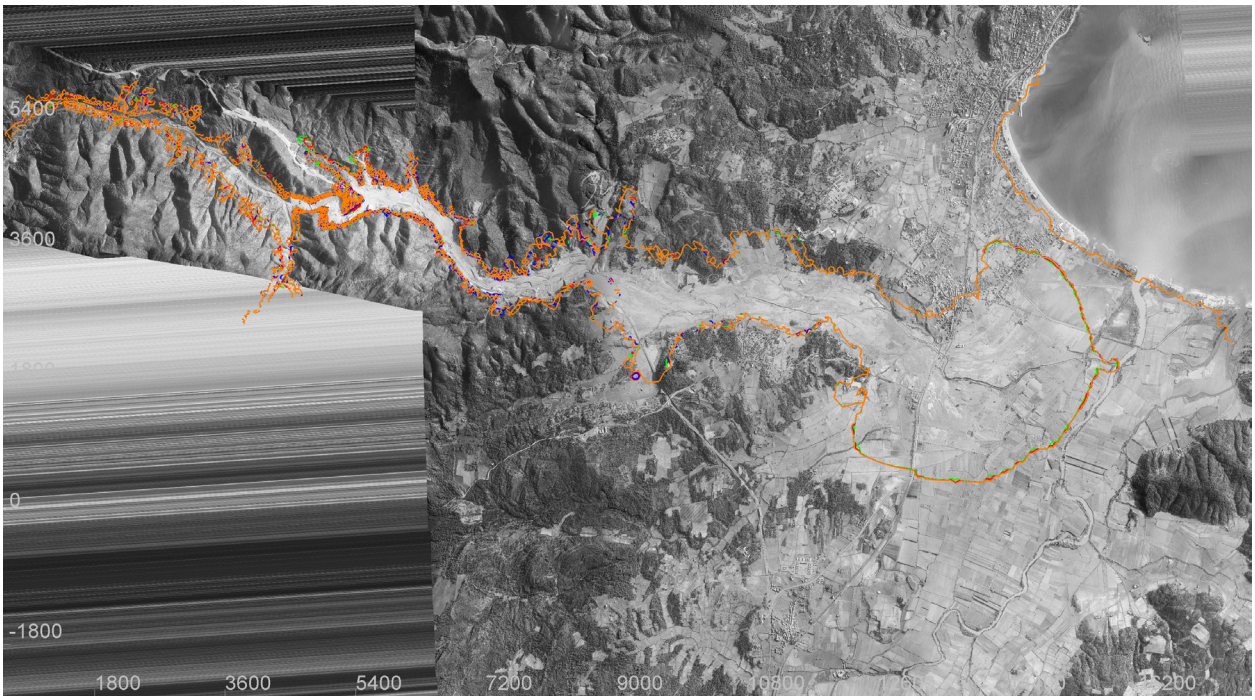

Figure 5-90

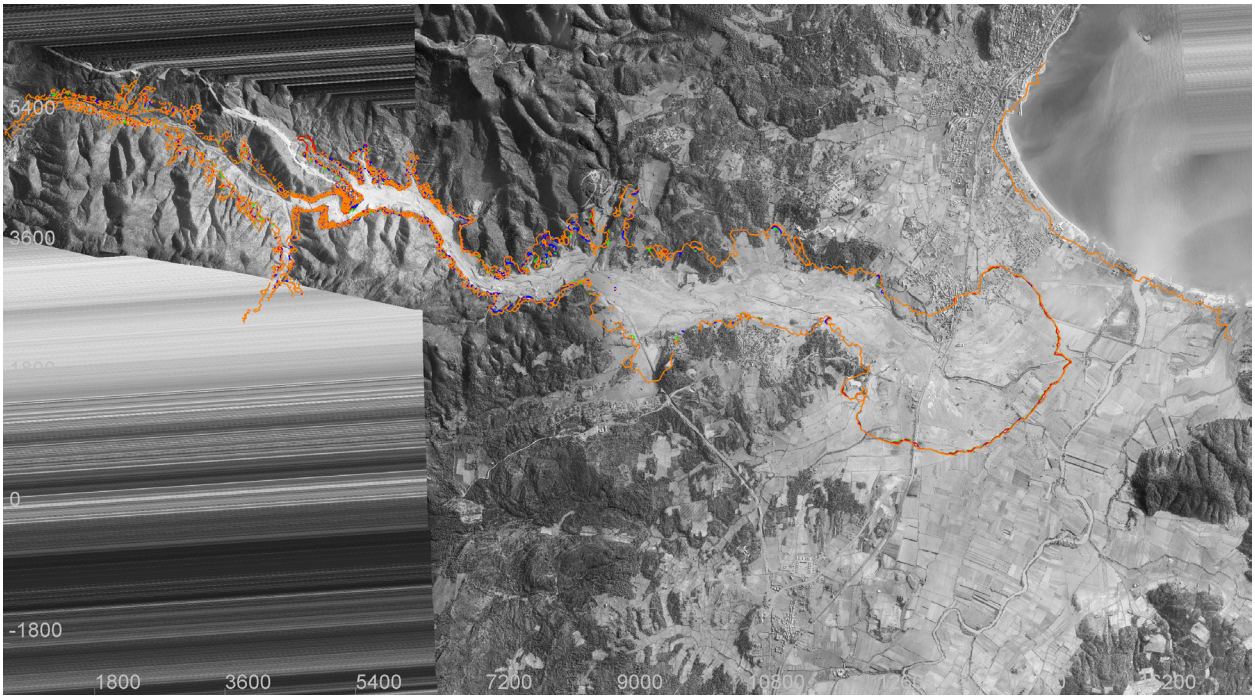

Figure 5-91

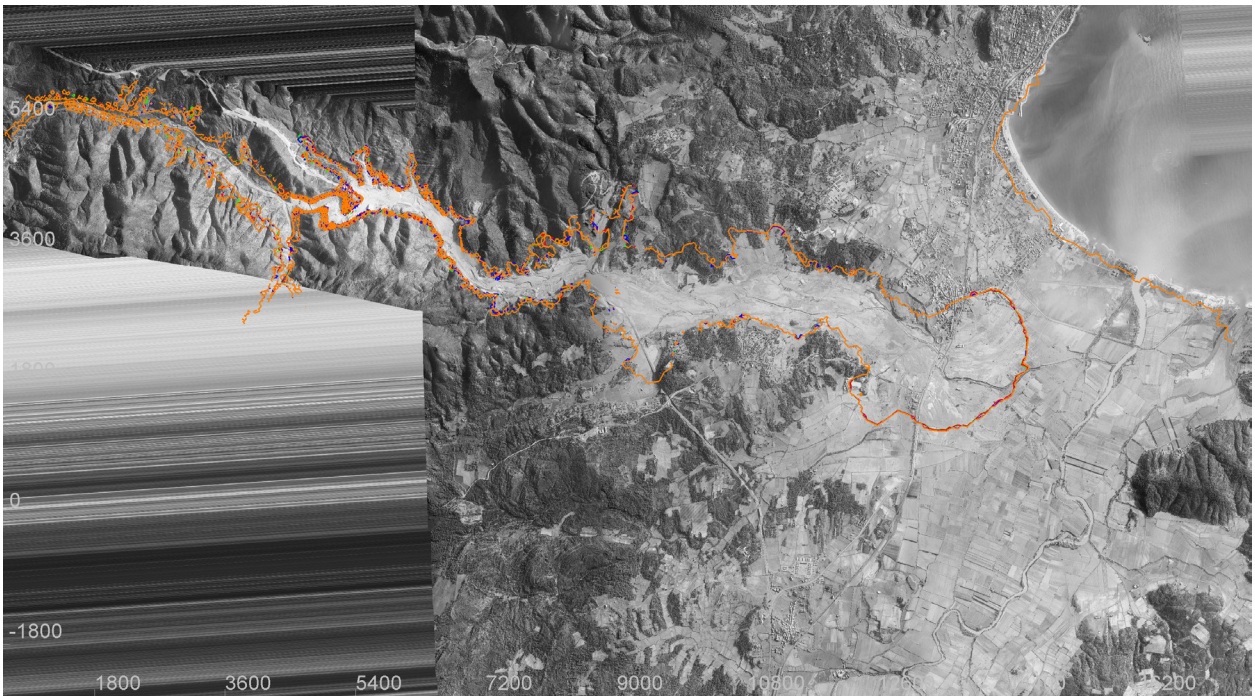

Figure 5-92

Figure 5-90: Extent of inundation 30 minutes after dam-break on a mobile-bed with $n_g = 0.025$, $n_v = 0.000$, $\phi' = 40°$, and $d_{50} = 1\ mm$ (orange – $d_b = 2\ m$, blue – $d_b = 5\ m$, red – $d_b = 10\ m$, green – $d_b = 15\ m$) (aerial photograph of Frejus [FR 177-150, #1 to #104] in 1959 © IGN, 2012, by permission)

Figure 5-91: Extent of inundation 30 minutes after dam-break on a mobile-bed with $n_g = 0.030$, $n_v = 0.000$, $\phi' = 40°$, and $d_{50} = 1\ mm$ (orange – $d_b = 2\ m$, blue – $d_b = 5\ m$, red – $d_b = 10\ m$, green – $d_b = 15\ m$) (aerial photograph of Frejus [FR 177-150, #1 to #104] in 1959 © IGN, 2012, by permission)

Figure 5-92: Extent of inundation 30 minutes after dam-break on a mobile-bed with $n_g = 0.035$, $n_v = 0.000$, $\phi' = 40°$, and $d_{50} = 1\ mm$ (orange – $d_b = 2\ m$, blue – $d_b = 5\ m$, red – $d_b = 10\ m$, green – $d_b = 15\ m$) (aerial photograph of Frejus [FR 177-150, #1 to #104] in 1959 © IGN, 2012, by permission)

Table 5-3: Flood-wave propagation time after dam-break to the Mediterranean Sea on mobile-bed with varied d_b

n_g	n_v	$\phi'(°)$	$d_{50}\ (m)$	$d_b\ (m)$	$t\ (min)$
0.025	0.000	40	0.001	2	32
0.025	0.000	40	0.001	5	32
0.025	0.000	40	0.001	10	32
0.025	0.000	40	0.001	15	33
0.030	0.000	40	0.001	2	36
0.030	0.000	40	0.001	5	36
0.030	0.000	40	0.001	10	36
0.030	0.000	40	0.001	15	36
0.035	0.000	40	0.001	2	39
0.035	0.000	40	0.001	5	39
0.035	0.000	40	0.001	10	39
0.035	0.000	40	0.001	15	39

6 SUMMARY

6.1 CONCLUSIONS

This thesis develops a model using the TELEMAC suite that is suitable for simulating mobile-bed dam-breaks in 2D, then tests it on the Malpasset dam-break as a case study. To develop a model capable of simulating dam-break flows over a mobile bed, a number of TELEMAC2D and SYSIPHE subroutines were created or altered. The final version of the coupled TELEMAC2D-SISYPHE dam-break model has the following capabilities and features:

- set unique critical shear stresses for each of 10 different sediment size classes;
- set unique friction coefficients on nodes inside boundaries defined by input files;
- temporally vary friction coefficients based on total erosion or deposition that has occurred at each computational node;
- compute sediment transport based on developed combination **Meyer-Peter and Muller (1948)** and **Wilson (1966)** equation;
- adjust computed sediment transport to account for the presence of vegetation;
- spatially vary and stratify sediment; and
- spatially define bedrock (rigid boundary) elevation.

Due to a lack of available data to calibrate the mobile-bed version of the Malpasset dam-break model, it was decided that a sensitivity analysis would be performed on the parameters of grain roughness (n_g), vegetation density (n_v and ϕ'), mean grain size (d_{50}), and depth to bedrock (d_b) to examine its effects on inundation and flood-wave propagation characteristics (namely travel time).

6.1.1 SENSITIVITY ANALYSIS

In **Section 5.1**, increasing n_g was found to impact the inundation and flood-wave propagation in such a way that

- the HWM increased in some cross-sections and decreased in others, indicating a varied effect, the magnitude of which is amplified by n_g, on the extent of flood plain inundation;

- erosion and deposition decreased, indicating an inverse relationship between τ^* and n_g; and
- flood-wave celerity decreased, yielding an increased time required to propagate a set distance.

In **Section 5.2**, increasing vegetation density (n_v and ϕ') was found to impact the inundation and flood-wave propagation in such a way that

- the HWM increased in some cross-sections and decreased in others, indicating a varied effect, the magnitude of which is amplified by vegetation density, on the extent of flood plain inundation; this is further supported by the steady-state hydrodynamic simulations modelling a mean annual flood;
- erosion and deposition decreased, indicating a decrease in the τ^*_{grain} partition of τ^*; and
- flood-wave celerity decreased, yielding an increased time required to propagate a set distance.

In **Section 5.3**, increasing d_{50} was found to impact the inundation and flood-wave propagation in such a way that

- the HWM increased in some cross-sections and decreased in others, indicating a varied effect, the magnitude of which is amplified by n_g, on the extent of flood plain inundation;
- erosion and deposition increased; and
- flood-wave celerity increased, yielding a decreased time required to propagate a set distance.

In **Section 5.4**, increasing d_b was found to impact the inundation and flood-wave propagation in such a way that

- no effect was observed on the HWM, indicating that flood plain inundation is not impacted by d_b;
- only the depth of erosion increased in regions of high τ^*, with no change observed in the size of erosion and deposition zones; and
- no effect was observed on flood-wave celerity.

6.1.2 THE FIXED-BED ASSUMPTION

From the case studies mentioned in **Section 1.2** and **Section 4.1**, it is clear that the fixed-bed assumption used in industry standard dam-break analyses is flawed. Models created with this assumption cannot account for morphological changes to the flow paths that occur over the course of a dam-break. However, the fixed-bed assumption is adequate in some instances, for example, the difference in flood-wave propagation time between a fixed-bed and mobile-bed simulation (**Figure 5-24** and **Figure 5-29**) is 1.5 minutes (5%) when all other simulation parameters are held constant. If only flood-wave propagation time were of interest, a fixed-bed model would be sufficient to model the Malpasset dam-break. For other analyses, such as comparing pre- and post-dam-break inundation extents, morphologic changes induced by the propagation of a flood-wave would be more significant as discussed in **Section 5.2.4**. With current computing capabilities, there is no reason why industry should not adopt mobile-bed models in dam-break analyses, especially when performing inundation studies. The fixed-bed assumption is valid only when no significant impact to simulation results is expected from morphological change.

6.1.3 RESEARCH CONTRIBUTION

The development of a mobile-bed dam-break model provides an initial step towards improved dam-break simulations and predictions of morphological change. Although at present this model is still primitive, a comparison of results against a fixed-bed model could identify potential planning and design deficiencies that warrant further investigation.

6.2 LIMITATIONS

The following are limitations of this mobile-bed dam-break model:

- The secondary flow correction algorithm built into SISYPHE requires further development and is inferior to the River2D-Morphology algorithm created by Stephen Kwan. It is possible to reprogram the SISYPHE algorithm in the future.
- The **Meyer-Peter and Muller (1948)** and **Wilson (1966)** combination sediment transport equation does not account for debris flows, which are known to exist during dam-breaks. It was originally intended that the **Hanes (1985)** equation be used in place of **Wilson**

(1966), but the **Hanes (1985)** equation caused simulations to become highly unstable and eventually crash. It is very possible that sediment transport rates are underestimated.

- Infrastructure in the Malpasset model, such as buildings, was assumed to impact flow the same way that vegetation would. This is inaccurate, as buildings tend to be impermeable. Future work on this model would require a better method of accounting for the presence of infrastructure.
- Global values of n_g, n_v, ϕ', d_{50}, and d_b were used for the sensitivity analysis on the Malpasset model. However, a switch to local values would better represent the physical world and hopefully yield more realistic results.
- Manning's n was chosen to represent bed roughness. Perhaps another method could be chosen since effects of bed roughness vary with water depth, and Manning's n is unable to capture this.

6.3 FUTURE WORK

The end result of any future work for this research would be to improve upon the created mobile-bed dam-break model. A number of suggestions for future work were outlined in the limitations section. Additional suggestions are listed below:

- Conduct and model a laboratory flume experiment with a variety of conditions to model performance.
- Simulate real-case dam-breaks that have pre- and post-dam-break topography available in order to further examine model performance and validity.
- Extend all of this work to create a 3D mobile-bed dam-break model.

REFERENCES

Bagnold, R. A. (1966). "An Approach to the Sediment Transport Problem for General Physics." *Rep. No. Geological Survey Professional Paper 422-I,* Washington, D.C.

Cao, Z., Pender, G., Wallis, S., and Carling, P. (2004). "Computational dam-break hydraulics over erodible sediment bed." *J.Hydraul.Eng.,* 130(7), 689-703.

Capart, H., Spinewine, B., Young, D. L., Zech, Y., Brooks, G. R., Leclerc, M., and Secretan, Y. (2007). "The 1996 Lake Ha! Ha! breakout flood, Quebec: Test data for geomorphic flood routing methods." *Journal of Hydraulic Research,* 45, 97-109.

Capart, H., and Young, D. L. (1998). "Formation of a jump by the dam-break wave over a granular bed." *J.Fluid Mech.,* 372, 165-187.

Cheng, N. (2002). "Exponential formula for bedload transport." *J.Hydraul.Eng.,* 128(10), 942-946.

Dewals, B., Archambeau, P., Erpicum, S., Mouzelard, T., and Pirotton, M. (2002). "Dam-break hazard assessment with geomorphic flow computation, using WOLF 2D hydrodynamic software." *Third International Conference Computer Simulation in Risk Analysis and Hazard Mitigation, Risk Analysis III, June 19, 2002 - June 21,* WITPress, Sintra, Portugal, 59-68.

DHL (Delft Hydraulics Laboratory). (1982). "Initiation of Motion and Suspension, Development of Concentration Profiles in a Steady, Uniform Flow Without Initial Sediment Load." Report M1531-III.

EDF (Electricité de France). (2010). "TELEMAC modelling system and SISYPHE user manual version 6.0." Electricité de France: Research & Development, France.

Einstein, H. A. (1950). "The Bedload Function for Bedload Transportation in Open Channel Flows." *Technical Bulletin no. 1026,* 1-71.

Engelund, F. (1965). "A Criterion for the Occurrence of Suspended Load." *La Houille Blanche,* (8), 7.

Engelund, F., and Fredsoe, J. (1976). "Sediment Transport Model for Straight Alluvial Channels." *Nordic Hydrol.,* 7(5), 293-306.

EWRI (Environmental and Water Resources Institute). (2008). "Sedimentation Engineering: Processes, Measurements, Modeling, and Practice." *Rep. No. 110,* American Society of Civil Engineers, USA.

Ferrari, A., Fraccarollo, L., Dumbser, M., Toro, E. F., and Armanini, A. (2010). "Three-dimensional flow evolution after a dam break." *J.Fluid Mech.,* 663, 456-477.

Gilbert, G. K. (1914). "The Transportation of Debris by Running Water." U.S. Geological Survey Professional Paper 86, 263.

Hanes, D. M. (1985). "GRAIN FLOWS AND BED-LOAD SEDIMENT TRANSPORT: REVIEW AND EXTENSION." Acta Mech., 63(1-4), 131-142.

Hardy, R. J., Lane, S. N., Lawless, M. R., Best, J. L., Elliott, L., and Ingham, D. B. (2005). "Development and testing of a numerical code for treatment of complex river channel topography in three-dimensional CFD models with structured grids." *Journal of Hydraulic Research*, 43(5), 468-480.

Hervouet, J. (2000). "A high resolution 2-D dam-break model using parallelization." *Hydrol.Process.*, 14(13), 2211-2230.

Hervouet, J., and Petitjean, A. (1999). "Malpasset dam-break revisited with two-dimensional computations." *Journal of Hydraulic Research/De Recherches Hydrauliques*, 37(6), 777-788.

Leal, J. G. A. B., Ferreira, R. M. L., and Cardoso, A. H. (2002). "Dam-Break Waves on Movable Bed." *Proceedings River Flow 2002 Conference,* River Flow 2002, Louvain-la-Neuve, Belgium, 981-990.

Li, S., and Millar, R. G. (2011). "A two-dimensional morphodynamic model of gravel-bed river with floodplain vegetation." *Earth Surf.Process.Landforms,* 36(2), 190-202.

Liu, N., Chen, Z., Zhang, J., Lin, W., Chen, W., and Xu, W. (2010). "Draining the Tangjiashan barrier lake." *J.Hydraul.Eng.,* 136(11), 914-923.

Mays, L. (1999). "Sedimentation and Erosion Hydraulics." *Hydraulic Design Handbook,* McGraw-Hill, 6.1.

Meland, N., and Normann, J. O. (1966). "Transport Velocities of Single Particles in Bed-Load Motion." *Geografiska Annaler,* 48(A).

Meyer-Peter, E., and Muller, R. (1948). "Formulas for Bed-Load Transport." *Proceedings of the 2nd Congress, International Association for Hydraulic Structures Research,* 39-64.

Newlin, B. (2007). "Dam Failure Analysis: Current methods for analysis and the implications for emergency action planning." Retrieved June 21, 2011: http://mafsm.org/pdf/2007Conf/Dam_Failure.pdf.

Parker, G. (1979). "Hydraulic Geometry of Active Gravel Rivers." *J.Hydraul.Eng.,* 105(9), 1185-1201.

Quanhong, L. (2009). "Numerical Simulation of Sediment Transport and Morphological Evolution." PhD thesis, National University of Singapore, Singapore.

Soares Frazao, S., Poncin, M. P., Paquier, V., Spinewine, B., and Zech, Y. (2001). "Dam-break induced bank erosion: exploratory investigation and perspectives." *Proceedings of Congress of International Association for Hydraulic Research,* 29, Theme C, 246-251.

Soares Frazao, S., and Zech, Y. (2002). "Dam break in channels with 90 bend." *J.Hydraul.Eng.,* 128(11), 956-968.

Steffler, P. M., and Blackburn, J. (2002). "River2D: Two-dimensional depth-averaged model of river hydrodynamics and fish habitats." University of Alberta, Edmonton, AB.

USACE. (1997). "Engineering and Design: Hydrologic Engineering Requirements for Reservoirs." *Rep. No. EM 1110-2-1420,* U.S. Army Corps of Engineers, Washington, D.C.

van Rijn, L. C. (1984). "Sediment Transport, Part II: Suspended Load Transport." *J.Hydraul.Eng.,* 110(11), 1613-1641.

Vasquez, J. A. (2005). "Two-dimensional finite element river morphology model." PhD thesis, University of British Columbia, Vancouver, BC.

Vasquez, J. A., and Leal, J. G. A. B. (2006). "Two-dimensional dam-break simulation over movable beds with an unstructured mesh." *International Conference on Fluvial Hydraulics - River Flow 2006, September 6, 2006 - September 8,* Taylor and Francis/Balkema, Lisbon, Portugal, 1483-1491.

Vasquez, J. A., Millar, R. G., and Steffler, P. M. (2007). "Two-dimensional finite element river morphology model." National Research Council of Canada, Ottawa, ON, 752-760.

Vasquez, J. A., and Roncal, J. J. (2009). "Testing River2D and Flow-3D for sudden dam-break flow simulations." *Canadian Dam Association 2009 Annual Conference,* Canadian Dam Association, Whistler, BC .

Wilson, K. C. (1966). "Bedload Transport at High Shear Stresses." *Journal of the Hydraulics Division, ASCE,* 92(HY6), 49-59.

Wong, M., and Parker, G. (2006). "Reanalysis and correction of bed-load relation of Meyer-Peter and Muller using their own database."*J.Hydraul.Eng.,* 132(11), 1159-1168.

Xia, J., Lin, B., Falconer, R. A., and Wang, G. (2010). "Modelling dam-break flows over mobile beds using a 2D coupled approach." *Adv.Water Resour.,* 33(2), 171-183.

APPENDIX A – SAMPLE TELEMAC2D INPUT FILE

```
FICHIER DE GEOMETRIE = geometry.slf
FICHIER FORTRAN = fortran.f
FICHIER DES CONDITIONS AUX LIMITES = boundary.cli
FICHIER DES RESULTATS = t2d_results.slf
TITRE = 'Le barrage de MALPASSET'

SUITE DE CALCUL = NON
VARIABLES POUR LES SORTIES GRAPHIQUES =
U,V,H,S,B,F,Q,M,W,N,O,MAXZ,TMXZ,MAXV,TMXV,US
NOMBRE DE TABLEAUX PRIVES = 2
BILAN DE MASSE = VRAI
NOMBRE DE PAS DE TEMPS = 72000   PAS DE TEMPS = 0.1
PERIODE POUR LES SORTIES GRAPHIQUES = 50

PERIODE DE SORTIE LISTING = 10
PRECONDITIONNEMENT = 2
BANCS DECOUVRANTS = VRAI
FORME DE LA CONVECTION = 14;5
OPTION DE SUPG = 0;0
MAXIMUM D'ITERATIONS POUR LE SOLVEUR = 200
SOLVEUR = 7  OPTION DU SOLVEUR = 3  PRECISION DU SOLVEUR = 0.0001
STOCKAGE DES MATRICES : 3     PRODUIT MATRICE-VECTEUR : 2
IMPLICITATION POUR LA HAUTEUR = 0.55
IMPLICITATION POUR LA VITESSE = 0.55
MASS-LUMPING SUR H = 1.
CLIPPING DE H = NON

LOI DE FROTTEMENT SUR LE FOND = 4
COEFFICIENT DE FROTTEMENT : 0.

MODELE DE TURBULENCE = 1 COEFFICIENT DE DIFFUSION DES VITESSES = 1.
COTE INITIALE = 0.
EQUATIONS : 'SAINT-VENANT EF'
OPTION DE TRAITEMENT DES BANCS DECOUVRANTS : 1
TRAITEMENT DU SYSTEME LINEAIRE : 2 SOLVEUR : 1 PRECONDITIONNEMENT : 2
COMPATIBILITE DU GRADIENT DE SURFACE LIBRE : 0.9

FICHIER DES PARAMETRES DE SISYPHE  = sisyphe.cas
COUPLAGE AVEC = 'SISYPHE'
TRAITEMENT DES HAUTEURS NEGATIVES=2
CORRECTION DE CONTINUITE=OUI

&FIN
```

APPENDIX B – SAMPLE SISYPHE INPUT FILE

```
/----------------------------------------------------------------------/
/         SISYPHE
/----------------------------------------------------------------------/

FICHIER DES CONDITIONS AUX LIMITES       = boundary.cli
FICHIER DE GEOMETRIE                     = geometry.slf

/----------------------------------------------------------------------/
/         GENERAL OPTIONS
/----------------------------------------------------------------------/

VARIABLES POUR LES SORTIES GRAPHIQUES =
R,CHESTR,TOB,E,KS,D50
FICHIER DES RESULTATS                    = sis_results.slf

/----------------------------------------------------------------------/
/         NUMERICAL OPTIONS
/----------------------------------------------------------------------/

BILAN DE MASSE = OUI
/STEADY CASE                             = YES

/----------------------------------------------------------------------/
/         PHYSICAL OPTIONS
/----------------------------------------------------------------------/

FORMULE DE TRANSPORT SOLIDE = 1
RAPPORT D'EVOLUTION CRITIQUE = 0.1
EPAISSEUR DE COUCHE ACTIVE = 1.0
NOMBRE DE CLASSES GRANULOMETRIQUES = 3
DIAMETRE MOYEN DES GRAINS = 0.001;0.001;0.001
COURANTS SECONDAIRES = OUI

VOLUMES FINIS = OUI
OPTION DE TRAITEMENT DES FONDS NON ERODABLES = 4

&FIN
```

APPENDIX C – SAMPLE FORTRAN INPUT FILE

```
C   SET SHIELDS PARAMETER (AC) FOR EACH SEDIMENT SIZE CLASS
!       ***********************
        SUBROUTINE INIT_SEDIMENT
!       ***********************
!
     &(NSICLA,ELAY,ZF,ZR,NPOIN,AVAIL,FRACSED_GF,AVA0,
     & LGRAFED,CALWC,XMVS,XMVE,GRAV,VCE,XWC,FDM,
     & CALAC,AC,SEDCO,ES,NCOUCH_TASS,CONC_VASE,
     & MS_SABLE,MS_VASE,ACLADM,UNLADM,TOCE_SABLE)
C
!~~~~~~~~~~~~~~~~~~~~~~~~~~~~~~~~~~~~~~~~~~~~~~~~~~~~~~~~~~~~~~~~~~~~~~~~~~~~~~~~
!| AC             |<->| CRITICAL SHIELDS PARAMETER
!| ACLADM         |-->| MEAN DIAMETER OF SEDIMENT
!| AT0            |<->| TIME IN S
!| AVAIL          |<->| VOLUME PERCENT OF EACH CLASS
!| CALAC          |---| ****
!| CALWC          |-->| ****
!| CONC_VASE      |<->| MUD CONCENTRATION FOR EACH LAYER
!| ELAY           |<->| THICKNESS OF SURFACE LAYER
!| ES             |<->| LAYER THICKNESSES AS DOUBLE PRECISION
!| FDM            |-->| DIAMETER DM FOR EACH CLASS
!| FRACSED_GF     |-->|(A SUPPRIMER)
!| GRAV           |-->| ACCELERATION OF GRAVITY
!| LGRAFED        |-->|(A SUPPRIMER)
!| MS_SABLE       |<->| MASS OF SAND PER LAYER (KG/M2)
!| MS_VASE        |<->| MASS OF MUD PER LAYER (KG/M2)
!| NCOUCH_TASS    |-->| NUMBER OF LAYERS FOR CONSOLIDATION
!| NPOIN          |-->| NUMBER OF POINTS
!| NSICLA         |-->| NUMBER OF SEDIMENT CLASSES
!| SEDCO          |-->| LOGICAL, SEDIMENT COHESIVE OR NOT
!| UNLADM         |-->| MEAN DIAMETER OF ACTIVE STRATUM LAYER
!| VCE            |-->| WATER VISCOSITY
!| XMVE           |-->| FLUID DENSITY
!| XMVS           |-->| WATER DENSITY
!| XWC            |-->| SETTLING VELOCITY
!| ZF             |-->| ELEVATION OF BOTTOM
!| ZR             |-->| NON ERODABLE BED
!~~~~~~~~~~~~~~~~~~~~~~~~~~~~~~~~~~~~~~~~~~~~~~~~~~~~~~~~~~~~~~~~~~~~~~~~~~~~~~~~

      USE BIEF
      USE INTERFACE_SISYPHE, EX_INIT_SEDIMENT => INIT_SEDIMENT
!
      IMPLICIT NONE
      INTEGER LNG,LU
```

```
      COMMON/INFO/LNG,LU
C
C+-+-+-+-+-+-+-+-+-+-+-+-+-+-+-+-+-+-+-+-+-+-+-+-+-+-+-+-+-+-+-+-+-+-+-+-+-+-+-+-+-+-+-+-+-+-+-+-+-+-+-+-+
C
      INTEGER,          INTENT(IN)    :: NSICLA,NPOIN,NCOUCH_TASS
      TYPE(BIEF_OBJ),   INTENT(INOUT) :: ELAY,ZF,ZR
      TYPE(BIEF_OBJ), INTENT(INOUT)    :: MS_SABLE, MS_VASE
      TYPE(BIEF_OBJ),   INTENT(INOUT) :: ACLADM, UNLADM
      LOGICAL,          INTENT(IN)    :: LGRAFED,CALWC
      LOGICAL,          INTENT(IN)    :: CALAC
      DOUBLE PRECISION, INTENT(IN)    :: XMVS,XMVE,GRAV,VCE
      DOUBLE PRECISION, INTENT(INOUT) :: AVA0(NSICLA)
      DOUBLE PRECISION, INTENT(INOUT) :: AVAIL(NPOIN,10,NSICLA)
      DOUBLE PRECISION, INTENT(INOUT) :: FRACSED_GF(NSICLA)
      DOUBLE PRECISION, INTENT(INOUT) :: FDM(NSICLA),XWC(NSICLA)
      DOUBLE PRECISION, INTENT(INOUT) :: AC(NSICLA),TOCE_SABLE
C
      LOGICAL,          INTENT(IN)    :: SEDCO(NSICLA)
C
C IF SEDCO(1) OR SEDCO(2) = YES --> CONSOLIDATION MODEL
C
C
      DOUBLE PRECISION, INTENT(IN)    :: CONC_VASE(10)
      DOUBLE PRECISION, INTENT(INOUT) :: ES(NPOIN,10)
C
C+-+-+-+-+-+-+-+-+-+-+-+-+-+-+-+-+-+-+-+-+-+-+-+-+-+-+-+-+-+-+-+-+-+-+-+-+-+-+-+-+-+-+-+-+-+-+-+-+-+-+-+-+
C
      INTEGER           :: I,J
      DOUBLE PRECISION  :: DENS,DSTAR
      LOGICAL           :: MIXTE
!
!=====================================================================
==!
!=====================================================================
==!
C                       PROGRAM                       !
!=====================================================================
==!
!=====================================================================
==!
!
C  ------ BED COMPOSITION
!
       CALL OS('X=Y-Z   ',X=ELAY,Y=ZF,Z=ZR)
!
C     ONLY ONE CLASS
```

```
C
      IF(NSICLA.EQ.1) THEN
        DO I=1,NPOIN
         AVAIL(I,1,1) = 1.D0
         ACLADM%R(I) = FDM(1)
        ENDDO
C     PURE MUD ONLY
        IF(SEDCO(1)) CALL INIT_MIXTE(XMVS,NPOIN,AVAIL,NSICLA,ES,
     &                          ELAY%R,NCOUCH_TASS,CONC_VASE,
     &                            MS_SABLE%R,MS_VASE%R,ZF%R,
     &                                  ZR%R,AVA0)
C
      ELSE
C
C     NON-COHESIVE, MULTI-CLASSES
C
        IF(.NOT.SEDCO(2)) THEN
         CALL INIT_AVAI
C         CALL MEAN_GRAIN_SIZE
C THIS PART CAN BE INTEGRATED INTO INIT_AVAI
         DO J=1,NPOIN
          ACLADM%R(J) = 0.D0
          UNLADM%R(J) = 0.D0
          DO I=1,NSICLA
           IF(AVAIL(J,1,I).GT.0.D0) THEN
            ACLADM%R(J) = ACLADM%R(J) + FDM(I)*AVAIL(J,1,I)
            UNLADM%R(J) = UNLADM%R(J) + FDM(I)*AVAIL(J,2,I)
           ENDIF
          ENDDO
          ACLADM%R(J)=MAX(ACLADM%R(J),0.D0)
          UNLADM%R(J)=MAX(UNLADM%R(J),0.D0)
         ENDDO
        ELSE
C
C        MIXED (so far only 2 classes: NON COHESIVE /COHESIVE)
C
         MIXTE=.TRUE.
         CALL INIT_MIXTE(XMVS,NPOIN,AVAIL,NSICLA,ES,ELAY%R,
     &                   NCOUCH_TASS,CONC_VASE,MS_SABLE%R,
     &                   MS_VASE%R,ZF%R,ZR%R,AVA0)
         DO I=1,NPOIN
          ACLADM%R(I) = FDM(1)
         ENDDO
        ENDIF
C
      ENDIF
```

```
C
      IF(LGRAFED) THEN
        DO I=1, NSICLA
          FRACSED_GF(I)=AVA0(I)
        ENDDO
      ENDIF
C
C
C ------ SETTLING VELOCITY
C
      IF(.NOT.CALWC) THEN
        DENS = (XMVS - XMVE) / XMVE
        DO I = 1, NSICLA
          CALL VITCHU_SISYPHE(XWC(I),DENS,FDM(I),GRAV,VCE)
        ENDDO
      ENDIF
C
C------ SHIELDS PARAMETER
C
      WRITE(*,*)
      WRITE(*,*) 'INPUT SEDIMENT CLASSES AND SHIELDS PARAMETER'
      WRITE(*,*)
C
      IF(.NOT.CALAC) THEN
        DENS  = (XMVS - XMVE )/ XMVE
        AC(1)=0.056*tan(40*3.141592654/180)
        AC(2)=0.056*tan(40*3.141592654/180)
        AC(3)=999999
      ENDIF

      DO I = 1, NSICLA
         WRITE(*,*) 'D50 = ', FDM(I), ', AC = ', AC(I)
      ENDDO


C     IF(.NOT.CALAC) THEN
C       DENS  = (XMVS - XMVE )/ XMVE
C       DO I = 1, NSICLA
C         DSTAR = FDM(I)*(GRAV*DENS/VCE**2)**(1.D0/3.D0)
C         IF (DSTAR <= 4.D0) THEN
C           AC(I) = 0.24*DSTAR**(-1.0D0)
C         ELSEIF (DSTAR <= 10.D0) THEN
C           AC(I) = 0.14D0*DSTAR**(-0.64D0)
C         ELSEIF (DSTAR <= 20.D0) THEN
C           AC(I) = 0.04D0*DSTAR**(-0.1D0)
C         ELSEIF (DSTAR <= 150.D0) THEN
```

```
C           AC(I) = 0.013D0*DSTAR**(0.29D0)
C         ELSE
C           AC(I) = 0.055D0
C         ENDIF
C      AC(3)=9999
C         WRITE(*,*) 'D50 = ', FDM(I), ', AC = ', AC(I)
C       ENDDO
C      ENDIF

      WRITE(*,*)

C pour les sédiments mixtes (suspension_flux_mixte)
      IF(MIXTE) TOCE_SABLE=AC(1)*FDM(1)*GRAV*(XMVS - XMVE)
C
C-----------------------------------------------------------------------
C
      RETURN
      END

C    INITIALIZE FRICTION COEFFICIENT IN BOTH TELEMAC2D AND SISYPHE
!       *****************
        SUBROUTINE FONSTR
!       *****************
!
     &(H,ZF,Z,CHESTR,NGEO,NFON,NOMFON,MESH,FFON,LISTIN)
!
!***********************************************************************
! BIEF   V6P1                              21/08/2010
!***********************************************************************
!
!brief    LOOKS FOR 'BOTTOM' IN THE GEOMETRY FILE.
!+
!+          LOOKS FOR 'BOTTOM FRICTION' (COEFFICIENTS).
!
!note     THE NAMES OF THE VARIABLES HAVE BEEN DIRECTLY
!+        WRITTEN OUT AND ARE NOT READ FROM 'TEXTE'.
!+        THIS MAKES IT POSSIBLE TO HAVE A GEOMETRY FILE
!+        COMPILED IN ANOTHER LANGUAGE.
!
!history  J-M HERVOUET (LNH)
!+        17/08/94
!+        V5P6
!+
!
!history  N.DURAND (HRW), S.E.BOURBAN (HRW)
!+        13/07/2010
```

```
!+        V6P0
!+   Translation of French comments within the FORTRAN sources into
!+   English comments
!
!history  N.DURAND (HRW), S.E.BOURBAN (HRW)
!+        21/08/2010
!+        V6P0
!+   Creation of DOXYGEN tags for automated documentation and
!+   cross-referencing of the FORTRAN sources
!
!~~~~~~~~~~~~~~~~~~~~~~~~~~~~~~~~~~~~~~~~~~~~~~~~~~~~~~~~~~~~~~~~~~~~~~~~~~~~~~~~
!| CHESTR        |<--| FRICTION COEFFICIENT (DEPENDING ON FRICTION LAW)
!| FFON          |-->| FRICTION COEFFICIENT IF CONSTANT
!| H             |<--| WATER DEPTH
!| LISTIN        |-->| IF YES, WILL GIVE A REPORT
!| MESH          |-->| MESH STRUCTURE
!| NFON          |-->| LOGICAL UNIT OF BOTTOM FILE
!| NGEO          |-->| LOGICAL UNIT OF GEOMETRY FILE
!| NOMFON        |-->| NAME OF BOTTOM FILE
!| Z             |<--| FREE SURFACE ELEVATION
!| ZF            |-->| ELEVATION OF BOTTOM
!~~~~~~~~~~~~~~~~~~~~~~~~~~~~~~~~~~~~~~~~~~~~~~~~~~~~~~~~~~~~~~~~~~~~~~~~~~~~~~~~
!
      USE BIEF, EX_FONSTR => FONSTR
      USE DECLARATIONS_TELEMAC2D, only: NPOIN, inpoly, X, Y
!
      IMPLICIT NONE
      INTEGER LNG,LU,I,J,N
      COMMON/INFO/LNG,LU
!
!+-+-+-+-+-+-+-+-+-+-+-+-+-+-+-+-+-+-+-+-+-+-+-+-+-+-+-+-+-+-+-+-+-+-+-+-+-+-+-+
!
      TYPE(BIEF_OBJ), INTENT(INOUT) :: H,ZF,Z,CHESTR
      CHARACTER(LEN=72), INTENT(IN) :: NOMFON
      TYPE(BIEF_MESH), INTENT(IN)   :: MESH
      DOUBLE PRECISION, INTENT(IN)  :: FFON
      LOGICAL, INTENT(IN)           :: LISTIN
      INTEGER, INTENT(IN)           :: NGEO,NFON
!
!+-+-+-+-+-+-+-+-+-+-+-+-+-+-+-+-+-+-+-+-+-+-+-+-+-+-+-+-+-+-+-+-+-+-+-+-+-+-+-+
!
      INTEGER ERR
!
      DOUBLE PRECISION BID
      REAL, ALLOCATABLE :: W(:)
!
```

```
LOGICAL CALFON,CALFRO,OK,LUZF,LUH,LUZ


INTEGER NPMAX2
PARAMETER (NPMAX2=200)

INTEGER NP1
DOUBLE PRECISION X1(NPMAX2),Y1(NPMAX2)
INTEGER NP2
DOUBLE PRECISION X2(NPMAX2),Y2(NPMAX2)
INTEGER NP3
DOUBLE PRECISION X3(NPMAX2),Y3(NPMAX2)
INTEGER NP4
DOUBLE PRECISION X4(NPMAX2),Y4(NPMAX2)
INTEGER NP5
DOUBLE PRECISION X5(NPMAX2),Y5(NPMAX2)
INTEGER NP6
DOUBLE PRECISION X6(NPMAX2),Y6(NPMAX2)
INTEGER NP7
DOUBLE PRECISION X7(NPMAX2),Y7(NPMAX2)
INTEGER NP8
DOUBLE PRECISION X8(NPMAX2),Y8(NPMAX2)
INTEGER NP9
DOUBLE PRECISION X9(NPMAX2),Y9(NPMAX2)
INTEGER NP10
DOUBLE PRECISION X10(NPMAX2),Y10(NPMAX2)
INTEGER NP11
DOUBLE PRECISION X11(NPMAX2),Y11(NPMAX2)
INTEGER NP12
DOUBLE PRECISION X12(NPMAX2),Y12(NPMAX2)
INTEGER NP13
DOUBLE PRECISION X13(NPMAX2),Y13(NPMAX2)
INTEGER NP14
DOUBLE PRECISION X14(NPMAX2),Y14(NPMAX2)
INTEGER NP15
DOUBLE PRECISION X15(NPMAX2),Y15(NPMAX2)
INTEGER NP16
DOUBLE PRECISION X16(NPMAX2),Y16(NPMAX2)
INTEGER NP17
DOUBLE PRECISION X17(NPMAX2),Y17(NPMAX2)
INTEGER NP18
DOUBLE PRECISION X18(NPMAX2),Y18(NPMAX2)
INTEGER NP19
DOUBLE PRECISION X19(NPMAX2),Y19(NPMAX2)
INTEGER NP20
DOUBLE PRECISION X20(NPMAX2),Y20(NPMAX2)
```

```
      INTEGER NP21
      DOUBLE PRECISION X21(NPMAX2),Y21(NPMAX2)
      INTEGER NP22
      DOUBLE PRECISION X22(NPMAX2),Y22(NPMAX2)
      INTEGER NP23
      DOUBLE PRECISION X23(NPMAX2),Y23(NPMAX2)
      INTEGER NP24
      DOUBLE PRECISION X24(NPMAX2),Y24(NPMAX2)
      INTEGER NP25
      DOUBLE PRECISION X25(NPMAX2),Y25(NPMAX2)
      INTEGER NP26
      DOUBLE PRECISION X26(NPMAX2),Y26(NPMAX2)
!
!-----------------------------------------------------------------------
!
      ALLOCATE(W(MESH%NPOIN),STAT=ERR)
      IF(ERR.NE.0) THEN
        IF(LNG.EQ.1) WRITE(LU,*) 'FONSTR : MAUVAISE ALLOCATION DE W'
        IF(LNG.EQ.2) WRITE(LU,*) 'FONSTR: WRONG ALLOCATION OF W'
        STOP
      ENDIF
!
!-----------------------------------------------------------------------
!
!     ASSUMES THAT THE FILE HEADER LINES HAVE ALREADY BEEN READ
!     WILL START READING THE RESULT RECORDS
!
!-----------------------------------------------------------------------
!
!     INITIALISES
!
      LUH  =  .FALSE.
      LUZ  =  .FALSE.
      LUZF =  .FALSE.
      CALFRO = .TRUE.
!
!-----------------------------------------------------------------------
!
!     LOOKS FOR THE FRICTION COEFFICIENT IN THE FILE
!
      IF(LNG.EQ.1) CALL FIND_IN_SEL(CHESTR,'FROTTEMENT      ',NGEO,W,OK,
     &                              TIME=BID)
      IF(LNG.EQ.2) CALL FIND_IN_SEL(CHESTR,'BOTTOM FRICTION ',NGEO,W,OK,
     &                              TIME=BID)
!     CASE OF A GEOMETRY FILE IN ANOTHER LANGUAGE
      IF(.NOT.OK.AND.LNG.EQ.1) THEN
```

```
      CALL FIND_IN_SEL(CHESTR,'BOTTOM FRICTION ',NGEO,W,OK,TIME=BID)
     ENDIF
     IF(.NOT.OK.AND.LNG.EQ.2) THEN
      CALL FIND_IN_SEL(CHESTR,'FROTTEMENT      ',NGEO,W,OK,TIME=BID)
     ENDIF
     IF(OK) THEN
      CALFRO = .FALSE.
      IF(LNG.EQ.1) WRITE(LU,5)
      IF(LNG.EQ.2) WRITE(LU,6)
5     FORMAT(1X,'FONSTR : COEFFICIENTS DE FROTTEMENT LUS DANS',/,
    &        1X,'        LE FICHIER DE GEOMETRIE')
6     FORMAT(1X,'FONSTR : FRICTION COEFFICIENTS READ IN THE',/,
    &        1X,'        GEOMETRY FILE')
     ENDIF
!
!    LOOKS FOR THE BOTTOM ELEVATION IN THE FILE
!
     IF(LNG.EQ.1) CALL FIND_IN_SEL(ZF,'FOND           ',NGEO,W,OK,
    &                         TIME=BID)
     IF(LNG.EQ.2) CALL FIND_IN_SEL(ZF,'BOTTOM         ',NGEO,W,OK,
    &                         TIME=BID)
     IF(.NOT.OK.AND.LNG.EQ.1) THEN
      CALL FIND_IN_SEL(ZF,'BOTTOM         ',NGEO,W,OK,TIME=BID)
     ENDIF
     IF(.NOT.OK.AND.LNG.EQ.2) THEN
      CALL FIND_IN_SEL(ZF,'FOND           ',NGEO,W,OK,TIME=BID)
     ENDIF
!    MESHES FROM BALMAT ?
     IF(.NOT.OK) CALL FIND_IN_SEL(ZF,'ALTIMETRIE      ',NGEO,W,OK,
    &                         TIME=BID)
!    TOMAWAC IN FRENCH ?
     IF(.NOT.OK) CALL FIND_IN_SEL(ZF,'COTE_DU_FOND    ',NGEO,W,OK,
    &                         TIME=BID)
!    TOMAWAC IN ENGLISH ?
     IF(.NOT.OK) CALL FIND_IN_SEL(ZF,'BOTTOM_LEVEL    ',NGEO,W,OK,
    &                         TIME=BID)
     LUZF = OK
!
     IF(.NOT.LUZF) THEN
!     LOOKS FOR WATER DEPTH AND FREE SURFACE ELEVATION
      IF(LNG.EQ.1) CALL FIND_IN_SEL(H,'HAUTEUR D''EAU   ',NGEO,W,OK,
    &                          TIME=BID)
      IF(LNG.EQ.2) CALL FIND_IN_SEL(H,'WATER DEPTH     ',NGEO,W,OK,
    &                          TIME=BID)
      IF(.NOT.OK.AND.LNG.EQ.1) THEN
       CALL FIND_IN_SEL(H,'WATER DEPTH     ',NGEO,W,OK,TIME=BID)
```

```
      ENDIF
      IF(.NOT.OK.AND.LNG.EQ.2) THEN
        CALL FIND_IN_SEL(H,'HAUTEUR D''EAU   ',NGEO,W,OK,TIME=BID)
      ENDIF
      LUH = OK
      IF(LNG.EQ.1) CALL FIND_IN_SEL(Z,'SURFACE LIBRE   ',NGEO,W,OK,
     &                              TIME=BID)
      IF(LNG.EQ.2) CALL FIND_IN_SEL(Z,'FREE SURFACE    ',NGEO,W,OK,
     &                              TIME=BID)
      IF(.NOT.OK.AND.LNG.EQ.1) THEN
        CALL FIND_IN_SEL(Z,'FREE SURFACE    ',NGEO,W,OK,TIME=BID)
      ENDIF
      IF(.NOT.OK.AND.LNG.EQ.2) THEN
        CALL FIND_IN_SEL(Z,'SURFACE LIBRE   ',NGEO,W,OK,TIME=BID)
      ENDIF
      LUZ = OK
    ENDIF
!
!   INITIALISES THE BOTTOM ELEVATION
!
    IF(LUZF) THEN
!
      CALFON = .FALSE.
!
    ELSE
!
      IF (LUZ.AND.LUH) THEN
!
        CALL OS( 'X=Y-Z   ' , ZF , Z , H , BID )
        IF(LNG.EQ.1) WRITE(LU,24)
        IF(LNG.EQ.2) WRITE(LU,25)
24        FORMAT(1X,'FONSTR (BIEF) : ATTENTION, FOND CALCULE AVEC',/,
     &            '              PROFONDEUR ET SURFACE LIBRE',/,
     &            '              DU FICHIER DE GEOMETRIE')
25        FORMAT(1X,'FONSTR (BIEF): ATTENTION, THE BOTTOM RESULTS',/,
     &            '              FROM DEPTH AND SURFACE ELEVATION',
     &           /,'              FOUND IN THE GEOMETRY FILE')
        CALFON = .FALSE.
!
      ELSE
!
        CALFON = .TRUE.
!
      ENDIF
!
    ENDIF
```

```
!
!---------------------------------------------------------------------
!
! BUILDS THE BOTTOM IF IT WAS NOT IN THE GEOMETRY FILE
!
      IF(NOMFON(1:1).NE.' ') THEN
!       A BOTTOM FILE WAS GIVEN, (RE)COMPUTES THE BOTTOM ELEVATION
        IF(LISTIN) THEN
          IF(LNG.EQ.1) WRITE(LU,2223) NOMFON
          IF(LNG.EQ.2) WRITE(LU,2224) NOMFON
          IF(.NOT.CALFON) THEN
            IF(LNG.EQ.1) WRITE(LU,2225)
            IF(LNG.EQ.2) WRITE(LU,2226)
          ENDIF
        ENDIF
2223    FORMAT(/,1X,'FONSTR (BIEF) : FOND DANS LE FICHIER : ',A72)
2224    FORMAT(/,1X,'FONSTR (BIEF): BATHYMETRY GIVEN IN FILE : ',A72)
2225    FORMAT(  1X,'              LE FOND TROUVE DANS LE FICHIER',/,
     &          1X,'             DE GEOMETRIE EST IGNORE',/)
2226    FORMAT(  1X,'             BATHYMETRY FOUND IN THE',/,
     &          1X,'            GEOMETRY FILE IS IGNORED',/)
!
        CALL FOND(ZF%R,MESH%X%R,MESH%Y%R,MESH%NPOIN,NFON,
     &           MESH%NBOR%I,MESH%KP1BOR%I,MESH%NPTFR)
!
      ELSEIF(CALFON) THEN
        IF(LISTIN) THEN
          IF(LNG.EQ.1) WRITE(LU,2227)
          IF(LNG.EQ.2) WRITE(LU,2228)
        ENDIF
2227    FORMAT(/,1X,'FONSTR (BIEF) : PAS DE FOND DANS LE FICHIER DE',
     &        /,1X,'              GEOMETRIE ET PAS DE FICHIER DES',
     &        /,1X,'              FONDS. LE FOND EST INITIALISE A'
     &        /,1X,'              ZERO MAIS PEUT ENCORE ETRE MODIFIE'
     &        /,1X,'              DANS CORFON.',
     &        /,1X)
2228    FORMAT(/,1X,'FONSTR (BIEF): NO BATHYMETRY IN THE GEOMETRY FILE',
     &        /,1X,'             AND NO BATHYMETRY FILE. THE BOTTOM',
     &        /,1X,'             LEVEL IS FIXED TO ZERO BUT STILL',
     &        /,1X,'             CAN BE MODIFIED IN CORFON.',
     &        /,1X)
        CALL OS( 'X=C     ' , ZF , ZF , ZF , 0.D0 )
      ENDIF
!
!---------------------------------------------------------------------
!
```

```
! COMPUTES THE BOTTOM FRICTION COEFFICIENT
!
      IF(CALFRO) THEN
        CALL OS( 'X=C     ' , CHESTR , CHESTR , CHESTR , FFON )
      ENDIF
      CALL STRCHE


C
C-----------------------------------------------------------------------

      WRITE(*,*)
      WRITE(*,*) 'SET FRICTION ACCORDING TO FOLLOWING BOUNDARIES'
      WRITE(*,*)

      OPEN (61,file='../BOUNDARIES/V1.xyz',status='old')
      read (61,*) NP1
      DO n=1, NP1
        read (61,*) X1(n),Y1(n)
      ENDDO
      print *,'FIN LECTURE V1.xyz', NP1
      CLOSE(61)

      OPEN (61,file='../BOUNDARIES/V2.xyz',status='old')
      read (61,*) NP2
      DO n=1, NP2
        read (61,*) X2(n),Y2(n)
      ENDDO
      print *,'FIN LECTURE V2.xyz', NP2
      CLOSE(61)

      OPEN (61,file='../BOUNDARIES/V3.xyz',status='old')
      read (61,*) NP3
      DO n=1, NP3
        read (61,*) X3(n),Y3(n)
      ENDDO
      print *,'FIN LECTURE V3.xyz', NP3
      CLOSE(61)

      OPEN (61,file='../BOUNDARIES/V4.xyz',status='old')
      read (61,*) NP4
      DO n=1, NP4
        read (61,*) X4(n),Y4(n)
      ENDDO
      print *,'FIN LECTURE V4.xyz', NP4
      CLOSE(61)
```

```
OPEN (61,file='../BOUNDARIES/V5.xyz',status='old')
read (61,*) NP5
DO n=1, NP5
  read (61,*) X5(n),Y5(n)
ENDDO
print *,'FIN LECTURE V5.xyz', NP5
CLOSE(61)

OPEN (61,file='../BOUNDARIES/V6.xyz',status='old')
read (61,*) NP6
DO n=1, NP6
  read (61,*) X6(n),Y6(n)
ENDDO
print *,'FIN LECTURE V6.xyz', NP6
CLOSE(61)

OPEN (61,file='../BOUNDARIES/V7.xyz',status='old')
read (61,*) NP7
DO n=1, NP7
  read (61,*) X7(n),Y7(n)
ENDDO
print *,'FIN LECTURE V7.xyz', NP7
CLOSE(61)

OPEN (61,file='../BOUNDARIES/V8.xyz',status='old')
read (61,*) NP8
DO n=1, NP8
  read (61,*) X8(n),Y8(n)
ENDDO
print *,'FIN LECTURE V8.xyz', NP8
CLOSE(61)

OPEN (61,file='../BOUNDARIES/V9.xyz',status='old')
read (61,*) NP9
DO n=1, NP9
  read (61,*) X9(n),Y9(n)
ENDDO
print *,'FIN LECTURE V9.xyz', NP9
CLOSE(61)

OPEN (61,file='../BOUNDARIES/V10.xyz',status='old')
read (61,*) NP10
DO n=1, NP10
  read (61,*) X10(n),Y10(n)
ENDDO
```

```
print *,'FIN LECTURE V10.xyz', NP10
CLOSE(61)

OPEN (61,file='../BOUNDARIES/V11.xyz',status='old')
read (61,*) NP11
DO n=1, NP11
  read (61,*) X11(n),Y11(n)
ENDDO
print *,'FIN LECTURE V11.xyz', NP11
CLOSE(61)

OPEN (61,file='../BOUNDARIES/V12.xyz',status='old')
read (61,*) NP12
DO n=1, NP12
  read (61,*) X12(n),Y12(n)
ENDDO
print *,'FIN LECTURE V12.xyz', NP12
CLOSE(61)

OPEN (61,file='../BOUNDARIES/V13.xyz',status='old')
read (61,*) NP13
DO n=1, NP13
  read (61,*) X13(n),Y13(n)
ENDDO
print *,'FIN LECTURE V13.xyz', NP13
CLOSE(61)

OPEN (61,file='../BOUNDARIES/V14.xyz',status='old')
read (61,*) NP14
DO n=1, NP14
  read (61,*) X14(n),Y14(n)
ENDDO
print *,'FIN LECTURE V14.xyz', NP14
CLOSE(61)

OPEN (61,file='../BOUNDARIES/V15.xyz',status='old')
read (61,*) NP15
DO n=1, NP15
  read (61,*) X15(n),Y15(n)
ENDDO
print *,'FIN LECTURE V15.xyz', NP15
CLOSE(61)

OPEN (61,file='../BOUNDARIES/V16.xyz',status='old')
read (61,*) NP16
DO n=1, NP16
```

```
  read (61,*) X16(n),Y16(n)
ENDDO
print *,'FIN LECTURE V16.xyz', NP16
CLOSE(61)

OPEN (61,file='../BOUNDARIES/V17.xyz',status='old')
read (61,*) NP17
DO n=1, NP17
  read (61,*) X17(n),Y17(n)
ENDDO
print *,'FIN LECTURE V17.xyz', NP17
CLOSE(61)

OPEN (61,file='../BOUNDARIES/V18.xyz',status='old')
read (61,*) NP18
DO n=1, NP18
  read (61,*) X18(n),Y18(n)
ENDDO
print *,'FIN LECTURE V18.xyz', NP18
CLOSE(61)

OPEN (61,file='../BOUNDARIES/V19.xyz',status='old')
read (61,*) NP19
DO n=1, NP19
  read (61,*) X19(n),Y19(n)
ENDDO
print *,'FIN LECTURE V19.xyz', NP19
CLOSE(61)

OPEN (61,file='../BOUNDARIES/V20.xyz',status='old')
read (61,*) NP20
DO n=1, NP20
  read (61,*) X20(n),Y20(n)
ENDDO
print *,'FIN LECTURE V20.xyz', NP20
CLOSE(61)

OPEN (61,file='../BOUNDARIES/B1.xyz',status='old')
read (61,*) NP21
DO n=1, NP21
  read (61,*) X21(n),Y21(n)
ENDDO
print *,'FIN LECTURE B1.xyz', NP21
CLOSE(61)

OPEN (61,file='../BOUNDARIES/B2.xyz',status='old')
```

```
read (61,*) NP22
DO n=1, NP22
  read (61,*) X22(n),Y22(n)
ENDDO
print *,'FIN LECTURE B2.xyz', NP22
CLOSE(61)

OPEN (61,file='../BOUNDARIES/B3.xyz',status='old')
read (61,*) NP23
DO n=1, NP23
  read (61,*) X23(n),Y23(n)
ENDDO
print *,'FIN LECTURE B3.xyz', NP23
CLOSE(61)

OPEN (61,file='../BOUNDARIES/B4.xyz',status='old')
read (61,*) NP24
DO n=1, NP24
  read (61,*) X24(n),Y24(n)
ENDDO
print *,'FIN LECTURE B4.xyz', NP24
CLOSE(61)

OPEN (61,file='../BOUNDARIES/B5.xyz',status='old')
read (61,*) NP25
DO n=1, NP25
  read (61,*) X25(n),Y25(n)
ENDDO
print *,'FIN LECTURE B5.xyz', NP25
CLOSE(61)

OPEN (61,file='../BOUNDARIES/B6.xyz',status='old')
read (61,*) NP26
DO n=1, NP26
  read (61,*) X26(n),Y26(n)
ENDDO
print *,'FIN LECTURE B6.xyz', NP26
CLOSE(61)

DO J=1,NPOIN
  IF (inpoly(X(J),Y(J),X1,Y1,NP1).OR.
&     inpoly(X(J),Y(J),X2,Y2,NP2).OR.
&     inpoly(X(J),Y(J),X3,Y3,NP3).OR.
&     inpoly(X(J),Y(J),X4,Y4,NP4).OR.
&     inpoly(X(J),Y(J),X5,Y5,NP5).OR.
&     inpoly(X(J),Y(J),X6,Y6,NP6).OR.
```

```
     &      inpoly(X(J),Y(J),X7,Y7,NP7).OR.
     &      inpoly(X(J),Y(J),X8,Y8,NP8).OR.
     &      inpoly(X(J),Y(J),X9,Y9,NP9).OR.
     &      inpoly(X(J),Y(J),X10,Y10,NP10).OR.
     &      inpoly(X(J),Y(J),X11,Y11,NP11).OR.
     &      inpoly(X(J),Y(J),X12,Y12,NP12).OR.
     &      inpoly(X(J),Y(J),X13,Y13,NP13).OR.
     &      inpoly(X(J),Y(J),X14,Y14,NP14).OR.
     &      inpoly(X(J),Y(J),X15,Y15,NP15).OR.
     &      inpoly(X(J),Y(J),X16,Y16,NP16).OR.
     &      inpoly(X(J),Y(J),X17,Y17,NP17).OR.
     &      inpoly(X(J),Y(J),X18,Y18,NP18).OR.
     &      inpoly(X(J),Y(J),X19,Y19,NP19).OR.
     &      inpoly(X(J),Y(J),X20,Y20,NP20).OR.
     &      inpoly(X(J),Y(J),X21,Y21,NP21).OR.
     &      inpoly(X(J),Y(J),X22,Y22,NP22).OR.
     &      inpoly(X(J),Y(J),X23,Y23,NP23).OR.
     &      inpoly(X(J),Y(J),X24,Y24,NP24).OR.
     &      inpoly(X(J),Y(J),X25,Y25,NP25).OR.
     &      inpoly(X(J),Y(J),X26,Y26,NP26)) THEN

            CHESTR%R(J)=0.025+0.000
          ELSE
            CHESTR%R(J)=0.025
          ENDIF
        ENDDO
!
        WRITE(*,*)
!
!-----------------------------------------------------------------------
!
        DEALLOCATE(W)
!
!-----------------------------------------------------------------------
!
        RETURN
        END

C       SPECIFY HOW FRICTION COEFFICIENT WILL VARY WITH TIME IN TELEMAC2D
!       ****************
        SUBROUTINE CORSTR
!       ****************
!brief    CORRECTS THE FRICTION COEFFICIENT ON THE BOTTOM
!+              WHEN IT IS VARIABLE IN TIME.
        USE BIEF
        USE DECLARATIONS_TELEMAC2D
```

```
      USE DECLARATIONS_SISYPHE, ONLY: ESOMT,ZR

      IMPLICIT NONE
      INTEGER LNG,LU
      COMMON/INFO/LNG,LU

      INTEGER I

!-----------------------------------------------------------------------

C MAYBE THIS SHOULD ONLY BE APPLIED INTO THE FLOODPLAIN???
      DO I=1,NPOIN
        IF(ESOMT%R(I)<-1.0) THEN
          CHESTR%R(I)=0.025
        ENDIF
      ENDDO


      RETURN
      END

C     SPECIFY HOW FRICTION COEFFICIENT WILL VARY WITH TIME IN SISYPHE
!       ************************
        SUBROUTINE CORSTR_SISYPHE
!       ************************
!
!
!***********************************************************************
! SISYPHE   V6P1                              21/07/2011
!***********************************************************************
!
!brief    CORRECTS THE BOTTOM FRICTION COEFFICIENT
!+             (IF VARIABLE IN TIME).
!
      USE BIEF
      USE DECLARATIONS_SISYPHE
!
      IMPLICIT NONE
      INTEGER LNG,LU
      COMMON/INFO/LNG,LU

      INTEGER I

!-----------------------------------------------------------------------

C MAYBE THIS SHOULD ONLY BE APPLIED INTO THE FLOODPLAIN???
```

```
      DO I=1,NPOIN
        IF(ESOMT%R(I)<-1.0) THEN
           CHESTR%R(I)=0.025
        ENDIF
      ENDDO


      RETURN
      END

C    BEDLOAD TRANSPORT EQUATION INCORPORATING VEGETATION EFFECTS
C    COMBINATION OF MEYER PETER MULLER AND WILSON EQUATIONS
C        ************************
        SUBROUTINE BEDLOAD_MEYER
C        ************************
C
     &  (TETAP, HIDING, HIDFAC, DENS, GRAV, DM, AC,
     &   ACP, QSC, SLOPEFF, COEFPN)
C
C brief    MEYER-PETER BEDLOAD TRANSPORT FORMULATION.
C~~~~~~~~~~~~~~~~~~~~~~~~~~~~~~~~~~~~~~~~~~~~~~~~~~~~~~~~~~~~~~~~~~~~~~
~
C| AC            |<->| CRITICAL SHIELDS PARAMETER
C| ACP           |<->| MODIFIED SHIELDS PARAMETER
C| COEFPN        |<->| CORRECTION OF TRANSORT FOR SLOPING BED EFFECT
C| DENS          |-->| RELATIVE DENSITY
C| DM            |-->| SEDIMENT GRAIN DIAMETER
C| GRAV          |-->| ACCELERATION OF GRAVITY
C| HIDFAC        |-->| HIDING FACTOR FORMULAS
C| HIDING        |-->| HIDING FACTOR CORRECTION
C| QSC           |<->| BED LOAD TRANSPORT
C| SLOPEFF       |-->| LOGICAL, SLOPING BED EFFECT OR NOT
C| TETAP         |-->| ADIMENSIONAL SKIN FRICTION
C~~~~~~~~~~~~~~~~~~~~~~~~~~~~~~~~~~~~~~~~~~~~~~~~~~~~~~~~~~~~~~~~~~~~~~
~
C
      USE INTERFACE_SISYPHE,
     &    EX_BEDLOAD_MEYER => BEDLOAD_MEYER
      USE BIEF
      USE DECLARATIONS_SISYPHE, only : MPM_ARAY, ESOMT
      USE DECLARATIONS_TELEMAC2D, only : CHESTR, NPOIN
      USE DECLARATIONS_TELEMAC2D, only : PRIVE1, PRIVE2

      IMPLICIT NONE
      INTEGER LNG,LU
      COMMON/INFO/LNG,LU
```

```
C 2/ GLOBAL VARIABLES
C -------------------
      TYPE(BIEF_OBJ),   INTENT(IN)    :: TETAP, HIDING
      INTEGER,          INTENT(IN)    :: HIDFAC, SLOPEFF
      DOUBLE PRECISION, INTENT(IN)    :: DENS, GRAV, DM, AC
C WORK ARRAY T1
      TYPE(BIEF_OBJ),   INTENT(INOUT) :: ACP
      TYPE(BIEF_OBJ),   INTENT(INOUT) :: QSC, COEFPN
C N1=GRAIN ROUGHNESS
C N2=VEGETATION ROUGHNESS
C PRIVE1=SHEAR STRESS FOR SEDIMENT TRANSPORT

C 3/ LOCAL VARIABLES
C -------------------
      DOUBLE PRECISION :: C2, N1, N2, MY,WY,MX,WX
      INTEGER          :: I

C=======================================================================
===C
C=======================================================================
===C
C                        PROGRAM                        C
C=======================================================================
===C
C=======================================================================
===C

      CALL CPSTVC(QSC,ACP)
      CALL OS('X=C     ', X=ACP, C=AC)
C     WRITE(*,*) AC
C ************************************* C
C ADJUST SHEAR STRESS FOR SED TRANSPORT    C (_IMP_)
C ************************************* C

      DO I=1,NPOIN
      IF(ESOMT%R(I)<-1) THEN
        PRIVE1(I)=TETAP%R(I)
      ELSEIF(ESOMT%R(I)>0) THEN
        PRIVE1(I)=TETAP%R(I)
      ELSEIF(CHESTR%R(I)<N1) THEN
        PRIVE1(I)=TETAP%R(I)
      ELSE
        N1=0.025
        N2=CHESTR%R(I)-N1
        PRIVE1(I)=TETAP%R(I)*N1/(N1**2+N2**2)**0.5
```

```
      ENDIF
      PRIVE2(I)=TETAP%R(I)
      ENDDO

C ************************************** C
C 0 - SLOPE EFFECT: SOULBY FORMULATION     C (_IMP_)
C ************************************** C
      IF(SLOPEFF == 2) THEN
        CALL OS('X=XY    ', X=ACP, Y=COEFPN )
      ENDIF

C ************************************** C
C III - BEDLOAD TRANSPORT CORRECTED       C (_IMP_)
C       FOR EXTENDED GRAIN SIZE           C (_IMP_)
C       WITH VARIABLE MPM_COEFFICIENT     C
C ************************************** C
      C2 = SQRT(GRAV*DENS*DM**3)

      DO I=1,NPOIN
        IF (PRIVE1(I)-ACP%R(I)>=0) THEN
          IF (PRIVE1(I)<0.18) THEN
C             MEYER-PETER MULLER 1948
            QSC%R(I)=8*C2*(PRIVE1(I)-ACP%R(I))**1.5
C             WRITE(*,*) 'MPM', PRIVE1(I)
C           ELSEIF (PRIVE1(I)>0.5) THEN
          ELSEIF (PRIVE1(I)>0.5) THEN
C             WILSON 1966
            QSC%R(I)=12*C2*(PRIVE1(I)-ACP%R(I))**1.5
C             WRITE(*,*) 'WILSON', PRIVE1(I)
          ELSE
C             INTERPOLATE BETWEEN WILSON AND MPM
            MX=0.18
            MY=8*C2*(MX-ACP%R(I))**1.5
            WX=0.5
            WY=12*C2*(WX-ACP%R(I))**1.5
            QSC%R(I)=MY*(PRIVE1(I)/MX)**(LOG(WY/MY)/LOG(WX/MX))
C             WRITE(*,*) 'OTHER', PRIVE1(I)
          ENDIF
        ELSE
          QSC%R(I)=0
        ENDIF
      ENDDO


C     IF ((HIDFAC == 1) .OR. (HIDFAC == 2) ) THEN
C
```

```
C      DO I=1,NPOIN
C        IF (PRIVE1(I)-ACP%R(I) >= 0) THEN
C      QSC%R(I)=MPM_ARAY%R(I)*C2*(PRIVE1(I)-ACP%R(I)*HIDING%R(I))**1.5D0
C        ELSE
C      QSC%R(I)=0
C        ENDIF
C      ENDDO
C
C      ELSE
C
C      DO I=1,NPOIN
C        IF (PRIVE1(I)-ACP%R(I) >= 0) THEN
C      QSC%R(I)=MPM_ARAY%R(I)*HIDING%R(I)*C2*(PRIVE1(I)-ACP%R(I))**1.5D0
C        ELSE
C      QSC%R(I)=0
C        ENDIF
C      ENDDO
C
C      ENDIF
C=====================================================================
===C
C=====================================================================
===C
      RETURN
      END

C    SPATIAL AND STRATIFICATION OF SEDIMENT
!       ********************
        SUBROUTINE INIT_COMPO
!       ********************
!
     &(NCOUCHES)
!
!***********************************************************************
! SISYPHE   V6P1                                21/07/2011
!***********************************************************************
!
!brief    INITIAL FRACTION DISTRIBUTION, STRATIFICATION,
!+              VARIATION IN SPACE.
!
!~~~~~~~~~~~~~~~~~~~~~~~~~~~~~~~~~~~~~~~~~~~~~~~~~~~~~~~~~~~~~~~~~~~~~~~~~~~~~~~~
!| NCOUCHES      |-->| NUMBER OF LAYER FOR EACH POINT
!~~~~~~~~~~~~~~~~~~~~~~~~~~~~~~~~~~~~~~~~~~~~~~~~~~~~~~~~~~~~~~~~~~~~~~~~~~~~~~~~
!
      USE BIEF
      USE DECLARATIONS_SISYPHE
```

```
!
      IMPLICIT NONE
      INTEGER LNG,LU
      COMMON/INFO/LNG,LU
!
!+-+-+-+-+-+-+-+-+-+-+-+-+-+-+-+-+-+-+-+-+-+-+-+-+-+-+-+-+-+-+-+-+-+-+-+-+-+-+
!
!                            NPOIN
      INTEGER, INTENT (INOUT)::NCOUCHES(*)
!
!+-+-+-+-+-+-+-+-+-+-+-+-+-+-+-+-+-+-+-+-+-+-+-+-+-+-+-+-+-+-+-+-+-+-+-+-+-+-+
!
      INTEGER I, J, N
C-----------------------------------------------------------------------
C
      INTEGER NPMAX2
      PARAMETER (NPMAX2=200)

      INTEGER NP1
      DOUBLE PRECISION X1(NPMAX2),Y1(NPMAX2)
      INTEGER NP2
      DOUBLE PRECISION X2(NPMAX2),Y2(NPMAX2)
      INTEGER NP3
      DOUBLE PRECISION X3(NPMAX2),Y3(NPMAX2)
      INTEGER NP4
      DOUBLE PRECISION X4(NPMAX2),Y4(NPMAX2)
      INTEGER NP5
      DOUBLE PRECISION X5(NPMAX2),Y5(NPMAX2)
      INTEGER NP6
      DOUBLE PRECISION X6(NPMAX2),Y6(NPMAX2)
      INTEGER NP7
      DOUBLE PRECISION X7(NPMAX2),Y7(NPMAX2)
      INTEGER NP8
      DOUBLE PRECISION X8(NPMAX2),Y8(NPMAX2)
      INTEGER NP9
      DOUBLE PRECISION X9(NPMAX2),Y9(NPMAX2)
      INTEGER NP10
      DOUBLE PRECISION X10(NPMAX2),Y10(NPMAX2)
      INTEGER NP11
      DOUBLE PRECISION X11(NPMAX2),Y11(NPMAX2)
      INTEGER NP12
      DOUBLE PRECISION X12(NPMAX2),Y12(NPMAX2)
      INTEGER NP13
      DOUBLE PRECISION X13(NPMAX2),Y13(NPMAX2)
      INTEGER NP14
      DOUBLE PRECISION X14(NPMAX2),Y14(NPMAX2)
```

```
      INTEGER NP15
      DOUBLE PRECISION X15(NPMAX2),Y15(NPMAX2)
      INTEGER NP16
      DOUBLE PRECISION X16(NPMAX2),Y16(NPMAX2)
      INTEGER NP17
      DOUBLE PRECISION X17(NPMAX2),Y17(NPMAX2)
      INTEGER NP18
      DOUBLE PRECISION X18(NPMAX2),Y18(NPMAX2)
      INTEGER NP19
      DOUBLE PRECISION X19(NPMAX2),Y19(NPMAX2)
      INTEGER NP20
      DOUBLE PRECISION X20(NPMAX2),Y20(NPMAX2)
      INTEGER NP21
      DOUBLE PRECISION X21(NPMAX2),Y21(NPMAX2)
      INTEGER NP22
      DOUBLE PRECISION X22(NPMAX2),Y22(NPMAX2)
      INTEGER NP23
      DOUBLE PRECISION X23(NPMAX2),Y23(NPMAX2)
      INTEGER NP24
      DOUBLE PRECISION X24(NPMAX2),Y24(NPMAX2)
      INTEGER NP25
      DOUBLE PRECISION X25(NPMAX2),Y25(NPMAX2)
      INTEGER NP26
      DOUBLE PRECISION X26(NPMAX2),Y26(NPMAX2)
C
C-----------------------------------------------------------------------

      WRITE(*,*)
      WRITE(*,*) 'SET SEDIMENT SIZES ACCORDING TO FOLLOWING BOUNDARIES'
      WRITE(*,*)

      OPEN (61,file='../BOUNDARIES/V1.xyz',status='old')
      read (61,*) NP1
      DO n=1, NP1
        read (61,*) X1(n),Y1(n)
      ENDDO
      print *,'FIN LECTURE V1.xyz', NP1
      CLOSE(61)

      OPEN (61,file='../BOUNDARIES/V2.xyz',status='old')
      read (61,*) NP2
      DO n=1, NP2
        read (61,*) X2(n),Y2(n)
      ENDDO
      print *,'FIN LECTURE V2.xyz', NP2
      CLOSE(61)
```

```
OPEN (61,file='../BOUNDARIES/V3.xyz',status='old')
read (61,*) NP3
DO n=1, NP3
  read (61,*) X3(n),Y3(n)
ENDDO
print *,'FIN LECTURE V3.xyz', NP3
CLOSE(61)

OPEN (61,file='../BOUNDARIES/V4.xyz',status='old')
read (61,*) NP4
DO n=1, NP4
  read (61,*) X4(n),Y4(n)
ENDDO
print *,'FIN LECTURE V4.xyz', NP4
CLOSE(61)

OPEN (61,file='../BOUNDARIES/V5.xyz',status='old')
read (61,*) NP5
DO n=1, NP5
  read (61,*) X5(n),Y5(n)
ENDDO
print *,'FIN LECTURE V5.xyz', NP5
CLOSE(61)

OPEN (61,file='../BOUNDARIES/V6.xyz',status='old')
read (61,*) NP6
DO n=1, NP6
  read (61,*) X6(n),Y6(n)
ENDDO
print *,'FIN LECTURE V6.xyz', NP6
CLOSE(61)

OPEN (61,file='../BOUNDARIES/V7.xyz',status='old')
read (61,*) NP7
DO n=1, NP7
  read (61,*) X7(n),Y7(n)
ENDDO
print *,'FIN LECTURE V7.xyz', NP7
CLOSE(61)

OPEN (61,file='../BOUNDARIES/V8.xyz',status='old')
read (61,*) NP8
DO n=1, NP8
  read (61,*) X8(n),Y8(n)
ENDDO
```

```
print *,'FIN LECTURE V8.xyz', NP8
CLOSE(61)

OPEN (61,file='../BOUNDARIES/V9.xyz',status='old')
read (61,*) NP9
DO n=1, NP9
  read (61,*) X9(n),Y9(n)
ENDDO
print *,'FIN LECTURE V9.xyz', NP9
CLOSE(61)

OPEN (61,file='../BOUNDARIES/V10.xyz',status='old')
read (61,*) NP10
DO n=1, NP10
  read (61,*) X10(n),Y10(n)
ENDDO
print *,'FIN LECTURE V10.xyz', NP10
CLOSE(61)

OPEN (61,file='../BOUNDARIES/V11.xyz',status='old')
read (61,*) NP11
DO n=1, NP11
  read (61,*) X11(n),Y11(n)
ENDDO
print *,'FIN LECTURE V11.xyz', NP11
CLOSE(61)

OPEN (61,file='../BOUNDARIES/V12.xyz',status='old')
read (61,*) NP12
DO n=1, NP12
  read (61,*) X12(n),Y12(n)
ENDDO
print *,'FIN LECTURE V12.xyz', NP12
CLOSE(61)

OPEN (61,file='../BOUNDARIES/V13.xyz',status='old')
read (61,*) NP13
DO n=1, NP13
  read (61,*) X13(n),Y13(n)
ENDDO
print *,'FIN LECTURE V13.xyz', NP13
CLOSE(61)

OPEN (61,file='../BOUNDARIES/V14.xyz',status='old')
read (61,*) NP14
DO n=1, NP14
```

```
  read (61,*) X14(n),Y14(n)
ENDDO
print *,'FIN LECTURE V14.xyz', NP14
CLOSE(61)

OPEN (61,file='../BOUNDARIES/V15.xyz',status='old')
read (61,*) NP15
DO n=1, NP15
  read (61,*) X15(n),Y15(n)
ENDDO
print *,'FIN LECTURE V15.xyz', NP15
CLOSE(61)

OPEN (61,file='../BOUNDARIES/V16.xyz',status='old')
read (61,*) NP16
DO n=1, NP16
  read (61,*) X16(n),Y16(n)
ENDDO
print *,'FIN LECTURE V16.xyz', NP16
CLOSE(61)

OPEN (61,file='../BOUNDARIES/V17.xyz',status='old')
read (61,*) NP17
DO n=1, NP17
  read (61,*) X17(n),Y17(n)
ENDDO
print *,'FIN LECTURE V17.xyz', NP17
CLOSE(61)

OPEN (61,file='../BOUNDARIES/V18.xyz',status='old')
read (61,*) NP18
DO n=1, NP18
  read (61,*) X18(n),Y18(n)
ENDDO
print *,'FIN LECTURE V18.xyz', NP18
CLOSE(61)

OPEN (61,file='../BOUNDARIES/V19.xyz',status='old')
read (61,*) NP19
DO n=1, NP19
  read (61,*) X19(n),Y19(n)
ENDDO
print *,'FIN LECTURE V19.xyz', NP19
CLOSE(61)

OPEN (61,file='../BOUNDARIES/V20.xyz',status='old')
```

```
read (61,*) NP20
DO n=1, NP20
  read (61,*) X20(n),Y20(n)
ENDDO
print *,'FIN LECTURE V20.xyz', NP20
CLOSE(61)

OPEN (61,file='../BOUNDARIES/B1.xyz',status='old')
read (61,*) NP21
DO n=1, NP21
  read (61,*) X21(n),Y21(n)
ENDDO
print *,'FIN LECTURE B1.xyz', NP21
CLOSE(61)

OPEN (61,file='../BOUNDARIES/B2.xyz',status='old')
read (61,*) NP22
DO n=1, NP22
  read (61,*) X22(n),Y22(n)
ENDDO
print *,'FIN LECTURE B2.xyz', NP22
CLOSE(61)

OPEN (61,file='../BOUNDARIES/B3.xyz',status='old')
read (61,*) NP23
DO n=1, NP23
  read (61,*) X23(n),Y23(n)
ENDDO
print *,'FIN LECTURE B3.xyz', NP23
CLOSE(61)

OPEN (61,file='../BOUNDARIES/B4.xyz',status='old')
read (61,*) NP24
DO n=1, NP24
  read (61,*) X24(n),Y24(n)
ENDDO
print *,'FIN LECTURE B4.xyz', NP24
CLOSE(61)

OPEN (61,file='../BOUNDARIES/B5.xyz',status='old')
read (61,*) NP25
DO n=1, NP25
  read (61,*) X25(n),Y25(n)
ENDDO
print *,'FIN LECTURE B5.xyz', NP25
CLOSE(61)
```

```
      OPEN (61,file='../BOUNDARIES/B6.xyz',status='old')
      read (61,*) NP26
      DO n=1, NP26
        read (61,*) X26(n),Y26(n)
      ENDDO
      print *,'FIN LECTURE B6.xyz', NP26
      CLOSE(61)

C     SPECIFY NUMBER OF LAYERS, AND LAYER THICKNESSES
      DO J=1,NPOIN
        IF (inpoly(X(J),Y(J),X1,Y1,NP1).OR.
     &      inpoly(X(J),Y(J),X2,Y2,NP2).OR.
     &      inpoly(X(J),Y(J),X3,Y3,NP3).OR.
     &      inpoly(X(J),Y(J),X4,Y4,NP4).OR.
     &      inpoly(X(J),Y(J),X5,Y5,NP5).OR.
     &      inpoly(X(J),Y(J),X6,Y6,NP6).OR.
     &      inpoly(X(J),Y(J),X7,Y7,NP7).OR.
     &      inpoly(X(J),Y(J),X8,Y8,NP8).OR.
     &      inpoly(X(J),Y(J),X9,Y9,NP9).OR.
     &      inpoly(X(J),Y(J),X10,Y10,NP10).OR.
     &      inpoly(X(J),Y(J),X11,Y11,NP11).OR.
     &      inpoly(X(J),Y(J),X12,Y12,NP12).OR.
     &      inpoly(X(J),Y(J),X13,Y13,NP13).OR.
     &      inpoly(X(J),Y(J),X14,Y14,NP14).OR.
     &      inpoly(X(J),Y(J),X15,Y15,NP15).OR.
     &      inpoly(X(J),Y(J),X16,Y16,NP16).OR.
     &      inpoly(X(J),Y(J),X17,Y17,NP17).OR.
     &      inpoly(X(J),Y(J),X18,Y18,NP18).OR.
     &      inpoly(X(J),Y(J),X19,Y19,NP19).OR.
     &      inpoly(X(J),Y(J),X20,Y20,NP20).OR.
     &      inpoly(X(J),Y(J),X21,Y21,NP21).OR.
     &      inpoly(X(J),Y(J),X22,Y22,NP22).OR.
     &      inpoly(X(J),Y(J),X23,Y23,NP23).OR.
     &      inpoly(X(J),Y(J),X24,Y24,NP24).OR.
     &      inpoly(X(J),Y(J),X25,Y25,NP25).OR.
     &      inpoly(X(J),Y(J),X26,Y26,NP26)) THEN

          NCOUCHES(J) = 3
          ES(J,1)=1
          ES(J,2)=1
          ES(J,3)=98

          AVAIL(J,1,1) = 1
          AVAIL(J,1,2) = 0
          AVAIL(J,1,3) = 0
```

```
          AVAIL(J,2,1) = 0
          AVAIL(J,2,2) = 1
          AVAIL(J,2,3) = 0
          AVAIL(J,3,1) = 0
          AVAIL(J,3,2) = 0
          AVAIL(J,3,3) = 1

        ELSE

          NCOUCHES(J) = 2
          ES(J,1)=2
          ES(J,2)=99

          AVAIL(J,1,1) = 0
          AVAIL(J,1,2) = 1
          AVAIL(J,1,3) = 0
          AVAIL(J,2,1) = 0
          AVAIL(J,2,2) = 0
          AVAIL(J,2,3) = 1

        ENDIF
      ENDDO

      WRITE(*,*)
!
!-----------------------------------------------------------------------
!
      RETURN
      END

C    SPATIAL DEFINITION OF BEDROCK (RIGID BOUNDARY) ELEVATION
C       ****************
        SUBROUTINE NOEROD
C       ****************
C
     * (H , ZF , ZR , Z , X , Y , NPOIN , CHOIX , NLISS )
C
C**********************************************************************
C SISYPHE VERSION 5.1                    C. LENORMANT
C
C COPYRIGHT EDF-DTMPL-SOGREAH-LHF-GRADIENT
C**********************************************************************
C
C     FONCTION  : IMPOSE LA VALEUR DE LA COTE DU FOND NON ERODABLE  ZR
C
C
```

```
C     RQ: LES METHODES DE TRAITEMENT DES FONDS NON ERODABLES PEUVENT
CONDUIRE
C     A ZF < ZR A CERTAINS PAS DE TEMPS, POUR PALLIER A CELA ON PEUT
CHOISIR
C     CHOISIR DE LISSER LA SOLUTION OBTENUE i.e NLISS > 0.
C
C     FUNCTION  : IMPOSE THE RIGID BED LEVEL  ZR
C
C----------------------------------------------------------------------
C                         ARGUMENTS
C .__________________.____.______________________________________________
C |      NOM       |MODE|                ROLE
C |__________________|____|______________________________________________
C |   H            | -->| WATER DEPTH
C |   ZF           | -->| BED LEVEL
C |   ZR           |<-- | RIGID BED LEVEL
C |   Z            | -->| FREE SURFACE
C |   X,Y          | -->| 2D COORDINATES
C |   NPOIN        | -->| NUMBER OF 2D POINTS
C |   CHOIX        | -->| SELECTED METHOD FOR THE TREATMENT OF RIGID BEDS
C |   NLISS        |<-->| NUMBER OF SMOOTHINGS
C |________________|____|______________________________________________
C MODE : -->(INPUT), <--(RESULT), <-->(MODIFIED DATA)
C----------------------------------------------------------------------
C
      USE BIEF
C       USE DECLARATIONS_SISYPHE, ONLY : MESH,NPTFR
C
      IMPLICIT NONE
      INTEGER LNG,LU
      COMMON/INFO/LNG,LU
C
C+-+-+-+-+-+-+-+-+-+-+-+-+-+-+-+-+-+-+-+-+-+-+-+-+-+-+-+-+-+-+-+-+-+-+-+
C
      INTEGER, INTENT(IN):: NPOIN , CHOIX
      INTEGER, INTENT(INOUT):: NLISS
C
      DOUBLE PRECISION, INTENT(IN)::  Z(NPOIN) , ZF(NPOIN)
      DOUBLE PRECISION , INTENT(IN)::  X(NPOIN) , Y(NPOIN), H(NPOIN)
      DOUBLE PRECISION , INTENT(INOUT)::  ZR(NPOIN)
C
C+-+-+-+-+-+-+-+-+-+-+-+-+-+-+-+-+-+-+-+-+-+-+-+-+-+-+-+-+-+-+-+-+-+-+-+
C
      INTEGER I
      INTEGER k, n
      DOUBLE PRECISION C
```

```
      DOUBLE PRECISION ZEMAX, XMAX
      INTEGER NPMAX2
      PARAMETER (NPMAX2=200)

      INTEGER NP1
      DOUBLE PRECISION X1(NPMAX2),Y1(NPMAX2)
      INTEGER NP2
      DOUBLE PRECISION X2(NPMAX2),Y2(NPMAX2)
      INTEGER NP3
      DOUBLE PRECISION X3(NPMAX2),Y3(NPMAX2)
      INTEGER NP4
      DOUBLE PRECISION X4(NPMAX2),Y4(NPMAX2)
      INTEGER NP5
      DOUBLE PRECISION X5(NPMAX2),Y5(NPMAX2)
      INTEGER NP6
      DOUBLE PRECISION X6(NPMAX2),Y6(NPMAX2)
      INTEGER NP7
      DOUBLE PRECISION X7(NPMAX2),Y7(NPMAX2)
      INTEGER NP8
      DOUBLE PRECISION X8(NPMAX2),Y8(NPMAX2)
      INTEGER NP9
      DOUBLE PRECISION X9(NPMAX2),Y9(NPMAX2)
      INTEGER NP10
      DOUBLE PRECISION X10(NPMAX2),Y10(NPMAX2)

C
C--------------------
C RIGID BEDS POSITION
C--------------------
C
C     DEFAULT VALUE:       ZR=ZF-100.
C
C     ZEMAX: EPAISSEUR MAX DU LIT
      ZEMAX=100.D0
      CALL OV( 'X=Y+C     ',ZR,ZF,ZF,-ZEMAX,NPOIN)

C     print *,'DANS NOEROD...'

C     OPEN (61,file='../BOUNDARIES/1.xyz',status='old')
C     read (61,*) NP1
C     DO n=1, NP1
C        read (61,*) X1(n),Y1(n)
C     ENDDO
C     print *,'FIN LECTURE 1.xyz', NP1
C     CLOSE(61)
```

```
C      DO N=1,NPOIN
C        ZR(N) = ZF(N)-2.0
C      IF (inpoly(x(N),y(N),X1,Y1,NP1)) THEN
C        ZR(N)= ZF(N)-0.5
C      ELSEIF (inpoly(x(N),y(N),X2,Y2,NP2)) THEN
C        ZR(N)= ZF(N)-1.0
C      ENDIF
C      ENDDO
C
C------------------
C SMOOTHING OPTION
C------------------
C
C     NLISS : NUMBER OF SMOOTHING IF  (ZF - ZR ) NEGATIVE
C           DEFAULT VALUE : NLISS = 0 (NO SMOOTHING)
C
      NLISS = 0
C
C---------------------------------------------------------------------
C
      RETURN
      END

C    TELEMAC2D GRAPHICAL OUTPUT
!      *************************
       SUBROUTINE NOMVAR_TELEMAC2D
!      *************************
!
     &(TEXTE,TEXTPR,MNEMO,NPERIAF,NTRAC,NAMETRAC)
!
!***********************************************************************
! TELEMAC2D   V6P1                                   21/08/2010
!***********************************************************************
!
!brief    GIVES THE VARIABLE NAMES FOR THE RESULTS AND GEOMETRY
!+              FILES (IN TEXTE) AND FOR THE PREVIOUS COMPUTATION
!+              RESULTS FILE (IN TEXTPR).
!+
!+              TEXTE AND TEXTPR ARE GENERALLY EQUAL EXCEPT IF THE
!+              PREVIOUS COMPUTATION COMES FROM ANOTHER SOFTWARE.
!
!history  J-M HERVOUET (LNHE)
!+        31/08/2007
!+        V5P8
!+
```

```
!
!history  N.DURAND (HRW), S.E.BOURBAN (HRW)
!+        13/07/2010
!+        V6P0
!+   Translation of French comments within the FORTRAN sources into
!+   English comments
!
!history  N.DURAND (HRW), S.E.BOURBAN (HRW)
!+        21/08/2010
!+        V6P0
!+   Creation of DOXYGEN tags for automated documentation and
!+   cross-referencing of the FORTRAN sources
!
!~~~~~~~~~~~~~~~~~~~~~~~~~~~~~~~~~~~~~~~~~~~~~~~~~~~~~~~~~~~~~~~~~~~~~~~
!| MNEMO          |<--| MNEMONIC FOR 'VARIABLES FOR GRAPHIC OUTPUTS'
!| NAMETRAC       |-->| NAME OF TRACERS (GIVEN BY KEYWORDS)
!| NPERIAF        |-->| NUMBER OF PERIODS FOR FOURRIER ANALYSIS
!| NTRAC          |-->| NUMBER OF TRACERS
!| TEXTE          |<--| SEE ABOVE
!| TEXTPR         |<--| SEE ABOVE
!~~~~~~~~~~~~~~~~~~~~~~~~~~~~~~~~~~~~~~~~~~~~~~~~~~~~~~~~~~~~~~~~~~~~~~~
!
      IMPLICIT NONE
      INTEGER LNG,LU
      COMMON/INFO/LNG,LU
!
!+-+-+-+-+-+-+-+-+-+-+-+-+-+-+-+-+-+-+-+-+-+-+-+-+-+-+-+-+-+-+-+-+-+-+-+
!
      CHARACTER(LEN=32), INTENT(INOUT) :: TEXTE(*),TEXTPR(*)
      CHARACTER(LEN=8),  INTENT(INOUT) :: MNEMO(*)
      INTEGER, INTENT(IN)              :: NPERIAF,NTRAC
      CHARACTER(LEN=32), INTENT(IN)    :: NAMETRAC(32)
!
!+-+-+-+-+-+-+-+-+-+-+-+-+-+-+-+-+-+-+-+-+-+-+-+-+-+-+-+-+-+-+-+-+-+-+-+
!
      CHARACTER(LEN=2) I_IN_2_LETTERS(32)
      DATA I_IN_2_LETTERS /'1 ','2 ','3 ','4 ','5 ','6 ','7 ','8 ','9 ',
     &                     '10','11','12','13','14','15','16','17','18',
     &                     '19','20','21','22','23','24','25','26','27',
     &                     '28','29','30','31','32'/
      INTEGER I
!
!-----------------------------------------------------------------------
!
!  ENGLISH
!
```

```
      IF(LNG.EQ.2) THEN
!
      TEXTE (1 ) = 'VELOCITY U      M/S           '
      TEXTE (2 ) = 'VELOCITY V      M/S           '
      TEXTE (3 ) = 'CELERITY        M/S           '
      TEXTE (4 ) = 'WATER DEPTH     M             '
      TEXTE (5 ) = 'FREE SURFACE    M             '
      TEXTE (6 ) = 'BOTTOM          M             '
      TEXTE (7 ) = 'FROUDE NUMBER                 '
      TEXTE (8 ) = 'SCALAR FLOWRATE M2/S          '
      TEXTE (9 ) = 'EX TRACER                     '
      TEXTE (10) = 'TURBULENT ENERG.JOULE/KG      '
      TEXTE (11) = 'DISSIPATION     WATT/KG       '
      TEXTE (12) = 'VISCOSITY       M2/S          '
      TEXTE (13) = 'FLOWRATE ALONG XM2/S          '
      TEXTE (14) = 'FLOWRATE ALONG YM2/S          '
      TEXTE (15) = 'SCALAR VELOCITY M/S           '
      TEXTE (16) = 'WIND ALONG X    M/S           '
      TEXTE (17) = 'WIND ALONG Y    M/S           '
      TEXTE (18) = 'AIR PRESSURE    PASCAL        '
      TEXTE (19) = 'BOTTOM FRICTION               '
      TEXTE (20) = 'DRIFT ALONG X   M             '
      TEXTE (21) = 'DRIFT ALONG Y   M             '
      TEXTE (22) = 'COURANT NUMBER                '
      TEXTE (23) = 'GRAIN SHEAR     NONDIMENSIONAL '
      TEXTE (24) = 'TOTAL SHEAR     NONDIMENSIONAL '
      TEXTE (25) = 'VARIABLE 25     UNIT   ??     '
      TEXTE (26) = 'VARIABLE 26     UNIT   ??     '
      TEXTE (27) = 'HIGH WATER MARK M             '
      TEXTE (28) = 'HIGH WATER TIME S             '
      TEXTE (29) = 'HIGHEST VELOCITYM/S           '
      TEXTE (30) = 'TIME OF HIGH VELS             '
      TEXTE (31) = 'FRICTION VEL.   M/S           '
!
! TEXTPR IS USED TO READ PREVIOUS COMPUTATION FILES.
! IN GENERAL TEXTPR=TEXTE BUT YOU CAN FOLLOW UP A COMPUTATION
! FROM ANOTHER CODE WITH DIFFERENT VARIABLE NAMES, WHICH MUST
! BE GIVEN HERE:
!
      TEXTPR (1 ) = 'VELOCITY U      M/S          '
      TEXTPR (2 ) = 'VELOCITY V      M/S          '
      TEXTPR (3 ) = 'CELERITY        M/S          '
      TEXTPR (4 ) = 'WATER DEPTH     M            '
      TEXTPR (5 ) = 'FREE SURFACE    M            '
      TEXTPR (6 ) = 'BOTTOM          M            '
      TEXTPR (7 ) = 'FROUDE NUMBER                '
```

```
      TEXTPR (8 ) = 'SCALAR FLOWRATE M2/S          '
      TEXTPR (9 ) = 'EX TRACER                     '
      TEXTPR (10) = 'TURBULENT ENERG.JOULE/KG      '
      TEXTPR (11) = 'DISSIPATION     WATT/KG       '
      TEXTPR (12) = 'VISCOSITY       M2/S          '
      TEXTPR (13) = 'FLOWRATE ALONG XM2/S          '
      TEXTPR (14) = 'FLOWRATE ALONG YM2/S          '
      TEXTPR (15) = 'SCALAR VELOCITY M/S           '
      TEXTPR (16) = 'WIND ALONG X    M/S           '
      TEXTPR (17) = 'WIND ALONG Y    M/S           '
      TEXTPR (18) = 'AIR PRESSURE    PASCAL        '
      TEXTPR (19) = 'BOTTOM FRICTION               '
      TEXTPR (20) = 'DRIFT ALONG X   M             '
      TEXTPR (21) = 'DRIFT ALONG Y   M             '
      TEXTPR (22) = 'COURANT NUMBER                '
      TEXTPR (23) = 'GRAIN SHEAR     NONDIMENSIONAL '
      TEXTPR (24) = 'TOTAL SHEAR     NONDIMENSIONAL '
      TEXTPR (25) = 'VARIABLE 25     UNIT   ??     '
      TEXTPR (26) = 'VARIABLE 26     UNIT   ??     '
      TEXTPR (27) = 'HIGH WATER MARK M             '
      TEXTPR (28) = 'HIGH WATER TIME S             '
      TEXTPR (29) = 'HIGHEST VELOCITYM/S           '
      TEXTPR (30) = 'TIME OF HIGH VELS             '
      TEXTPR (31) = 'FRICTION VEL.   M/S           '
!
!-----------------------------------------------------------------------
!
!  FRANCAIS OU AUTRE
!
      ELSE
!
      TEXTE (1 ) = 'VELOCITY U      M/S            '
      TEXTE (2 ) = 'VELOCITY V      M/S            '
      TEXTE (3 ) = 'CELERITY        M/S            '
      TEXTE (4 ) = 'WATER DEPTH     M              '
      TEXTE (5 ) = 'FREE SURFACE    M              '
      TEXTE (6 ) = 'BOTTOM          M              '
      TEXTE (7 ) = 'FROUDE NUMBER                  '
      TEXTE (8 ) = 'SCALAR FLOWRATE M2/S           '
      TEXTE (9 ) = 'EX TRACER                      '
      TEXTE (10) = 'TURBULENT ENERG.JOULE/KG       '
      TEXTE (11) = 'DISSIPATION     WATT/KG        '
      TEXTE (12) = 'VISCOSITY       M2/S           '
      TEXTE (13) = 'FLOWRATE ALONG XM2/S           '
      TEXTE (14) = 'FLOWRATE ALONG YM2/S           '
      TEXTE (15) = 'SCALAR VELOCITY M/S            '
```

```
      TEXTE (16) = 'WIND ALONG X    M/S           '
      TEXTE (17) = 'WIND ALONG Y    M/S           '
      TEXTE (18) = 'AIR PRESSURE    PASCAL        '
      TEXTE (19) = 'BOTTOM FRICTION               '
      TEXTE (20) = 'DRIFT ALONG X   M             '
      TEXTE (21) = 'DRIFT ALONG Y   M             '
      TEXTE (22) = 'COURANT NUMBER                '
      TEXTE (23) = 'GRAIN SHEAR     NONDIMENSIONAL  '
      TEXTE (24) = 'TOTAL SHEAR     NONDIMENSIONAL  '
      TEXTE (25) = 'VARIABLE 25     UNIT   ??       '
      TEXTE (26) = 'VARIABLE 26     UNIT   ??       '
      TEXTE (27) = 'HIGH WATER MARK M             '
      TEXTE (28) = 'HIGH WATER TIME S             '
      TEXTE (29) = 'HIGHEST VELOCITYM/S           '
      TEXTE (30) = 'TIME OF HIGH VELS             '
      TEXTE (31) = 'FRICTION VEL.   M/S           '
!
! TEXTPR IS USED TO READ PREVIOUS COMPUTATION FILES.
! IN GENERAL TEXTPR=TEXTE BUT YOU CAN FOLLOW UP A COMPUTATION
! FROM ANOTHER CODE WITH DIFFERENT VARIABLE NAMES, WHICH MUST
! BE GIVEN HERE:
!
      TEXTPR (1 ) = 'VELOCITY U      M/S           '
      TEXTPR (2 ) = 'VELOCITY V      M/S           '
      TEXTPR (3 ) = 'CELERITY        M/S           '
      TEXTPR (4 ) = 'WATER DEPTH     M             '
      TEXTPR (5 ) = 'FREE SURFACE    M             '
      TEXTPR (6 ) = 'BOTTOM          M             '
      TEXTPR (7 ) = 'FROUDE NUMBER                 '
      TEXTPR (8 ) = 'SCALAR FLOWRATE M2/S          '
      TEXTPR (9 ) = 'EX TRACER                     '
      TEXTPR (10) = 'TURBULENT ENERG.JOULE/KG      '
      TEXTPR (11) = 'DISSIPATION     WATT/KG       '
      TEXTPR (12) = 'VISCOSITY       M2/S          '
      TEXTPR (13) = 'FLOWRATE ALONG XM2/S          '
      TEXTPR (14) = 'FLOWRATE ALONG YM2/S          '
      TEXTPR (15) = 'SCALAR VELOCITY M/S           '
      TEXTPR (16) = 'WIND ALONG X    M/S           '
      TEXTPR (17) = 'WIND ALONG Y    M/S           '
      TEXTPR (18) = 'AIR PRESSURE    PASCAL        '
      TEXTPR (19) = 'BOTTOM FRICTION               '
      TEXTPR (20) = 'DRIFT ALONG X   M             '
      TEXTPR (21) = 'DRIFT ALONG Y   M             '
      TEXTPR (22) = 'COURANT NUMBER                '
      TEXTPR (23) = 'GRAIN SHEAR     NONDIMENSIONAL  '
      TEXTPR (24) = 'TOTAL SHEAR     NONDIMENSIONAL  '
```

```
      TEXTPR (25) = 'VARIABLE 25     UNIT   ??      '
      TEXTPR (26) = 'VARIABLE 26     UNIT   ??      '
      TEXTPR (27) = 'HIGH WATER MARK M             '
      TEXTPR (28) = 'HIGH WATER TIME S             '
      TEXTPR (29) = 'HIGHEST VELOCITYM/S           '
      TEXTPR (30) = 'TIME OF HIGH VELS             '
      TEXTPR (31) = 'FRICTION VEL.   M/S           '
!
      ENDIF
!
!---------------------------------------------------------------------
!
!   ALIASES FOR THE VARIABLES IN THE STEERING FILE
!
!     UVCHSBFQTKEDIJMXYPWAGLNORZ
!     VELOCITY COMPONENT U
      MNEMO(1)   = 'U      '
!     VELOCITY COMPONENT V
      MNEMO(2)   = 'V      '
!     CELERITY
      MNEMO(3)   = 'C      '
!     WATER DEPTH
      MNEMO(4)   = 'H      '
!     FREE SURFACE ELEVATION
      MNEMO(5)   = 'S      '
!     BOTTOM ELEVATION
      MNEMO(6)   = 'B      '
!     FROUDE
      MNEMO(7)   = 'F      '
!     FLOW RATE
      MNEMO(8)   = 'Q      '
!     EX TRACER
      MNEMO(9)   = '?      '
!     TURBULENT ENERGY
      MNEMO(10)   = 'K      '
!     DISSIPATION
      MNEMO(11)   = 'E      '
!     TURBULENT VISCOSITY
      MNEMO(12)   = 'D      '
!     FLOWRATE ALONG X
      MNEMO(13)   = 'I      '
!     FLOWRATE ALONG Y
      MNEMO(14)   = 'J      '
!     SPEED
      MNEMO(15)   = 'M      '
!     WIND COMPONENT X
```

```
      MNEMO(16)   = 'X       '
!     WIND COMPONENT Y
      MNEMO(17)   = 'Y       '
!     ATMOSPHERIC PRESSURE
      MNEMO(18)   = 'P       '
!     FRICTION
      MNEMO(19)   = 'W       '
!     DRIFT IN X
      MNEMO(20)   = 'A       '
!     DRIFT IN Y
      MNEMO(21)   = 'G       '
!     COURANT NUMBER
      MNEMO(22)   = 'L       '
!     VARIABLE 23
      MNEMO(23)   = 'N       '
!     VARIABLE 24
      MNEMO(24)   = 'O       '
!     VARIABLE 25
      MNEMO(25)   = 'R       '
!     VARIABLE 26
      MNEMO(26)   = 'Z       '
!     VARIABLE 27
      MNEMO(27)   = 'MAXZ    '
!     VARIABLE 28
      MNEMO(28)   = 'TMXZ    '
!     VARIABLE 29
      MNEMO(29)   = 'MAXV    '
!     VARIABLE 30
      MNEMO(30)   = 'TMXV    '
!     VARIABLE 31
      MNEMO(31)   = 'US      '
!
!-----------------------------------------------------------------------
!
!     FOURIER ANALYSES
!
      IF(NPERIAF.GT.0) THEN
        DO I=1,NPERIAF
          IF(LNG.EQ.1) THEN
            TEXTE(32+NTRAC+2*(I-1)) =  'AMPLI PERIODE '
     &                  //I_IN_2_LETTERS(I)
     &                  //'M             '
            TEXTE(33+NTRAC+2*(I-1)) =  'PHASE PERIODE '
     &                  //I_IN_2_LETTERS(I)
     &                  //'DEGRES        '
            TEXTPR(32+NTRAC+2*(I-1)) =  'AMPLI PERIODE '
```

```
     &                    //I_IN_2_LETTERS(I)
     &                    //'M             '
          TEXTPR(33+NTRAC+2*(I-1)) =  'PHASE PERIODE '
     &                    //I_IN_2_LETTERS(I)
     &                    //'DEGRES        '
        ELSE
          TEXTE(32+NTRAC+2*(I-1)) =  'AMPLI PERIOD  '
     &                    //I_IN_2_LETTERS(I)
     &                    //'M             '
          TEXTE(33+NTRAC+2*(I-1)) =  'PHASE PERIOD  '
     &                    //I_IN_2_LETTERS(I)
     &                    //'DEGRES        '
          TEXTPR(32+NTRAC+2*(I-1)) =  'AMPLI PERIOD  '
     &                    //I_IN_2_LETTERS(I)
     &                    //'M             '
          TEXTPR(33+NTRAC+2*(I-1)) =  'PHASE PERIOD  '
     &                    //I_IN_2_LETTERS(I)
     &                    //'DEGRES        '
        ENDIF
        MNEMO(32+NTRAC+2*(I-1)) = 'AMPL'//I_IN_2_LETTERS(I)//'  '
        MNEMO(33+NTRAC+2*(I-1)) = 'PHAS'//I_IN_2_LETTERS(I)//'  '
       ENDDO
     ENDIF
!
!-----------------------------------------------------------------------
!
!    TRACERS
!
     IF(NTRAC.GT.0) THEN
       DO I=1,NTRAC
         TEXTE(31+I)  = NAMETRAC(I)
         TEXTPR(31+I) = NAMETRAC(I)
         MNEMO(31+I)  = 'T'//I_IN_2_LETTERS(I)//'   '
       ENDDO
     ENDIF
!
!-----------------------------------------------------------------------
!
     RETURN
     END

C    SISYPHE GRAPHICAL OUTPUT
!       ************************
       SUBROUTINE NOMVAR_SISYPHE
!       ************************
!
```

```
    &( TEXTE ,TEXTPR , MNEMO , NSICLA , UNIT )
!
!*********************************************************************
! SISYPHE   V6P1                                   21/07/2011
!*********************************************************************
!
!brief    GIVES THE VARIABLE NAMES FOR THE RESULTS AND
!+                GEOMETRY FILES.
!
!history  E. PELTIER; C. LENORMANT; J.-M. HERVOUET
!+        11/09/95
!+
!+
!
!history  M. GONZALES DE LINARES; C.VILLARET
!+        2003
!+
!+
!
!history  JMH
!+        03/11/2009
!+        V6P0
!+   MODIFIED AFTER JACEK JANKOWSKI DEVELOPMENTS
!
!history  N.DURAND (HRW), S.E.BOURBAN (HRW)
!+        13/07/2010
!+        V6P0
!+   Translation of French comments within the FORTRAN sources into
!+   English comments
!
!history  N.DURAND (HRW), S.E.BOURBAN (HRW)
!+        21/08/2010
!+        V6P0
!+   Creation of DOXYGEN tags for automated documentation and
!+   cross-referencing of the FORTRAN sources
!
!~~~~~~~~~~~~~~~~~~~~~~~~~~~~~~~~~~~~~~~~~~~~~~~~~~~~~~~~~~~~~~~~~~~~~~~~~~~~
!| MNEMO          |<--| SYMBOLS TO SPECIFY THE VARIABLES FOR OUTPUT
!|                |   | IN THE STEERING FILE
!| NSICLA         |-->| NUMBER OF SIZE CLASSES FOR BED MATERIALS
!| TEXTE          |<--| NAMES OF VARIABLES (PRINTOUT)
!| TEXTPR         |<--| NAMES OF VARIABLES (INPUT)
!| UNIT           |-->| LOGICAL, FILE NUMBER
!~~~~~~~~~~~~~~~~~~~~~~~~~~~~~~~~~~~~~~~~~~~~~~~~~~~~~~~~~~~~~~~~~~~~~~~~~~~~
!
```

```
    USE DECLARATIONS_SISYPHE, ONLY :
MAXVAR,NSICLM,NLAYMAX,NOMBLAY,
   &                          NPRIV
!
    IMPLICIT NONE
    INTEGER LNG,LU
    COMMON/INFO/LNG,LU
!
!+-+-+-+-+-+-+-+-+-+-+-+-+-+-+-+-+-+-+-+-+-+-+-+-+-+-+-+-+-+-+-+-+-+-+-+-+-+-+-+-+-+-+-+-+-+-+-+-+-+-+-+-+
!
    INTEGER, INTENT(IN)        :: NSICLA
    CHARACTER*8, INTENT(INOUT)  :: MNEMO(MAXVAR)
    CHARACTER*32, INTENT(INOUT) :: TEXTE(MAXVAR),TEXTPR(MAXVAR)
    LOGICAL, INTENT(IN)        :: UNIT
!
!+-+-+-+-+-+-+-+-+-+-+-+-+-+-+-+-+-+-+-+-+-+-+-+-+-+-+-+-+-+-+-+-+-+-+-+-+-+-+-+-+-+-+-+-+-+-+-+-+-+-+-+-+
!
    INTEGER I,J,K,ADD
!
    CHARACTER(LEN=32) TEXTE_AVAI(NLAYMAX*NSICLM),TEXTE_QS(NSICLM)
    CHARACTER(LEN=32) TEXTE_CS(NSICLM),TEXTE_QSC(NSICLM)
    CHARACTER(LEN=32) TEXTE_QSS(NSICLM),TEXTE_ES(NLAYMAX)
    CHARACTER(LEN=8)  MNEMO_AVAI(NLAYMAX*NSICLM),MNEMO_QS(NSICLM)
    CHARACTER(LEN=8)  MNEMO_CS(NSICLM),MNEMO_ES(NLAYMAX)
    CHARACTER(LEN=8)  MNEMO_QSC(NSICLM),MNEMO_QSS(NSICLM)
    CHARACTER(LEN=2)  CLA
    CHARACTER(LEN=1)  LAY
!
!---------------------------------------------------------------------
! CV 3010 +1
    ADD=27+MAX(4,NPRIV)+NSICLA*(NOMBLAY+4)+NOMBLAY
!V     ADD=26+MAX(4,NPRIV)+NSICLA*(NOMBLAY+4)+NOMBLAY
    IF(ADD.GT.MAXVAR) THEN
      IF(LNG.EQ.1) THEN
       WRITE(LU,*) 'NOMVAR_SISYPHE : MAXVAR DOIT VALOIR AU MOINS ',ADD
      ENDIF
      IF(LNG.EQ.2) THEN
       WRITE(LU,*) 'NOMVAR_SISYPHE: MAXVAR SHOULD BE AT LEAST ',ADD
      ENDIF
      CALL PLANTE(1)
      STOP
    ENDIF
!
!---------------------------------------------------------------------
!    2 3RD FRACTION MEANS FRACTION OF SEDIMENT OF CLASS 3 IN 2ND LAYER
!
```

```
      IF(NOMBLAY.GT.9.OR.NSICLA.GT.99) THEN
        WRITE (LU,*) 'REPROGRAM NOMVAR_SISYPHE DUE TO CONSTANT FORMATS'
        CALL PLANTE(1)
        STOP
      ENDIF
!
      DO I=1,NSICLA
        DO J=1,NOMBLAY
          K=(I-1)*NOMBLAY+J
          WRITE(LAY,'(I1)') J
          IF(I.LT.10) THEN
            WRITE(CLA,'(I1)') I
          ELSE
            WRITE(CLA,'(I2)') I
          ENDIF
          TEXTE_AVAI(K) = TRIM('FRAC LAY '//LAY//' CL '//CLA)
          MNEMO_AVAI(K) = TRIM(LAY//'A'//CLA)
        ENDDO
      ENDDO
!
      DO J=1,NSICLA
        IF(J<10) THEN
          WRITE(CLA,'(I1)') J
        ELSE
          WRITE(CLA,'(I2)') J
        ENDIF
        TEXTE_QS(J)  = TRIM('QS CLASS '//CLA)
        TEXTE_QSC(J) = TRIM('QS BEDLOAD CL'//CLA)
        TEXTE_QSS(J) = TRIM('QS SUSP. CL'//CLA)
        IF(UNIT) THEN
          TEXTE_CS(J) = TRIM('CONC MAS CL'//CLA)
          TEXTE_CS(J)(17:19) = 'G/L'
        ELSE
          TEXTE_CS(J) = TRIM('CONC VOL CL'//CLA)
        ENDIF
        MNEMO_QS(J)  = TRIM('QS'//CLA)
        MNEMO_QSC(J) = TRIM('QSBL'//CLA)
        MNEMO_QSS(J) = TRIM('QSS'//CLA)
        MNEMO_CS(J)  = TRIM('CS'//CLA)
      ENDDO
!
      DO K=1,NOMBLAY
        WRITE(LAY,'(I1)') K
!V        TEXTE_ES(K)(1:16)  = 'LAY. '//LAY//' THICKNESS'
        TEXTE_ES(K)(1:16)  = 'LAYER'//LAY//' THICKNESS'
        TEXTE_ES(K)(17:32) = 'M               '
```

```
      MNEMO_ES(K) = LAY//'ES    '
    ENDDO
!
!---------------------------------------------------------------------
!
    IF(LNG.EQ.2) THEN
!
!     ENGLISH VERSION
!
      TEXTE(01) = 'VELOCITY U      M/S           '
      TEXTE(02) = 'VELOCITY V      M/S           '
      TEXTE(03) = 'WATER DEPTH     M              '
      TEXTE(04) = 'FREE SURFACE    M              '
      TEXTE(05) = 'BOTTOM          M             '
      TEXTE(06) = 'FLOWRATE Q      M3/S/M         '
      TEXTE(07) = 'FLOWRATE QX     M3/S/M         '
      TEXTE(08) = 'FLOWRATE QY     M3/S/M         '
      TEXTE(09) = 'RIGID BED       M              '
      TEXTE(10) = 'FRICTION COEFT                 '
      TEXTE(11) = 'BED SHEAR STRESSN/M2        '
      TEXTE(12) = 'WAVE HEIGHT HM0 M              '
      TEXTE(13) = 'PEAK PERIOD TPR5S              '
      TEXTE(14) = 'MEAN DIRECTION  DEG            '
      TEXTE(15) = 'SOLID DISCH     M2/S           '
      TEXTE(16) = 'SOLID DISCH X   M2/S           '
      TEXTE(17) = 'SOLID DISCH Y   M2/S           '
      TEXTE(18) = 'EVOLUTION       M              '
      TEXTE(19) = 'RUGOSITE TOTALE M              '
      TEXTE(20) = 'FROT. PEAU MU                  '
!V 2010
      TEXTE(21) = 'MEAN DIAMETER M                '
! CV 2010 +1
      ADD=NSICLA*(NOMBLAY+2)
      TEXTE(22+ADD)='QS BEDLOAD      M2/S          '
      TEXTE(23+ADD)='QS BEDLOAD X    M2/S          '
      TEXTE(24+ADD)='QS BEDLOAD Y    M2/S          '
      TEXTE(25+ADD)='QS SUSPENSION   M2/S          '
      TEXTE(26+ADD)='QS SUSPENSION X M2/S          '
      TEXTE(27+ADD)='QS SUSPENSION Y M2/S          '
!
    ELSE
!
!     FRENCH VERSION
!
      TEXTE(01) = 'VELOCITY U      M/S           '
      TEXTE(02) = 'VELOCITY V      M/S           '
```

```
      TEXTE(03) = 'WATER DEPTH     M             '
      TEXTE(04) = 'FREE SURFACE    M            '
      TEXTE(05) = 'BOTTOM         M            '
      TEXTE(06) = 'FLOWRATE Q      M3/S/M        '
      TEXTE(07) = 'FLOWRATE QX     M3/S/M        '
      TEXTE(08) = 'FLOWRATE QY     M3/S/M        '
      TEXTE(09) = 'RIGID BED       M            '
      TEXTE(10) = 'FRICTION COEFT               '
      TEXTE(11) = 'BED SHEAR STRESSN/M2       '
      TEXTE(12) = 'WAVE HEIGHT HM0 M            '
      TEXTE(13) = 'PEAK PERIOD TPR5S            '
      TEXTE(14) = 'MEAN DIRECTION  DEG          '
      TEXTE(15) = 'SOLID DISCH     M2/S         '
      TEXTE(16) = 'SOLID DISCH X   M2/S         '
      TEXTE(17) = 'SOLID DISCH Y   M2/S         '
      TEXTE(18) = 'EVOLUTION       M            '
      TEXTE(19) = 'RUGOSITE TOTALE M            '
      TEXTE(20) = 'FROT. PEAU MU                '
!V 2010
      TEXTE(21) = 'MEAN DIAMETER M              '
! CV 2010 +1
      ADD=NSICLA*(NOMBLAY+2)
      TEXTE(22+ADD)='QS BEDLOAD      M2/S          '
      TEXTE(23+ADD)='QS BEDLOAD X    M2/S          '
      TEXTE(24+ADD)='QS BEDLOAD Y    M2/S          '
      TEXTE(25+ADD)='QS SUSPENSION   M2/S          '
      TEXTE(26+ADD)='QS SUSPENSION X M2/S          '
      TEXTE(27+ADD)='QS SUSPENSION Y M2/S          '
!
    ENDIF
!
!    AVAIL: ALL LAYERS OF CLASS 1, THEN ALL LAYERS OF CLASS 2, ETC.
!         SAME ORDER AS IN POINT_SISYPHE
!
    DO J=1,NOMBLAY
      DO I=1,NSICLA
!V 2010    +1
        TEXTE(21+(I-1)*NOMBLAY+J) = TEXTE_AVAI((I-1)*NOMBLAY+J)
        MNEMO(21+(I-1)*NOMBLAY+J) = MNEMO_AVAI((I-1)*NOMBLAY+J)
      ENDDO
    ENDDO
!
    DO I=1,NSICLA
!V 2010    +1
      TEXTE(21+I+NOMBLAY*NSICLA)    = TEXTE_QS(I)
      MNEMO(21+I+NOMBLAY*NSICLA)    = MNEMO_QS(I)
```

```
      TEXTE(21+I+(NOMBLAY+1)*NSICLA) = TEXTE_CS(I)
      MNEMO(21+I+(NOMBLAY+1)*NSICLA) = MNEMO_CS(I)
      TEXTE(27+I+NSICLA*(NOMBLAY+2)) = TEXTE_QSC(I)
      MNEMO(27+I+NSICLA*(NOMBLAY+2)) = MNEMO_QSC(I)
      TEXTE(27+I+NSICLA*(NOMBLAY+3)) = TEXTE_QSS(I)
      MNEMO(27+I+NSICLA*(NOMBLAY+3)) = MNEMO_QSS(I)
    ENDDO
!
!V 2010    +1
    DO I=1,NOMBLAY
      TEXTE(27+I+NSICLA*(NOMBLAY+4)) = TEXTE_ES(I)
      MNEMO(27+I+NSICLA*(NOMBLAY+4)) = MNEMO_ES(I)
    ENDDO
!
    ADD=NSICLA*(NOMBLAY+4)+NOMBLAY
    TEXTE(28+ADD)='PRIVE 1                    '
    TEXTE(29+ADD)='PRIVE 2                    '
    TEXTE(30+ADD)='PRIVE 3                    '
    TEXTE(31+ADD)='PRIVE 4                    '
!   NPRIV MAY BE GREATER THAN 4
!   TEXTE(31+ADD)='PRIVE 5                    '
!
!V 2010 +1
    DO I=1,31+NSICLA*(NOMBLAY+4)+NOMBLAY
      TEXTPR(I)=TEXTE(I)
    ENDDO
!
!---------------------------------------------------------------------
!
!   OTHER NAMES FOR OUTPUT VARIABLES (STEERING FILE)
!
!   VELOCITY U
    MNEMO(1)   = 'U       '
!   VELOCITY V
    MNEMO(2)   = 'V       '
!   WATER DEPTH
    MNEMO(3)   = 'H       '
!   FREE SURFACE
    MNEMO(4)   = 'S       '
!   BOTTOM
    MNEMO(5)   = 'B       '
!   SCALAR FLOW RATE
    MNEMO(6)   = 'Q       '
!   SCALAR FLOW RATE X
    MNEMO(7)   = 'I       '
!   SCALAR FLOW RATE Y
```

```
      MNEMO(8)   = 'J       '
!     RIGID BED
      MNEMO(9)   = 'R       '
!     FRICTION COEFFICIENT
      MNEMO(10)   = 'CHESTR  '
!     MEAN BOTTOM FRICTION
      MNEMO(11)   = 'TOB     '
!     WAVE HEIGHT
      MNEMO(12)   = 'W       '
!     PEAK PERIOD
      MNEMO(13)   = 'X       '
!     WAVE DIRECTION
      MNEMO(14)   = 'THETAW  '
!     SOLID DISCHARGE
      MNEMO(15)   = 'M       '
!     SOLID DISCHARGE X
      MNEMO(16)   = 'N       '
!     SOLID DISCHARGE Y
      MNEMO(17)   = 'P       '
!     EVOLUTION
      MNEMO(18)   = 'E       '
!     KS
      MNEMO(19)   = 'KS      '
!     MU
      MNEMO(20)   = 'MU      '
! CV 2010
      MNEMO(21)   = 'D50     '
! +1
      MNEMO(22+NSICLA*(NOMBLAY+2)) = 'QSBL    '
      MNEMO(23+NSICLA*(NOMBLAY+2)) = 'QSBLX   '
      MNEMO(24+NSICLA*(NOMBLAY+2)) = 'QSBLY   '
      MNEMO(25+NSICLA*(NOMBLAY+2)) = 'QSSUSP  '
      MNEMO(26+NSICLA*(NOMBLAY+2)) = 'QSSUSPX '
      MNEMO(27+NSICLA*(NOMBLAY+2)) = 'QSSUSPY '
!
      ADD=NSICLA*(NOMBLAY+4)+NOMBLAY
      MNEMO(28+ADD) = 'A       '
      MNEMO(29+ADD) = 'G       '
      MNEMO(30+ADD) = 'L       '
      MNEMO(31+ADD) = 'O       '
!     THE NUMBER OF PRIVATE ARRAYS IS A KEYWORD
!     MNEMO(31+ADD) = '????????'
!
!----------------------------
! CV 2010: +1
      ADD=NSICLA*(NOMBLAY+4)+NOMBLAY+27+MAX(NPRIV,4)
```

```
      IF(ADD.LT.MAXVAR) THEN
        DO I=ADD+1,MAXVAR
          MNEMO(I) =' '
          TEXTE(I) =' '
          TEXTPR(I)=' '
        ENDDO
      ENDIF
!
!-----------------------------------------------------------------------
!
      RETURN
      END

C     ORIGINAL SUBROUTINE IN MALPASSET SIMULATION
C       ****************
        SUBROUTINE CONDIN
C       ****************
C
C
C**********************************************************************
C TELEMAC-2D VERSION 5.0        19/08/98  J-M HERVOUET TEL: 30 87 80 18
C
C**********************************************************************
C
C     FONCTION  : INITIALISATION DES GRANDEURS PHYSIQUES H, U, V ETC
C
C-----------------------------------------------------------------------
C                           ARGUMENTS
C .__________________.____._____________________________________________
C |      NOM       |MODE|                   ROLE
C |________________|____|_____________________________________________
C |                | -- |
C |________________|____|_____________________________________________
C MODE : -->(DONNEE NON MODIFIEE), <--(RESULTAT), <-->(DONNEE MODIFIEE)
C**********************************************************************
C
      USE BIEF
      USE DECLARATIONS_TELEMAC2D
C
      IMPLICIT NONE
      INTEGER LNG,LU
      COMMON/INFO/LNG,LU
C
C+-+-+-+-+-+-+-+-+-+-+-+-+-+-+-+-+-+-+-+-+-+-+-+-+-+-+-+-+-+-+-+-+-+-+-+
C
C
C+-+-+-+-+-+-+-+-+-+-+-+-+-+-+-+-+-+-+-+-+-+-+-+-+-+-+-+-+-+-+-+-+-+-+-+
```

```
C
      INTEGER ITRAC
C
C-----------------------------------------------------------------------
C
C   INITIALISATION DU TEMPS
C
      AT = 0.D0
C
C-----------------------------------------------------------------------
C
C   INITIALISATION DES VITESSES : VITESSES NULLES
C
      CALL OS( 'X=C     ' , X=U , C=0.D0 )
      CALL OS( 'X=C     ' , X=V , C=0.D0 )
C
C-----------------------------------------------------------------------
C
C   INITIALISATION DE H , LA HAUTEUR D'EAU
C
      IF(CDTINI(1:10).EQ.'COTE NULLE') THEN
        CALL OS( 'X=C     ' , H , H  , H , 0.D0 )
        CALL OS( 'X=X-Y   ' , H , ZF , H , 0.D0 )
      ELSEIF(CDTINI(1:14).EQ.'COTE CONSTANTE') THEN
        CALL OS( 'X=C     ' , H , H  , H , COTINI )
        CALL OS( 'X=X-Y   ' , H , ZF , H , 0.D0   )
      ELSEIF(CDTINI(1:13).EQ.'HAUTEUR NULLE') THEN
        CALL OS( 'X=C     ' , H , H  , H , 0.D0  )
      ELSEIF(CDTINI(1:13).EQ.'PARTICULIERES') THEN
C  ZONE A MODIFIER
       STOP 'CONDITIONS PARTICULIERES A PROGRAMMER'
C  FIN DE LA ZONE A MODIFIER
      ELSE
        WRITE(LU,*) 'CONDIN : CONDITION INITIALE NON PREVUE : ',CDTINI
        STOP
      ENDIF
C
      CALL CORSUI(H%R,U%R,V%R,ZF%R,X,Y,NPOIN)
C
C-----------------------------------------------------------------------
C
C   INITIALISATION DU TRACEUR
C
      IF(NTRAC.GT.0) THEN
        DO ITRAC=1,NTRAC
          CALL OS('X=C     ',X=T%ADR(ITRAC)%P,C=TRAC0(ITRAC))
```

```
      ENDDO
    ENDIF
C
C-----------------------------------------------------------------
C
C INITIALISATION DE LA VISCOSITE
C
    CALL OS( 'X=C     ' , VISC , VISC , VISC , PROPNU )
C
C-----------------------------------------------------------------
C
    RETURN
    END

C   ORIGINAL SUBROUTINE IN MALPASSET SIMULATION
C      ************************************************
       DOUBLE PRECISION FUNCTION DISTAN(X1,Y1,X2,Y2,X3,Y3)
C      ************************************************
C
C*********************************************************************
C PROGICIEL : TELEMAC          23/07/91
C
C*********************************************************************
C
C   FONCTION : CETE FONCTION CALCULE LA DISTANCE ENTRE UNE DROITE
C ET UN POINT SUR LE MAILLAGE
C-----------------------------------------------------------------
C                        ARGUMENTS
C .__________________.____.______________________________________________.
C |     NOM       |MODE|                ROLE                    |
C |__________________|____|________________________________________________|
C |    X1         | -->  ABSCISSE DU PREMIER POINT SUR LA DROITE
C |    Y1         | -->| COORDONNEE DU PREMIER POINT SUR LA DROITE
C |    X2         | -->  ABSCISSE DU DEUXIEME POINT SUR LA DROITE
C |    Y2         | -->| COORDONNEE DU DEUXIEME POINT SUR LA DROITE
C |    X          | -->| ABSCISSE DU POINT POUR LEQUEL ON CHERCHE DIST1
C |    Y          | -->| COORDONNEE DU POINT POUR LEQUEL ON CHERCHE DIS
C |    DISTAN     |<-- |  DISTANCE ENTRE LA DROITE ET LE POINT
C |__________________|____|_____________________________________________
C MODE : -->(DONNEE NON MODIFIEE), <--(RESULTAT), <-->(DONNEE MODIFIEE)
C*********************************************************************
C
C
    IMPLICIT NONE
    DOUBLE PRECISION X1,X2,X3,Y1,Y2,Y3
    DOUBLE PRECISION A1,B1,C1,DET
```

```
      INTRINSIC SQRT
      A1=Y1-Y2
      B1=-X1+X2
      C1=X1*Y2-X2*Y1
      DET=SQRT((A1**2)+(B1**2))
      DISTAN=((A1*X3)+(B1*Y3)+C1)/DET
      RETURN
      END

C     ORIGINAL SUBROUTINE IN MALPASSET SIMULATION
C       ****************
        SUBROUTINE CORSUI
C       ****************
C
C
     *(H,U,V,ZF,X,Y,NPOIN)
C
C*======================================================================
C PROGICIEL : TELEMAC           01/03/90    J-M HERVOUET
C*======================================================================
C
C  FONCTION  : FONCTION DE CORRECTION DES FONDS RELEVES
C
C             CE SOUS-PROGRAMME UTILITAIRE NE FAIT RIEN DANS LA
C             VERSION STANDARD. IL EST A LA DISPOSITION DES
C             UTILISATEURS, POUR LISSER OU CORRIGER DES FONDS SAISIS
C             PAR EXEMPLE.
C
C----------------------------------------------------------------------
C                         ARGUMENTS
C .__________________.____.______________________________________________
C |      NOM         |MODE|                  ROLE
C |__________________|____|______________________________________________
C |      ZF          |<-->| FOND A MODIFIER.
C |      X,Y,(Z)     | -->| COORDONNEES DU MAILLAGE (Z N'EST PAS EMPLOYE).
C |      NPOIN       | -->| NOMBRE DE POINTS DU MAILLAGE.
C |__________________|____|______________________________________________
C MODE : -->(DONNEE NON MODIFIEE), <--(RESULTAT), <-->(DONNEE MODIFIEE)
C----------------------------------------------------------------------
C
C PROGRAMME APPELANT : TELMAC
C PROGRAMMES APPELES : RIEN EN STANDARD
C
C*======================================================================
C
      IMPLICIT NONE
```

```
C
      INTEGER NPOIN,I
C
      DOUBLE PRECISION H(*),X(*),Y(*),ZF(*),U(*),V(*)
C
      DOUBLE PRECISION DISTAN,X1,X2,Y1,Y2,HD
      EXTERNAL DISTAN
C
C-----------------------------------------------------------------------
C
C   INITIALISATION DES VARIABLES POUR LE CALCUL DE LA SITUATION DU
POINT
C   X1,Y1,X2,Y2 POINT DEFINISANT LA DROITE DE LIMITE DE BARRAGE
C   X3,Y3 POINT DEFINISANT LES COORDONNEES D POINT A DROITE DE LIMITE
DE
C
       X1= 4701.183D0
       Y1= 4143.407D0
       X2= 4655.553D0
       Y2= 4392.104D0
C
       DO 99 I=1,NPOIN
         HD=DISTAN(X1,Y1,X2,Y2,X(I),Y(I))
         IF(HD.GT.0.001D0) THEN
           H(I) = 100.D0 - ZF(I)
           U(I) = 0.D0
           V(I) = 0.D0
         ENDIF
C
C  ZONE DERRIERE LE BARRAGE MAIS QUI N'EST PAS DANS
C  LA RETENUE.
C
         IF((X(I)-4500.D0)**2+(Y(I)-5350.D0)**2.LT.200.D0**2) THEN
           H(I)=0.D0
         ENDIF
C
99     CONTINUE
C
C-----------------------------------------------------------------------
C
      RETURN
      END
```